The Analyst

The Analytical Journal of The Royal Society of Chemistry

Information for Authors

Full details of how to submit material for publication in *The Analyst* are given in the Instructions to Authors in the January issue. Separate copies are available on request.

The Analyst publishes papers on all aspects of the theory and practice of analytical chemistry, fundamental and applied, inorganic and organic, including chemical, physical, biochemical, clinical, pharmaceutical, biological, automatic and computer-based methods. Papers on new approaches to existing methods, new techniques and instrumentation, detectors and sensors, and new areas of application with due attention to overcoming limitations and to underlying principles are all equally welcome. There is no page charge.

The following types of papers will be considered:

Full papers, describing original work.

Short papers: the criteria regarding originality are the same as for full papers, but short papers generally report less extensive investigations or are of limited breadth of subject matter

Communications, which must be on an urgent matter and be of obvious scientific importance. Rapidity of publication is enhanced if diagrams are omitted, but tables and formulae can be included. Communications receive priority and are usually published within 5–8 weeks of receipt. They are intended for brief descriptions of work that has progressed to a stage at which it is likely to be valuable to workers faced with similar problems. A fuller paper may be offered subsequently, if justified by later work.

Reviews, which must be a critical evaluation of the existing state of knowledge on a particular facet of analytical chemistry.

Every paper (except Communications) will be submitted to at least two referees, by whose advice the Editorial Board of *The Analyst* will be guided as to its acceptance or rejection. Papers that are accepted must not be published elsewhere except by permission. Submission of a manuscript will be regarded as an undertaking that the same material is not being considered for publication by another journal.

Regional Advisory Editors. For the benefit of potential contributors outside the United Kingdom, a Panel of Regional Advisory Editors exists. Requests for help or advice on any matter related to the preparation of papers and their submission for publication in *The Analyst* can be sent to the nearest member of the Panel. Currently serving Regional Advisory Editors are listed in each issue of *The Analyst*

Manuscripts (three copies typed in double spacing) should be addressed to:
The Editor, *The Analyst,*
Royal Society of Chemistry,
Burlington House,
Piccadilly,
LONDON W1V 0BN, UK

Particular attention should be paid to the use of standard methods of literature citation, including the journal abbreviations defined in Chemical Abstracts Service Source Index. Wherever possible, the nomenclature employed should follow IUPAC recommendations, and units and symbols should be those associated with SI.

All queries relating to the presentation and submission of papers, and any correspondence regarding accepted papers and proofs, should be directed to the Editor, *The Analyst* (address as above). Members of the Analytical Editorial Board (who may be contacted directly or via the Editorial Office) would welcome comments, suggestions and advice on general policy matters concerning *The Analyst.*
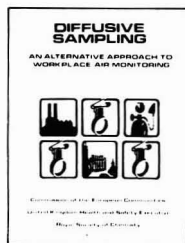
Fifty reprints of each published contribution are supplied free of charge, and further copies can be purchased.

Extraction, Clean-up and Chromatographic Determination of Organophosphate, Pyrethroid and Carbamate Insecticides in Grain and Grain Products
A Review

Gerard J. Sharp, John G. Brayan, Sergio Dilli* and Paul R. Haddad
Department of Analytical Chemistry, University of New South Wales, P.O. Box 1, Kensington, New South Wales 2033, Australia

James M. Desmarchelier
CSIRO, Division of Entomology, P.O. Box 1700, Canberra City, ACT 2601, Australia

Summary of Contents

Keywords: *Pesticide residue analysis; extraction; clean-up; gas chromatography; high-performance liquid chromatography*

1. Introduction

Because grains and their processed products, such as bread or cooked rice, form a major part of the diet of humans and domestic animals, the subject of insecticide residue analysis in grains is important. Despite the obvious importance of the analytical chemistry of insecticides on such stored commodities and their products, it appears that there is no critical appraisal of the subject currently available and it is with this in mind that we have attempted to meet the need in this review.

The scope of the review covers the period from 1962 to the end of 1986 and endeavours to examine critically the existing methodologies and techniques, including residue extraction, clean-up, chromatography and general method evaluation, as they apply to the organophosphate, pyrethroid and carbamate insecticides. Among these, carbaryl and several of the organophosphate pesticides are the most commonly used compounds although, in conjunction with piperonyl butoxide, pyrethroids are used for specific pests. Comprehensive details (such as sample types, columns and detectors) have been tabulated in order to make them more useful and readily accessible. These deal with (i) the broad analytical details; (ii) methods based on gas chromatography (GC); and (iii) methods based on high-performance liquid chromatography (HPLC) and follow the sequence of the general discussion. For easier use, references in the tables have been sorted into each of the three classes of pesticides under review and, in addition, chronologically within each class.

There are two principal sources of insecticides in stored commodities, namely, carry-over from insecticide applications to growing crops and intentional admixture of insecticides with stored commodities (that is, from post-harvest treatment). Here, special attention is given to the latter use, where such insecticides are often described as grain protectants. This usage has recently been comprehensively reviewed[1] for insecticides approved (or likely to be approved) by the Codex Alimentarius Commission, but this did not

include a critical review of the analytical chemistry involved. It is likely, however, that techniques appropriate for the quantification of insecticides admixed in storage will also apply to those from application to the growing crops, although this may not be true of the pesticide degradation products.

In general, a quantitative analytical procedure based on a chromatographic technique is valid only if each of the following five conditions is satisfied: (i) extraction is complete and the extract truly represents the insecticide level in the commodity; (ii) clean-up, when used, is effective and recovery is quantitative; (iii) chromatographic resolution is adequate, if not a base-line resolution; (iv) detection of the insecticide(s) and measurement of the response of the detector are sensitive, specific or selective and reproducible; and (v) comparison of the "unknown" with calibration standards is reproducible. Of these, steps (ii)–(iv) can be validated from the response of "spiked" samples. Step (i) can only be validated from studies of the completeness of the extraction procedures using aged† residues[4] and step (v) requires replication of standards. For good results, each step requires that studies on each type of sample to be analysed be carried out, because a procedure involving extraction, clean-up, separation and quantification on, for example, paddy rice, cannot be assumed to be appropriate for cooked rice. Further, some of these steps (such as the extraction step) may be studied carefully on a few occasions and the resulting methodology used thereafter, whereas others, such as the replication of standards, are required in all determinations. It is important, too, that recoveries of "spiked" samples be included with each batch of determinations to guard against, among other possibilities, variations in the batches of materials used for the clean-up step. Undoubtedly, these general considerations are fundamental to meaningful studies on the fate of residues during the storage and processing of food.

---

† The term is used here to refer to pesticides applied to grain in the field[2] or in storage[3] and then stored for a realistic length of time before being extracted from the grain for quantification.

---

* To whom correspondence should be addressed.

Although perhaps peripheral to this discussion, it follows that a suitable protocol for such studies would involve: (i) extraction studies on aged residues for each commodity (for example, oats, oat hulls, groats or rolled oats); (ii) the preparation of calibration standards, at least in duplicate; and (iii) the determination of recoveries from "spiked" samples for each commodity of interest. If it is accepted that such studies are necessary, then much work remains to be carried out as there are few reports dealing with the completeness of the extraction of insecticides from maize, oats, barley, oil-seeds and legumes. Although it is possible that procedures validated for wheat will also be satisfactory for other grains, this hypothesis requires verification for other products.

2. Extraction of Pesticide Residues from Grains and Grain Products

A wide variety of extraction procedures have been used to remove pesticide residues from grains for analysis (see Table 1), varying from simply standing the grain in a solvent overnight[43] to the more exhaustive techniques such as Soxhlet extraction.[19] A number of different solvents have been used, ranging from non-polar solvents, e.g., hexane, to those of high polarity such as methanol and acetone - water. The extraction procedure, however, has been thoroughly investigated in only a few instances.[2,3,26,61]

Whereas the problems associated with the extraction of aged residues have been well documented,[4,13,63–66] for most of the methods summarised in Table 1 the grain is spiked with the pesticide immediately prior to extraction, and percentage recoveries have then been listed. Such an approach may prove the validity of the clean-up method, but it does not evaluate satisfactorily the effectiveness of the extraction procedure. In order to do this it is necessary to ensure that the maximum amount of pesticide can be extracted from grains containing "aged" residues. This is because pesticides that have been in contact with the grain for some time may interact with it and, as a result, be more difficult to extract than pesticides that have been applied more recently. Attempts to distinguish further the available and total pesticide levels have involved the use of radiolabelled pesticides to determine solvent extractable material in a grain[13,23,67] in addition to the bound pesticide following acid digestion of the grain.[50]

Several methods have been used to evaluate extraction efficiency from grains and other crops. Hence, Bowman et al.[2] compared a number of solvents and methods for extracting six organophosphate pesticides from field-treated crops. From this work, a Soxhlet extraction with 10% methanol in chloroform was found to extract higher levels of pesticides than other techniques such as blending with benzene. In another study, Desmarchelier[3] found that methanol or ethanol extracted higher levels of organophosphates from grains than hexane, but light petroleum was as effective as a number of other solvents for extracting pyrethroids. It was also found that light petroleum extracted the same amount of fenitrothion from grain in 36 h that could be extracted with methanol in 4 h.

In the extraction of carbaryl, Hargreaves and Melksham[61] concluded that methanol was more effective than several other solvents. This comparison was made by standing the grain overnight in one of the solvents, viz., hexane, acetone, dichloromethane or methanol, then decanting the extract and immediately re-extracting the grain with methanol. Ambrus et al.[26] also used multiple extractions to evaluate the usefulness of acetone for the extraction of organophosphates and carbaryl from field-treated crops. Krause[23,67] carried out experiments with ^{14}C-labelled carbaryl and found that methanol extracts up to 15% more carbamate residues from various crops than either acetonitrile or acetone.

Results from several sources suggest that methanol is the most suitable solvent for extracting organophosphates and carbamates from grains. Less work has been carried out on the pyrethroids but it appears that non-polar solvents may also be useful in this instance. Whereas the commodities investigated have been mainly field crops such as maize and wheat in storage, much less is known about the conditions required for the extraction of pesticides from other crops such as paddy rice, oil-seeds and legumes, or, from wet cooked products. It is very likely that the amount of insecticide extracted by non-polar solvents from commodities decreases as the moisture content increases, as is found with cooked products. Similarly, it is probably true that those solvents that can be used to extract insecticides from whole grains can also be used to recover them, probably more quickly, from milled products (such as flour) because of the greater ratio of surface area to volume.

In general, the results obtained using methods for which the extraction procedure has not been evaluated are questionable and, in some instances, the pesticide levels may be seriously under-estimated.

3. Clean-up of Pesticide Residue Extracts from Grains and Grain Products

As shown in Table 1, there are a large and varied number of clean-up procedures available. In many instances, although some of the procedures gave good results, it was not demonstrated conclusively that the clean-up was either necessary or that it had been optimised. Further, as comparatively little is known of the exact chemical composition of co-extractives from grains, there is still no systematic approach for separating them from insecticides, except on a trial and error basis. It is interesting to note that the techniques and cost-effectiveness of some clean-up procedures have been reviewed.[68,69]

The two major approaches to clean-up involve the use of partitioning and column chromatography, although some of the lesser used techniques include gel permeation chromatography, sweep co-distillation and steam distillation. Where column chromatography is employed, the common stationary phases are alumina, silica and Florisil. The amount of packing required is empirical and is determined by the difficulty of the separation and/or the level of co-extractives present. In general, the complexity of the clean-up is determined by the level and type of co-extractives and, to a lesser extent, the type of detection used. However, use of the more selective detectors, such as the nitrogen - phosphorus detector (NPD) or the flame photometric detector (FPD), may largely eliminate the clean-up stage prior to the gas chromatographic determination of the organophosphates.

One problem in clean-up that has received little attention is the effect of water on those procedures that require removal of solvent (as, for example, before the use of an adsorbent or commercial cartridge such as Sep-Pak). Procedures suitable for grains (containing about 10–15% water) may not be suitable for cooked grains (with 60–80% water) in which the water either impedes extraction with a water-immiscible solvent or is taken up by a water-miscible solvent from which the water must then be removed.

A final point deserving comment concerns the end-use of the analytical results, because a clean-up procedure published, or intended, for multi-residue analyses in regulatory laboratories might not be appropriate for the determination of residues of grain protectants for which the need is different. For example, in those instances where the aim of the analysis is to determine the variation of residue levels of a known insecticide admixed with grain in commercial storages, it may be better to measure levels in many samples using minimal clean-up, rather than in a few samples following extensive clean-up. Uncomplicated procedures also have merit in the quality control situations facing grain handlers or millers.

Table 1. Summary of extraction and clean-up procedures for grain protectants

Pesticide	Sample	Extraction			Clean-up		Analysis mode	Reference
		Sample treatment	Solvent	Partitioning solvent	Column (or other)	Eluent		
Organophosphates	Crops	Chopped and blended	Ethyl acetate		Adsorption chromatography (or sweep co-distillation)			5
Malathion	Wheat	Ground; Soxhlet extraction	Hexane		None		GC	6
Malathion and dichlorvos	Wheat	Ground	Hexane		None		GC	7
Six organophosphates	Crops include corn and grass	Blended; Soxhlet extraction	Extraction study includes benzene - chloroform and chloroform - methanol				GC	2
Malathion and its hydrolytic products	Grain	Blended	Acidified acetone	Hexane			GC	8
Dichlorvos	Crops	Ground and macerated	Dichloromethane or ethyl acetate		(Steam distillation)		GC	9
Dichlorvos and malathion	Wheat	Ground and macerated	Methanol		Charcoal and Celite	Acetone	GC	10
Organophosphates	Non-fatty foods	Chopped and blended	Acetonitrile	Dichloromethane	Charcoal, Sea Sorb 43 and Celite 545	Acetonitrile - benzene (1 + 1)	GC	11
Dichlorvos and malathion	Grain	Ground and homogenised	Methanol		None		GC	12
Fonofos	Wheat	Chopped and macerated	Extraction study: (1) ethyl acetate; (2) benzene; (3) acetonitrile				Liquid scintillation counter	13
Malathion, tetrachlorvinphos and fenitrothion	Paddy rice, wheat, sorghum, milled products and cooked products	Agitation	Methanol		Agitating filtrate with 1 g of Nuchar Attaclay for 2 h		GC	14
15 organophosphates	Wheat	Ground and shaken with stainless-steel balls	Diethyl ether - hexane (3 + 97)		None		GC	15
11 organophosphates	Rice and wheat	Powdered sample; Soxhlet extraction	Extraction study: (1) acetone; (2) hexane; (3) benzene	Hexane-saturated acetonitrile	Sodium sulphate and activated charcoal	Acetone - hexane (1 + 1)	GC	16
Dichlorvos and malathion	Grain dust	Standing overnight	Methanol - acetic acid (99 + 1)		None		GC	17
Organophosphates	Wheat	Whole grain, standing 40 ± 12 h	Extraction study: (1) methanol; (2) acetone; (3) hexane		None		GC	18

Table 1. Summary of extraction and clean-up procedures for grain protectants—*continued*

Pesticide	Sample	Extraction — Sample treatment	Extraction — Solvent	Partitioning solvent	Clean-up — Column (or other)	Clean-up — Eluent	Analysis mode	Reference
Etrimfos	Corn and alfalfa	Chopped; Soxhlet extraction	Dichloromethane - methanol (9 + 1)		(1) Sephadex; (2) silica gel	(1) Benzene - methanol (9 + 1); (2) benzene - acetone (9 + 1)	GC	19
Organophosphates and pyrethroids ..	Cereal products		Light petroleum - diethyl ether (1 + 1)	Acetonitrile to petroleum to dichloromethane	Florisil (for pyrethroids)		GC - ECD; GC - MS (resmethrin and bioresmethrin)	20
Nine organophosphates	Grain	Ground and homogenised	Methanol		Not stated		GC	21
Methidathion and its monoxone metabolite	Safflower seed, meal and oil	Blended	Acetonitrile	Light petroleum to acetonitrile	Florisil	Diethyl ether - benzene (6 + 94)	GC	22
Organophosphates, carbaryl and pyrethroids ..	Wheat, barley, oats, sorghum and rice	Various	Extraction study: (1) methanol or (2) ethanol or (3) hexane; (4) acetone (carbaryl); (5) light petroleum (pyrethroids); (6) dichloromethane (carbaryl)	(1) No clean-up for organophosphates; (2) carbaryl was derivatised			GC	3
Carbamates, organophosphates and piperonyl butoxide ..	Fruits, vegetables and grains	Ground and homogenised	Methanol	Acetonitrile	Nuchar, 5-N silanised Celite	Toluene - acetonitrile (1 + 3)	HPLC - fluorimetry	23, 24
Malathion and an alteration product ..	Rice	Whole grain	Water - acetonitrile (35 + 65) to acetonitrile	Light petroleum	Florisil	Diethyl ether - light petroleum (6 + 94), (15 + 85) and (50 + 50)	GC	25
Organophosphates and carbaryl	Low fat content crops, e.g., cereal grains	Ground and shaken for 1 h	Dichloromethane	Acetone - water	Basic alumina	(1) Hexane; (2) hexane - diethyl ether (2 + 1)	GC	26
Fenitrothion and its metabolites ..	Wheat	Shaken	Acidified acetone or methanol	Benzene	Silica gel and sodium sulphate	Ethanol - benzene (10 + 90)	GC	27
Dichlorvos, trichlorfon and methomyl ..	Hulled rice and rice straw		Aqueous acetonitrile		Inactivated Florisil and magnesium oxide		GC	28
Organophosphates ..	Oil-seeds and high fat, low moisture products	Ground and blended	(1) Light petroleum; (2) light petroleum - diethyl ether (1 + 1); (3) ethanol	Acetonitrile	Sodium sulphate		GC	29

Table 1. Summary of extraction and clean-up procedures for grain protectants—*continued*

Pesticide	Sample	Sample treatment	Extraction		Clean-up		Analysis mode	Reference
			Solvent	Partitioning solvent	Column (or other)	Eluent		
Organophosphates and carbamates	Low fat, low moisture products	Ground and blended	Water - acetone (35 + 65)	Light petroleum - dichloromethane	Carbon	Dichloromethane, acetone - dichloromethane (2 + 1)	GC - FPD; GC - Hall electrolytic conductivity detector	30
Organophosphates, synthetic pyrethroids, carbaryl and piperonyl butoxide	Grain, barley and wheat	Ground and homogenised	Acetone - methanol (1 + 1)	Dichloromethane	Florisil; Alumina: no clean-up for OPs and carbaryl	Diethyl ether - hexane; Dichloromethane	GC - FPD; HPLC - UV	31
Organophosphates	Unpolished rice	Ground and shaken for 10 min	Acetonitrile - water (1 + 1)	(1) Dichloromethane; (2) hexane	Removal of fats by zinc acetate addition; charcoal column	Acetonitrile - water (1 + 1)	GC	32
33 nitrogen and/or phosphate containing pesticides	Rice and rice straw		Methanol - acetone (1 + 1)	Hexane - acetonitrile	Amberlite XAD-2 (or 4) and Florisil and silica Sep-Pak cartridges		GC	33
Organophosphates	Wheat middling	Ground	Water - acetone (35 + 65)	Light petroleum	Florisil	Diethyl ether - light petroleum	HPLC - electro-chemical GC - FPD	34
Eight organophosphates	Grain	Ground and homogenised	Water - acetone (1 + 8)	Dichloromethane	Silica	Acetone - toluene - dichloromethane (1 + 1 + 5)	GC	35
Piperonyl butoxide	Cereal products		Light petroleum - diethyl ether				GC	36
Piperonyl butoxide	Rice, wheat, barley, soy-bean, rye, oats, red bean and corn	Ground	Hexane	Acetonitrile	None		HPLC - fluorimetric	37
Resmethrin	Wheat flour and cornmeal		Hexane	Acetonitrile	Alumina		GC	38
Resmethrin	Corn, cornmeal, flour and wheat	Ground wheat and corn	Pentane-saturated acetonitrile	Pentane	Florisil	Ethyl acetate - pentane (3 + 97)	GC - FID	39
Pyrethroids	Grain	Standing overnight; whole grain	Light petroleum (b.p. 30–40 °C)		TLC - silica	Benzene	GC	40
cis-trans-Permethrin	Grain, wheat, corn, cornmeal and flour	Ground and tumbled for 3 h	Pentane	Pentane-saturated acetonitrile	Alumina	Ethyl acetate - pentane (3 + 97)	GC - FID	41
cis-trans-Permethrin	Soy-beans, cottonseeds and others	Macerated	Hexane		Florisil and anhydrous sodium sulphate	Hexane - diethyl ether (9 + 1)	GC	42
Bioresmethrin	Wheat	Standing for 24 h	Acetone - hexane (1 + 3)		Alumina	Dichloromethane - hexane (3 + 7)	HPLC - UV	43
Fenvalerate	Cottonseeds	Blended then Soxhlet extraction for 18 h	Chloroform	Propylene carbonate	Florisil and sodium sulphate	Acetone - light petroleum (1 + 99)	GC	44
Bioresmethrin and piperonyl butoxide	Whole grain wheat	Whole wheat; standing	Hexane		None		GC	45

Table 1. Summary of extraction and clean-up procedures for grain protectants—*continued*

Pesticide	Sample	Extraction			Clean-up		Analysis mode	Reference
		Sample treatment	Solvent	Partitioning solvent	Column (or ether)	Eluent		
Permethrin, phenothrin, fenvalerate and deltamethrin	Wheat		Methanol	Hexane	Alumina	(1) Diethyl ether - hexane (1 + 10) for permethrin; (2) ethyl acetate - hexane (1 + 10) for others	HPLC - UV	46
Pyrethroids and natural pyrethrins	Wheat, soy-bean and corn		Acetonitrile	Hexane	Florisil		GC	47
Cypermethrin and fenvalerate	Wheat and milled fractions	Ground and shaken	Acetone hexane (1 + 1)	Hexane	Florisil	Benzene	GC - ECD	48
Cypermethrin	Crops including wheat and sorghum	Ground and macerated	Water - acetonitrile - hexane	Hexane	"Bond Elut" cartridge	*tert*-Butyl methyl ether - hexane (5 + 95)	GC - ECD	49
Carbofuran	Corn	Chopped, blended and stirred	Hydrolyse with hydrochloric acid (0.25 M)	Dichloromethane	Nuchar Attaclay	Dichloromethane - hexane - ethyl acetate (3 + 1)	GC	50
Aldicarb	Corn, green beans and other crops	Blended for 10 min	Acetone - dichloromethane (1 + 1)		Florisil	(1) Acetone - hexane (3 + 7); (2) acetone - hexane (1 + 1); (3) acetone	GC - FPD	51
Landrin	Corn	Blended	Acetonitrile	Hexane - diethyl ether (3 + 1)	Alumina	Hexane - diethyl ether (3 + 1)	GC - ECD	52
Propoxur	Corn, barley, rye, wheat, oats and other crops	Ground and blended	Acetone then chloroform	Hexane	Florisil	Chloroform	GC - ECD	53
Methyl carbamates as their 2,4-dinitrophenyl ether derivatives	Crops	Macerated	Acetonitrile	Light petroleum to acetonitrile to dichloromethane			GC	54
Carbamates	Corn, wheat and other crops	Blended	Acetone	Hexane - dichloromethane	Florisil	Acetone - hexane (15 + 85)	HPLC - UV	55
Carbamates	Hulled rice, and rice straw	Macerated	Water, isopropanol; acetone - methanol (1 + 1)	Coagulated with H_3PO_4 - NH_4Cl	Alumina - silver nitrate; Florisil		GC - NPD	56
Carbaryl	Wheat	Standing overnight	Acetone (1) Acetone; (2) acetone - methanol (3) acetone - ethyl acetate		None		GC	57
Eight carbamates	Hulled rice and rice straw						GC - NPD	58
Seven carbamates	Hulled rice and rice straw		Aqueous acetonitrile		(1) Alkyl(trichloro) silane cartridge; (2) Florisil or silica		GC	59
Carbaryl	Rice, wheat and jowar	Blended	Acetonitrile		Silica gel	Acetonitrile	Spectrophotometry	60
Carbaryl	Wheat	Whole; standing	Methanol		None	Ethyl acetate - hexane (3 + 7)	HPLC - UV	61
Bendiocarb	Corn	Blended	Ethyl acetate		Nuchar activated charcoal - Whatman CF-11 cellulose		GC	62

Therefore, for grain handlers, the main purpose of the analysis may be to distinguish instances of low levels of insecticide, where the grain is at risk of becoming infested with insects (hence, requiring rapid despatch to the miller), from higher levels that must be used in order to allow degradation of the insecticide. For such purposes, speed and cost are important considerations. In this context, straightforward procedures for clean-up and the consequent savings in space and expensive solvents, compared with those used in official procedures, cannot be ignored.

4. Gas Chromatographic Determination of Organophosphate, Pyrethroid and Carbamate Insecticides

Table 2 summarises the gas chromatographic methods available for the analysis of grain protectants; this table includes commodities other than grains and grain products and is intended to be of assistance where a single or multi-residue method, using GC, is required. The chromatographic conditions stated for many of the pyrethroid and organophosphate insecticides are relevant irrespective of the commodity that has been extracted prior to the analysis.

It is surprising that, despite the number of GC procedures available [employing different detectors, different types of columns (packed or capillary) and column variations] and their individual requirements and experience, their relative advantages are not often discussed. In our experience, the main disadvantages of gas chromatographic analysis are: (i) the lack of a published method for separating resmethrin and piperonyl butoxide; (ii) the relatively high detection limits of resmethrin and phenothrin; and (iii) the failure of multi-residue methods to include resmethrin, phenothrin and carbaryl.

Organophosphates

Many papers have been published covering the determination of organophosphates in grain and grain products using GC. In addition, the quantification of this class of pesticides has been comprehensively reviewed[91] and the nomenclature and chemical structures of the various organophosphates have been well documented.[91,92] Generally, the methods have been confined to GC[3,9,15,21,32] using packed columns and the more specific nitrogen - phosphorus or flame photometric detectors. As a rule, these two detectors reduce or eliminate the need for elaborate clean-up procedures with packed columns[15,17,18] but, of course, this depends on the level of co-extractives, the number of pesticides to be quantified and the required reporting level. Also, with these detectors, the high resolution of a capillary column is not usually required unless a multi-residue method is desired.[31,75] Stan and Goebel[93] have compared the reliability of on-column and splitless injection techniques for pesticide residue analysis.

Pyrethroids

Miyamoto[94] and Papadopoulou-Mourkidou[95] have both presented excellent reviews of the quantification of this class of insecticides. Although much work has been published dealing with the gas chromatographic determination of the pyrethroids, there have been few reports of their determination with capillary columns. Bottomley and Baker[31] have shown that the main advantages of using capillary columns for screening purposes are improved resolution and shorter analysis times.

It is worth noting that pyrethroids are usually more difficult to determine than the organophosphates because of their appreciably lower levels of application. Further, for two of the common pyrethroids, phenothrin and bioresmethrin, the determinations are even more difficult as these compounds do

not contain either a significant electrophore for the electron-capture detector (ECD) or nitrogen or phosphorous suitable for the thermionic or flame photometric detectors. Another problem is encountered with the compound resmethrin and the synergist piperonyl butoxide, which is often used in combination with pyrethroid grain protectants (hence, its inclusion in Table 2). The resolution of these two compounds (which have the same relative molecular mass) by GC on a packed column is difficult, if not impossible. Resmethrin, however, has been determined alone with a packed column using flame ionisation[39,76] and a mass spectrometer operated in the chemical ionisation mode.[45]

Unlike the organophosphate and carbamate insecticides, an unusual difficulty arises with the synthetic pyrethroids because these compounds (the structures and generic names of which have been well documented by several authors[83,94]) consist of a mixture of stereoisomers. With the exception of fenvalerate, all of the pyrethroids are esters of chrysanthemic acid and have two chiral centres at C-1 and C-3 of the cyclopropane ring, giving rise to four stereoisomers independent of chirality in the alcohol moiety. Hence, permethrin consists of four stereoisomers [namely, (1R, trans), (1R, cis), (1S, trans) and (1S, cis)] in which the cis to trans ratio varies depending on the method of synthesis. Whereas separation of these diastereoisomers is possible by GC on a packed column, the separation is more straightforward with capillary columns.

The cis and trans isomers of permethrin can be separated on a packed column[39,41,42] or can be co-eluted depending on the requirements.[96] Chapman and Harris[82] have reported the separation of the enantiomers of permethrin and cypermethrin on a non-chiral phase after conversion into the diastereoisomers.

Carbamates

Several workers have reviewed comprehensively the determination of carbamate pesticides.[97-100] Others[101-105] have chosen to determine a derivative of the carbamates as this approach provides the opportunity and advantages of introducing a strong electrophore into the resulting derivative, with improved sensitivity using the ECD. Wallbank[57] has reported the use of an in situ derivatisation method.

Of the carbamates, carbaryl has always been more difficult to determine by GC because of its thermal instability. However, it can be determined directly[87] at relatively high levels or, with excellent sensitivity and no decomposition,[88,89] by using Carbowax 20M on modified supports. Nevertheless, the degradation of carbaryl to α-naphthol has always been a problem when using packed columns. Capillary GC seems to be the method of choice but the mode of injection is critical. Splitless injection requires very high injection port temperatures, which obviously promote decomposition; however, Ripley and Braun[106] reported very little decomposition of N-methylcarbamates using this technique. Wehner and Seiber[90] have reported a direct determination by using split injection with an NPD. The increased flow through the injection port together with split injection ensures that the residence time at the high temperature is decreased. However, sensitivity is lost through splitting the sample. On-column injection would seem to be the solution as direct injection into a cooled column followed by slow temperature programming of the column oven would then avoid the thermal shock associated with split or splitless methods. The use of supercritical fluid chromatography for the determination of thermally labile compounds, such as carbaryl, or involatile compounds, has also been described.[107]

Packed versus Capillary Column Gas Chromatography

There are occasions when a packed column can be an advantage because of the retention of involatile co-extractives

Table 2. Summary of gas chromatographic methods for the determination of grain protectants

Pesticide	Sample	Column(s)	Conditions	Detector	Reference
Malathion	Wheat	Glass, 5 ft × 0.125 in o.d. with 5% QF-1 on 60/80 Diatoport H.M.D.S.	N_2 carrier gas, 60 ml min⁻¹; isothermal, 195 °C	CsBr - alkali FID	6
Malathion and dichlorvos	Wheat	Glass, 1.83 m × 4 mm i.d. with 15% silicone gum MS 2211 on 80–100 Gas-Chrom Q	N_2 carrier gas, 26 ml min⁻¹; isothermal, 210 °C	KCl - thermionic detector	7
Malathion and its hydrolytic products	Stored grain	(1) Glass, 6 ft with 3% DC-11 on 60–80 mesh silanised Gas-Chrom P; (2) glass, 5 ft × 0.125 in with 5% QF-1 on 100–120 mesh Aeropack 30	(1) N_2 carrier gas, 36 ml min⁻¹; isothermal, 200 °C; (2) N_2 carrier gas, 20 ml min⁻¹, isothermal, 175 °C	(1) ECD; (2) phosphorus detection	8
Dichlorvos	Crops including cereal grains	Glass, 1 m × 3 mm i.d. with 10% phenyl-diethanolamine succinate on 100–120 Gas-Chrom Q	Isothermal, 140 °C	ECD, FPD or thermionic detectors	9
Dichlorvos and malathion	Wheat	Glass column, 1.5 m × 3 mm i.d. with either (1) Apiezon L (1.3%) and Epikote (0.1%) on 100–120 AW- Chrom G or (2) butane-1,4-diol succinate (1.3%) and Epikote (0.1%) on the same solid support as (1)	N_2 carrier gas, 15–20 ml min, isothermal, 220 °C for malathion; isothermal, 190 °C for dichlorvos	CsBr thermionic detector	10
Organophosphates	Non-fatty foods	Glass column, 6 ft × 4 mm i.d. with either (1) 2% DEGS on 80–100 Gas-Chrom Q or (2) 6% DC-200 on 80–100 Chromosorb W (HP)	Not stated . . .	KCl thermionic detector; FPD	11
Dichlorvos and malathion	Grain	Collaborative study: 19 columns used	N_2 carrier gas; all conditions are isothermal	Thermionic and FPD	12
15 organophosphates	Wheat	Glass, 6 ft × 3.5 mm i.d. with either (1) 4% SE-30 - 6% QF-1 on 60–80 Chrom W (AW and DMCS) or (2) 3% OV-1 on 60–80 Chrom W (AW and DMCS)	N_2 carrier gas, 80 ml min⁻¹; isothermal, 180 °C	FPD	15
Dichlorvos	Grain	Glass, 1.5 m × 3.0 mm i.d. packed with either (1) 10% DC-200 on Gas-Chrom Q or (2) neopentylglycol succinate on Chromosorb G	N_2 carrier gas: (1) 60 ml min⁻¹; (2) 50 ml min⁻¹; isothermal: (1) 180 °C; (2) 150 °C	FPD	70
Malathion, tetrachlorvinphos and fenitrothion	Paddy, wheat, sorghum, milled products and cooked products	Glass, 6 ft × 2 mm i.d. packed with 1.5% OV-225 on Chrom W	N_2 carrier gas, 14–40 ml min⁻¹; isothermal, 210 °C	CsBr alkali FID	14
Organophosphates	Fruit and vegetables	Five columns used including (1) DEGS and (2) OV-101, all on 80–100 Chrom W (HP), glass, 6 ft × 4 mm i.d.	N_2 carrier gas, 60–120 ml min⁻¹; isothermal, 200 °C	KCl thermionic detector	71
11 organophosphates	Rice and wheat	Five sets of columns including (1) DC-200 + OV-17 and (2) DEGS + H_3PO_4	N_2 carrier gas, 1.0 kg cm⁻²; isothermal, 180 or 190 °C	FID	16
Fenitrothion	Soy-beans and others	1.5 m × 4 mm glass column with 10% silicone DC-200 and 20% silicone DC QF-1 (1 + 1) on Chromosorb W (AW-DMCS) 60–80 mesh	Helium carrier gas, 50 ml min⁻¹; isothermal 210 °C	FPD	72
Dichlorvos and malathion	Grain dust	5% NPGS on Chromosorb W 80–100 mesh	N_2 carrier gas, 70 ml min⁻¹; 180 °C (1 min) . . . ramp . . . 240 °C	Phosphorus - FPD	17
Five organophosphates	Wheat	DC-200 or OV-101	Not stated	Specific phosphorus detector	18
Organophosphates	Fruit and vegetables	Various columns recommended including (1) 3 or 5% OV-17 with Epikote 1001 (0.02%) on 60–80 Gas-Chrom Q and (2) glass column with 1.3% Apiezon L on 80–100 AW-Chrom G	(1) 130 °C for dichlorvos; (2) 210–250 °C for others	Alkali FID; FPD; ECD	73
Etrimfos	Corn and alfalfa	1 m × 4 mm i.d. glass column with 5% OV-101 on 80–100 Gas-Chrom Q	N_2 carrier gas, 160 ml min⁻¹ (FPD); isothermal, 160 °C (FPD)	ECD - ⁶³Ni; FPD : NPD	19
Nine organophosphates	Grain	5% OV-17 (0.02%); Epikote 1001 (0.02%)	Not stated	Thermionic	21

Table 2. Summary of gas chromatographic methods for the determination of grain protectants—*continued*

Pesticide	Sample	Column(s)	Conditions	Detector	Reference
Organophosphates	Fruit and vegetables	Glass column, 1.8 m × 3 mm i.d. with (1) 2% DC-200 + 3% QF-1; (2) 1.5% OV-17 + 1.95% QF-1; (3) DC-200 all on 80–100 Gas-Chrom Q	N_2 carrier gas, 40 ml min^{-1}; isothermal, 160–220 °C	Rb_2SO_4 thermionic	74
Methidathion and its monoxone metabolites	Safflower seed, meal and oil	(1) Glass column, 1.8 m × 2 mm i.d. with 10% SE-30 on 80–100 Gas-Chrom Q; (2) glass, 1.06 m × 2 mm i.d. with 12% SE-30 on 80–100 Gas-Chrom Q (for the oil)	N_2 carrier gas, 40 ml min^{-1}; isothermal, 210–215 °C	FPD	22
Malathion and an alteration product	Rice	(1) 5% OV-101 + 7.5% OV-210; (2) 5% OV-101 both 2 m × 4 mm i.d. glass with 80–100 Gas-Chrom Q	Isothermal, 200 °C	FPD: mass spectrometry	25
Organophosphates	Standards	14.5 m × 0.25 mm WCOT OV-1	Hydrogen carrier gas, 0.2 bar; 115 °C . . . 4 °C min^{-1} . . . 190 °C then 8 °C min^{-1} up to 260 °C	NPD	75
Dichlorvos, trichlorfon and methomyl	Hulled rice and rice straw	Glass capillary columns	NA*	Thermionic detector	28
Fenitrothion and its metabolites	Wheat	1.5 m × 4 mm i.d. glass column with either 5% OV-101 or 3% OV-225 on Chromosorb W HP 80/100	N_2 carrier gas, 40 ml min^{-1}; FPD - isothermal, 80, 120 or 175 °C; ECD - isothermal, 140 °C	FPD and ^{3}H-ECD	27
Organophosphates	Unpolished rice	Glass, 2 m × 3 mm i.d., with 10% DC-200 on 60–80 Chromosorb (AW and DMCS)	N_2 carrier gas, 50 ml min^{-1}; isothermal, 210 °C	FPD	32
33 nitrogen and/or phosphate containing compounds	Rice and straw rice	Fused silica capillary columns	NA*	Thermionic detector	33
Eight organophosphates	Grain	2 m × 4 mm i.d. glass column with 10% OV-17 on Gas-Chrom Q	Not stated	FPD and thermionic detectors	35
Synthetic pyrethroids and organophosphates	Grain	(1) 25 m × 0.23 mm i.d. WCOT fused-silica with OV-101, film thickness 0.12 μm; (2) OPs - 3% OV-225 on Gas-Chrom Q (80–100 mesh) 1 m × 4 mm i.d. glass column	(1) Capillary: Ar - CH$_4$ (9 + 1), 1.0 ml min^{-1}; pyrethroid temperature programme: 60 °C (2 min) . . . 30 °C min^{-1} . . . 215 °C (55 min); OPs: 100 (10) 3 °C min^{-1} 195 (15); spitless injection (30 s); make up gas, Ar - CH$_4$ (9 + 1) 20 ml min^{-1} (2) Packed column: N_2, 50 ml min^{-1}; temperature programme: 130 °C (2 min) . . . 10 °C min^{-1} . . . 220 °C (2 min)	OPs: FPD; pyrethroids: ECD	31
Resmethrin	Corn, cornmeal flour and wheat	Stainless-steel 183 cm × 4 mm o.d. with 10% UC-W 98 on 80–100 Chromosorb W (HP)	N_2 carrier gas, 86 ml min^{-1}; isothermal, 245 °C	FID	76
Pyrethroids	Grain	Not stated	Not stated	FID	40
Permethrin	Potatoes	Glass, 1.2 m × 2 mm i.d. with 3% SE-30 on 60–80 mesh Gas-Chrom Q	N_2 carrier gas, 70 ml min^{-1}; isothermal, 195 °C	^{63}Ni - ECD	77
cis- and trans-Permethrin	Grain and grain products	Glass, 122 cm × 4 mm i.d. with 5% OV-225 on 80–100 Gas-Chrom Q	N_2 carrier gas, 28 ml min^{-1}; isothermal, 250 °C	FID	41
Four pyrethroids	Standards	Glass column, 120 cm × 4 mm i.d. with 5% OV-101 on 100–200 Gas-Chrom Q	N_2 carrier gas, 70 ml min^{-1}; isothermal, 230 °C	^{63}Ni - ECD	78
Fenvalerate	Cabbage	0.5 m × 2 mm stainless-steel with 3% OV-101 + 3% Apiezon L on 80–100 mesh Gas-Chrom Q	N_2 carrier gas, 60 ml min^{-1}; isothermal, 225 °C	^{3}H - ECD	79

Table 2. Summary of gas chromatographic methods for the determination of grain protectants—*continued*

Pesticide	Sample	Column(s)	Conditions	Detector	Reference
cis- and *trans*-Permethrin	Soy-beans, cotton-seeds and others	Glass column, 6 ft × 2 mm i.d. with 1% SP-2330 on Supelcoport 80–100 mesh	N_2 carrier gas, 20 ml min^{-1}; isothermal, 215 °C	^{63}Ni - ECD; Coulson electrolytic conductivity detector (halogen mode)	42
Deltamethrin	Vegetable products	(1) DC-200; (2) OV-101; (3) OV 1 all on Chromosorb AW DMCS	Isothermal, 245 °C	^{63}Ni-ECD	80
Fenvalerate	Cabbage and lettuce	1.8 m × 2 mm glass column packed with either (1) 5% OV-101 on 80–100 Chromosorb W or (2) 4% SE-30 - 6% QF-1 on 100–200 Chromosorb W	Ar - CH$_4$ (95 + 5) carrier gas: (1) 60 ml min^{-1}; (2) 45 ml min^{-1}; isothermal, 225 °C	^{63}Ni-ECD	81
Enantiomers of cypermethrin and permethrin; conversion into diastereoisomers	Standards	60 cm × 4 mm i.d. packed with 2.5% OV-210 on Varaport 30 (100–120 mesh)	Ar - CH$_4$ (95 + 5) carrier gas; isothermal, 125 °C	^{63}Ni - ECD	82
Piperonyl butoxide	Cereal products	10% SE-30 on Chromosorb W	NA*	FID	36
Allethrin, resmethrin and permethrin	Standards	6 ft × 3 mm i.d. glass, 10% SILAR-10-C on Gas-Chrom Q, 100–200 mesh	N_2 carrier gas, 35 ml min^{-1}; isothermal, 250 °C	FID	39
Fenvalerate	Grapes, peppers, apples and cotton-seeds	Glass column, 1.1 m × 2 mm i.d. with 2% XE-60 on 80–100 Supelcoport	N_2 carrier gas, 30 ml min^{-1}; isothermal, 215 °C	^{3}H-ECD	44
Bioresmethrin and piperonyl butoxide	Whole grain wheat	Glass column, 1.5 m × 2 mm i.d. with OV-101 on Gas-Chrom Q (60–80)	CH$_4$ carrier gas, 20 ml min^{-1}; isothermal, 230 °C	Chemical ionisation mass spectrometry	45
Permethrin, cypermethrin and fenvalerate	Celery and animal products	1.8 m × 2 mm i.d. Pyrex packed Ultra-Bond 20M	N_2 carrier gas, 20 ml min^{-1}; isothermal, 240 °C	^{63}Ni - ECD	83
Nine synthetic pyrethroids	Fruit and vegetables	(1) Glass column, 1 m × 4 mm i.d., 3% OV-7 on Gas-Chrom Q 80–100 mesh; (2) 25 m × 0.23 mm fused silica, WCOT OV-101, thickness 0.12 μm	(1) Isothermal, 235 °C; N$_2$ carrier gas, 50 ml min^{-1}; (2) splitless injection (30 s); N$_2$ carrier gas, 1.0 ml min^{-1}; 50 °C (2 min) . . . 25 °C min^{-1} . . . 210 °C (80 min)	^{63}Ni - ECD; make-up gas for capillary: Ar - CH$_4$ (9 + 1); 20 ml min^{-1}	84
Deltamethrin	Biological samples	1 m × 4 mm i.d. packed with 3% SE-30 on 80–100 Chromosorb W HP	Ar - CH$_4$ (95 + 5), 35 ml min^{-1}; isothermal, 260 °C	^{63}Ni - ECD	85
Pyrethroids and pyrethrins	Wheat, soy-bean and corn	(1) 2% XE-60 + 2% OV-17; (2) SE-30	(1) 215 or 210 °C; (2) 210 °C	ECD	47
Cypermethrin, fenvalerate	Wheat and milled fractions	Glass, 0.6 m × 4 mm i.d. with 3% OV-210 on Gas-Chrom Q 90–100 mesh	N$_2$ carrier gas, 80 ml min^{-1}; isothermal, 200 °C	^{3}H - ECD	48
Cypermethrin	Crops	Fused silica (FSOT) 25 m × 0.32 mm i.d. SE-54 (0.5-μm film thickness)	Helium carrier gas, 1.5 ml min^{-1}; 40 °C . . . 20 °C min^{-1} . . . 180 °C . . . 1 °C min^{-1} . . . 250 °C; splitless injection	ECD	49
Fenvalerate, permethrin, cypermethrin and deltamethrin	Fruit and vegetables	50 cm × 3 mm i.d. stainless-steel column with 5% OV-101 on 100–120 mesh Gas-Chrom Q	N$_2$ carrier gas, 100 ml min^{-1}; isothermal, 240 °C	^{63}Ni - ECD	86
Carbofuran	Corn	2 ft × 0.25 in o.d. aluminium packed with 3.5 g of 20% SE-30 on 60–80 Gas-Chrom Z	H$_2$ carrier gas, 20 p.s.i. at inlet; isothermal, 165 °C	Dohrmann micro-coulometric nitrogen detector	50
Carbaryl (direct chromatography)	Standard	0.5–2% Apiezon L on SE-30 on 100–120 mesh silanised Gas-Chrom P 2 m × 3 mm i.d. glass column	150–170 °C	KCl-treated thermionic FID	87

Table 2. Summary of gas chromatographic methods for the determination of grain protectants—*continued*

Pesticide				Sample	Column(s)	Conditions	Detector	Reference
Methyl-carbamates as their 2,4-dinitrophenyl ether derivatives	..	..		Crops	18 in × 0.25 in o.d. glass column with 10% DC-200 on 60–70 Anakrom ABS	N_2 carrier gas, 60 ml min^{-1}; isothermal, 212 °C	^{3}H - ECD	54
Carbaryl (direct chromatography)	..	..		Standards	Glass, 174 cm × 2 mm i.d. with 60–80 acid-washed Chromosorb W, surface modified with Carbowax 20M	N_2 carrier gas, 7.2 cm s^{-1} (10 ml min^{-1}); isothermal, 183 °C	(1) FID; (2) Rb_2SO_4 FID	88
Organophosphates and carbaryl	..	..		Wheat, barley, oats, sorghum and rice	(1) OPs: 4% SE-30–6% SP2401 on Chrom W, 100–120; (2) carbaryl: 5% SE-30 on Chromosorb W 60–80; detected as 2-chloroacetylnaphth-1-ol	N_2 carrier gas, 70 ml min^{-1}; (1) ranging from 150 °C for dichlorvos to 210 °C for fenitrothion; (2) 175 °C for carbaryl	(1) FPD; (2) ECD	3
Carbamates	..	..		Standards	Glass, 6 ft × 2 mm i.d. silanised Carbowax 20M - modified support	Helium carrier gas, 25 ml min^{-1}; temperature programme: 110 °C . . . 10 °C min^{-1} . . . 185 °C	Hall electrolytic conductivity detector	89
Carbaryl	..	..		Wheat	50 mm reaction bed of KOH-treated glass beads at 215 °C, which formed the initial part of the column of 1.8 m × 2 mm i.d. with 100–200 Porapak PS	N_2 carrier gas, 31 ml min^{-1}; isothermal, 200 °C; detected as N-methylcarbamate	Rb_2SO_4 alkali FID	57
Eight carbamates	..	..		Hulled rice and rice straw	Glass capillary, 25 m × 0.3 mm i.d. with SP-2100 silicone OV-1	NA*	Thermionic detector	58
N-Methyl-carbamates	..	..		Standards	18 m × 0.31 mm i.d. FSOT SE-52	Helium carrier gas, linear velocity 46 cm s^{-1}; split ratio 86 : 1; temperature programme: 170 °C (0 min) . . . 4 °C min^{-1} . . . 190 °C (2 min)	FID	90
Seven carbamates	..	..		Hulled rice and rice straw	Glass capillary columns	NA*	Nitrogen-sensitive detection	59

* NA = information not available.

Table 3. Summary of high-performance liquid chromatographic methods for the determination of grain protectants

Pesticide				Sample	Column	Mobile phase*	Approximate analysis time/min	Detector	Reference
Etrimphos and its degradation products	..	..		Corn and alfalfa	μBondapak C-18	Water - methanol (60 + 40) (1.0 ml min^{-1})	8	UV at 254 nm	19
Organophosphates	..	..		Wheat middling	C-18 (various brands)	Methanol - 0.1 M NaOH	20	Electrochemical after in-line photolysis	34
Ethyl and methyl parathion				Green vegetables	5-μm Regis octadecyl	Acetonitrile - aqueous electrolyte, such as KCl, CH_3COOK (1.0 ml min^{-1})	10	UV at 270 nm; electrochemical	120
Coumaphos, ethyl azinphos and trichlorfon	..	..		Cabbage and tomatoes	5-μm LiChrosorb RP-18	Methanol - water (80 + 20) (30–40 μl min^{-1})	8	UV at 254 nm; thermionic detector	121
Piperonyl butoxide	..	..		Rice, wheat, barley, rye, oats, corn and beans	Hitachi: Gel 3010	Ethanol (1.0 ml min^{-1})	5	Fluorimetry	37
Permethrin	..	..		Cotton	(a) Whatman Partisil ODS (column 40 °C)	Methanol - water (65 + 35) (1 ml min^{-1}); heptane - acetonitrile (999 + 1) (1.6 ml min^{-1})	20	UV at 254–280 nm	122
					(b) Brownlee Labs. Si-5A				
Bioresmethrin	..	..		Wheat	Spherisorb 5 10 W	Propanol - hexane (3 + 997) (1 ml min^{-1})	4	UV at 220 nm	122
Pyrethroids	..	..		Wheat	μBondapak C-18	Methanol - water (80 + 20) (2.5 ml min^{-1})	NA†	UV at 225 nm	43
Permethrin	..	..		Lettuce	5-μm Partisil	1-Tetradecane - dichloromethane - cyclohexane (3 + 70 + 27) (0.9 ml min^{-1})	15	UV at 235 nm	46
							10	Infrared; UV at 254 nm	123

Table 3. Summary of high-performance liquid chromatographic methods for the determination of grain protectants—*continued*

Pesticide	Sample	Column	Mobile phase*	Approximate analysis time/min	Detector	Reference
Pyrethroids and carbaryl ..	Barley and wheat	5-μm Spherisorb ODS; 5-μm Spherisorb silica	Methanol - water (80 + 20); 2,2,4-trimethylpentane - propan-2-ol (90 + 10)	up to 30; 10	UV at 206 nm; UV at 224 nm	31
Carbamates	Cabbage, corn, potatoes and wheat	5-μm LiChrosorb Si 60	Propan-2-ol - isooctane (5 + 95) (0.5–1.0 ml min⁻¹)	up to 12	UV at 254 nm	55
Carbofuran and its metabolites ..	Carrots, cabbage, corn, peas, potatoes and turnips	5-μm LiChrosorb Si 60	Propan-2-ol - trimethylpentane (3 + 97) to (8 + 92) (1.0 ml min⁻¹)	up to 12	UV at 254 nm; UV at 280 nm	124
Cabofuran and its metabolites ..	Vegetables	μBondapak C-18 RCSS C-8 Radial Pak	Methanol - water (30 + 70) to (50 + 50) (1.0–2.0 ml min⁻¹)	10	UV at 200 or 203 nm	125
Carbaryl	Potato and corn	5-μm Lichrosorb Si 60	Propan-1-ol - trimethylpentane (4 + 96) (1.0 ml min⁻¹)	6	UV at 254 or fluorescence detection of dansyl derivative	126
Carbofuran and its metabolites ..	Carrots, corn and potatoes	5-μm LiChrosorb Si 60	Acetone - 2,2,4-trimethylpentane (3 + 97) to (15 + 85) (0.8–1.8 ml min⁻¹)	up to 30	Fluorimetry (of dansyl derivative)	127
Carbamates	Fruit and vegetables	(1) Nucleosil-Nitril, 5 μm; (2) LiChrosorb-Diol, 10 μm; (3) LiChrosorb Si 100, 10 μm	2,2,4-Trimethylpentane - dioxane (9 + 1) (1–1.25 ml min⁻¹)	30	UV (wavelength varied depending on pesticide)	128, 129
Carbamates.	Vegetables	μBondapak C-18	Methanol - water (20 + 80) to (55 + 45) (20 min programme) (1.6 ml min⁻¹)	30	Fluorimetry (post-column derivatisation)	130
Carbamates	Fruit and vegetables	LiChrosorb Si 60	2,2,4-Trimethylpentane - dioxane: (1) 97 + 3; (2) 76 + 24 (6 ml min⁻¹)	up to 40	UV at 254 nm	131
Carbofuran and 3-hydroxy-carbofuran ..	Rape plants	Spherisorb ODS	Methanol - water (20 + 80) to (30 + 70) (1.0 ml min⁻¹)	10–20	UV at 280 nm	132
Carbamates, piperonyl butoxide and organo-phosphates ..	Fruit and vegetables	6-μm Zorback C-8 (heated to 35 °C)	Acetonitrile - water (12 + 88) to (70 + 30) (30 min gradient) (1.5 ml min⁻¹)	30	Fluorimetry (post-column labelling)	24
Aldicarb and its degradation products ..	Potatoes	10-μm LiChrosorb RP-18 or μBondapak C-18	Acetonitrile - pH 7.6 buffer; (4 + 96) for metabolites; (30 + 70) for aldicarb (2.0 ml min⁻¹)	20	UV at 220 nm for metabolites; UV at 247 nm for aldicarb	77
Carbaryl and organo-phosphates ..	Fruit and vegetables	Waters Radpak A (ODS 10 μm)	Acetonitrile - water (60 + 40) (1.5 ml min⁻¹)	NA†	UV at 280 nm	133
Carbaryl	Wheat	Whatman Partisil 5	Hexane - ethanol (90 + 10) (1.5 ml min⁻¹)	5	UV at 280 nm	61

* Flow-rate given in parentheses.
† NA = information not available.

either in a glass-wool plug or in the first few centimetres of the column. Capillary columns, by the very nature of their open tubular design, will not prevent material of low volatility from eventually reaching the detector. It can be concluded that it is far easier to change the glass-wool every few hundred injections than to clean a detector; this is particularly true when the ECD is used.

Undoubtedly, the effect of involatile material (or material of low volatility) in a quantitative procedure is a concern. By employing splitless injection, Grob and Bossard[108] have demonstrated the dramatic detrimental effect on quantification of injecting standards containing involatile material compared with the injection of "clean" standards. This effect has been confirmed by Ripley and Braun[106] who injected extracts containing a high lipid content. Hence, it is plausible that solute transfer from the injector to the column is affected more by "dirty" samples and, although clean samples are to be preferred when using the Grob splitless injection method, direct injection of extracts is possible provided that the effect of any co-extractives on the transfer of solute into the column is carefully studied. Grob and Neukom[109] have also shown that use of a light plug of silanised glass-wool in the injector insert improves the quantification of a sample containing involatile material. Similar effects were reported by Zenon-Roland et al.[110] for the adsorption of polar pesticides when using on-column injection after injection of crop extracts. Again, with on-column injection, it is necessary to be aware of the effect of co-extractives on the peak shape and the quantification of solutes. Of course this can be expected to vary from one commodity to another and to depend on the lipid content of the commodity.

Generally, there is a trend towards the use of capillary columns for pesticide residue analysis, where the shorter analysis times and enhanced resolution are very attractive features. However, the packed column is still an option if only a small number of pesticides are to be determined with specific detectors which, as mentioned earlier, can sometimes eliminate the need for a clean-up step.

Multi-residue Analysis

Multi-residue analyses are included in Table 2 for both pyrethroid and organophosphate pesticides in various commodities. Ambrus and Thier[111] have presented an excellent review of the use of multi-residue procedures in pesticide residue analysis. In addition, several multi-residue methods are available[112,113] for the determination of organophosphates in various commodities. For this type of work, the resolution attainable with capillary columns is invaluable. For example, using capillary column GC - ECD, Bottomley and Baker[31] have reported a method that can be used to screen most of the currently used pyrethroid and organophosphate insecticides. Unfortunately, the lack of response of resmethrin and phenothrin is a problem in this screening method. In other work, aided by automated data processing, Goebel and Stan[114] demonstrated the power of capillary columns for multi-residue analysis by diverting the effluent from one column to two detectors (NPD and ECD) and then confirming the identification on another column of different polarity. Several papers have described the behaviour and relative retention of the organophosphates on various phases for either packed or capillary columns under specified conditions.[106,115–119]

5. High-performance Liquid Chromatographic Determination of Organophosphate, Pyrethroid and Carbamate Insecticides

Table 3 lists published methods which use high-performance liquid chromatography (HPLC) for the analysis of pesticide residues in grain and other low-fat products, such as fruits and vegetables. The latter have been included because, with appropriate modification, these methods may also be applicable to grains.

The majority of the reports are concerned with carbamates. Of these, carbaryl has been studied fairly extensively,[31,61,126,133] probably as a result of the difficulty of determining this thermally labile compound by GC. Conversely, there are few reports concerning the organophosphates,[19,34,120,121] probably because these can easily be determined by using GC coupled with a phosphorus-specific detector. A number of other reports deal with the pyrethroids[43,46,122,123] and piperonyl butoxide.[37]

A major problem in using HPLC for residue analysis has been the lack of a highly selective or sensitive detector. In an attempt to overcome this problem, Papadopoulou-Mourkidou et al.[123] used on-line infrared detection for the determination of permethrin (in lettuce); other techniques used have included electrochemical detection for organophosphates[34,120] and the application of GC detectors to liquid chromatography.[121] A cholinesterase inhibition autoanalyser has also been used for the determination of organophosphates and carbamates.[134] Fluorescence detection has been applied frequently, either directly[37] or through the use of derivatives.[126,127] So far, none of these options has gained widespread acceptance; hence the UV spectrophotometer is still the most common detector employed for residue analysis by HPLC.

The reports cited in Table 3 are fairly evenly divided between reversed-phase and normal-phase methods. In most instances a clean-up procedure was employed prior to injection of the sample into the HPLC system. However, in some instances a second column was used for on-line clean-up, as in the work of Fogy et al.[128,129] who used two normal-phase columns to separate carbamates from plant co-extractives. On the other hand Gunew[43] used a pre-column for the separation of bioresmethrin from the co-extractives of wheat. In this instance, the co-extractives were trapped at the beginning of the pre-column and removed by back-flushing after the bioresmethrin had been eluted. Hargreaves and Melksham[61] used a similar method for the determination of carbaryl on wheat. Obviously, this approach saves both time and materials in clean-up operations; the use of column-switching (a further refinement of this approach) has recently[135] been reviewed.

Many of the methods summarised in Table 3 are multi-residue procedures, but most only deal with one class of pesticide, such as the carbamates.[131] Only in a few instances have several classes of pesticide been determined using one system[24,133] or has HPLC been used in combination with GC for multi-residue analysis.[31]

Overall, although it lacks a sensitive and specific detector (such as the NPD), HPLC still offers some unique (and, arguably, minor) advantages for residue analysis. These advantages include its suitability for the carbamates and the possibility of determining all pyrethroids with a single detector at one wavelength. Pyrethroid enantiomers have also been separated using HPLC.[136] HPLC can also incorporate either reversed- or normal-phase modes, each with the possibility of on-line clean-up. In fact, it can be said that the use of reversed-phase HPLC, with its potential for the direct injection of "dirty" extracts in water-miscible solvents and for on-line clean-up, has not been fully realised for this type of analysis. It seems, too, that the potential of HPLC for multi-residue analysis has also not been fully exploited.

6. Conclusion

In retrospect, determination by GLC is relatively straightforward for the organophosphates using a specific phosphorus-sensitive detector, or for halogenated pyrethroids using an ECD. In contrast, HPLC has both advantages and disadvantages compared with GLC. The main advantages are the

determination of all pyrethroids at a single wavelength (e.g., 230 nm), compared with the need for two detectors with GLC (ECD and the flame ionisation detector), and the determination of the thermally unstable carbaryl. However, sensitivity in HPLC is relatively low and problems may arise in the determination of insecticides in oil-rich commodities. Further advantages may be obtained from studies based on reversed-phase HPLC, in addition to those on normal-phase HPLC. This is particularly true when the extracting solvent is miscible with water, as analysis by reversed-phase HPLC may then be possible without clean-up. Both HPLC and capillary GLC show potential for use in studies of the degradation products of insecticides such as phenols or dimethylthiophosphoric acids.

In our opinion, future studies of analytical methodology should concentrate on those aspects that are concerned with new applications of capillary column gas - liquid chromatography, simplified clean-up procedures, particularly for HPLC and the ECD, and multi-residue methods. As priorities for work on the determination of insecticides on other commodities, we would nominate maize, rice and their products because of their importance in the diet and the relative lack of information available compared with wheat. Oil-seeds and legumes may also need to be examined. As for the fate of residues on, for example, wheat, there is still a need to determine residues in milled products (e.g., flour, germ and bran), processed products (e.g., noodles and deactivated bran) and cooked products (e.g., bread and boiled noodles). Ideally, each step of the analytical procedure would be assessed on the individual products using aged residues, bearing in mind that a solvent suitable for the extraction of insecticides from wheat may not necessarily be suitable for a wet product such as bread, or that a clean-up procedure satisfactory for wheat may be unsuitable for the oily wheat-germ. Clearly, a balanced judgement is needed involving the ultimate end-use of the analytical information and the best and cheapest means of obtaining it.

7. References

1. Snelson, J. T., "Grain Protectants," Australian Centre for International Agricultural Research, Canberra, 1987.
2. Bowman, M. C., Beroza, M., and Leuck, D. B., J. Agric. Food Chem., 1968, **16**, 796.
3. Desmarchelier, J., Nippon Noyaku Gakkaishi, 1980, **5**, 521.
4. Gunther, F. A., Adv. Pest Control Res., 1962, **5**, 191.
5. Watts, R. T. R., and Storherr, R. W., J. Assoc. Off. Anal. Chem., 1965, **48**, 1158.
6. Elms, K. D., J. Stored Prod. Res., 1967, **3**, 393.
7. Minett, W., and Belcher, R. S., J. Stored Prod. Res., 1969, **5**, 417.
8. Kadoum, A. M., J. Agric. Food Chem., 1969, **17**, 1178.
9. Elgar, K. E., Marlow, R. G., and Mathews, B. L., Analyst, 1970, **95**, 875.
10. Crisp, S., and Tarrant, K. R., Analyst, 1971, **96**, 310.
11. Storherr, R. W., Ott, P., and Watts, R. R., J. Assoc. Off. Anal. Chem., 1971, **54**, 513.
12. Committee for Analytical Methods for Residues of Pesticides and Veterinary Products in Foodstuffs of the Ministry of Agriculture, Fisheries and Food, Analyst, 1973, **98**, 19.
13. Saha, M., Summer, A. K., and Saha, J. G., J. Assoc. Off. Anal. Chem., 1973, **56**, 45.
14. Lockwood, L. M., Majumder, S. K., and Lineback, D. R., Cereal Sci. Today, 1974, **19**, 330.
15. Levi, I., and Nowicki, T. W., J. Assoc. Off. Anal. Chem., 1974, **57**, 924.
16. Aoki, Y., Takeda, M., and Uchiyama, M., J. Assoc. Off. Anal. Chem., 1975, **58**, 1286.
17. Desmarchelier, J. M., and Hogan, J. P., Aust. J. Exp. Agric. Anim. Husb., 1977, **18**, 453.
18. Desmarchelier, J., Bengston, M., Connell, M., Minett, W., Moore, B., Phillips, M., Snelson, J., Sticka, R., and Tucker, K., Pestic. Sci., 1977, **8**, 473.
19. Bowman, M. C., Holder, C. L., and Rushing, L. G., J. Agric. Food Chem., 1978, **26**, 35.
20. Mestres, R., Atmawijaya, S., and Chevallier, C., Ann. Falsif. Expert. Chim., 1979, **72**, 577.
21. Committee for Analytical Methods for Residues of Pesticides and Veterinary Products in Foodstuffs and the Working Party on Pesticide Residues of the Ministry of Agriculture, Fisheries and Food, Analyst, 1980, **105**, 515.
22. Winterlin, W., Whitehead, E., and Mourer, C., J. Assoc. Off. Anal. Chem., 1980, **63**, 1105.
23. Krause, R. T., J. Assoc. Off. Anal. Chem., 1980, **63**, 1114.
24. Krause, R. T., and August, M., J. Assoc. Off. Anal. Chem., 1983, **66**, 234.
25. Hansen, L. B., Castillo, G. D., and Biehl, E. T., J. Assoc. Off. Anal. Chem., 1981, **64**, 1232.
26. Ambrus, A., Lantos, J., Visi, E., Csatlos, I., and Sarvari, L., J. Assoc. Off. Anal. Chem., 1981, **64**, 733.
27. Abdel-Kader, M. H. K., and Webster, G. R. B., Int. J. Environ. Anal. Chem., 1982, **11**, 153.
28. Nishijima, O., Noyaku Kensasho Hokoku, 1982, **22**, 28.
29. Sawyer, L. D., J. Assoc. Off. Anal. Chem., 1982, **65**, 1122.
30. Luke, M. A., and Doose, J. M., Bull. Environ. Contam. Toxicol., 1983, **30**, 110.
31. Bottomley, P., and Baker, P. G., Analyst, 1984, **109**, 85.
32. Adachi, K., Ohokuni, N., and Mitsuhashi, T., J. Assoc. Off. Anal. Chem., 1984, **67**, 798.
33. Nishijima, O., Noyaku Kensasho Hokoku, 1984, **24**, 35.
34. Ding, X.-D., and Krull, I. S., J. Agric. Food Chem., 1984, **32**, 622.
35. Committee for Analytical Methods for Residues of Pesticides and Veterinary Products in Foodstuffs and the Working Party on Pesticide Residues of the Ministry of Agriculture, Fisheries and Food, Analyst, 1985, **110**, 765.
36. Mestres, R., and Susilo, H., Trav. Soc. Pharm. Montpellier, 1980, **40**, 277.
37. Isshiki, K., Tsumura, S., and Watanabe, T., Bull. Environ. Contam. Toxicol., 1978, **19**, 518.
38. Brown, B. B., in Zweig, G., and Sherma, J., Editors, "Analytical Methods for Pesticides and Plant Growth Regulators," Volume 7, Academic Press, New York, 1974, p. 441.
39. Ogierman, L., and Slilowiecki, A., Chromatographia, 1981, **14**, 459.
40. Desmarchelier, J. M., J. Stored Prod. Res., 1976, **12**, 245.
41. Simonaitis, R. A., and Cail, R. S., in Elliot, M., Editor, "ACS Symposium Series No. 42 (Synthetic Pyrethroids Symposium)," American Chemical Society, Washington, DC, 1977, p. 211.
42. Fujie, G. H., and Fullmer, O. H., J. Agric. Food Chem., 1978, **26**, 395.
43 Gunew, D. S., in Zweig, G., Editor, "Analytical Methods for Pesticides and Plant Growth Regulators," Volume 10, Academic Press, New York, 1978, p. 19.
44 Greenberg, R. S., J. Agric. Food. Chem., 1981, **29**, 856.
45 Cave, S. J., Pestic. Sci., 1981, **12**, 156.
46 Noble, R. M., Hamilton, D. J., and Osborne, W. J., Pestic. Sci., 1982, **13**, 246.
47. Okadu, T., Uno, M., Nozawa, M., and Tanigawa, K., Shokuhin Eiseigaku Zasshi, 1983, **24**, 147.
48. Joia, B. S., Sarna, L. P., and Webster, G. R. B., Int. J. Environ. Anal. Chem., 1985, **21**, 179.
49. Forbes, S., and Dutton, A. J., Pestic. Sci., 1985, **16**, 404.
50. Cook, R. F., Stanovick, R. P., and Cassil, C. C., J. Agric. Food Chem., 1969, **17**, 277.
51. Carey, W. F., and Helrich, K., J. Assoc. Off. Anal. Chem., 1970, **53**, 1296.
52. Lau, S. C., and Marzxmiller, R. L., J. Agric. Food Chem., 1970, **18**, 413.
53. Stanley, C. W., and Thornton, J. S., J. Agric. Food Chem., 1972, **20**, 1265.
54. Holden, E. H., J. Assoc. Off. Anal. Chem., 1973, **56**, 713.
55. Lawrence, J. F., J. Agric. Food Chem., 1977, **25**, 211.
56. Nishijima, O., and Tanaka, M., Noyaku Kensasho Hokoku, 1980, **20**, 59.
57. Wallbank, B. E., J. Chromatogr., 1981, **208**, 305.
58. Nishijima, O., Noyaku Kensasho Hokoku, 1981, **21**, 54.
59. Nishijima, O., Noyaku Kensasho Hokoku, 1982, **22**, 32.

60. Appraiah, K. M., Ramakrishna, R., Subbarao, K. R., and Kapur, O., *J. Assoc. Off. Anal. Chem.*, 1982, **65**, 32.
61. Hargreaves, P. A., and Melksham, K. J., *Pestic. Sci.*, 1983, **14**, 347.
62. Szeto, S. Y., Wilkinson, A. T. S., and Brown, M. J., *J. Agric. Food Chem.*, 1984, **32**, 78.
63. Sandell, E. B., *in* Kolthoff, I. M., and Elving, P. J., *Editors*, "Treatise on Analytical Chemistry, Part 1," Volume 1, Interscience, New York, 1959.
64. Thornburg, W. W., *J. Assoc. Off. Anal. Chem.*, 1965, **48**, 1023.
65. Wheeler, W. B., and Frear, D. E. H., *Residue Rev.*, 1966, **16**, 86.
66. Watts, R. R., *J. Assoc. Off. Anal. Chem.*, 1971, **54**, 953.
67. Krause, R. T., *J. Agric. Food Chem.*, 1978, **26**, 1333.
68. Taylor, I., and Thier, H. P., *Pure Appl. Chem.*, 1979, **51**, 1603.
69. Hemingway, R. J., *Pure Appl. Chem.*, 1984, **56**, 1131.
70. Hoodless, R. A., Jackson, F. J., Tarrant, K. R., and Griffith, B. E., *Pestic. Sci.*, 1974, **5**, 555.
71. Luke, M. A., Froberg, J. E., and Masumoto, H. T., *J. Assoc. Off. Anal. Chem.*, 1975, **58**, 1020.
72. Takimoto, Y., and Miyamoto, J., *Residue Rev.*, 1976, **60**, 83.
73. Committee for Analytical Methods for Residues of Pesticides and Veterinary Products in Foodstuffs and the Working Party on Pesticide Residues of the Ministry of Agriculture, Fisheries and Food, *Analyst*, 1977, **102**, 858.
74. Ferreira, J. R., and Silva Fernandes, A. M. S., *J. Assoc. Off. Anal. Chem.*, 1980, **63**, 517.
75. Wolf, M., Deleu, R., and Copin, A., *J. High Resolut. Chromatogr. Chromatogr. Commun.*, 1981, **4**, 346.
76. Simonaitis, R. A., and Cail, R. S., *J. Assoc. Off. Anal. Chem.*, 1975, **58**, 1032.
77. Cochrane, W. P., and Lanouette, M., *J. Assoc. Off. Anal. Chem.*, 1981, **64**, 724.
78. Chapman, R. A., and Simmons, H. S., *J. Assoc. Off. Anal. Chem.*, 1977, **60**, 977.
79. Talekar, N. S., *J. Assoc. Off. Anal. Chem.*, 1977, **60**, 908.
80. Mestres, R., Chevallier, C., Espinoza, C., and Cornet, R., *Trav. Soc. Pharm. Montpellier*, 1978, **38**, 183.
81. Lee, Y. W., Westcott, N. D., and Reichle, R. A., *J. Assoc. Off. Anal. Chem.*, 1978, **61**, 869.
82. Chapman, R. A., and Harris, C. R., *J. Chromatogr.*, 1979, **174**, 369.
83. Braun, H. E., and Stanek, K., *J. Assoc. Off. Anal. Chem.*, 1982, **65**, 685.
84. Baker, P. G., and Bottomley, P., *Analyst*, 1982, **107**, 206.
85. Akhtar, M. H., *J. Chromatogr.*, 1982, **246**, 81.
86. Awasthi, M. D., *J. Food Sci. Technol.*, 1985, **22**, 4.
87. Riva, M., and Carisano, A., *J. Chromatogr.*, 1969, **42**, 464.
88. Lorah, E. J., and Hemphill, D. D., *J. Assoc. Off. Anal. Chem.*, 1974, **57**, 570.
89. Hall, R. C., and Harris, D. E., *J. Chromatogr.*, 1979, **169**, 245.
90. Wehner, T. A., and Seiber, J. N., *J. High Resolut. Chromatogr. Chromatogr. Commun.*, 1981, **4**, 348.
91. Bowman, M. C., *in* Moye, H. A., *Editor*, "Chemical Analysis (Analysis of Pesticide Residues)," Volume 58, Wiley-Interscience, New York, 1981, p. 263.
92. Chau, A. S. Y., and Ripley, B. D., *Anal. Pestic. Water*, 1982, **2**, 61.
93. Stan, H. J., and Goebel, H., *J. Chromatogr.*, 1984, **314**, 413.
94. Miyamoto, J., *Pure Appl. Chem.*, 1981, **53**, 1967.
95. Papadopoulou-Mourkidou, E., *Residue Rev.*, 1983, **89**, 179.
96. Williams, I. H., *Pestic. Sci.*, 1976, **7**, 336.
97. Mount, M. E., and Oehme, F. W., *Residue Rev.*, 1981, **80**, 1.
98. Magallona, E. D., *Residue Rev.*, 1975, **56**, 1.
99. Dorough, H. W., and Thortenson, J. H., *J. Chromatogr. Sci.*, 1975, **13**, 212.
100. Seiber, J. N., *in* Moye, H. A., *Editor*, "Chemical Analysis (Analysis of Pesticide Residues)," Volume 58, Wiley-Interscience, New York, 1981, p. 333.
101. Tilden, R. I., and Van Middlem, C. H., *J. Agric. Food Chem.*, 1970, **18**, 154.
102. Moye, H. A., *J. Agric. Food. Chem.*, 1975, **23**, 415.
103. Ripley, B. D., and Chau, S. Y., *Anal. Pestic. Water*, 1982, **3**, 1.
104. Lawrence, J. F., Lewis, D. A., and McLeod, H. A., *J. Chromatogr.*, 1977, **138**, 143.
105. Cochrane, W. P., *in* Harvey, J., Jr., and Zweig, G., *Editors*, "ACS Symposium Series No. 136 (Pesticide Analytical Methodology)," American Chemical Society, Washington, DC, 1980, p. 231.
106. Ripley, B. D., and Braun, H. E., *J. Assoc. Off. Anal. Chem.*, 1983, **66**, 1084.
107. Wright, B. W., and Smith, R. D., *J. High Resolut. Chromatogr. Chromatogr. Commun.*, 1986, **9**, 73.
108. Grob, K., Jr., and Bossard, M., *J. Chromatogr.*, 1984, **294**, 65.
109. Grob, K., Jr., and Neukom, H. P., *Chromatographia*, 1984, **18**, 517.
110. Zenon-Roland, L., Agneessens, R., and Nangnlot, P., *J. High Resolut. Chromatogr. Chromatogr. Commun.*, 1984, **7**, 480.
111. Ambrus, and Thier, H. P., *Pure Appl. Chem.*, 1986, **58**, 1035.
112. Luke, M. A., Froberg, J. E., Doose, G. M., and Masumoto, H. T., *J. Assoc. Off. Anal. Chem.*, 1981, **64**, 1187.
113. Blaha, J. J., and Jackson, P. J., *J. Assoc. Off. Anal. Chem.*, 1985, **68**, 1095.
114. Goebel, H., and Stan, H. J., *J. Chromatogr.*, 1983, **279**, 523.
115. Fehringer, H. V., and Walters, S. M., *J. Assoc. Off. Anal. Chem.*, 1984, **67**, 91.
116. Prinsloo, S. M., and DeBeer, P. R., *J. Assoc. Off. Anal. Chem.*, 1985, **68**, 1100.
117. Osselton, M. D., and Snelling, R. D., *J. Chromatogr.*, 1986, **368**, 265.
118. Thompson, J. F., Mann, J. B., Apodaca, A. O., and Kantor, E. J., *J. Assoc. Off. Anal. Chem.*, 1975, **58**, 1037.
119. Ambrus, A., Visi, E., Zakar, F., Hargital, E., Szabo, L., and Papa, A., *J. Assoc. Off. Anal. Chem.*, 1981, **64**, 749.
120. Clark, G. J., Goodin, R. R., and Smiley, J. W., *Anal. Chem.*, 1985, **57**, 2223.
121. Gluckman, J. C., Barcelo, G., DeJong, G. J., Frei, J. W., Maris, F. A., and Brinkman, U. A. Th., *J. Chromatogr.*, 1986, **367**, 35.
122. Kikta, E. J., and Shierling, J. P., *J. Chromatogr.*, 1978, **150**, 229.
123. Papadopoulou-Mourkidou, E., Iwata, Y., and Gunther, F. A., *J. Agric. Food Chem.*, 1983, **31**, 629.
124. Lawrence, J. F., and Leduc, R., *J. Agric. Food Chem.*, 1977, **25**, 1362.
125. Spittler, T. D., and Marafioti, R. A., *J. Chromatogr.*, 1983, **255**, 191.
126. Lawrence, J. F., and Leduc, R., *J. Assoc. Off. Anal. Chem.*, 1978, **61**, 872.
127. Lawrence, J. F., and Leduc, R., *J. Chromatogr.*, 1978, **152**, 507.
128. Fogy, I., Schmid, E. R., and Huber, J. F. K., *Z. Lebensm. Unters. Forsch.*, 1979, **169**, 438.
129. Fogy, I., Schmid, E. R., and Huber, J. F. K., *Z. Lebensm. Unters. Forsch.*, 1980, **170**, 194.
130. Muth, G. L., and Erro, F., *Bull. Environ. Contam. Toxicol.*, 1980, **24**, 759.
131. Blaicher, G., Pfannhauser, W., and Woidich, H., *Chromatographia*, 1980, **13**, 438.
132. Lee, Y. W., and Westcott, N. A., *J. Agric. Food Chem.*, 1980, **28**, 719.
133. Funch, F. H., *Z. Lebensm. Unters. Forsch.*, 1981, **173**, 95.
134. Ramsteiner, K. A., and Hormann, W. A., *J. Chromatogr.*, 1975, **104**, 438.
135. Ramsteiner, K., *Int. J. Environ. Anal. Chem.*, 1986, **25**, 49.
136. Cayley, G. R., and Simpson, B. W., *J. Chromatogr.*, 1986, **356**, 123.

Evaluation of an Apparatus Designed for the Collection of Sidestream Tobacco Smoke

Christopher J. Proctor, Cathy Martin, John L. Beven and Harry F. Dymond
BAT (UK and Export) Ltd., Research and Development Centre, Regent's Park Road, Southampton SO9 1PE, UK

A method for the routine analysis of sidestream tobacco smoke has been developed. Fundamental to the analysis is the design of a glass fishtail chimney that sits over a burning cigarette and allows the smoke to be directed in a controlled manner to various trapping and analysing devices. The analytical variability of the method is given for the determination of particulate matter, nicotine, carbon monoxide and carbon dioxide in sidestream smoke.

Keywords: *Cigarette smoke; sidestream tobacco smoke; smoke collection*

Sidestream tobacco smoke is, effectively, all the smoke emitted from a cigarette other than the mainstream smoke. Yields of the constituents of sidestream smoke have been reported by many workers[1-4] and often used as a means of predicting the concentrations of compounds in ambient air due to tobacco smoke.[5] Such predictions are false because the composition and physical nature of sidestream smoke change dramatically as it ages and is greatly diluted.[6,7] However, as sidestream smoke is the major source of environmental tobacco smoke (ETS), its accurate analysis is important.

Mainstream smoke, the smoke that leaves the mouth end of the cigarette on inhalation, has been measured on a routine basis for many years. Sidestream smoke, however, is difficult to control as it is carried away by draughts and convection and the point of origin moves as the cigarette burns down. These factors make considerable demands on any collection system for sidestream smoke.

Several workers have published details of sidestream collection devices and designs vary greatly.[4] The majority of such devices distort the mainstream smoking characteristics of the cigarette and few are amenable to routine analysis of large numbers of cigarettes.

This paper describes a collection apparatus, the fishtail chimney, that can be used for the routine analysis of sidestream smoke. The device is easily attached to a standard smoking engine, maintains normal mainstream smoking conditions and provides a method for the precise measurement of both the particulate and gaseous phase of sidestream smoke.

Design Criteria for a Sidestream Smoke Collection Apparatus

The way in which cigarettes are smoked by machines is specifically detailed by International Standards Organisation (ISO) methods.[8] This ensures that cigarette deliveries are meaningful and comparable regardless of which laboratory performs the analysis.

Cigarettes vary and so a statistically determined number of cigarettes belonging to the same sample must be smoked before an analysis can be considered to give a reliable result. Other factors, such as the ambient conditions of the smoking laboratory, the moisture content of the cigarette and the air flowing over the cigarette while it is burning, all have significant effects on cigarette yields. It is most important when defining a standard method for sidestream smoke analysis that all of the conditions laid down for mainstream smoke analysis are maintained.

When designing a collection apparatus for sidestream smoke the following considerations must be taken into account. The device must not affect the normal combustion of the cigarette, either when it is being puffed or when it is smouldering. To achieve this the device must allow the cigarette to burn at ambient temperature and pressure in an atmosphere of air (not of the cigarette's own smoke).[9] Further, the air flow over the cigarette must be within the range defined by ISO, *i.e.*, 4–7 linear feet per minute.[8] The effect of the device on the combustion of the cigarette can easily be monitored by measuring mainstream smoke yields with and without the collection apparatus in place. Also, sampling should provide a true representation of the sidestream smoke.

Smoke components can broadly be divided into three phases. The particulate phase is that which is trapped on a Cambridge filter-pad, which is a glass-fibre disc bonded with 5% resin (Cambridge Filter Corp., USA). It is generally referred to as "tar" and is quoted as the gravimetric mass minus the mass of nicotine and of water. The vapour phase contains the more volatile components that pass through the pad and the third phase consists of gases such as carbon monoxide and carbon dioxide. A collection system should allow the analysis of each of these phases.

The smoke leaving the burning end of the cigarette is warm and particularly prone to condensation on cold surfaces, hence the collection method must allow recovery of any deposited substances. Further, if more than one cigarette is to be analysed per port of a smoking engine, then the yields must be additive from 1 to *n* cigarettes.

The device must be readily adapted to a standard smoking engine and it should preferably allow multiple, simultaneous analyses of both mainstream and sidestream smoke at a rate appropriate to routine measurement. In addition, the apparatus should permit easy insertion and ignition of the cigarettes in addition to an automatic butt-length (end-point) determination.

Previously Described Sidestream Smoke Collection Devices

There have been several attempts to design collection devices for sidestream smoke. All have used glass chambers or hoods although the design has varied according to the type of research undertaken. As early as 1964, Neurath and Ehmke[10] described a water-cooled chamber of 170-ml volume that entirely surrounded the cigarette. Entrance and exit ports allowed smoke to be passed through the chamber at a flow-rate of 20–25 ml s⁻¹ resulting in a total atmosphere change every 7–10 s. However, this arrangement had the disadvantage of uneven burning of the cigarette, did not allow separation of particulate and vapour phases and the small chamber severely distorted the mainstream combustion. Brunnemann and Hoffmann[11] tried to improve this design 10
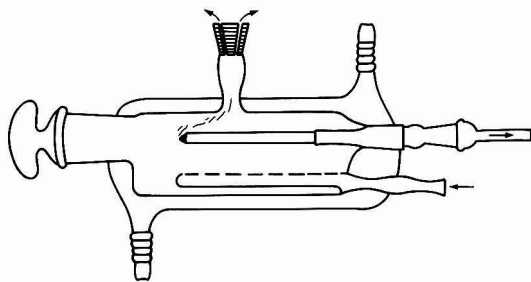
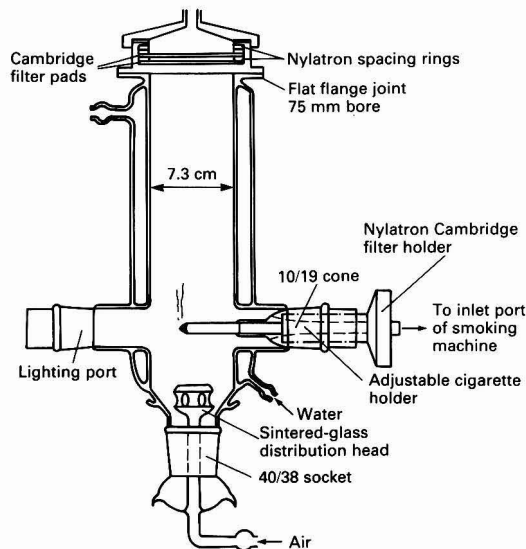**Fig. 1.** Sidestream collection apparatus used by Brunnemann and Hoffmann[2]

Fig. 2. The smoking cartridge devised by Johnson et al.[12] The inlet and lighting ports are standard Quickfit 24/29 sockets

Fig. 3. Sidestream collection apparatus designed by Sakuma et al.[3] A, Glass chimney for collecting sidestream smoke; B, ash tray; C, Cambridge filter holder; D, alkali solution trap; E, mist trap; F, charcoal trap; and G, flow meter

Sakuma and co-workers,[3,16,17] in a series of papers reporting on the distribution of acidic, basic and higher boiling compounds in sidestream smoke, described an apparatus that limits the deposition of smoke on the walls (Fig. 3). This pear-shaped apparatus uses an air flow-rate of 2 l min^{-1}. The distance between the cigarette and the filter-pad is less than that in the cartridge designed by Johnson and so the smoke is likely to be impacting while still warm. In addition, the design incorporates an ash-collection tray directly beneath the cigarette so it is difficult to ascertain the precise air flow-rate over the cigarette.

A different approach was taken by Chortyk and Schlotzhauer.[18] Their experimental design consists of a large glass funnel held above a rotary smoking engine. This allows 30 cigarettes to be smoked simultaneously and so overcomes variation between them. Because of the large air flow-rates involved, particulate trapping is not possible with this arrangement. Instead, they used a series of liquid traps to collect the smoke.

Hence several devices have been described, each having its own advantages relevant to the experiments for which it was designed. None, however, is appropriate to the routine analysis of sidestream smoke.

Fishtail Chimney

The fishtail chimney, shown in Fig. 4, was developed as an apparatus specifically for the routine analysis of sidestream smoke. Rather than totally enclosing the cigarette, the chimney sits over the cigarette. In its sampling position, the chimney sits within the apparatus having one side and the bottom of the "fishtail" open. Smoke is drawn up the chimney at a rate of 2 l min^{-1}. At this volumetric flow-rate, the linear flow-rate over the cigarette is approximately 6 linear feet per minute (within the ISO specification).

The device is easily mounted on a standard linear smoking engine. Typically, these machines have 8 or 20 ports to allow 8 or 20 cigarettes to be smoked simultaneously. The detailed design modifications necessary for any smoking engine are described elsewhere[19] but, to summarise, the chimneys are positioned one per port so that they can be raised to allow positioning and ignition of the cigarettes and then lowered again over the lighted cigarettes. The end-point of smoking is determined by means of a microswitch arrangement that deactivates the mainstream puffing once a piece of cotton, wound around a Y-shaped support, burns and breaks. At this point, each cigarette is extinguished by squeezing the burning end with specially designed tweezers.

A series of design variations based on the general chimney principle have been investigated. Both the shape and the height were varied and the collection efficiency was assessed. Both variables were found to have a significant effect.

years later by providing a perforated air-inlet tube, positioned below the cigarette, for their study of the pH of sidestream smoke. This allowed a more uniform combustion of the cigarette, but the system, illustrated in Fig. 1, falls short of fulfilling the criteria necessary for a standard sidestream smoke collection system.

In 1973 a different approach was taken by Johnson et al.[12] and Houseman.[13] In studies aimed at defining mainstream to sidestream smoke ratios for a wide range of compounds they devised the vertical smoking cartridge. This apparatus, illustrated in Fig. 2, was designed with a much greater distance between the cigarette and the Cambridge filter-pad (ca. 22 cm) than that in the Neurath chamber. It also made provision for lighting the cigarette in position although automatic butt termination was not possible. A sintered-glass distribution head ensured minimum turbulence in the incoming air, which was drawn through by creating a partial vacuum at the top of the chamber. In the course of the work no account was taken of condensation on the walls of the apparatus, although this does occur, and the system is still cumbersome for routine analyses. A similar device was used by Browne et al. in 1980.[14]

In 1983, Norman et al.[15] used a horizontal collection device similar to that originated by Neurath, although of larger volume. The experiments were designed to investigate oxides of nitrogen and hydrogen cyanide in sidestream smoke and no effort was made to improve the particulate collection of the apparatus.
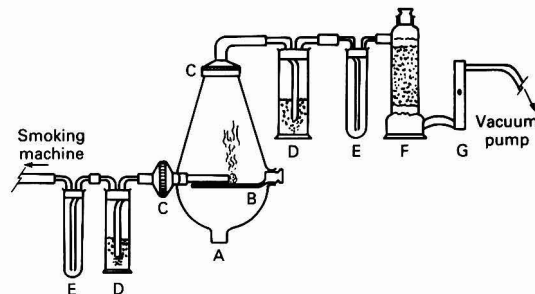
Fig. 4. The fishtail chimney. Internal dimensions in mm

Table 1. Effect of distance between the burning cigarette and the Cambridge filter-pad on nicotine and PMWNF sidestream yields

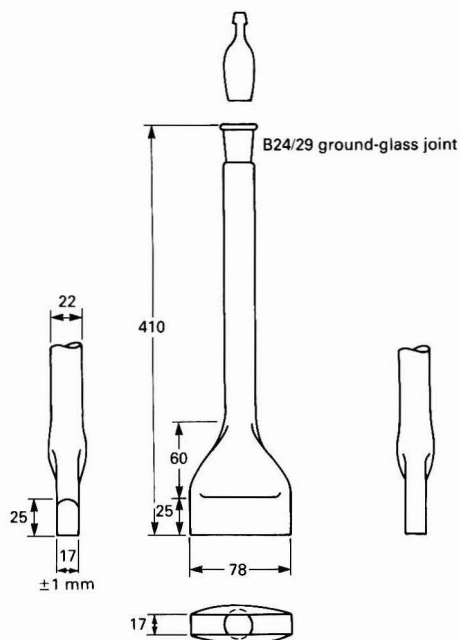| Height/ cm	Nicotine/ mg per cigarette			PMWNF/mg per cigarette		
	Pad	Chimney	Total	Pad	Chimney	Total
25.5	3.71	0.63	4.34	22.41	3.92	26.3
29.0	4.01	1.42	5.43	24.08	4.34	28.4
32.5	4.18	1.54	5.72	25.85	4.54	30.4
36.0	4.36	1.71	6.07	26.00	5.39	31.4
46.0	4.21	1.71	5.92	25.69	5.69	31.4
51.0	4.29	1.71	6.00	26.24	5.46	31.7

Fig. 5. Sidestream smoke analysis using the fishtail chimney

Assessment of the Fishtail Chimney

A series of experiments were performed to ensure that the chimney did not affect the normal combustion of the cigarettes. To do this, a set of cigarettes with a range of mainstream smoke deliveries was analysed with and without the fishtail chimney in place. No significant differences were found and so it was assumed that the collection apparatus did not affect the normal combustion of the cigarette.

When analysing mainstream smoke, three yields are usually quoted: tar, nicotine and carbon monoxide. Tar is a measurement of the particulate phase of smoke. It is defined as the smoke trapped on a Cambridge filter-pad and is quantified gravimetrically. A significant proportion of the material collected on the pad is water, the amount of which can vary even when conditions are strictly controlled. Hence, tar is normally quoted as the gravimetric mass minus the mass of nicotine and of water (both determined by gas chromatography) and called PMWNF (particulate matter, water and nicotine free). Nicotine in mainstream smoke is almost completely associated with the particulate phase[20] and is determined by GC analysis of an extract of the filter-pad.[21] Carbon monoxide is determined by near-infrared spectroscopy. The performance of the sidestream collection device was assessed by determining these three components and carbon dioxide.

The concentrations of carbon monoxide and carbon dioxide are determined by subsampling the gas flow from four ports manifolded together using two near-infrared analysers. Hence, an eight-port smoking engine requires two carbon monoxide and two carbon dioxide analysers. The signal from the analysers is integrated over each smoking run using a microcomputer and yields are calculated with correction for temperature, pressure and flow-rate. Flow-rates are determined by a series of calibrated rotameters. Care is taken to minimise any pressure differences that might arise in the system in order to permit accurate gas analysis.

The total nicotine yield is determined by taking into account the analysis of the propanol extract of each pad and the analysis of the propanol used to wash the chimney. PMWNF must also be corrected for deposition on the chimney. This is achieved by comparing the pad extract and the washings from the chimney by measuring the UV absorbance at 310 nm in a 10-mm quartz cell.

Table 1 presents the results of the nicotine and particulate matter determinations in chimneys similar to that shown in Fig. 4 except for the distance between the cigarette and the Cambridge filter-pad, which was varied. The nicotine and particulate values obtained decrease as the chimney is made progressively shorter than 36 cm. Above 36 cm the deliveries are stable. The final design specifies a distance of 45 cm between the burning cigarette and the Cambridge filter-pad used for particulate collection. This height effect is likely to be a function of both the smoke temperature (affecting the efficiency of the filter-pad) and the aerosol-forming processes (affecting the distribution between the particulate and vapour phases). These findings have implications for other designs of sidestream collection apparatus.

The shape of the apparatus also has an effect on the efficiency of transport of the smoke to the filter-pad. In order to fit a series of collection devices side by side on the smoking engine, the width of the device must be relatively narrow. This inevitably leads to deposition of smoke on the glass walls. Further, as the device is open at the bottom the apparatus must be designed to ensure that there is no smoke "fall out." Fall-out is eliminated and deposition limited when the shape of the apparatus is the same as that shown in Fig. 4. The apparatus then acts as a chimney, the flue effect carrying the smoke efficiently to the traps.

It is known that the particle size distribution, the average particle size and the distribution of compounds between the particulate and vapour phases can be different in fresh sidestream smoke compared with mainstream smoke. Hence, it was important to determine whether the nicotine had remained in the particulate phase and whether the Cambridge filter-pad was trapping efficiently. To investigate this, sidestream smoke was collected in a cooled acidic liquid trap placed between the pad and the pump. Any nicotine passing through the particulate trap is collected in the acid trap. Over 95% of the nicotine present was found on the pad and the chimney, so at this collection point the nicotine is almost entirely associated with the particulate phase.

Table 2. Analytical variability of the nicotine yield in sidestream smoke for four cigarette types

Cigarette type	Analytical run	Machine port	Pad nicotine*	Chimney nicotine*	Total nicotine*
Cigarette 1	1	2	4.31	1.17	5.5
	1	6	4.54	1.17	5.7
	2	3	4.38	1.09	5.5
	2	7	4.34	1.13	5.5
	3	1	4.34	1.21	5.6
	3	5	4.48	1.13	5.6
	4	4	4.34	1.09	5.4
	4	8	4.34	1.17	5.5
Cigarette 2	1	3	4.24	0.77	5.0
	1	7	4.61	1.29	5.9
	2	4	4.18	1.09	5.3
	2	8	4.34	1.38	5.7
	3	2	4.44	1.34	5.8
	3	6	4.54	1.34	5.9
	4	1	4.28	1.25	5.5
	4	5	4.31	1.38	5.7
Cigarette 3	1	4	3.37	0.92	4.3
	1	8	3.61	1.09	4.7
	2	1	3.67	1.04	4.7
	2	5	3.74	1.09	4.8
	3	3	3.74	1.00	4.7
	3	7	3.66	1.17	4.8
	4	2	3.51	1.04	4.6
	4	6	3.71	1.22	4.9
Cigarette 4	1	1	4.07	0.84	4.9
	1	5	4.54	0.92	5.5
	2	2	4.18	0.88	5.1
	2	6	3.87	0.79	4.7
	3	4	4.18	0.92	5.1
	3	8	4.07	0.92	5.0
	4	3	3.94	0.92	4.9
	4	7	4.18	1.04	5.2

* All nicotine values in mg per cigarette.

Table 3. Analytical variability of the PMWNF yields in sidestream smoke for four cigarette types

Cigarette type	Analytical run	Machine port	Pad PMWNF*	Chimney PMWNF*	Total PMWNF*
Cigarette 1 . .	1	2	26.31	4.90	31.2
	1	6	27.25	5.17	32.4
	2	3	27.38	5.06	32.4
	2	7	26.31	5.31	31.6
	3	1	24.79	6.08	30.9
	3	5	25.84	5.45	31.3
	4	4	28.25	4.17	32.4
	4	8	27.55	5.13	32.7
Cigarette 2 . .	1	3	26.52	4.40	30.9
	1	7	28.55	5.67	34.2
	2	4	26.61	4.84	31.5
	2	8	28.21	5.34	33.5
	3	2	28.98	6.45	35.4
	3	6	29.15	7.01	36.2
	4	1	27.71	4.80	32.5
	4	5	28.18	5.15	33.3
Cigarette 3 . .	1	4	22.03	4.14	26.2
	1	8	23.02	4.93	28.0
	2	1	22.53	4.68	27.2
	2	5	22.09	4.78	26.9
	3	3	23.48	4.89	28.4
	3	7	23.08	4.94	28.0
	4	2	22.21	4.40	26.6
	4	6	24.41	4.88	29.3
Cigarette 4 . .	1	1	24.06	4.04	28.1
	1	5	25.49	4.63	30.1
	2	2	23.98	4.09	28.1
	2	6	23.09	3.88	27.0
	3	4	24.04	4.91	29.0
	3	8	23.36	4.73	28.1
	4	3	23.58	4.01	27.6
	4	7	25.14	5.03	30.2

* All PMWNF values are in mg per cigarette.

Table 4. Arithmetic means (x), sample standard deviations (with $n - 1$ degrees of freedom, SD) and coefficients of variation (CV) for total nicotine and total PMWNF yields in the sidestream smoke of four cigarette types. Yields of both nicotine and PMWNF are in mg per cigarette

Cigarette type				Total nicotine	Total PMWNF
Cigarette 1	. .	. .	x	5.5	31.9
			SD	0.09	0.7
			CV	1.2%	2.2%
Cigarette 2	. .	. .	x	5.6	33.4
			SD	0.3	1.8
			CV	5.7%	5.4%
Cigarette 3	. .	. .	x	4.7	27.6
			SD	0.2	1.0
			CV	4.3%	3.7%
Cigarette 4	. .	. .	x	5.0	28.5
			SD	0.2	1.2
			CV	4.8%	4.0%

Nicotine and PMWNF yields were found to be additive for one to three cigarettes smoked per port, but not for more than three cigarettes. Hence, in order to provide a statistically significant sample that took into account the variability between individual cigarettes, four ports, each with three cigarettes, were smoked for each sample cigarette. That is, the yield quoted will always be the average of the analysis of 12 cigarettes. The experimental set-up is illustrated in Fig. 5.

Tables 2 and 3 present the data from the analysis of four different types of cigarette (a UK and US commercial and two experimental). Each figure in the table is the average of three cigarettes smoked. Smoking engine ports were randomised to reduce any machine effect. With randomisation it is not possible to run gaseous analyses (as that is based on collecting the smoke from four fixed ports). Table 4 summarises the statistical analysis of these data. For both nicotine and PMWNF a coefficient of variation better than 6%, which is similar to that achieved in the corresponding mainstream analyses, is easily attained. A further study found carbon monoxide and carbon dioxide measurements to be even more precise, with coefficients of variation better than 5% (Table 5).

Conclusions

This study indicates that the fishtail chimney can be used as the basis for a routine method of sidestream smoke analysis. Using this collection device, standard analytical methods that allow the accurate and simultaneous measurement of mainstream and sidestream tar, nicotine and carbon monoxide levels can be defined.

Some deposition of the warm sidestream smoke does occur on the walls. On average, 20% of both the total nicotine and the tar are recovered by washing out smoke deposited on the chimney. Even so, the method takes this quantity into account without any significant loss in precision.

The experimental set-up shown in Fig. 5 should be easily adaptable to the collection of either whole smoke or compounds in the vapour phase simply by the inclusion of liquid traps between the chimney and the rotary pump.

It should be emphasised that any measurement of sidestream smoke is a measurement at one point in time of an entity that is constantly changing. Hence, sidestream smoke yields cannot be related directly to concentrations of smoke found in the environment (ETS). As the sidestream smoke ages and is diluted by an ambient atmosphere the relative

Table 5. Analytical variability of the CO and CO_2 yields in the sidestream smoke of two cigarette types, X and Y

	CO		CO_2	
Run	Cigarette X/ mg per cigarette	Cigarette Y/ mg per cigarette	Cigarette X/ mg per cigarette	Cigarette Y/ mg per cigarette
1	73.0	69.8	614.7	605.5
2	70.6	72.6	612.7	602.6
3	72.5	73.5	623.3	647.5
4	74.2	74.4	638.5	638.5
5	73.9	72.3	638.3	626.5
6	74.1	73.1	633.5	624.9
7	73.4	76.1	626.4	625.6
8	72.3	68.5	618.1	596.8
9	64.0	68.1	578.9	608.9
10	69.5	67.3	611.0	592.1
Mean	71.7	71.6	619.5	618.7
SD	3.1	3.0	17.5	17.7
CV, %	4.6	4.2	2.8	2.9

composition and nature of the smoke will change dramatically.

Nicotine is an important example of a compound that disappears from air at a rapid rate as it evaporates into the vapour phase and becomes absorbed at surfaces.[6] However, because sidestream smoke is the origin of and main contributor to ETS it is important that there is a standard method for its analysis.

The fishtail chimney allows the application of a method for the routine measurement of sidestream smoke. It may be attached easily to standard smoking engines and does not affect the combustion of the cigarette. Finally, it enables precise and reproducible data to be acquired on a routine basis.

References

1. Klus, H., and Kuhn, H., *Beitr. Tabakforsch.*, 1982, **11**, 229.
2. Brunnemann, K. D., and Hoffmann, D., *J. Chromatogr. Sci.*, 1975, **13**, 159.
3. Sakuma, H., Kusama, M., Munakatu, S., Ohsumi, T., and Sugawara, S., *Beitr. Tabakforsch.*, 1983, **12**, 63.
4. O'Neill, I. K., Brunnemann, K. D., Dodet, B., and Hoffmann, D., *Editors*, "Environmental Carcinogens. Methods of Analysis and Exposure Measurement," Volume 9, IARC Scientific Publications, Lyon, No. 81, 1987.
5. Hugod, C., Hawkins, L. H., and Astrup, P., *Int. Arch. Occup. Environ. Health*, 1978, **42**, 21.
6. Nystrom, C. W., and Green, C. R., paper presented at the ASHREA Conference IAQ 86, Managing Indoor Air for Health and Energy Conservation, Atlanta, Georgia, April 20th–23rd, 1986.
7. Reasor, M. J., *J. Environ. Health*, 1987, **50**, 20.
8. "Tobacco and Tobacco Products—Routine Analytical Cigarette-smoking Machine—Definitions, Standard Conditions and Auxiliary Equipment," ISO 3308 - 1977 (E), International Standards Organisation, Geneva, 1977.
9. "Tobacco and Tobacco Products—Atmospheres for Conditioning and Testing," ISO 3402 - 1978, International Standards Organisation, Geneva, 1978.
10. Neurath, G., and Ehmke, H., *Beitr. Tabakforsch.*, 1964, **2**, 117.
11. Brunnemann, K. D., and Hoffmann, D., *Food Cosmet. Toxicol.*, 1974, **12**, 115.
12. Johnson, W. R., Hale, R. W., Nedlock, J. W., Grubbs, H. J., and Powell, D. H., *Tob. Sci.*, 1973, **17**, 141.
13. Houseman, T. H., *Beitr. Tabakforsch.*, 1973, **7**, 142.
14. Browne, C. L., Keith, C. H., and Allen, R. E., *Beitr. Tabakforsch.*, 1980, **10**, 81.
15. Norman, V., Ihrig, A. M., Larson, T. M., and Moss, B. L., *Beitr. Tabakforsch.*, 1984, **12**, 55.
16. Sakuma, H., Kusama, M., Yamaguchi, K., Matsuki, T., and Sugawara, S., *Beitr. Tabakforsch.*, 1984, **12**, 199.
17. Sakuma, H., Kusama, M., Yamaguchi, K., and Sugawara, S., *Beitr. Tabakforsch.*, 1984, **12**, 251.
18. Chortyk, O. T., and Schlotzhauer, W. S., *Tob. Sci.*, 1986, 122.
19. Proctor, C. J., Martin, C., Beven, J. L., and Dymond, H. F., in preparation
20. Schmeltz, I., Wenger, A., Hoffmann, D., and Tso, T. C., *J. Agric. Food Chem.*, 1979, **27**, 602.
21. "Standard Methods for the Analysis of Cigarette Smoke," Research Paper 11, Third Edition, Tobacco Advisory Council, London, 1986.

Improved Method for the Determination of the Total Glucosinolate Content of Rapeseed by Determination of Enzymically Released Glucose

Robert K. Heaney, E. Ann Spinks and G. Roger Fenwick
Division of Molecular Science, AFRC Institute of Food Research, Norwich Laboratory, Colney Lane, Norwich NR4 7UA, UK

A method is described for the determination of the total glucosinolate content of rapeseed. The method is an improvement of a previously described procedure and avoids the necessity for a defatting step. The new and old methods are compared with each other and with a high-performance liquid chromatographic method.

Keywords: *Total glucosinolates; rapeseed; glucose release*

Rapeseed is an increasingly important crop grown primarily for its oil. Production within the European Economic Community currently exceeds 3.5 million tonnes, a quarter of this total coming from the UK. Removal of the oil from the crushed seed leaves a residue or meal, which contains about 40% protein and hence is a valued component of animal feed formulations.[1] Rapeseed meal, however, contains a group of sulphur-containing glycosides called glucosinolates which can undergo chemical or enzymic hydrolysis to produce a range of products, some of which possess antinutritional properties.[2] The presence of such glucosinolates therefore limits the potential of rapeseed meal and consequently much effort has been directed towards the reduction or removal of these compounds from rapeseed.

The Commission of the European Communities (CEC) has encouraged the move towards rapeseed cultivars with a low glucosinolate content by currently offering premium payments for loads with less than 35 µmol of glucosinolates per gram of seed (at 9% moisture content). It is further proposed that by 1991 financial support will be withdrawn for all batches of seed having glucosinolate contents in excess of 20 µmol g⁻¹.

Such developments have stimulated many studies into methods of glucosinolate analysis and these can be divided into two groups:

1. Methods that provide qualitative and quantitative data about the glucosinolate content of a sample, *e.g.*, gas chromatography (GC)[3–5] and high-performance liquid chromatography (HPLC).[6–8] Development of these methods has been supported by the CEC and a temperature-programmed GC method is the present Official Method.[9] More recently, HPLC methods have been studied by an Expert Committee of the CEC and the conditions optimised. The resulting procedure has been submitted to the CEC as an alternative Official Method and is currently being considered.

2. Methods that indicate only the total glucosinolate content and provide no information about the nature or relative proportions of the individual components. These include "wet" methods such as the measurement of the glucose released following hydrolysis with the enzyme myrosinase (thioglucose glycohydrolase, E. C. 3.2.3.1)[10–12] and also such non-specific techniques as the measurement of the colour resulting from the complexing of glucosinolates with tetrachloropalladate reagent.[13,14] Considerable efforts have also been directed recently towards the study of indirect physical methods such as near-infrared reflectance spectroscopy (NIRS)[15–17] and X-ray fluorescence spectroscopy (XFS),[18,19] as only methods such as these would be expected to meet the demands of industry and plant breeders for rapid sample throughput.

Two methods based on the measurement of enzymically released glucose have been submitted to the CEC by the UK authorities and have been provisionally accepted, subject to certain conditions, as alternatives to the Official Method.[10,12] One of these[10] was originally developed for the analysis of rapeseed meal and is no longer strictly appropriate as the current CEC regulations require glucosinolate content to be expressed in terms of micromoles per gram of whole seed. The adjustment back to whole seed of a value expressed in terms of defatted meal has inherent difficulties, as such a calculation requires an accurate knowledge of the oil content of the seed and of the extent of its removal during defatting. An additional criticism of the method is that newer varieties of rapeseed with a low total glucosinolate content possess a relatively high proportion of 4-hydroxyindolyl glucosinolate, a compound having relatively low stability, the extraction of which would be better conducted under milder conditions. In this work this method has been modified to take account of the above factors. The original and amended methods were compared directly and with the HPLC method developed and agreed under the auspices of the CEC.

Experimental

Apparatus and Reagents

In addition to general laboratory equipment, a bench-top centrifuge (*e.g.*, MSE Centaur 2) and a rotary evaporator (Büchi Rotavapor R110) are required. Rapeseed samples are milled in a laboratory mill or high-speed coffee mill (*e.g.*, Krups 50) ideally modified to reduce its capacity. A water-bath or heating block (*e.g.*, Grant BT3; Grant Instruments, Barrington, Cambridge) is necessary and solution absorbance values are measured with a suitable spectrophotometer (*e.g.*, Perkin-Elmer 550S). The preparation of miniature ion-exchange columns (mini-columns) of DEAE-Sephadex A-25 using Pasteur pipettes is described in detail in the Appendix. Reagents are of analytical-reagent grade unless specified otherwise. Methanol (700 ml) is diluted to 1000 ml with distilled water. Pyridine acetate buffer (0.5 M, pH 5) is prepared by diluting pyridine (40 ml) and glacial acetic acid (30 ml) to 1000 ml with distilled water. Pyridine acetate buffer (0.02 M, pH 5) is prepared by diluting 0.5 M buffer (40 ml) to 1000 ml with distilled water.

Myrosinase is prepared by the method of Appelqvist and Josefsson[20] and purified as described by Heaney *et al.*[10] A myrosinase preparation is also available commercially (Biocatalysts, Treforest Industrial Estate, Pontypridd, Mid-Glamorgan). It is suggested that the activity of the enzyme preparation as determined by the method of Wilkinson *et al.*[21] but without ascorbate, should be not less than 0.1 Unit.

To prepare the myrosinase solution, dissolve 25 mg of myrosinase enzyme (Biocatalysts) in 0.02 M pyridine acetate buffer (1 ml), 250 µl of this solution being required for each determination. Prepare a suspension of DEAE-Sephadex A-25 (Pharmacia, Hounslow, Middlesex) by first stirring the dry gel with an excess of 0.5 M pyridine acetate buffer. Filter the suspension, wash it with 0.02 M pyridine acetate and finally suspend it in the 0.02 M buffer such that the total volume is twice that of the settled gel. Assay glucose with Glucose Kit No. 115-A (Sigma Chemical, Poole, Dorset), the reagents being prepared according to the manufacturer's instructions.

Extraction of Glucosinolates

If the seed is moist it is recommended that a sample (10–20 g) be dried overnight in a forced-air oven at 45 °C, a procedure that facilitates the next step. Grind the seed in a laboratory mill or coffee mill. If a coffee mill is used, the seed (5–10 g) should be milled for 20 s, mixed and then milled for a further 10 s. As some separation of meal components occurs during this process, the final product should be thoroughly mixed and be fine enough to pass through a standard 30-mesh sieve. If the result is to be expressed at a defined moisture content (e.g., for CEC purposes a 9% moisture content is specified) it is recommended that an accurate moisture determination be made on the above milled seed.

Without unnecessary delay, weigh ground seed meal (200 mg) into a clean, dry test-tube (Sovirel type) and, after pre-heating the tube (2 min) in a water-bath or heating block controlled at 75–76 °C, add approximately 3 ml of 70% V/V methanol (pre-heated to boiling point), stirring the suspension regularly for 10 min. Centrifuge the mixture and carefully decant and save the supernatant. Repeat the extraction and centrifugation steps twice more, heating for 5 min each time. Combine the three extracts and remove the methanol by rotary evaporation to give a volume of about 1 ml. Adjust the volume of this solution to exactly 10 ml with distilled water, mix well and freeze the solution (−18 °C) until required for analysis (solution A).

For each determination, prepare a Sephadex mini-column as described in the Appendix and wash the column by filling twice with distilled water, allowing it to drain each time. The flow through the column ceases when the water or solution reaches the surface of the gel.

Add solution A (4 ml) to the Sephadex mini-column, taking care to avoid disturbing the gel bed. Allow the column to drain and wash with water (2 × 0.5 ml) followed by 0.02 M pyridine acetate buffer (2 × 0.5 ml), allowing each addition to drain completely. Discard all effluents. Wipe the column tip clean, place a clean, dry vial beneath the column and add myrosinase solution (0.25 ml) to the surface of the gel, collecting the effluent.

After 2 h at room temperature (25 °C), elute the liberated glucose by adding water (0.5 ml) and allowing the column to drain fully before adding a further aliquot of water (0.5 ml). Collect the effluent (final volume 1.25 ml) (solution B). If necessary, solution B may be kept frozen (−18 °C) until required for glucose assay.

Determination of Glucose

When the Glucose Kit No. 115A is used in accordance with the manufacturer's instructions low absorbances result and it is recommended that the volume of test solutions and of the standard glucose solution (1 mg ml⁻¹ of glucose) be increased from 10 to 100 µl. A linear response is obtained up to approximately 1.2 mg ml⁻¹ of glucose but above this concentration there is a marked deviation from linearity. If a glucose value higher than 1.0 mg ml⁻¹ is obtained, dilute the original solution B and repeat the assay.

Calculation

Let the mass of milled seed extracted be M g and the volume of solution A applied to the Sephadex mini-column be V ml. Then,

glucosinolates in seed (µmol g⁻¹)

$$= \frac{\text{glucose in solution B (mg ml}^{-1}) \times 1.25 \times 10 \times 1000}{M \times V \times 180}$$

$$= \frac{\text{glucose in solution B (mg ml}^{-1}) \times 69.4}{M \times V}$$

where 10 ml is the total volume of solution A, 1.25 ml is the total volume of solution B and 180 is the relative molecular mass of glucose.

Results and Discussion

To test the efficiency of the extraction, two samples of rapeseed were milled as described above and 200 mg of each weighed into separate dry tubes. The tubes and their contents was pre-heated at 75 °C and hot 70% V/V methanol (3 ml) was added to each. The resulting suspension was stirred regularly (10 min), cooled and centrifuged. The supernatant was decanted and saved and the residue was re-extracted with 70% V/V methanol (3 ml) for 5 min and then centrifuged. This procedure was repeated a further three times with the supernatant being saved separately each time. After removal of excess of methanol by rotary evaporation the whole of each extract was applied to separate DEAE-Sephadex A-25 mini-columns and the total glucosinolate content of each extract was determined as described above. The results (Table 1) show that the removal of glucosinolates was quantitatively achieved with three extractions.

To determine the time necessary to effect complete on-column hydrolyses under the specified conditions, 4 g of rapeseed were finely ground, extracted three times with aqueous methanol (70% V/V) and, after removal of the methanol by rotary evaporation, the volume was adjusted to 200 ml with water (equivalent to 200 mg of rapeseed in 10 ml).

Solutions of progoitrin (2.04 mg ml⁻¹), gluconapin (1.78 mg ml⁻¹) and glucobrassicin (2.26 mg ml⁻¹) were prepared.

Five different times of hydrolysis were compared for each of the following column loadings: extract (4 ml) + water (0.5 ml); extract (4 ml) + progoitrin solution (0.5 ml); extract (4 ml) + gluconapin solution (0.5 ml); and extract (4 ml) + glucobrassicin solution (0.5 ml).

After washing, all columns were treated with the same amount (0.25 ml) of myrosinase solution (25 mg ml⁻¹) and eluted with water (2 × 0.5 ml) at intervals of 1, 1.5, 2, 3 and 4 h after addition of the enzyme. The results (Table 2) indicate that the hydrolysis of endogenous glucosinolates and added glucosinolates is effectively complete after 1.5–2 h and it may be concluded that, under the conditions specified, 2 h is a sufficient time for the quantitative release of glucose from rapeseed glucosinolates.

In the recommended procedure an improvement in sensitivity, particularly for low-glucosinolate rapeseed, is obtained by

Table 1. Effect of repeated extractions on the glucosinolate content of two samples of rapeseed

Extract (3 ml)	Time/min	Glucosinolate in seed/µmol g⁻¹	
		Sample A	Sample B
1	10	43.94	26.48
2	5	9.97	5.47
3	5	1.72	0.94
4	5	0.13	0.13
5	5	0.03	—

Table 2. Effect of the time of on-column hydrolysis on the measured glucosinolate content of a rapeseed extract with and without added glucosinolates

Hydrolysis time/h	Glucosinolate content in seed/μmol g^{-1}			
	Extract + water	Extract + progoitrin	Extract + gluconapin	Extract + glucobrassicin
1	20.3	47.7	48.3	44.6
1.5	21.5	48.9	48.8	45.8
2.0	20.9	49.2	48.5	46.8
3.0	20.5	48.9	47.3	46.0
4.0	21.3	49.0	48.5	46.4

Table 3. Effect of column loading on accuracy

Column loading/ ml	Glucose found/ mg ml^{-1}	Rapeseed glucosinolate content in seed/ μmol g^{-1}
1	0.192 0.190	66.0
2	0.387 0.386	66.7
3	0.580 0.582	67.2
4	0.763 0.772	66.6

Table 4. Analysis of eight rapeseed samples for glucosinolate content using the modified method and comparison with two other methods. All results are expressed as μmol g^{-1} of seed at 9% moisture

		Glucose release				CEC HPLC method	
		Old method		Modified method			
	Sample	Results	Mean	Results	Mean	Results	Mean
A	.. .. ..	62.70 64.38	63.54	64.93 65.85	65.39	66.71 69.65	68.18
B	.. .. ..	33.88 33.57	33.73	35.28 33.90	34.59	36.22 36.34	36.28
C	.. .. ..	59.50 60.44	59.97	60.21 59.53	59.87	64.93 64.39	64.66
D	.. .. ..	66.14 66.64	66.40	67.30 67.39	67.35	62.58 62.47	62.53
E	.. .. ..	58.94 60.16	59.59	61.95 59.18	60.57	56.93 58.09	57.51
F	.. .. ..	61.82 61.42	61.62	60.39 61.85	61.12	65.01 63.69	64.35
G	.. .. ..	31.10 32.25	31.68	33.93 33.05	33.49	34.72 33.56	34.14
H	.. .. ..	64.20 66.63	65.42	67.75 69.02	68.38	68.47 66.63	67.55

the addition of 4 ml of extract to the DEAE-Sephadex A-25 mini-columns. Table 3 shows that column loadings of up to 4 ml of a normal rapeseed extract can be safely used without loss of accuracy.

To check the reproducibility of the method, a sample of rapeseed was analysed on ten occasions during 4 weeks. Each analysis was performed in triplicate (including milling) and the mean results were 60.9, 61.8, 60.8, 59.2, 60.3, 62.7, 63.0, 60.9, 62.8 and 59.6 μmol g^{-1}, with an over-all mean of 61.2 μmol g^{-1}. The standard deviation was 1.24 μmol g^{-1} and the coefficient of variation was 2.03%.

Eight samples of rapeseed were analysed using the proposed procedure and the results were compared with those obtained using the original method (Table 4). The same samples were also analysed by the HPLC procedure submitted to the CEC. The total glucosinolate content was determined by adding the individual glucosinolate contents.

The results in Table 4 show that there is close agreement between the two glucose release methods, indicating that the removal of oil prior to extraction of glucosinolates is an unnecessary complication. Comparison of the glucose release figures with those obtained by HPLC shows that there is reasonable agreement.

Conclusions

Quantitative removal of oil, as recommended in the earlier method, is a difficult step which may account to a significant extent for the relatively poor agreement found between laboratories using this procedure. The proposed method eliminates this problem and, although it is possible that procedures could be further improved or simplified, it is considered that it is a reliable means of determining the glucosinolate content of rapeseed.

Appendix

Prepare DEAE-Sephadex A-25 mini-columns as follows. Warm the end of a Pasteur pipette (short-form) in a flame and insert a 2-μl Microcap pipette (Drummond Scientific Broomall, PA, USA) such that it protrudes approximately 1 cm. Hold the Pasteur pipette horizontal and introduce a drop of molten paraffin wax into the gap between the two pipettes, allowing the wax to fill the gap. Firmly plug the bottom of the Pasteur pipette with fine glass-wool and wash with distilled water. Add a suspension of DEAE-Sephadex A-25 (1 ml) and allow the column to drain. After washing with distilled water the column is ready for use. With practice it is simple to produce columns with reproducible flow-rates and performance and at very low cost.

References

1. Bunting, E. S., *Editor*, "Production and Utilization of Protein in Oilseed Crops," Martinus Nijhoff for CEC, The Hague, 1981.
2. Fenwick, G. R., *J. Assoc. Publ. Anal.*, 1984, **22**, 117.
3. Heaney, R. K., and Fenwick, G. R., *J. Sci. Food Agric.*, 1980, **31**, 593.
4. Daun, J. K., and McGregor, D. I. "Glucosinolate Analysis of Rapeseed," Method of the Canadian Grain Commission, Agriculture Canada, Winnipeg, 1983.
5. Slominski, B. A., and Campbell, L. D., *J. Sci. Food Agric.*, 1987, **40**, 131.

6. Møller, P., Olsen, O., Plöger, A., Rasmussen, K. W., and Sørensen, H., *in* Sørensen, H., *Editor*, "Advances in the Production and Utilization of Cruciferous Crops," Nijhoff/Junk for CEC, Dordrecht, 1985, pp. 111–126.
7. Sang, J. P., and Truscott, R. J. W., *J. Assoc. Off. Anal. Chem.*, 1984, **67**, 829.
8. Spinks, E. A., Sones, K., and Fenwick, G. R., *Fette Seifen Anstrichm.*, 1984, **86**, 228.
9. "Rape and Rapeseed: Determination of Glucosinolate Content," Official Journal of the European Community No. L210/55. Community Regulation (EEC) No. 2435/86, 29th July, 1986.
10. Heaney, R. K., Spinks, E. A., Hanley, A. B., and Fenwick, G. R., "Analysis of Glucosinolates in Rapeseed," Agriculture and Food Research Council Technical Bulletin, AFRC Food Research Institute, Norwich, 1984, pp. 1–25.
11. Thies, W., *Fette Seifen Anstrichm.*, 1985, **87**, 347.
12. Smith, C. A., and Dacombe, C., *J. Sci. Food Agric.*, 1987, **38**, 141.
13. Thies, W., *Fette Seifen Anstrichm.*, 1982, **84**, 338.
14. Møller, P., Plöger, A., and Sørensen, H., *in* Sørensen, H., *Editor*, "Advances in the Production and Utilization of Cruciferous Crops," Nijhoff/Junk for CEC, Dordrecht, 1985, pp. 97–110.
15. Starr, C., Suttle, J., Morgan, A. G., and Smith, D. B., *J. Agric. Soc. Camb.*, 1985, **104**, 317.
16. Biston, R., Dardenne, P., Cwikowski, M., Wathelet, J.-P., and Severin, M., *in* Wathelet, J.-P., *Editor*, "Glucosinolates in Rapeseed—Analytical Aspects," Nijhoff/Junk for CEC, Dordrecht, 1987, pp. 163–172.
17. Renard, M., Bernard, C., Deschamps, M., Furtoss, V., Lila, M., Quinsac, A., Regnier, J. M., and Ribaillier, D., *in* Wathelet, J.-P., *Editor*, "Glucosinolates in Rapeseed—Analytical Aspects," Nijhoff/Junk for CEC, Dordrecht, 1987, pp. 173–176.
18. Schnug, E., and Haneklaus, S., *Fett. Wiss. Tech.*, 1987, **89**, 32.
19. Schnug, E., and Haneklaus, S., *Fresenius Z. Anal. Chem.*, 1987, **326**, 441.
20. Appelqvist, L. A., and Josefsson, E., *J. Sci. Food Agric.*, 1967, **1**, 510.
21. Wilkinson, A. P., Rhodes, M. J. C., and Fenwick, G. R., *Anal. Biochem.*, 1984, **139**, 284.

Optical Sensors

Part 34. Fibre Optic Glucose Biosensor With an Oxygen Optrode as the Transducer

Wolfgang Trettnak, Marc J. P. Leiner and Otto S. Wolfbeis*
Analytical Division, Institute of Organic Chemistry, Karl-Franzens University, A-8010 Graz, Austria

A biosensor for the continuous determination of glucose is presented. Glucose oxidase was immobilised covalently on a nylon membrane and the consumption of oxygen was measured by following, via fibre optic bundles, the changes in the fluorescence of an oxygen-sensitive dye whose fluorescence is quenched dynamically by molecular oxygen. The dye is dissolved in a very thin silicone membrane placed beneath the enzyme layer. As a result of the oxidation by the enzyme a certain amount of oxygen is consumed. This amount is indicated by the fluorescent dye. The measurements were performed in flowing air-saturated solutions containing 0.1 M pH 7.0 phosphate buffer. The effects of the amount of immobilised enzyme and the thickness of the indicator layer on response times (t_{90} = 1–6 min), analytical ranges (0.1–20 mM) and relative signal changes (up to 26%) were investigated.

Keywords: *Glucose biosensor; oxygen optrode*

The determination of glucose in clinical analysis is essential for the diagnosis of diabetic patients and for the development of an artificial endocrine pancreas. In the microbiological and food industries a glucose sensor is considered to be very desirable for process control. A variety of methods for the determination of glucose are known, of which the enzyme-based assays are considered to be the most specific. Of these methods, those that utilise the enzyme glucose oxidase (GOD) are the most widespread. GOD catalyses the oxidation of glucose according to the following equation:

$$\text{D-Glucose} + \text{O}_2 \xrightarrow{\text{GOD}} \text{D-gluconolactone} + \text{H}_2\text{O}_2 \quad .. \quad (1)$$
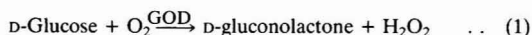
Glucose can be determined by measuring (a) the production of hydrogen peroxide, (b) the production of gluconic acid, into which D-gluconolactone is rapidly converted and which lowers the pH of the solution or (c) the consumption of oxygen.

The first amperometric enzyme electrode using immobilised glucose oxidase in combination with an oxygen electrode was developed by Clark and Lyons.[1] These workers measured the consumption of oxygen due to the activity of the enzyme and developed a device that is now referred to as a "glucose biosensor." The system was later improved by Updike and Hicks[2] who used two amperometric oxygen electrodes to remove interferences due to variations in the levels of oxygen; glucose oxidase was immobilised in polyacrylamide. Further improvements were made by Mascini and co-workers[3,4] and by Bardeletti *et al.*[5] by immobilising the enzyme on nylon nets or nylon membranes.

This paper describes a fibre optic glucose sensor, based on the same enzymatic reaction as the biocatalytic recognition process, but which is coupled to a fibre optic oxygen transducer. Although an optical glucose sensor (an enzyme "optode") has already been described by Uwira *et al.*,[6] their approach is somewhat impractical. These workers used pyrenebutyric acid (PBA) as a fluorescence indicator and glucose oxidase immobilised in a glutaraldehyde - bovine serum albumin matrix. The most serious drawback of this type of device is that it cannot easily be coupled to a conventional fibre optic system because PBA has an excitation wavelength in the UV region and this is not compatible with the transmission characteristics of glass or plastic fibres. In addition, the indicator was not actually immobilised, but rather dissolved in a viscous solvent; hence, it is subject to slow wash-out because of its appreciable solubility in water; the experimental arrangement is also fragile. A similar device, but using an unspecified indicator dissolved in a polymer layer, has been described by Kroneis and Marsoner.[7]

Experimental

Materials

Glucose oxidase (E.C. 1.1.3.4.; Type II, from *Aspergillus niger*) with a specific activity of 24 000 U per gram of solid was obtained from Sigma (Munich, FRG). The Immunodyne immunoaffinity membrane, which was made of nylon 6-6, having a porosity of 200 nm, a thickness of approximately 75 μm and with chemically activated carboxyl groups on the surface, was obtained from Pall (Glen Cove, New York, USA).

Decacyclene, which has a low solubility in silicone, was rendered polymer-soluble by butylation according to a published method.[8] The transparent silicone pre-polymer (Elastosil E43) was obtained from Wacker-Chemie (Burghausen, Munich, FRG). All other chemicals were of analytical-reagent grade.

Apparatus

Optical measurements were performed with an Oriel 3090 fibre optic photometer (Chelsea Instruments, London, UK) equipped with a xenon lamp pulsed at 9 Hz. The excitation filter was a 410-nm narrow band pass interference filter. Light was guided through the input bundle of a bifurcated fibre optic to the flow-through cell and the fluorescence was collected and guided back to the photometer through the output bundle. The emission filter was a 450-nm cut-off glass filter (Schott KV 450), which showed good transmission above 450 nm. The light guide, consisting of a bifurcated fibre optic bundle formed from poly(methyl methacrylate) (Faseroptik Henning, Allersburg, FRG), was 1.5 m long with an internal diameter of 3.5 mm per single bundle (with 30 fibres per bundle) and of 4.5 mm at the common end.

The flow-through cell was machined from stainless steel and had a chamber volume of approximately 20 μl. The buffer and glucose solutions were pumped through the cell at a typical flow-rate of 1.2 ml min⁻¹. Fig. 1 shows a cross-section through the flow-through cell and the alignment of the fibre.

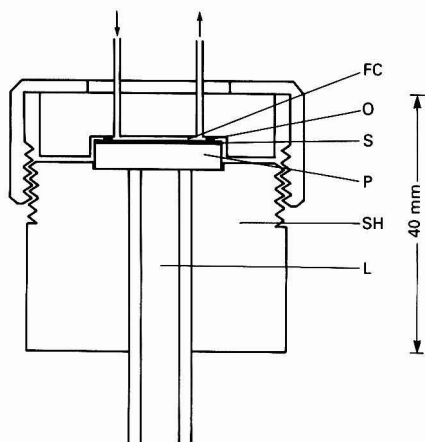* To whom correspondence should be addressed.

Fig. 1. Schematic diagram of the flow-through cell and alignment of the fibre end. FC, Flow-through chamber; O, O-ring; S, sensing platelet; P, Plexiglas disc; SH, stainless-steel housing; and L, light guide
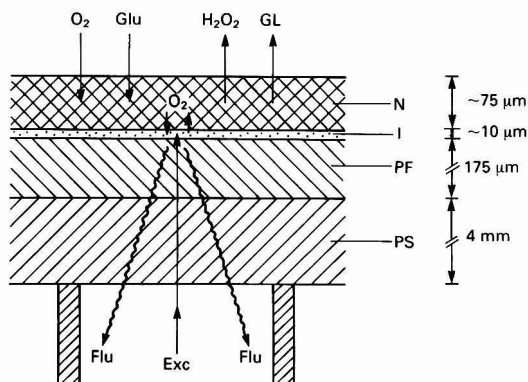

Fig. 2. Cross-section through the sensing layer of the fibre optic glucose sensor. PS, Plexiglas support; PF, polyester film; I, indicator layer (decacyclene dissolved in silicone); and N, nylon membrane with enzyme immobilised on its surface. The arrows indicate the diffusion processes involved (Glu, glucose; and GL, gluconolactone). The directions of the exciting light (Exc) and fluorescence (Flu) are also shown

Immobilisation Procedure

The immunoaffinity membrane, 2 cm in diameter, with a thickness of approximately 75 μm and with chemically activated carboxyl groups on its surface, was immersed in a solution of 8 mg of glucose oxidase in 2 ml of pH 7.4 phosphate-buffered saline for periods varying from 10 min to 24 h. The membrane was then washed with 0.1 M pH 7 phosphate buffer and stored in a refrigerator at 4 °C in the same buffer containing 0.1% sodium azide as a bactericide.

Preparation of the Oxygen Sensing Layer

A 20-mg amount of solubilised decacyclene was dissolved in 1.0 ml of toluene. This solution was mixed with 1.0 g of silicone pre-polymer, spread on to a 175-μm polyester film to a thickness of about 20 μm and then left to polymerise at 50 °C for 24 h. After evaporation of the solvent and curing of the residue in ambient air, the thickness of the indicator layer was approximately 10 μm. Similarly, 25 and 50 μm thick oxygen-sensitive layers were prepared by using 2.0 mg of solubilised decacyclene in 1.0 ml of toluene and 1.0 g of silicone. The use of 2.0 mg of indicator per millilitre of toluene was found to be sufficient in this instance because the thicker layers gave adequate fluorescence even at this low concentration of dye. Discs (20 mm) of the oxygen sensors were cut and stored in 0.1 M pH 7.0 phosphate buffer.

Assembly of the Glucose Sensor

The nylon 6-6 membrane containing the immobilised glucose oxidase was laid on to an oxygen sensor disc and both were placed in the flow-through cell, before being firmly attached together by means of a rubber O-ring (see Fig. 1). A schematic diagram of the arrangement and a representation of the glucose-sensitive chemistry at the fibre end, together with the diffusion processes involved, are shown in Fig. 2.

When not in use, the enzyme membranes were stored at 4 °C in 0.1 M pH 7.0 phosphate buffer containing 0.1% sodium azide. Glucose solutions were prepared fresh daily and air-saturated solutions in 0.1 M pH 7.0 phosphate buffer were used. All measurements were performed at 22 ± 1 °C.

Results

Enzyme Membrane

The immunoaffinity membrane is made from nylon that has a chemically pre-activated surface with a high density of

Fig. 3. Stern - Volmer plot of the quenching of the fluorescence of the glucose sensor by oxygen in aqueous solution at 22 °C and at a barometric pressure of 727 Torr (96.9 kPa). Curve A is plotted according to equation (2); curve B is false-light-corrected according to equation (3), with $K_{sv} = 0.0026$ Torr^{-1}. The calibration points are encircled

covalent binding sites. The immobilisation procedure is very simple and proceeds smoothly under mild conditions, viz., the membrane is immersed in a solution of the enzyme in a suitable buffer (such as phosphate-buffered saline) at room temperature. The enzyme is bound to the nylon membrane via the chemically activated carboxyl groups and the amount of enzyme immobilised can easily be regulated by selection of the appropriate reaction time.

The membrane shows good porosity and possesses a high surface area, chemical stability, mechanical resistance and flexibility. We found that the recommended method of immobilisation gave much more reproducible results than those methods based on a sequence of chemical reactions. The type of membrane described in this work has been used successfully in amperometric enzyme electrodes.[5]

Choice of Indicator

Decacyclene shows a high photostability and gives a quantum yield of 0.29 in toluene.[9,10] Its excitation maximum is at 385 nm, but because it gives a broad absorption band, it can also be excited in the visible region, for example at 410 nm, with
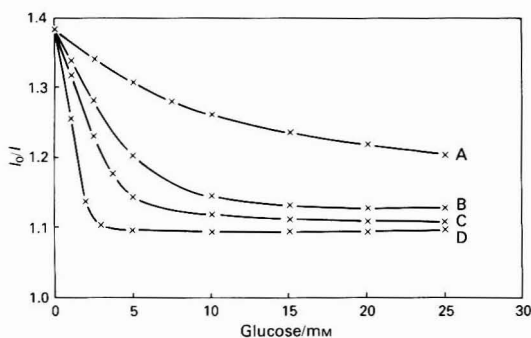
Fig. 4. Calibration graphs for four types of glucose sensor (A, B, C and D) with different amounts of immobilised enzyme; characteristic data for the sensors are given in Table 1. All measurements were performed in air-saturated 0.1 M phosphate-buffered solutions at pH 7.0 and 22 °C
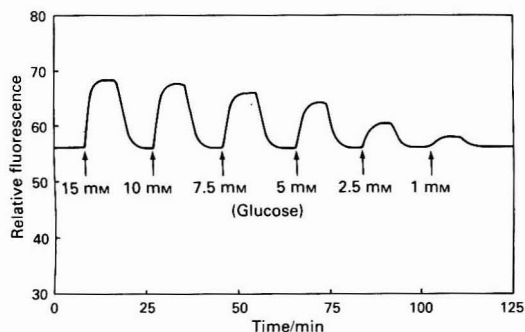

Fig. 5 Typical time-response curve for the glucose sensor B towards glucose solutions passing at a flow-rate of 1.2 ml min⁻¹ at 22 °C. All solutions were air-saturated and contained 0.1 M pH 7.0 phosphate buffer

adequate efficiency. The emission band is very broad, ranging from *ca.* 450 to *ca.* 600 nm, with a maximum at 510 nm. This band is due to an excimer emission and is only observed in fairly concentrated decacyclene solutions, whereas in very dilute solutions, the fluorescence is blue (from the monomer).

Solubilised decacyclene, in contrast to unmodified decacyclene, exhibits excellent solubility in solvents such as toluene and silicone, a property that is extremely important, because good polymer solubility is a prerequisite if thin indicator layers (*e.g.*, 0.01 mm) with sufficient fluorescence intensities are to be prepared.

A Stern - Volmer plot of the quenching by oxygen of the fluorescence of decacyclene in the glucose sensor in aqueous solution at 22 °C and at 727 Torr (96.9 kPa) is shown in Fig. 3. The false-light-corrected quenching constant K_{sv} is 0.0026 Torr⁻¹. A method for the calculation of false-light-corrected quenching constants is given in the Appendix.

Dynamic Response

Fig. 4 shows the calibration graphs obtained for four glucose sensors having different amounts of enzyme immobilised on the nylon membrane. The signal changes and analytical ranges of the sensor depend mainly on the total enzyme activity in the layer. A high enzyme activity is capable of producing and maintaining a larger oxygen gradient across the membrane and, therefore, giving a more distinct signal change. On the other hand, when large amounts of enzyme are used, saturation is soon reached, because oxygen is consumed rapidly in the membrane. Hence, the analytical range of the

sensor remains small, whereas with smaller amounts of immobilised enzyme larger analytical ranges are achieved.

The response time (Fig. 5) depends on the enzyme activity and the thickness of the indicator layer. A higher enzyme activity gives rise to a shorter response time, and *vice versa*. We ultimately used 10 μm thick indicator layers only, because thicker indicator layers (*e.g.*, 25 and 50 μm) resulted in prolonged response times with no change in the shape of the calibration graphs. Typical response times and other figures of merit for six glucose sensors are summarised in Table 1. The detection limit is between 0.05 and 0.1 mM glucose and the standard deviation for 10 replicate measurements is ±2.4%. The pH dependence of the glucose probe is shown in Fig. 6; a relatively broad pH maximum is observed, with a useful range from pH 4 to 7.5.

Discussion

The results demonstrate that a fibre optic glucose sensor based on an enzymatic reaction and coupled to an oxygen optrode can be a very simple, sensitive and highly specific system. The sensing layer consists of two parts: a nylon membrane with the glucose oxidase enzyme immobilised on its surface and an indicator layer of decacyclene in silicone.

For a mathematical treatment of the response curves various diffusion processes and kinetic parameters have to be considered (Fig. 2). Glucose and oxygen must diffuse to the enzyme in the nylon membrane, whereas gluconolactone (gluconic acid) and hydrogen peroxide diffuse out of the sensing indicator layer. In the sensing layer, an oxygen gradient is created, which leads to a change in the fluorescence because molecular oxygen is a dynamic quencher of the fluorescence of decacyclene. The oxygen gradient is influenced by the thickness of the nylon membrane, the diffusional constant of oxygen, the activity of the enzyme, the pH in the vicinity of the enzyme and the oxygen concentration in the sample solution.

The linear ranges of the calibration graphs can be described by using a modified form of the Stern - Volmer equation in which an additional term, K'[glucose], is subtracted; this term accounts for the consumption of oxygen[11]:

$$I_0/I = 1 + K_{sv}[O_2] - K'[glucose] \quad .. \quad .. \quad (2)$$

I_0 and I are the fluorescence intensities of the sensor in the absence and presence, respectively, of the oxygen quencher in the sample solution and K_{sv} is the Stern - Volmer constant. K' is an empirical parameter that accounts for the various diffusion processes and the kinetics of the enzyme reaction, which are difficult to describe mathematically. Unfortunately, K' is also a function of the concentration of oxygen from which it can be deduced that an unambiguous relationship between the glucose concentration and I only exists if the oxygen concentration is constant.

With regard to the lifetimes of the sensor, the sensors showed a stable response for at least 5 months, after an initial decrease in the relative signal change during the first week; this is probably due to enzyme molecules that are weakly linked to the polymeric surface leaching out. Similar observations have been reported by Mascini *et al.*[4]

The normal blood glucose level is about 5 mM, but in pathological cases it can increase to as high as 50 mM. To be of use in clinical chemistry and in *in vivo* monitoring, an analytical range of between 1 and 20 mM is preferable. Such a range is covered by this type of sensor, provided that the appropriate amount of enzyme is immobilised (Fig. 4). A similar analytical range is required when using glucose sensors in biotechnology, for which glucose is one of the preferred microbial substrates.

The system can easily be adapted for other applications by immobilising other enzymes or by using a combination of two

Table 1. Figures of merit for six glucose sensors with different amounts of immobilised enzyme and thicknesses of the indicator layer. All measurements were performed in air-saturated solutions of 0.1 M phosphate buffer at pH 7.0 and with glucose concentrations of 0–25 mM. The flow-rate was 1.2 ml min⁻¹

| Sensor | Thickness of indicator layer/μm | Time of enzyme immobilisation* | Analytical range/mM | Response time | | Washing time§/min |
				t_{90}†/min	t_{100}‡/min	
A	10	10 min	0.1–20.0	2.5–3.5	5.0–6.5	5.5–8.5
B	10	30 min	0.1–10.0	2.0–3.0	5.0–6.0	5.0–8.5
C	10	60 min	0.1–6.0	1.0–3.0	2.0–5.0	6.5–7.5
D	10	24 h	0.05–3.0	1.0–3.0	1.5–5.0	6.0–7.0
E	25	10 min	0.1–20.0	3.0–4.0	5.5–7.5	7.0–9.0
F	50	10 min	0.1–20.0	5.5–6.0	9.5–11.5	8.5–12.5

* Time for which the nylon membrane was immersed in the enzyme solution.
† Time after which 90% of the total signal change was reached.
‡ Time after which the signal remained constant.
§ Time taken for signal to return to the base line after washing with buffer.
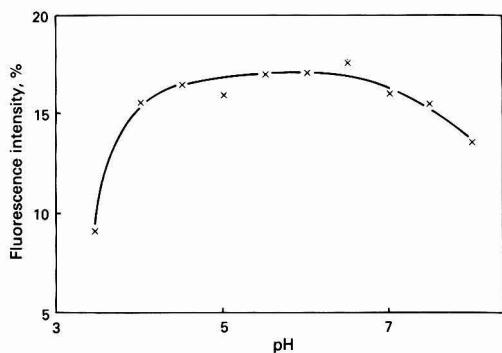
Fig. 6. Determination of the pH dependence of the response of the glucose sensor D towards a single dose of a 2 mM glucose solution. Measurements were performed in 0.1 M phosphate buffer at 22 °C in air-saturated solutions

or more enzymes. A typical bi-enzyme system has been incorporated in a sensor for the determination of maltose by using the enzymes amyloglucosidase and glucose oxidase,³ with a glucose-sensing electrode acting as a transducer.

Appendix

Determination of Quenching Constants in the Presence of Stray Light

The fluorescence intensity I_x of an indicator is related to the actual concentration of a quencher $[Q]_x$ (such as oxygen) by the Stern - Volmer equation

$$I_0/I_x = 1 + K_{sv}[Q]_x \quad .. \quad .. \quad .. \quad (3)$$

where I_0 and I_x are the fluorescence intensities in the absence and presence, respectively, of a quencher Q, and K_{sv} is the Stern - Volmer constant. To determine I_0 and K_{sv} from equation (2), a two-point calibration is required. For calibration at a zero oxygen concentration, water purged with pure nitrogen can be used together with another solution of defined oxygen concentration $[Q]_x$, e.g., water equilibrated with air.

In practice, we sometimes encountered difficulties in our experimental set-up in establishing a linear relationship between I_0/I_x and the oxygen concentration $[Q]_x$ (Fig. 3, curve A). This is due to the fact that a constant level of oxygen-independent light intensity is passing the filter system. In some commercial instruments, such blanks, together with the electronic and photomultiplier blanks ("noise"), can be set manually to zero and ambient background light can be subtracted electronically.

There are, however, some sources of error in intensity measurements that are responsible for a constant signal background level but cannot be removed by manual or electronic subtraction. We will refer to this type of light as "false light." It can be caused by: (a) light from the xenon lamp passing the blocking region of the interference filter; (b) "cross talk" between the fibres of the input and output bundles; (c) mirror-type reflection at the interface between the light guide and the sensor support; (d) diffuse reflection; (e) Rayleigh scattering by molecules or aggregates of molecules; (f) Mie scattering by particles of colloidal size in the sensing layers; and (g) the intrinsic background fluorescence of the sensor material and the fibres. This false light is often more intense than the fluorescence of the indicator itself; when it enters the output bundle it cannot be removed entirely by the secondary ("emission") filter.

As a typical example, the emission filter used in this work has a mean transmission of about 0.25% in the range 400–420 nm. Given the low intensity of the fluorescence, serious levels of false light are encountered because 0.25% of the reflected and scattered violet excitation light passes this filter. The use of a cut-off wavelength higher than 450 nm or of an interference filter as the emission (secondary) filter results in considerable losses in signal intensity.

Another important source of false light is Raman scatter caused by the presence of water in the enzyme layer. This occurs at a longer wavelength than the incident exciting light (the shift is ca. 3300 cm⁻¹) and can, therefore, pass the emission filter without any losses being incurred. A final source of false light in this work is the white light from the excitation beam, which first passes a narrow band pass interference filter (with transmissions of 58% at 410 nm and 0.5% at 400 and 420 nm). Although the mean transmission is only 10⁻⁵% outside the range 400–420 nm, this light passes the emission filter with almost no loss in intensity and gives rise to an oxygen-independent optical signal at the photomultiplier.

The intensity of this false light (I_f) can be determined by using a blank sensor containing no fluorescent indicator. However, because of the various thicknesses of the sensors, the sensitivity of the stray light intensity towards small positional changes and some stretching of the sensors in the flow-through cell, we found this approach to be of little practical value. A more attractive approach is to determine the false light together with K_{sv} by means of a three-point calibration, as described below.

As the apparent value, I'_0, measured by the instrument, is composed of the "true" value I_0 and a certain amount of false light, we can set I_0 equal to $(I'_0 - I_f)$ and, by analogy, I_x equal to $(I'_x - I_f)$. Equation (3) can now be rewritten¹⁰ as:

$$(I'_0 - I_f)/(I'_x - I_f) = 1 + K_{sv}[Q]_x .. \quad .. \quad (4)$$

I'_0 and I'_x are the intensities measured by the detector in the absence and presence, respectively, of the quencher at a concentration $[Q]_x$; I_f is considered to be independent of the concentration of the quencher.

Values for I_f and K_{sv} were calculated from the intensity values I'_1, I'_2 and I'_3, obtained from three measurements at three different quencher concentrations $[Q]_1$, $[Q]_2$ and $[Q]_3$, respectively (Fig. 3, curve B):

$$K_{sv} = \frac{I'_1([Q]_2 - [Q]_3) + I'_2([Q]_3 - [Q]_1) + I'_3([Q]_1 - [Q]_2)}{I'_1[Q]_1([Q]_3 - [Q]_2) + I'_2[Q]_2([Q]_1 - [Q]_3) + I'_3[Q]_3([Q]_2 - [Q]_1)} \quad (5)$$

and

$$I_f = \frac{I'_1(1 + K_{sv}[Q]_1) - I'_3(1 + K_{sv}[Q]_2)}{K_{sv}([Q]_1 - [Q]_3)} \quad \cdot\cdot \quad (6)$$

In practice, for tonometered (gas-equilibrated) liquids, it is difficult to obtain a calibration point for an absolutely oxygen-free aqueous solution (I'_0). The zero oxygen value was, therefore, calculated preferentially from the following equation, which can be derived from equation (4):

$$I'_0 = I'_1 + I'_1 K_{sv}[Q]_1 - I_f K_{sv}[Q]_1 \cdot\cdot \quad \cdot\cdot \quad (7)$$

All quenching constants given in this work are corrected for false light.

References

1. Clark, L. C., and Lyons, C., *Ann. N.Y. Acad. Sci.*, 1962, **102**, 29.
2. Updike, S. J., and Hicks, G. P., *Nature (London)*, 1967, **214**, 986.
3. Mascini, M., Iannello, M., and Palleschi, G., *Anal. Chim. Acta*, 1983, **146**, 135.
4. Mascini, M., Mazzei, F., Moscone, D., Calabrese, G., and Benedetti, M. M., *Clin. Chem.*, 1987, **33**, 591.
5. Bardeletti, G., Sechaud, F., and Coulet, P. R., *Anal. Chim. Acta*, 1986, **187**, 47.
6. Uwira, N., Opitz, N., and Lübbers, D. W., *Adv. Exp. Med. Biol.*, 1984, **169**, 913.
7. Kroneis, H. W., and Marsoner, H. J., *in* Schmid, R. D., Guilbault, G. G., Karube, I., Schmidt, H. L., and Wingard, L. B., *Editors*, "Biosensors International Workshop 1987," Verlag Chemie, Weinheim, 1987, p. 303.
8. Marsoner, H. J., Kroneis, H. W., and Wolfbeis, O. S., *Eur. Pat.*, 109 959, 1987; *US Pat.*, 4 587 101, 1987.
9. Wolfbeis, O. S., Posch, H. E., and Kroneis, H. W., *Anal. Chem.*, 1985, **57**, 2556.
10. Kroneis, H. W., *Dissertation*, Technical University of Graz, 1982, p. 60.
11. Völkl, K.-P., Grossmann, U., Opitz, N., and Lübbers, D. W., *Adv. Physiol. Sci.*, 1984, **25**, 99.

Chloride Chemical Sensor Based on an Organic Conducting Polypyrrole Polymer

Shaojun Dong, Zhisheng Sun and Ziling Lu

Changchun Institute of Applied Chemistry, Chinese Academy of Sciences, Changchun, Jilin 130021, People's Republic of China

The potential response behaviour of a chloride doped polypyrrole (PPy) polymer film electrode to chloride ion in solution has been examined. The effect of the polymerisation conditions on the characteristics of the potential response and response mechanism is discussed. A chloride ion-selective electrode based on a conducting PPy polymer film was prepared with a potential response slope of 58–60 mV (pCl$^-$)$^{-1}$ and a detection limit of 3.5×10^{-5} M of Cl$^-$. The optimum conditions for the preparation of the electrode were: pyrrole (Py), 0.05–0.2 M; LiCl, 0.1–1 M; scan range for electrochemical polymerisation, 0.5–1.2 V; polymerisation time, 10–30 min; and scan rate, 20–100 mV s^{-1}. The chemical sensor has a fast response, a low resistance, is easy to prepare and is not susceptible to poisoning.

Keywords: *Chloride ion-selective electrode; conducting polymers; polypyrrole; chemically modified electrode; electrochemical polymerisation*

Several investigations into organic conducting polymers have been carried out in recent years.[1–6] Much attention has been directed towards understanding the structure and properties of these polymers and to their possible uses as battery materials[7,8] and electrochromic devices,[9] etc. Our aim was to investigate the performance of a chemical sensor based on an organic conducting polymer film. This paper describes the stable potential response behaviour of a conducting polypyrrole (PPy) polymer film electrode prepared by electrochemical polymerisation on glassy carbon (GC) following doping with ions from an aqueous solution. As a result of these investigations, a chloride chemical sensor has been developed and information has been obtained on the interaction between the conducting polymer and the doping ions and also on the conducting mechanism involved.

Experimental

Reagents

Pyrrole (Py) (Fluka) was purified by distillation from CaH$_2$ and stored under a nitrogen atmosphere at low temperature, protected from light. LiCl and other reagents used were of analytical-reagent grade. Doubly distilled water was used throughout.

Electrochemical Polymerisation

The polypyrrole (PPy) polymer film was prepared on a glassy carbon (GC) surface from an aqueous solution containing Py and LiCl using cyclic voltammetry (CV) as described previously.[10] The thickness of the film was controlled by the polymerisation time, the number of scans made and the applied potential during the electrochemical polymerisation process. The electrochemical polymerisation was carried out with a CV 47 voltammograph (BAS). A conventional single compartment cell equipped with a platinum wire counter electrode and a saturated KCl - calomel reference electrode (SCE) with double salt bridges (whose external tube was filled with a 0.1 M Na$_2$SO$_4$ solution) was employed for the electrochemical polymerisation. The working electrode was a PTFE-coated GC disc electrode polished to a mirror finish with 0.3-µm Al$_2$O$_3$ powder.

Potential Measurement of the Film Electrode

A PPy polymer film electrode was used as the measuring electrode with the reference electrode described above. All potentials were measured on a Beckman Φ60 pH meter *versus* SCE. The electrochemical cell can be represented as follows:

Hg, Hg$_2$Cl$_2$, KCl (sat.) ‖ 0.1 M Na$_2$SO$_4$ |

Solution to be tested ‖ GC surface
PPy
film
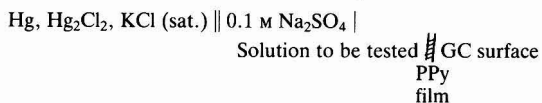
Results

Potential Response Behaviour of the PPy Polymer Film Electrode to Chloride Ion

The chloride doped PPy polymer film electrode shows a stable potential response in a solution containing Cl$^-$ ions after preparation and immersion in a Cl$^-$ solution for a period of time. Initially, the electrode potential drops rapidly with time, then more slowly after 2 h and reaches a stable value after 50 h. Hence, a suitable immersion time is about 2–3 d. After such treatment a Nernstian potential response is obtained in chloride ion solutions of different concentrations and the slope remains almost constant, but the response shifts to a more negative potential and the linear range becomes larger with increasing immersion times (see Fig. 1).

Effect of Preparation Conditions on the PPy Film Electrode Response Behaviour

Effect of Py concentration in the electrolyte solution

Fig. 2 shows the potential response curves of PPy film electrodes prepared in 0.1 M aqueous LiCl solutions containing various concentrations of Py. When the concentration of Py is low, the PPy polymer film obtained is thinner and the potential response is poor owing to the slowness of the polymerisation reaction. Hence, Py concentrations in the range 0.05–0.2 M were used.

Effect of Cl$^-$ doping ion concentration in the electrolyte solution

Table 1 gives the response behaviour of PPy film electrodes prepared in 0.05 M Py solutions containing various concentrations of the Cl$^-$ doping ion. When the Cl$^-$ doping ion concentration is less than 10^{-3} M, a Nernstian response is obtained, but the slope is low and unstable and the response disappears after 47 h. When the concentration of Cl$^-$ ions is 10^{-2} M, initially the potential response is almost Nernstian, but becomes non-linear after 24 h. However, when the PPy film
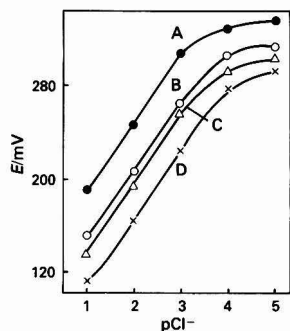
Fig. 1. Potential response of the Cl⁻ doped PPy polymer film electrode. Potential range, 0.5–1.2 V; polymerisation time, 20 min; scan rate, 20 mV s⁻¹. Solution 0.05 M Py + 0.1 M LiCl. Activation time: A, 5; B, 24; C, 46.5; and D, 75 h
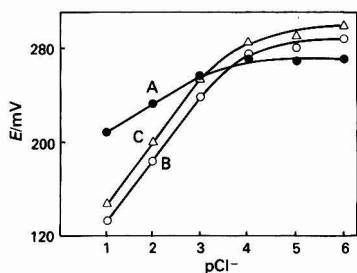

Fig. 2. Effect of Py concentration on the response behaviour of the Cl⁻ doped PPy polymer film electrode. Potential range, 0.5–1.0 V; polymerisation time, 20 min; scan rate 20 mV s⁻¹. Solution, 0.1 M LiCl. Py concentration: A, 0.01; B, 0.05 and C, 0.2 M

Table 1. Effect of Cl⁻ doping ion concentration in the electrolyte solution on the response behaviour of the PPy polymer film electrode. The polymerisation was carried out over the potential range 0.5–1.0 V for 20 min at 20 mV s⁻¹. Electrode area, 0.07 cm²

No.	Concentration of Cl⁻ doping ion/M	Activation time/h	Detection limit/M	Slope/mV (pCl⁻)⁻¹
D_1	10^{-3}	4	5.0×10^{-4}	37
		24	6.3×10^{-4}	23
		47	Non-linear response	
D_2	10^{-2}	4	1.0×10^{-3}	53
		24	2.5×10^{-3}	53
		47	Non-linear response	
D_3	10^{-1}	4	1.6×10^{-4}	60
		47	1.3×10^{-4}	60
		77	3.5×10^{-5}	60

electrode is prepared in a 10^{-1} M Cl⁻ solution, it gives a good stable Nernstian response with a low detection limit (see Table 1).

Response behaviour of PPy film electrodes prepared over various potential scan ranges

Fig. 3 shows the response curves of PPy film electrodes polymerised by CV over the potential ranges 0–0.5, 0.5–1.0, 1.0–1.5 and 0.7–1.2 V, respectively. It can be seen that the PPy film is not formed in the potential range 0–0.5 V, because no potential response is observed, *i.e.*, the electrochemical polymerisation reaction does not take place. Also, the PPy film electrode response becomes poor when the potential range is greater than 1.5 V owing to destruction of the film. The optimum scan range for electrochemical polymerisation is *ca.* 0.5–1.0 V.
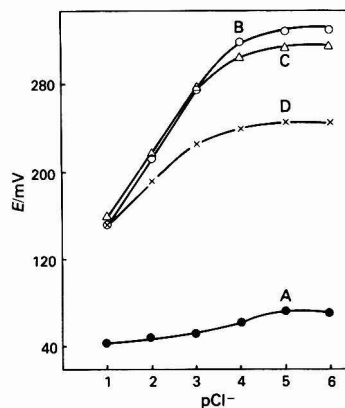
Fig. 3. Effect of potential scan range of the response behaviour of the Cl⁻ doped PPy polymer film electrode. Solution, 0.05 M Py + 0.1 M LiCl. Polymerisation time, 20 min; scan rate, 50 mV s⁻¹. Potential scan range: A, 0–0.5; B, 0.5–1.0; C, 0.7–1.2; and D, 1.0–1.5 V

Table 2. Effect of scan rate during polymerisation on the response behaviour of the Cl⁻ doped PPy polymer film electrode. Conditions: 0.05 M Py + 0.1 M LiCl; potential range, 0.5–1.2 V; polymerisation time, 20 min

No.	Scan rate/ mV s⁻¹	Activation time/h	Detection limit/M	Slope/mV (pCl⁻)⁻¹
B_1	20	5	3.2×10^{-4}	58
		24	1.8×10^{-4}	58
		75	7.9×10^{-5}	59
B_2	50	5	2.0×10^{-4}	60
		46.5	7.1×10^{-5}	60
		75	7.1×10^{-5}	60
B_3	100	5	2.5×10^{-4}	60
		24	1.3×10^{-4}	59
		46.5	2.5×10^{-4}	59
B_4	200	5	1.6×10^{-4}	60
		24	1.6×10^{-4}	60
		46.5	2.2×10^{-4}	60

Effect of potential scan rate during electrochemical polymerisation

The response of PPy film electrodes prepared by CV at various scan rates is shown in Table 2. Good response characteristics are observed for PPy film electrodes prepared in the scan rate range 20–200 mV s⁻¹, but the response becomes relatively poor when the scan rate is too fast, *i.e.*, greater than 200 mV s⁻¹.

Response behaviour of PPy film electrodes prepared at various final potentials

Table 3 gives the response of PPy film electrodes polymerised in 0.05 M Py + 0.1 M aqueous LiCl solutions over the potential range 0.5–1.0 V by CV scanning for 20 min, then kept at various final potentials for 5 min. The results show that all the PPy film electrodes prepared in this way exhibit good potential response characteristics regardless of the final potential. Because the ionic releasing and doping processes of PPy polymer films are different at different final potentials, the response potentials of these PPy film electrodes are also different—the response curves shift along the potential axis. As can be seen from Fig. 4, the more negative the final potential is, the more negative is the response.

Performance of a Chloride Ion-selective Electrode Based on a PPy Polymer Film

From the above experiments, the following conditions were selected for preparing the Cl⁻ doped PPy polymer film

Table 3. Response behaviour of Cl$^-$ doped PPy polymer film electrodes prepared at various final potentials. Conditions: 0.05 M Py + 0.1 M LiCl; potential range 0.5–1.0 V; polymerisation time, 20 min; and scan rate, 50 mV s^{-1}. Electrodes kept at the final potential for 5 min

No.	Final potential/V	Activation time/h	Detection limit/M	Slope/mV (pCl$^-$)$^{-1}$
E$_1$	0	2.5	1.3 × 10^{-4}	62
		21	7.9 × 10^{-5}	60
		45	6.3 × 10^{-5}	60
		75	4.5 × 10^{-5}	56
E$_2$	0.3	1	1.8 × 10^{-4}	60
		45	8.9 × 10^{-5}	60
E$_3$	0.7	1	2.5 × 10^{-4}	60
		21	1.3 × 10^{-4}	60
		45	7.9 × 10^{-5}	60
E$_4$	1.0	1	1.8 × 10^{-4}	58
		21	1.0 × 10^{-4}	58
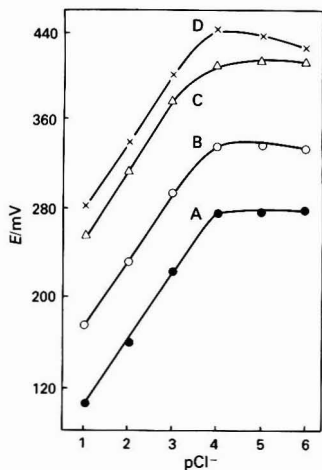
Fig. 4. Response behaviour of the Cl$^-$ doped PPy polymer film electrode prepared at various final potentials: A, 0; B, 0.3; C, 0.7; and D, 1.0 V. Scanned over 0.5–1.0 V in 0.05 M Py + 0.1 M LiCl for 20 min at 50 mV s^{-1}, then kept at the final potential for 5 min
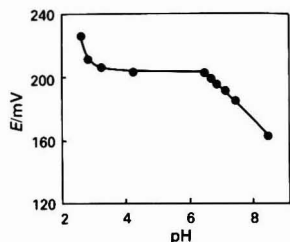
Fig. 5. Effect of pH on the potential response of the PPy film electrode in 10^{-3} M LiCl

electrodes: Py 0.05–0.2 M; LiCl 0.1–1 M; CV scan range, 0.5–1.2 V; polymerisation time, 10–30 min; and scan rate, 20–100 mV s^{-1}. The performance characteristics of the Cl$^-$ ion-selective electrode based on a PPy polymer film are as follows.

Detection limit and slope

A Nernstian response for 10^{-1}–10^{-4} M Cl$^-$ with a slope of 58–60 mV (pCl$^-$)$^{-1}$ is obtained with a detection limit down to 3.5 × 10^{-5} M of Cl$^-$. Although the detection limit is not particularly low, it is comparable to those of most other chloride-selective electrodes.

Appropriate pH range

Fig. 5 shows the relationship between pH and potential; it can be seen that the response potentials remain almost constant in the pH range 2.5–7 in a 10^{-3} M Cl$^-$ solution.

Selectivity

The interference effects of ten anions were studied and the resulting selectivity coefficients are given in Table 4. It can be seen that the potential response of the PPy film electrode is selective; those ions which cause the most severe interference are NO$_3$$^-$, HCOO$^-$, Br$^-$ and I$^-$.

Study of the Response Mechanism

The good potential response characteristics of the PPy polymer conducting material to chloride ions may be due to the formation of an ion associate between the large PPy cation, which has a highly conjugated structure, and the doping ion. During electrochemical polymerisation, Py is oxidised and polymerised to form a highly conjugated, linked cation, with the anion in solution entering the film to give simultaneous doping. It has been reported[10–12] that three or four Py groups can share a positive charge, so PPy is probably a large, highly conjugated series of linked cations with strong hydrophobic properties. When brought into contact with an aqueous solution, an interface is formed between the hydrophobic PPy film and the aqueous solution, resulting in an equilibrium distribution of chloride ions across the interface to yield a film potential, so that a potential response is observed for Cl$^-$ ions in aqueous solution. It is therefore expected that these large conjugated cations will give different ion associates with different anions, resulting in different properties for the conducting polymer films. As far as the potential response performance characteristics are concerned, the extent of this association should lead to an order of ionic selectivity. From the selectivity coefficients given in Table 4, the order of selectivity found is as follows: HCOO$^-$, NO$_3$$^-$ >I$^-$>IO$_4$$^-$>Br$^-$>ClO$_4$$^-$>F$^-$>CH$_3COO^-$>SSA$^-$ (5-sulphosalicylate) >SO$_4$$^{2-}$. The results show that the selectivity of the film is related to the ionic radius and charge of the anion. Anions such as NO$_3$$^-$, HCOO$^-$, Br$^-$ and I$^-$, whose unit charge radii are close to each other cause severe interference, whereas ions with small unit charge radii such as F$^-$ and SO$_4$$^{2-}$ and those with large unit charge radii such as ClO$_4$$^-$ and IO$_4$$^-$ cause slight interference. A large organic anion such as SSA$^-$ does not interfere. This means that repulsive interactions during polymerisation also play an important role in addition to the association process; hence, those ions that have similar ionic radii will mutually interfere. Therefore, it is possible to adjust the selectivity by changing the conditions used in the polymerisation process.

Table 5 gives the electrode potentials obtained for different cation solutions with the same Cl$^-$ ion concentration. It can be seen that the nature of the cation has no apparent effect on the potential, suggesting that under the experimental conditions used in this work, any cation present in the solution will not take part in the polymerisation process or enter the polymer film and will not, therefore, affect the performance of the PPy film electrode.

The most common use of chloride ion-selective electrodes has been as solid-state chloride electrodes.[13] Coetzee and Freiser[14,15] have prepared a liquid membrane electrode with an organic phase composed of Aliquat 336 S (i.e., salts of the tricaprylylmethylammonium ion) in decan-1-ol, and James et al.[16] have prepared a PVC membrane coated wire electrode. Compared with these liquid membrane and PVC membrane electrodes the electrode described here has a fast response, is easy to prepare and is not susceptible to poisoning, in contrast to the solid-state polymer membrane prepared by Oka et al.[17] Compared with the electrodes mentioned above, a notable

Table 4. Potential selectivity coefficients, $k_{i,j}{}^{\text{pot}}$, of Cl⁻ doped PPy polymer film electrodes

Interfering ion	$k_{i,j}{}^{\text{pot}}$	Interfering ion	$k_{i,j}{}^{\text{pot}}$
$SO_4{}^{2-}$	3.16×10^{-3}	$NO_3{}^-$	>1
F^-	1×10^{-1}	Br^-	3.98×10^{-1}
CH_3COO^- ..	6.3×10^{-2}	I^-	5.62×10^{-1}
$IO_4{}^-$	4.47×10^{-1}	SSA^-	1×10^{-2}
$ClO_4{}^-$	2.24×10^{-1}	$HCOO^-$ ..	>1

Table 5. Potential response of Cl⁻ doped PPy polymer film electrode in various cation electrolyte solutions

Electrolyte	Concentration/ M	Potential/ mV	Concentration/ M	Potential/ mV
LiCl	10^{-3}	183	10^{-2}	127
NaCl ..	10^{-3}	182	10^{-2}	126
KCl	10^{-3}	180	10^{-2}	124
NH_4Cl ..	10^{-3}	178	10^{-2}	126
$MgCl_2$ ..	5×10^{-4}	178	5×10^{-3}	123
$CaCl_2$ ..	5×10^{-4}	178	5×10^{-3}	125
$SrCl_2$ ..	5×10^{-4}	176	5×10^{-3}	123
$BaCl_2$ ..	5×10^{-4}	177	5×10^{-3}	127

feature of the electrode prepared in this work is that the film material is a conducting polymer and so the electrode resistance is very low. Further, the selectivity order of this type of electrode towards anions is different to that of other types of electrode and can be adjusted by varying the conditions of preparation.

Conclusion

An organic conducting PPy polymer film, prepared by electrochemical polymerisation in an aqueous solution containing Py and Cl⁻ ions, has been found to show a stable and selective potential response towards Cl⁻ ions in solution with a detection limit of 3.5×10^{-5} M of Cl⁻ and a slope of about 58–60 mV (pCl⁻)⁻¹. The electrode has a fast response, a low resistance and is insoluble in organic solvents.

References

1. Stotheim, T. A., Editor, "Handbook of Conducting Polymers," Volumes I and II, Marcel Dekker, New York, 1986.
2. Chiang, C. K., Fincher, C. R., Park, Y. W., Heeger, A. J., Shirakawa, H., Lowis, E. J., Gau, S. C., and MacDiarmid, A. G., *Phys. Rev. Lett.*, 1977, **39**, 1098.
3. Diaz, A. F., Kanazawa, K. K., and Gardini, G. P., *J. Chem. Soc., Chem. Commun.*, 1979, 635.
4. MacDiarmid, A. G., Mu, S., Somasiri, N. L. D., and Wu, W., *Mol. Cryst. Liq. Cryst.*, 1985, **121**, 187.
5. Garnier, F., Tourillon, G., Gazard, M., and Dubois, J. C., *J. Electroanal. Chem.*, 1983, **148**, 299.
6. Shacklette, L. W., Chance, R. R., Ivory, D. M., Miller, G. G., and Baughman, R. H., *Synth. Met.*, 1979, **1**, 307.
7. Kaufman, J. H., Mele, E. J., Heeger, A. J., Kaner, R., and MacDiarmid, A. G., *J. Electrochem. Soc.*, 1983, **130**, 571.
8. Kaufman, J. H., Chang, T. C., Heeger, A. J., and Wudl, F., *J. Electrochem. Soc.*, 1984, **131**, 2092.
9. Kobayashi, T., Yonegama, H., and Tamura, H., *J. Electroanal. Chem.*, 1984, **161**, 419.
10. Dong, S., and Ding, J., *Synth. Met.*, 1987, **20**, 119.
11. Salmon, M., Diaz, A. F., Logan, A. J., Kroubi, M., and Bargon, J., *Mol. Cryst. Liq. Cryst.*, 1982, **83**, 265.
12. Tourillon, G., and Garnier, F., *J. Electroanal. Chem.*, 1982, **135**, 173.
13. "Orion Specific Ion Electrode Model 92–17 Data Sheet," Orion Research, Cambridge, MA, 1980.
14. Coetzee, C. J., and Freiser, H., *Anal. Chem.*, 1968, **40**, 2071.
15. Coetzee, C. J., and Freiser, H., *Anal. Chem.*, 1969, **41**, 1128.
16. James, H., Carmack, G., and Freiser, H., *Anal. Chem.*, 1972, **44**, 856.
17. Oka, S., Sibazaki, Y., and Tahara, S., *Anal. Chem.*, 1981, **53**, 588.

Study of the Copper - Zinc Interference in Potentiometric Stripping Analysis

José Obiols, Ricardo Devesa and Antonio Malet

Department of Analytical Chemistry, C.E.T.S. Instituto Químico de Sarriá, Barcelona, Spain

The severe mutual interference between copper and zinc which occurs when working with a mercury film electrode in potentiometric stripping analysis has been studied. The results obtained are consistent with the formation of 1:1, 1:2 or 1:3 Cu - Zn compounds, depending on the experimental conditions. The gallium additions method, used for the elimination of this interference, does not give good results for solutions with a copper content that is very much greater than that of zinc, but it is effective for copper to zinc ratios of the order of unity or less, a situation that often occurs with environmental samples.

Keywords: *Potentiometric stripping analysis; copper - zinc interference; thin film electrode; gallium additions method*

Anodic stripping voltammetry (ASV) has been widely used for the determination of trace amounts of metals[1] owing to its excellent sensitivity, which is comparable to that of atomic absorption spectrometry (AAS), in the analysis of samples with a high saline content. In addition, the signal obtained by ASV is specific for labile species and, therefore, this technique is well suited to metal speciation studies, which are becoming increasingly important.

Potentiometric stripping analysis (PSA), a technique first proposed by Jagner and Graneli in 1976[2] and which has subsequently been applied successfully to a wide variety of samples, possesses the same advantages as ASV. This technique is based on the pre-concentration of a metallic cation by electrodeposition at a controlled potential and subsequent chemical stripping by means of an oxidising agent added to the system; a graph of stripping potential against time is then plotted.[3–5]

In 1958, Kémula *et al.*[6] described the interfering effect caused by the interaction of copper and zinc in the determination of these metals by ASV; this interference has subsequently been studied by many other workers. In contrast, the only comparable studies involving PSA have been those carried out by Jagner and co-workers.[3,7]

The studies carried out on interference effects in ASV have demonstrated the importance of the type of electrode used. Hence, with a hanging mercury drop electrode, interference was only observed when very concentrated solutions were electrolysed or when very long electrodeposition times were used.[8–13] On the other hand, with mercury film electrodes interfering effects were always observed irrespective of the experimental conditions employed.[11–18] The effects observed included a decrease in the stripping wave of zinc as the copper concentration increased to give a signal that appeared at a potential very close to that for the stripping of copper. In an extreme situation, complete suppression of the zinc signal was observed if the concentration of copper was sufficiently high.

Tracer studies carried out independently by Copeland *et al.*[12] and Crosmun *et al.*[14] with ^{65}Zn in the mid-1970s showed that a decrease in the zinc signal was not due to the electrodeposition of this metal being hindered by the presence of copper, but rather to the formation of an intermetallic compound in the amalgam of the working electrode with a stripping potential very close to that of copper. Since then, several reports have been published dealing with the most likely nature and stoicheiometry of the intermetallic copper - zinc compound formed in the amalgam and many stoicheiometries have been suggested. Although a 1:1 Cu - Zn compound has been proposed most often,[7,11,14,15,19] Schuman and Woodward[11] have proposed the formation of both 1:2 and 1:3 copper - zinc compounds. This suggests that the

stoicheiometry of the compound formed depends both on the ratio of the concentration of copper to zinc in the test solution (which will be almost the same as that in the amalgam as both metals have very similar accumulation coefficients) and on the absolute concentration of the two metals in the amalgam. The latter depends on the concentration of copper and zinc in the test solution, on the volume of mercury used for the electrode and on those parameters that control the transport of material to the electrode.

Owing to the complexity of the mercury - copper - zinc system,[19] attempts to remove the interference have concentrated on displacing the copper from its intermetallic compounds with zinc by the addition of gallium, which leads to the formation of a much more stable copper - gallium compound.[3,12,15,18] Other methods proposed have included the use of a two-electrode cell, which permits the separate deposition of each metal[17] and a numerical resolution using the standard additions method proposed by Saxberg and Kowalski,[20] which has been applied successfully to both ASV[21] and PSA.[22]

This paper describes a series of experiments that are directed towards observing the magnitude of the interfering effect between copper and zinc that occurs in a mercury film electrode using PSA under a variety of experimental conditions. This work was also aimed at evaluating the effectiveness of the gallium additions method in removing this interference.

Experimental

Instrumentation

A Radiometer ISS 820 potentiometric stripping analyser was used; it was equipped with a 50-ml glass cell containing a glassy carbon working electrode (surface area, 8 mm²), a platinum wire counter electrode and a standard calomel reference electrode. Stirring was achieved mechanically by means of a three-edged bar.

Reagents

Standard solutions of copper and zinc were prepared from their chlorides (Merck, analytical-reagent grade) and a standard solution of gallium from its nitrate (Merck, analytical-reagent grade). The mercury(II) solution used for plating and as an oxidising agent was prepared from its chloride (Panreac, analytical-reagent grade) in the same medium. The hydrochloric acid used was of Suprapur quality (Merck) and the water employed in the dilutions was purified with a Seta reverse osmosis and de-ionisation system. Blank signals were negligible in all instances.

The nitrogen employed for de-aeration of the samples was purified by bubbling it through two washing bottles containing pyrogallol and concentrated sulphuric acid.

Procedure

A 20-ml volume of the acidified solution to be analysed was placed in the glass cell, 0.4 ml of a 400 p.p.m. Hg^{II} solution was added and nitrogen was passed through the solution at a rate of about 200 ml min^{-1} for 20 min. The bubbler was raised above the solution, stirring was started and four plating - stripping cycles were carried out (for 2 min at -1.1 V versus SCE) so as to cover the working electrode with a mercury film. After the appropriate time and voltage for electrodeposition had been chosen (-1.05 V versus SCE for the selective deposition of copper and -1.25 V versus SCE for the reduction of both species), the sample signal was recorded together with those resulting from additions made to the sample. The additions were performed by means of a Brand 100-μl digital micropipette using solutions that were sufficiently concentrated so that the increase in the volume of the solution was negligible and aeration of the solution was not necessary.

Results and Discussion

Stoicheiometry of the Copper - Zinc Compounds

In order to study the magnitude of the copper - zinc interference when working with a mercury film electrode in PSA, a series of experiments were carried out in which the decrease in the stripping signal of zinc as the concentration of copper was increased was measured. These experiments were performed at three zinc concentrations, viz., 10^{-4}, 10^{-5} and 10^{-6} M. In the first two instances a 0.1 M HCl medium was used, whereas in the last instance the acidity was only 0.015 M in order to reduce the formation of hydrogen bubbles on the mercury film, given the long electrolysis times required at this low concentration. Also, because of the extremely short electrolysis times (ca. 15 s) which had to be used when working at the higher concentrations, the stripping curves were recorded in quadruplicate and the mean value was taken. The possibility of increasing the stripping times by decreasing the concentration of the oxidising agent was rejected because a mercury film with similar characteristics was required in all the experiments.

Fig. 1(b) shows the graph obtained for the lowest zinc concentration (10^{-6} M) in which the signal for this metal,

expressed as a function of the molar ratio of copper to zinc (r) in the test solution after each addition of copper, can be seen. The linear decrease observed, leading to suppression of the zinc signal at values of r close to unity, is consistent with the almost exclusive formation of a 1 : 1 Cu - Zn compound, which is in agreement with results obtained by other workers using ASV. The signal given by the intermetallic compound, the stripping wave of which overlaps that of free copper, is shown in Fig. 1(a); a straight line graph with a positive slope is obtained as might be expected from Fig. 1(b).

A different response of the system is evident from Fig. 2(b), which shows the graph obtained for 10^{-5} M zinc. In this instance an initial linear decrease in the zinc signal up to a molar ratio of copper to zinc of between 0.3 and 0.4 can be seen, the slope of the graph suggesting the formation of a 1 : 2 copper - zinc compound. Subsequently, the decrease in the slope (in absolute values) leads to the suppression of the signal for values of r close to unity; this can be explained by the increased formation of the 1 : 1 compound relative to the 1 : 2
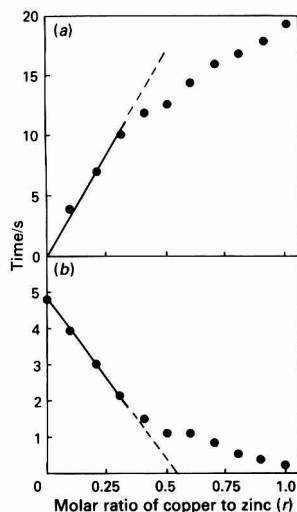
Fig. 2. Stripping time of (a) an intermetallic compound and (b) Zn vs. the molar ratio of Cu to Zn. [Zn] = 10^{-5} M; electrolysis time, 2 min

Fig. 1. Stripping time of (a) an intermetallic compound and (b) Zn vs. the molar ratio of Cu to Zn. [Zn] = 10^{-6} M; electrolysis time, 8 min
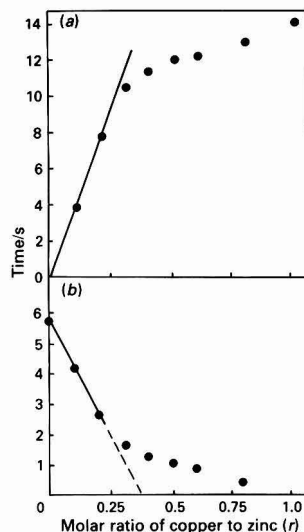
Fig. 3. Stripping time of (a) an intermetallic compound and (b) Zn vs. the molar ratio of Cu to Zn. [Zn] = 10^{-4} M; electrolysis time, 10 s

compound as the molar ratio of copper to zinc increases. As regards the stripping wave of the intermetallic compound, a decrease in the slope of the graph is observed [Fig. 2(a)] for the same r value, which is consistent with the hypothesis proposed earlier.

A similar experiment was performed with a 10^{-4} M zinc solution. The graphs obtained in this instance are shown in Fig. 3. The slope of the linear decrease at the beginning of the zinc signal can be attributed to the formation of the compound $CuZn_3$. The fact that this signal is lost for r values close to unity suggests that formation of the 1:1 copper - zinc compound predominates as the copper content of the solution increases.

The appearance of significant tailing in graphs similar to those described above is sometimes observed, as can be seen in Fig. 4; this is particularly so when thick mercury films are used in that a large excess of copper is then needed to achieve complete suppression of the zinc wave. A similar phenomenon has been observed in ASV[11,13,14] and has been attributed to the dissociation of the intermetallic copper - zinc compound. On the other hand, it has been shown that the magnitude of the interference decreases as the surface to volume ratio of the working electrode decreases. Fig. 5 shows the results obtained for the same solution when the thickness of the mercury film is varied.

Gallium Additions Method

The second objective of this work was to evaluate the effectiveness of the gallium additions method in removing the copper - zinc interference when working with a mercury film in PSA. Hence, several experiments were carried out in which the recovery of the zinc signal in the presence of copper was measured as a function of the amount of gallium added. All the experiments were performed at a constant concentration of zinc (10^{-6} M), the concentration of copper being varied so as to give values of the molar ratio of copper to zinc (r) of between 0.1 and 5. Because of the poor reproducibility of the technique as regards the signal produced by equal amounts of

Fig. 4. Zinc signal evolution (R, %) as a function of the copper concentration. Mercury film pre-formed at -0.9 V vs. SCE for 60 min. [Zn] = 10^{-5} M; electrolysis time, 2 min

Fig. 5. Zinc signal evolution (R, %) as a function of the copper concentration. Mercury film pre-formed for (▲) 8, (△) 68 and (●) 128 min. [Zn] = 10^{-5} M; electrolysis time, 2 min

metal in successive determinations, the procedure followed in all instances was to record initially the stripping signal of the 10^{-6} M zinc solution, then to add the amount of copper corresponding to the value of r required and finally to record again the free zinc signal. This signal was recorded after each addition of gallium had been made.

Fig. 6 shows plots of the recovery of the zinc signal for various values of r (expressed as the percentage ratio of the zinc signal obtained in the presence of copper after the addition of gallium to the initial signal in the absence of copper) versus the gallium concentration reached after each addition. In all instances the decrease in the zinc signal due to the addition of copper is consistent with the earlier discussion as regards the 1:1 stoicheiometry of the copper - zinc compound formed and its dissociation. As regards the recovery of the signal, the results obtained are very mixed. Hence, in solutions that are low in copper the recovery of the zinc signal is easily achieved; however, when working with concentrations of copper and zinc that are of the same order, it is necessary to have a large excess of gallium in the solution in order to obtain recoveries of about 90%, i.e., a molar ratio of gallium to copper of about 30 is required. For solutions with a copper concentration that is very much higher than that of zinc, the addition of gallium only permits a partial recovery of the zinc signal, e.g., when $r = 5$, the recovery is only about 50%.
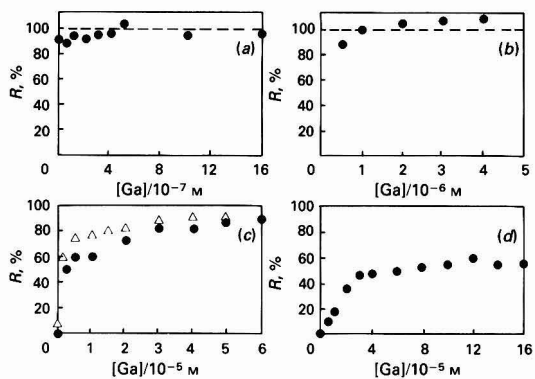
Fig. 6. Zinc signal recovery (R, %) vs. gallium concentration. Molar ratio of Cu to Zn (r): (a) 0.1, (b) 0.5, (c) 1 (△) and 2 (●) and (d) 5. [Zn] = 10^{-6} M; electrolysis time, 4 min
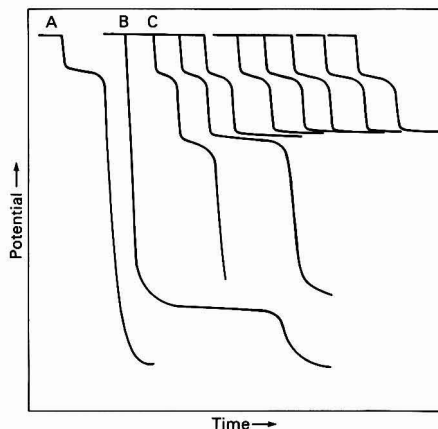
Fig. 7. Stripping curves for $r = 2$ in Fig. 6. A, Solution containing only zinc; B, after the addition of copper; and C, after the first addition of gallium

The good results obtained when the copper concentration in the solution is lower than that of zinc, which is the situation found most often,[12,15] confirm the usefulness of the proposed method for the determination of zinc under such conditions. However, in contrast to reports in the literature, the appearance of the stripping wave of free gallium does not necessarily mean that all the zinc has been released from the intermetallic copper - zinc compound. For example, the stripping curves for $r = 2$ are shown in Fig. 7 in which the appearance of the gallium wave can be seen (curve C), whereas the zinc signal has not been completely recovered. Further, although the addition of increasing amounts of gallium increases the percentage of zinc liberated, the most notable effect of these additions is to increase the wave of the free metal (*i.e.*, gallium) itself.

In those instances in which the copper content of the solution is higher than that of zinc, the gallium additions method lowers the magnitude of the interference but does not eliminate it completely; hence, other methods proposed in the literature (cited above) should be considered even though they are not simple or universally applicable. However, it should be noted that in environmental studies, in which the use of electrometric techniques such as pre-concentration have been very important, the zinc concentrations are generally much higher than those of copper. Therefore, the gallium additions method should be a simple and very versatile method for the determination of zinc in the presence of copper. On the other hand, the formation of a 1 : 1 copper - zinc compound for zinc concentrations of 10^{-7} M or less suggests that it should be possible to determine zinc below this level. This could be achieved not only by performing standard additions of zinc in the presence of gallium, but also by the method of Jagner and Kryger,[7] which involves successive additions of copper and then obtaining the molar concentration of this metal required for the suppression of the zinc signal by extrapolation, having previously determined the copper content in the plating solution at an anodic potential with respect to that required for the reduction of zinc.

References

1. Wang, J., *Environ. Sci. Technol.*, 1982, **16**, 104A.
2. Jagner, D., and Graneli, A., *Anal. Chim. Acta*, 1976, **83**, 19.
3. Jagner, D., Josefson, M., and Westerlund, S., *Anal. Chim. Acta*, 1981, **129**, 153.
4. Jagner, D., *Anal. Chem.*, 1978, **50**, 1924.
5. Jagner, D., *Analyst*, 1982, **107**, 593.
6. Kémula, W., Galus, Z., and Kublik, Z., *Nature (London)*, 1958, **182**, 1228.
7. Jagner. D., and Kryger, L., *Anal. Chim. Acta*, 1975, **80**, 255.
8. Lazar, B., Nishri, A., and Ben-Yaakov, S., *J. Electroanal. Chem.*, 1981, **125**, 295.
9. Chau, Y. K., and Lum-Shue-Cham, K., *Water Res.*, 1974, **8**, 383.
10. Ben-Bassat, A. H. I., Blinderman, J. M., Saloman, A., and Wakshal, E., *Anal. Chem.*, 1975, **47**, 534.
11. Shuman, M. S., and Woodward, G. P., Jr., *Anal. Chem.*, 1976, **48**, 1979.
12. Copeland, T. R., Osteryoung, R. A., and Skogerboe, R. K., *Anal. Chem.*, 1974, **46**, 2093.
13. Wise, J. A., Roston, D. A., and Heineman, W. R., *Anal. Chim. Acta*, 1983, **154**, 95.
14. Crosmun, S. T., Dean, J. A., and Stokely, J. R., *Anal. Chim. Acta*, 1975, **75**, 421.
15. Abdullah, M. I., Reusch, B., and Kilmex, R., *Anal. Chim. Acta*, 1976, **84**, 307.
16. Gardiner, J., and Stiff, M. J., *Water Res.*, 1975, **9**, 517.
17. Roston, D. A., Brooks, E. E., and Heineman, W. R., *Anal. Chem.*, 1979, **51**, 1728.
18. Neiman, E. Ya., Petrova, L. G., Ignatov, V. I., and Dolgopolova, G. M., *Anal. Chim. Acta*, 1980, **113**, 277.
19. Galus, Z., *CRC Crit. Rev. Anal. Chem.*, 1974, **4**, 359.
20. Saxberg, Bo. E. H., and Kowalski, B. R., *Anal. Chem.*, 1979, **51**, 1031.
21. Gerlach, R. W., and Kowalski, B. R., *Anal. Chim. Acta*, 1982, **134**, 119.
22. Hoyer, B., and Kryger, L., *Anal. Chim. Acta*, 1985, **167**, 11.

Medium Effects in the Stripping Voltammetry of Mercury

H. Gunasingham, K. P. Ang and C. C. Ngo
Department of Chemistry, National University of Singapore, Kent Ridge, Singapore 0511

The effect of the stripping medium on the stripping voltammetry of monolayer mercury films has been studied using a wall-jet electrode in conjunction with flow injection. A suitable methodology is proposed which allows the obviation of adsorption effects in the determination of trace levels of mercury. This approach can be used in routine analysis.

Keywords: *Stripping voltammetry; monolayer mercury films; medium effects; wall-jet electrode; flow injection*

Mercury-film electrodes (MFEs) have been the subject of intense interest as regards their application to stripping voltammetry, both for the determination of trace levels of mercury[1–4] and for the determination of heavy metals that form amalgams with mercury.[5–7] More recently, these electrodes have been applied to organic analysis.[8,9] Of the various electrode materials that have been employed for MFEs, glassy carbon has been the most widely used, primarily because of its larger cathodic potential range, relative stability and lesser susceptibility to poisoning.[10–12]

Studies on the nature of thin mercury films formed on glassy carbon electrodes have been carried out using cathodic linear sweep voltammetry,[13] direct current anodic stripping voltammetry,[14–19] optical microscopy,[15] spectroelectrochemistry,[20] flameless atomic absorption spectrometry,[21,22] potentiometric stripping analysis,[23] alternating current voltammetry[16] and oscillographic polarography.[24]

Stulikova[15] has shown that mercury is deposited on glassy carbon as fine droplets, the size of which depends on the plating potential. This finding has been supported by the work of Yoshida and Kihara[21] and Yoshida[22] who found that the mercury film is metallic and, in contrast to platinum, a strongly adsorbed film does not form on the electrode surface, even at the monolayer level. Johnson[25] has found that when trace levels of metals, such as silver, are co-deposited with mercury, a continuous thin film is produced, whereas droplets are formed in the absence of the trace metal. Also, Batley and Florence[14] have shown that a thin-film approximation is valid for very thin films (less than 0.5 μm).

Most of the work reported so far has been carried out with discrete solutions, primarily using a rotating disc electrode. In a previous paper, however, we described the use of a wall-jet electrode (WJE) as a continuous monitoring detector for such studies.[18] The experimental results correlated well with the theoretical values, based on a thin-layer approximation, for the irreversible stripping of a monolayer mercury film into a flowing HNO₃ - KNO₃ solution.

One of the advantages of the WJE is that, when used in conjunction with flow injection, it allows fine control of the pre-electrolysis and stripping steps, which can be performed in different media.[7,18] Of particular interest is the ability to carry out the stripping step in a flowing solution. In this instance, whereas the stripping peak current is still well defined theoretically, the flowing solution diminishes the concentration effects that arise from stationary solutions.[26] The other advantage is that, by the use of microprocessor control, it is feasible to measure accurately and rapidly the stripping profiles of films whose thickness is of the order of a monolayer or less. Sample changing is also simplified and requires minimal operator intervention.

In this paper we examine the effect of different plating and stripping media on the stripping peak current. The results are explained in terms of an irreversible or reversible stripping process.

Experimental

The wall-jet cell used in this work has been described previously.[18] The most noteworthy feature of this cell design is its large geometric cell volume. The working electrode was a 5.2-mm glassy carbon electrode, which was polished to a mirror finish with 1-μm diamond paste followed by 0.05-μm alumina. The reference electrode was a Ag - AgCl electrode (saturated KCl), and the counter electrode was a 5-mm platinum disc. The inlet diameter was 0.33 mm.

Experimental Set-up

Fig. 1 is a schematic diagram of the experimental set-up. In contrast to earlier work, a six-port stream selection valve (Rheodyne, Model 5010) was used together with a pneumatically actuated four-way injection valve (Rheodyne, Model 5020). The latter was used to inject the mercury sample during the pre-electrolysis step. Sample injection and control of the potentiostat (PAR 174A) sequencing (initial, scan and hold cycles) were carried out automatically using an Apple IIe computer. This enabled the plating and stripping of the mercury film to be controlled with great accuracy.

Reagents

All chemicals were of analytical-reagent grade and were used without further purification. Mercury solutions were prepared by dissolving the required amount of triply distilled mercury in concentrated nitric acid and diluting with distilled, de-ionised water. Solutions were purged with oxygen-free nitrogen for 15 min before use. Nitrogen was bubbled through the solution reservoirs throughout each run.

Results and Discussion

In our previous work it was shown that the theory of the stripping of mercury films at a WJE can be described using a thin-layer approximation, even though the stripping process is
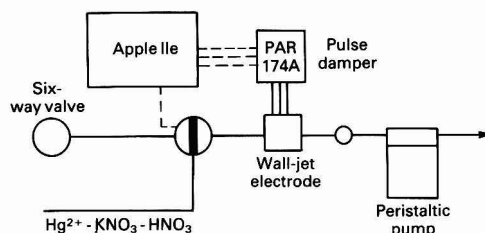
Fig. 1. Schematic diagram of the experimental set-up

carried out in a flowing electrolyte solution.[18] For a reversible process, the stripping current (i_p) is given by

$$i_p = \frac{0.35 n_p n_s F^2 r t D^{2/3} v^{-5/12} V^{3/4} a^{-1/2} X^{3/4}}{RT} \quad .. \quad (1)$$

and for an irreversible process, the peak current (i_p) is given by

$$i_p = \frac{0.5511 n_p \alpha n_s F^2 r t C D^{2/3} v^{-5/12} V^{3/4} a^{-1/2} X^{3/4}}{RT} \quad .. \quad (2)$$

where v is the kinematic viscosity, V the volume flow-rate, a the inlet diameter, X the electrode radius, n_p and n_s are the number of electrons in the plating and stripping steps, respectively, and α is the transfer coefficient. All the other terms have their usual meanings. For a KNO_3 - HNO_3 stripping solution, it was found that the stripping of a monolayer mercury film is an irreversible process in which αn_s varies between 0.5 and 0.75.

Effect of Stripping Medium

In order to study the effect of different stripping media, the mercury film was plated from a 0.1 M HNO_3 - 0.005 M KNO_3 solution. This is a suitable medium because the plating step is well defined by the limiting current equation for the wall-jet electrode at low mercury concentrations.[7] Each analytical stripping scan in a particular medium was followed by a reference scan carried out in 0.1 M KNO_3 - 0.005 M HNO_3. The reference scan was used to assess the state of the electrode, particularly with regard to electrode poisoning, and whether complete stripping of the mercury film was being achieved during the analytical scan. The entire sequence of analytical and reference scans was controlled by the microcomputer.

Table 1 gives the values of the peak current (αn_s) [calculated from equation (2)] and the peak potential (E_p) for the different stripping media examined. With the exception of the

Table 1. Effect of stripping medium on the stripping voltammetry of mercury. Deposition time ($t_{dep.}$), 20 s; stripping flow-rate, 2.38 ml min^{-1}; scan rate, 20 mV s^{-1}; and C_{Hg}, 4×10^{-5} M in 0.1 M KNO_3 - 0.005 M HNO_3

Stripping medium	i_p	αn_s	E_p
HNO_3 - KNO_3 (0.005 M - 0.1 M) ..	15.4 ± 0.4	0.6	0.48
Na_2SO_4 - HNO_3 (0.1 M - 0.1 M)	17.8 ± 0.5	0.7	0.44
$EDTA$ - HNO_3 (0.1 M - 0.1 M) ..	22 ± 0.2	0.86	0.16
KCl - HNO_3 (0.1 M - 0.005 M) ..	22 ± 0.5	—*	0.16
KBr - HNO_3 (0.1 M - 0.1 M)	32 ± 0.5	Reversible	0.06
KI - HNO_3 (0.1 M - 0.1 M)	32 ± 0.5	Reversible	-0.2
$KSCN$ - KNO_3 (0.1 M - 0.1 M)	31.5 ± 0.5	Reversible	0.04

* Stripping process complicated by the formation of $HgCl_2$ and Hg_2Cl_2.

Table 2. Dependence of mercury stripping efficiency on the potential scan rate. [Hg^{2+}], 4×10^{-5} M; deposition time, 20 s; deposition flow-rate, 2.32 ml min^{-1}; deposition potential, -1.0 V; and stripping electrolyte, KNO_3 (0.1 M) - HCl (0.005 M). Efficiency calculated on the basis of a one-electron reaction using equation (1)

Scan rate/mV s^{-1}	Stripping efficiency, %	
	Iodide	Chloride
2	190	204
5	220	174
10	212	140
20	170	96

bromide, iodide and thiocyanate media, the stripping process is irreversible with values of n_s varying from 0.5 to 0.85. The stripping current, i_p, obtained for the thiocyanate medium agreed with the theoretical value calculated from equation (1). For the chloride medium, calculation of the value of n_s is complicated by the fact that both $HgCl_2$ and Hg_2Cl_2 can be formed, depending on the stripping scan rate and the concentration of chloride in the stripping solution. Bilewicz et al.[19] showed that high chloride concentrations promote the formation of $HgCl_2$ and its complexes.

Table 2 shows the dependence of the mercury stripping efficiency on the stripping scan rate (calculated for a one-electron process). The near 200% efficiency obtained at slow scan rates indicates that the stripping process actually involves two electrons. By analogy with the work of Bilewicz et al.,[19] it is reasonable to assume that at slower scan rates sufficient chloride is admitted by the convective diffusion conditions of the wall jet to promote the formation of $HgCl_2$. As the scan rate increases, the efficiency decreases and, therefore, it can be assumed that both $HgCl_2$ and Hg_2Cl_2 are being formed. It is interesting to note that the efficiency obtained for the bromide and iodide media does not vary significantly with the scan rate, further supporting the view that the stripping process in these media is predominantly a two-electron process.

Effect of Electrode Pre-treatment

Much work has been carried out on the effect of electrode pre-treatment on the response of glassy carbon electrodes.[27–31] We have found that, provided the glassy carbon surface is polished to a scratch-free mirror finish, the use of different polishing procedures (including polishing with diamond paste and alumina on a glass plate) has only a small effect on the stripping peak current. Also, the electrode is less susceptible to de-activation after prolonged use, in contrast to the hexacyanoferrate(III) - hexacyanoferrate(II) system. This is consistent with the general supposition that mercury films do not interact strongly with glassy carbon surfaces.

One of the interesting aspects of this work is that the nominal electrode area shows good agreement with the actual active surface area in the calculation of the theoretical peak current. For the chloride, bromide and thiocyanate media, the experimental value differs by less than 10% from the theoretical value for a reversible stripping process. Even if this difference is attributed to surface roughness, the assumption is that the mercury is fairly evenly deposited on the glassy carbon surface. However, it should be noted that this assumption only holds for films whose thickness is of the order of a monolayer. As the film becomes thicker, the use of the nominal surface area is less valid.

In general, potential pre-treatment by cycling between negative and positive potentials, as suggested by Engstrom[30] and Engstrom and Strasser,[31] does not improve the reversibility of the stripping process. However, the electrode has to be pre-treated with chromic acid, otherwise a small second peak at $+0.58$ V occurs. This peak correlates with the $Hg(OH)_2$ peak found under dilute acidic conditions in the study of the effect of pH, described below. Presumably, this is because acidification of the electrode surface decreases the tendency of the mercury that is in contact with the electrode to hydrolyse.

Effect of pH

Whereas varying the pH appears to have little influence on the plating step, studies carried out using acetate buffers as the stripping solutions showed that the peak potential changed by about 31 mV pH^{-1} in the pH range 3–6. This slope is indicative of an irreversible stripping process in the acetate buffer. However, the peak current is little affected by the pH of the stripping solution.

Fig. 2. Replating of adsorbed Hg_2Cl_2 in nitrate medium. Nitrate medium: KNO_3 (A–G) 0.1 M plus HNO_3, (A) 1×10^{-2}, (B) 1×10^{-3}, (C) 5×10^{-4}, (D) 1×10^{-4}, (E) 5×10^{-5}, (F) 1×10^{-5} and (G) 5×10^{-6} M. The waiting time is the length of time for which the electrode is held at $+0.2$ V in the nitrate medium following the stripping run in the chloride medium. See text for details
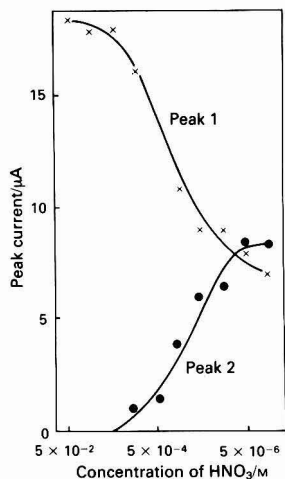

Fig. 3. Effect of acid concentration on the mercury stripping voltammogram. $E_{dep.}$, -1.0 V; scan rate, 20 mV s^{-1}; C, 4×10^{-5} M; $t_{dep.}$, 20 s; and V, 2.38 ml min^{-1}
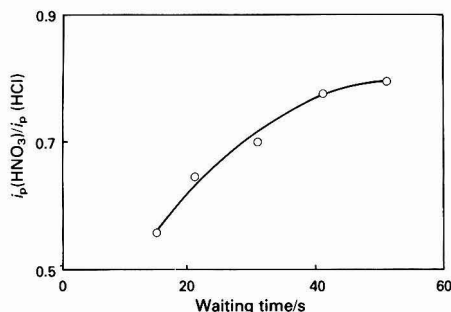
Fig. 4. Effect of acid concentration on the stripping peak current. Conditions as in Fig. 3

In very dilute acidic solutions, concentration effects are observed, owing to the formation of $Hg(OH)_2$. Fig. 2 shows the occurrence of a second peak at around $+0.58$ V when the HNO_3 concentration drops below 0.005 M. This second peak increases with decreasing acid concentration, whereas the usual peak at $+0.48$ V decreases. This effect can be seen more clearly in Fig. 3, which shows the change in peak current with varying acid concentrations.

In Situ Cleaning of Adsorbates

The adsorption of mercury compounds on the electrode surface is one of the fundamental difficulties associated with its routine determination by stripping voltammetry. Invariably, adsorption leads to blocking of the active surface of the electrodes, causing a decrease in the analytical current. It can also lead to erratic results and loss of precision.

Clearly, it is unsatisfactory to have to remove the electrode periodically in order to repolish the surface. Apart from the tediousness of the operation, repolishing the electrode can also alter its operating characteristics.

To demonstrate that adsorption occurs, a monolayer mercury film was plated and the potential was then scanned in a chloride medium to obtain a mercury stripping peak at $+0.15$ V. The scan was stopped at $+0.2$ V and the stripping medium was changed to HNO_3 - KNO_3. Then, after a waiting time, the scan was continued to $+0.7$ V. A second stripping peak was obtained at $+0.48$ V in the nitrate medium, the size of this peak depending on the length of the waiting time.

Fig. 4 shows a graph of the ratio of the peak current obtained in a nitrate medium (at $+0.48$ V) to that obtained in a chloride medium (at $+0.15$ V) against the waiting time. The ratio increases with increasing waiting time, indicating that more mercury is being replated and that mercury, stripped as Hg_2Cl_2, remains on the electrode surface long enough to be replated in a nitrate medium.

Although the above experiment illustrates the problem of adsorption, it also reveals how this problem can be overcome. For the Hg_2Cl_2 adsorbate, it was found that, by using a nitric acid cleaning step between analyses, it was possible to obviate completely the adsorption so that the glassy carbon electrode showed no memory effects. Nitric acid can also be used to remove phosphate and EDTA adsorbates.

Sensitivity

The use of the WJE results in a highly sensitive technique for the determination of mercury. Thiocyanate is the best stripping medium as it favours a two-electron stripping process and minimises adsorption. However, the plating step is best performed in an acidic medium, *e.g.*, dilute nitric acid.

It has been shown that, with the WJE, it is possible to determine monolayer amounts of mercury. In the direct current mode, detection limits below 10^{-7} M are feasible, and

in the differential-pulse mode the detection limit is below 10^{-8} M. These detection limits compare favourably with those reported in the literature.[2] In general, the precision of the method is less than 3%.

References

1. Perone, S. P., and Kretlow, W. J., *Anal. Chem.*, 1965, **37**, 969.
2. Jaya, S., Rao, T. P., and Rao, G. P., *Analyst*, 1985, **110**, 1361.
3. Jagner, D., *Anal. Chim. Acta*, 1979, **105**, 33.
4. Jagner, D., *Analyst*, 1982, **107**, 593.
5. Barendecht, E., *in* Bard, A. J., *Editor*, "Electroanalytical Chemistry," Volume 2, Edward Arnold, London, Marcel Dekker, New York, 1967, p. 53.
6. Wang, J., "Stripping Analysis," VCH, Florida, 1985.
7. Gunasingham, H., Ang, K. P., and Ngo, C. C., *J. Electroanal. Chem.*, 1986, **215**, 123.
8. Stojek, S., Stepnik, B., and Kublik, Z., *J. Electroanal. Chem.*, 1976, **74**, 277.
9. Gunasingham, H., Tay, B. T., and Ang, K. P., *Anal. Chem.*, 1986, **58**, 1578.
10. Florence, T. M., *J. Electroanal. Chem.*, 1970, **27**, 273.
11. Van der Linden, W. E., and Dieker, J. W., *Anal. Chim. Acta*, 1980, **119**, 1.
12. Zittel, H. E., and Miller, F. J., *Anal. Chem.*, 1965, **37**, 200.
13. Daneshwar, R. G., and Kulkarni, A. V., *J. Electroanal. Chem.*, 1979, **99**, 207.
14. Batley, G. E., and Florence, T. M., *J. Electroanal. Chem.*, 1974, **55**, 23.
15. Stulikova, M., *J. Electroanal. Chem.*, 1973, **48**, 33.
16. Stulikova, M., and Vydra, F., *J. Electroanal. Chem.*, 1973, **42**, 127.
17. Luang, L., and Vydra, F., *J. Electroanal. Chem.*, 1974, **50**, 379.
18. Gunasingham, H., Ang, K. P., and Ngo, C. C., *Anal. Chem.*, 1985, **57**, 505.
19. Bilewicz, R., Stojek, Z., and Kublik, Z., *J. Electroanal. Chem.*, 1979, **96**, 29.
20. Laser, D., and Ariel, M., *J. Electroanal. Chem.*, 1974, **50**, 474.
21. Yoshida, Z., and Kihara, S., *J. Electroanal. Chem.*, 1979, **95**, 159.
22. Yoshida, Z., *Bull. Chem. Soc. Jpn.*, 1981, **54**, 562.
23. Jagner, D., *Anal. Chim. Acta*, 1979, **100**, 33.
24. Subramaniam, G., and Rao, G. P., *J. Electroanal. Chem.*, 1976, **70**, 133.
25. Johnson, D. C., personal communication.
26. Almeidamota, A. M., Buffle, J., Kounaves, S. P., and Goncalves, M. S., *Anal. Chim. Acta*, 1985, **172**, 13.
27. Weisshaar, D., and Kuwana, T., *Anal. Chem.*, 1985, **57**, 378.
28. Thortan, D. C., Corby, K. T., Spendel, V. A., Jordan, J., Robbat, A., Rustrom, D. J., Gross, M., and Ritzler, G., *Anal. Chem.*, 1985, **57**, 150.
39. Fagan, D. T., Hu, I. F., Kazee, B., Weisshar, D., and Kuwana, T., "Extended Abstracts, Electroanalytical Symposium, 1985," BAS Press, West Lafayette, 1985, p. 134.
30. Engstrom, R. C., *Anal. Chem.*, 1982, **54**, 2310.
31. Engstrom, R. C., and Strasser, V. A., *Anal. Chem.*, 1984, **56**, 136.

Transient Responses of Glass Electrodes in Dilute Solutions and Freshwaters

William Davison and Terence R. Harbinson
The Freshwater Biological Association, The Ferry House, Ambleside, Cumbria LA22 0LP, UK

Glass electrodes respond slowly in dilute, nearly neutral solutions (I = 0.1–1 mmol dm^{-3}, pH 6–9) of either natural lake water or simple inorganic salts, taking *ca.* 10 min to equilibrate irrespective of whether the solution is flowing or static. Although buffer capacity and ionic strength influence the response, they are not critical factors. The transient effect is associated with low concentrations of cations. There was no great difference in response for the different cations tested, but the sluggishness appeared to increase in the order $K^+ \approx Ca^{2+} < Na^+ \approx Mg^{2+} < NH_4^+$. The time dependence of the response is consistent with it being due to a diffusional exchange process. Glass electrodes are inappropriate pH sensors for the determination of the pH of dilute neutral solutions by flow injection analysis.

Keywords: *Dilute solutions; freshwater; glass electrode; response time; flow injection*

The considerable attention recently devoted to the measurement of pH in dilute solutions has been stimulated by the phenomenon of acid rain and so work has concentrated on dilute acidic solutions.[1–6] Advances in understanding, particularly with regard to problems associated with liquid junctions,[1,4,7] have led to recommendations that dilute acids could be used as standards.[2,3,6]

Work on dilute solutions of nearly neutral pH has been more limited. Problems encountered in measuring the pH of dilute lake waters (pH 5.5–8.0) have led to suggestions that the pH measured by commercial glass electrodes is so unreliable that it is better to calculate the pH from measured components of the CO_2 - H_2O system.[8,9] However, some laboratories[10–12] have accurately determined the pH of dilute solutions of neutral buffers and shown that it is possible to obtain high-quality data. Conversely, similar measurements by other workers[3,4] have resulted in large errors, and the determination of the second dissociation constant of 10^{-3} mol kg^{-1} phosphoric acid from pH titrations has only really been successful when an experimental free diffusion junction has been used.[10,13] Whereas some of the inconsistency is probably associated with the use of electrodes with unsatisfactory performance, often attributable to an inappropriate or malfunctioning liquid junction, there may also be fundamental reasons for the discrepancies.

In recent work that considered the use of flow injection technology for the accurate measurement of pH, we observed that the electrode response was markedly worse in soft waters at pH *ca.* 7 than in dilute acids or acidic natural waters. We report here the results of an investigation of transient effects in dilute solutions.

Experimental

Equipment and Reagents

All solutions were prepared from AnalaR reagents. Salts for buffers were dried according to the recommendations of Bates.[14] Artificial lake water, prepared by combining salt solutions and then equilibrating with air, had a nearly neutral pH, an alkalinity of 500 µequiv. l^{-1} and the following composition; Na$^+$, 300; Ca^{2+}, 288; K$^+$, 60; Mg^{2+}, 60; NH$_4^+$, 25; Cl$^-$, 350; SO$_4^{2-}$, 90; and NO$_3^-$, 50 µM. Filtered lake water was taken from Windermere,[15] which typically has a nearly neutral pH, an alkalinity of 220 µequiv. l^{-1} and the following composition: Na$^+$, 200; Ca^{2+}, 150; K$^+$, 10; Mg^{2+}, 75; Cl$^-$, 240; SO$_4^{2-}$, 85; and NO$_3^-$, 30 µM. Acid stream water from Mosedale (pH *ca.* 5)[4] is dominated by the following ions: Na$^+$, 150; Ca^{2+}, 25; Mg^{2+}, 25; Cl$^-$, 150; and SO$_4^{2-}$ 50 µM.

Potential differences were measured using a high-impedance buffer amplifier simultaneously linked to a chart recorder and a digital multimeter which could discriminate to 1 µV.

Procedure

Most measurements were made using a flow cell, based on the design of Howson *et al.*,[16] but having a much smaller sample chamber (residual volume of 0.1 ml). The small, glass pH electrode (3-mm diameter), equipped with a screw thread and seal, was supplied by Pharmacia. A reference electrode (Radiometer K4112, calomel - saturated KCl) was sealed into a chamber containing saturated KCl. Two tubes were connected to the chamber: one led to a T-connection with the flowing sample stream, 1 cm downstream from the glass electrode, and the other to a motorised syringe, which continuously fed (0.2 ml min^{-1}) the KCl bridge solution to the liquid junction formed at the T-piece. Such a junction has been systematically evaluated[17] and shown to perform well.

A carrier solution of either 0.1 mmol dm^{-3} HCl + 0.4 mmol dm^{-3} KCl (pH 4.0) or 0.5 mmol dm^{-3} Na$_2$HPO$_4$ + 0.5 mmol dm^{-3} KH$_2$PO$_4$ (pH 7.1) was gravity fed through the cell at 3.8 ml min^{-1}. The low pH carrier solution was selected from various candidates as the one which exhibited the lowest long-term drift (Table 1). Test solutions were injected into this stream using a 26-ml sample loop. Hence the arrangement resembled that used in simple flow injection analysis (Fig. 1), with 0.8-mm bore tubing and a volume between the point of injection and the liquid junction of 0.142 ml. With such a large sample loop dispersion effects should be negligible.[18] Injection of 0.025 mol dm^{-3} KH$_2$PO$_4$ - 0.025 mol dm^{-3} Na$_2$HPO$_4$ into the low pH carrier stream operating at different flow-rates showed that with a flow-rate of 3.8 ml min^{-1} a drift of 0.01 pH min^{-1} is achieved in 2 min (Fig. 2).

Table 1. Long-term drift in the flow injection assembly for various carrier solutions, calculated from the maximum excursion in measured potential in a 4-h period. The amplitude of the high-frequency noise exhibited by the pen trace is also given

Solution	Drift/ pH h^{-1}	Noise/ mV
Distilled H$_2$O	0.15	±4
0.01 mmol dm^{-3} H$_2$SO$_4$	0.087	±1
0.1 mmol dm^{-3} KCl	0.055	±0.25
0.1 mmol dm^{-3} HCl - 0.4 mmol dm^{-3} KCl ..	0.036	±0.05
0.1 mmol dm^{-3} potassium hydrogen phthalate	0.066	±0.5
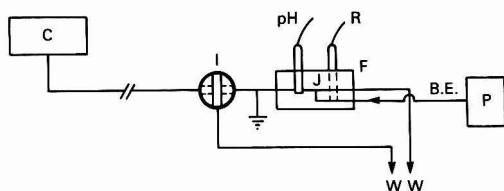
Fig. 1. Arrangement for pH measurement using a flow injection assembly. Carrier solution, C, is fed by gravity to injection valve, I. The flow cell, F, is equipped with pH and reference (R) electrodes. Bridge electrolyte, B.E., is continuously supplied from a syringe pump, P, to connect the reference electrode to the solution stream by liquid junction, J. W is waste
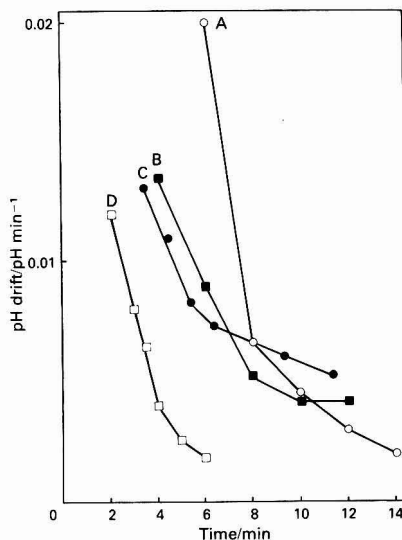

Fig. 3. Assembly for rapidly exchanging solutions for conventional electrodes. The electrode, E, is inserted into a small, capped plastic container, C, containing a stirrer bar, B, and connected via a tap, T, to a syringe, S, for injecting the sample. Syringe volume, 50 ml; volume of C, 2–3 ml

Fig. 2. Time dependence of the pH drift (pH min^{-1}), which is the slope of the pH *versus* time graph, for four different flow-rates when standard strength pH 6.88 phosphate buffer is injected into a carrier solution of 0.1 mmol dm^{-3} HCl + 0.4 mmol dm^{-3} KCl. Sample flow-rate: A, 0.5; B, 1.8; C, 2.8; and D, 3.8 ml min^{-1}

Fig. 4. Recorder traces illustrating injection of various solutions into the flow injection assembly. Injected solutions: (A) NBS pH 6.88 phosphate buffer; (B) solution A diluted 50×; (C) Windermere lake water; (D) artificial lake water; (E) 0.1 mmol dm^{-3} HCl; (F) distilled water; and (G) Mosedale stream water (pH 5.4). Except for E the carrier stream was 0.1 mmol dm^{-3} HCl + 0.4 mmol dm^{-3} KCl. The carrier for E was solution B

Measurements were also made using various combination electrodes inserted into a small plastic beaker fitted with a stirrer bar, an inlet port and a cover to minimise gaseous exchange (Fig. 3). The electrode was pre-equilibrated with the carrier solution, then the system was rapidly flushed by injecting the test solution using a syringe; the solution overflowed through the small gap between the electrode and the cover.

Conventional dip-mode measurements in a beaker used a reference electrode equipped with a previously described free diffusion junction.[13]

All measurements were thermostated at 20 ± 0.1 °C.

Results and Discussion

Typical recorder traces obtained by injecting various solutions into the flow injection assembly are shown in Fig. 4. Solutions of natural and artificial, nearly neutral lake water responded much more slowly than the rest. After 4 min the measured drift of 0.07 pH min^{-1} was one order of magnitude higher than that observed for the other solutions. Distilled water gave a rapid response, quickly establishing a plateau value, and demonstrating that within 1 min there is no appreciable modification of the pH by mixing with the carrier solution.

Phosphate buffer solution (pH 6.88) also gave a rapid response, both at normal strength and when diluted 50-fold. Failure of an acid stream sample (Mosedale, pH 5.4) to show a similar curvature to that observed for neutral Windermere water could have been associated with the smaller pH change from the pH 4 carrier solution. However, there was a rapid change of more than 3 pH when dilute phosphate buffer was added, and when the dilute phosphate solution was used as the carrier solution and 0.1 mol dm^{-3} hydrochloric acid was injected the response was similarly rapid. That the effect was not associated with the carrier solution was shown by injecting lake water into a stream of distilled water. The response curve

had the same rounded shape as that obtained using the dilute acid carrier solution.

The solutions of natural and artificial lake water were air equilibrated before measurement and so exchange of CO_2 should be minimal, especially in a sealed system. Solutions with different initial partial pressures of CO_2 gave the same response and confirmed that CO_2 exchange was not a problem.

Buffer capacity may be important in determining the response. That it is not the sole factor is illustrated by the good response for distilled water (Fig. 4).

To test whether the sluggish response was associated with the glass electrode or the liquid junction, measurements were made in a beaker with solutions of artificial lake water and distilled water. A dip-mode free diffusion junction[13] was formed in the solution in the beaker and allowed to stabilise, then the glass electrode from the flow cell was immersed while monitoring the response. A similar sluggish response to that observed for the flow cell was recorded for artificial lake water whereas distilled water gave a much flatter signal (Fig. 5). When the electrode was pre-equilibrated and the liquid junction re-formed, the response was immediately flat and stable for both solutions, showing that the poor response in artificial lake water was associated with the glass electrode.

There was a possibility that the observed effect was unique to the Pharmacia electrode, so measurements were made on artificial lake water, dilute phosphate buffer and distilled water using Amagruss, Russell, Radiometer and Orion Ross combination electrodes. They were fitted into a specially constructed assembly (Fig. 3) and the solution was rapidly exchanged. The observed responses were similar to those shown in Fig. 4. When a Corning glass electrode and the Pharmacia electrode from the flow cell were similarly tested, by additionally inserting a Radiometer K4112 reference electrode into the electrode chamber, the same phenomenon of a slow response in artificial lake water and a rapid response in distilled water and dilute buffer was observed.

Having established that in certain nearly neutral solutions of low ionic strength there is a transient effect common to glass electrodes, we tried to characterise the nature of the effect. As it is observable both in simple synthetic solutions and in natural waters it cannot be associated with organic components, such as humic acids, in the water.

Various salt solutions with an ionic strength of 1 mmol dm^{-3} were prepared. Except for $KHCO_3$ they were adjusted to pH 7 by adding small aliquots of their common acid or base while bubbling with argon to remove CO_2. Solutions of $KHCO_3$ were adjusted to pH 7 by varying the ratio of CO_2 to Ar in a gas mixture. The resulting solution was transferred by syringe into the injection assembly (Fig. 3) fitted with a Russell combination electrode designed for measuring low ionic strength solutions. In each instance the response was similar to that obtained for synthetic lake water.

Previous workers[19,20] have shown that response curves from glass electrodes can be linearised by plotting $\log(|E_\infty - E_t|/E_\infty)$ against $t^{\frac{1}{2}}$. Figs. 6 and 7 show such plots for the various solutions tested, E_∞ being taken as the value at 8 min. The slope of this plot is a measure of the speed of response. For five of the solutions the plots could be reasonably fitted by straight lines with similar slopes (Fig. 6). Sodium chloride gave a slightly higher slope, indicating a slower response, and the slope for NH_4Cl was higher still (Fig. 7). The only obvious non-linear response was for $MgCl_2$. These results indicate that it is the cation rather than the anion in solution which has the major influence on response time.

The reasonable linearity of most of the data suggests that the observed effect may be due to a diffusion process.[19] Perhaps on exchanging solutions the fresh cations have to establish a new equilibrium with exchange sites on the glass. This exchange will occur more rapidly when the glass surface is exposed to higher concentrations of the new cation. The more specific mechanism suggested by Kennedy[21] whereby protons are released into the hydration layer on the initial adsorption of metal ions is also consistent with the results. That the effect is not simply associated with the general ionic strength of the solution was shown by adding NaCl to a 0.2 mmol dm^{-3} solution of $KHCO_3$. Increasing the concentration of NaCl to 0.1 mol dm^{-3} changed the shape of the potential - time curve slightly, consistent with Figs. 6 and 7, but the response was still sluggish. Surprisingly, in view of the good response observed with distilled water, there was also little change in the response when the concentration of $KHCO_3$ was reduced to 0.01 mmol dm^{-3}.

Changing the pH of solutions of $KHCO_3$ by bubbling with gas mixtures with various ratios of CO_2 to Ar showed that the

Fig. 5. Response of Pharmacia glass electrode immersed in (A) and (B) artificial lake water and (C) and (D) distilled water contained in a beaker. The reference electrode used a free diffusion junction. (A) and (C), glass electrode inserted after pre-stabilisation of the junction; (B) and (D), junction re-formed after pre-stabilisation of the glass electrode
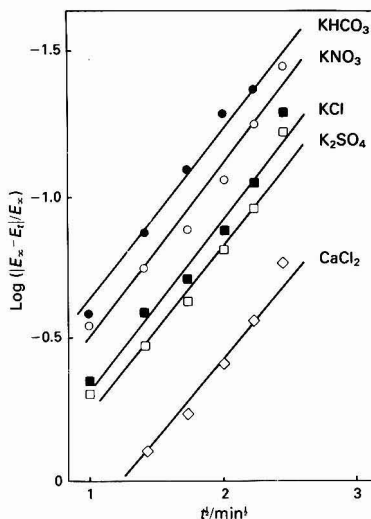
Fig. 6. Linearisation of response curves as $\log(|E_\infty - E_t|/E_\infty)$ *versus* $t^{\frac{1}{2}}$ (min$^{\frac{1}{2}}$) for various simple solutions ($I = 1$ mmol dm^{-3}; pH = 7.0 ± 0.3)
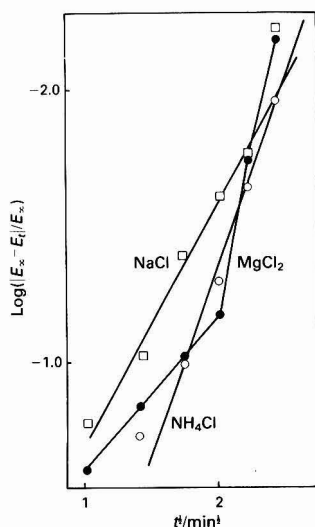
Fig. 7. Linearisation of response curves as $\log(|E_\infty - E_t|/E_\infty)$ versus $t^{\frac{1}{2}}$ (min$^{\frac{1}{2}}$) for various simple solutions ($I = 1$ mmol dm^{-3}; pH = 7.0 ± 0.3)

response was slowest in solutions with a pH near 8. More exchangeable sites may be available at nearly neutral pH where OH$^-$ and H$^+$ ions are less dominant. Alternatively, the effect may be simply related to the buffer capacity, which is at a minimum at pH 8 in dilute hydrogen carbonate solutions.[22]

Conclusion

The glass electrode responds slowly in nearly neutral, poorly buffered solutions, but if sufficient time is allowed (ca. 10 min) an equilibrium pH will be achieved. The sluggish response is not solely related to buffer capacity because there is a good response in distilled water, and the ionic strength does not appear to be a critical factor. It is associated with low concentrations of cations and the shape of the response curve indicates that a diffusional exchange process may be operating. There was no great difference in the effect for the different cations tested but it increased in the order K$^+ \approx$ Ca$^{2+} <$ Na$^+ \approx$ Mg$^{2+} <$ NH$_4^+$. The distinction between the various cations may depend on the solution used to pre-equilibrate the electrode, which in this instance was dilute HCl - KCl. Kennedy[21] has observed a similar transient effect with initial excursions of ca. 0.2 pH and a response of ca. 10 min when dilute solutions (20 µmol dm^{-3}) of Ca^{2+}, Ni^{2+}, Co^{2+}, Mn^{2+}, Zn^{2+}, Cd^{2+} and Hg^{2+} are introduced into a flowing stream.

Such an effect has profound implications for the measurement of pH in neutral dilute solutions such as freshwaters. Previous observations of slow response times[6,14,23] have been attributed to re-equilibrium by CO$_2$ or to solution memory effects, especially when the previous solution was a standard strength buffer. Both of these possible causes have been eliminated in this work, which has demonstrated that there is an inherent problem associated with low concentrations of cations and equilibrium at the glass electrode. Accurate measurements in dilute solutions can only be made if sufficient time (ca. 10 min) is allowed for a true equilibrium to be established.

These conclusions imply that it may be inappropriate to determine the pH of dilute neutral solutions by using glass

electrodes in flow injection analysis. Such a technique uses precise hydraulic control to make use of measurements that have not yet achieved equilibrium. However, if the sensor response is sluggish and variable from solution to solution, depending on its composition, the procedure fails. Problems using such a system for determining soil pH have been noted[24] and to some extent overcome by matching the buffer capacity of standards to soil solutions. A glass electrode worked well in a flowing system for the rapid determination of acidic rain water samples but the calibration graph was non-linear in the most neutral pH range considered, 4–5,[25] presumably due to the onset of poor response. It is possible that PVC-based pH-sensitive electrodes may not suffer from the same transient interference effects and so they may be more suitable than glass electrodes for use in flow injection analysis.[26,27]

References

1. Midgley, D., Atmos. Environ., 1987, 21, 173.
2. McQuaker, N. R., Kluckner, P. D., and Sandberg, D. K., Environ. Sci. Technol., 1983, 17, 431.
3. Metcalf, R. C., Z. Gletscherkd. Glazialgeol., 1984, 20, 41.
4. Davison, W., and Woof, C., Anal. Chem., 1985, 57, 2567.
5. Koch, W. F., and Marinenko, G., ASTM Spec. Tech. Publ., 1983, No. 823, 10.
6. Jones, C., Williams, D. W., and Marsicano, F., Sci. Total Environ., 1987, 64, 211.
7. Brezinski, D. P., Analyst, 1983, 108, 425.
8. Herczeg, A. L., Broecker, W. S., Anderson, R. F., Schiff, S. L., and Schindler, D. W., Nature (London), 1985, 315, 133.
9. Herczeg, A. L., and Hesslein, R. H., Geochim. Cosmochim. Acta, 1984, 48, 837.
10. Covington, A. K., Whalley, P. D., and Davison, W., Anal. Chim. Acta, 1985, 169, 221.
11. Boyle, P. F., Ross, J. W., Syncott, J. C., and James, C. L., in Isom, B. G., Dennis, S. D., and Bates, J. M., Editors, "Impact of Acid Rain and Deposition on Aquatic and Biological Systems," ASTM, Philadelphia, 1986, pp. 98–106.
12. Illingworth, J. A., Biochem. J., 1981, 195, 259.
13. Davison, W., and Harbinson, T. R., Analyst, 1988, 113, 709.
14. Bates, R. G., "Determination of pH," Wiley, New York, 1964.
15. Sutcliffe, D. W., Carrick, T. R., Heron, J., Rigg, E., Talling, J. F., Woof, C., and Lund, J. W. G., Freshwater Biol., 1982, 12, 451.
16. Howson, M. R., House, W. A., and Pethybridge, A. D., Analyst, 1986, 111, 1215.
17. Harbinson, T. R., and Davison, W., Anal. Chem., 1987, 59, 2450.
18. Růžička, J., and Hansen, E. H., "Flow Injection Analysis," Wiley, New York, 1981.
19. Eisenman, G., Editor, "Glass Electrodes for Hydrogen and Other Cations," Marcel Dekker, New York, 1967.
20. Rechnitz, G. A., and Kugler, G. C., Anal. Chem., 1967, 39, 1683.
21. Kennedy, C. D., Analyst, 1983, 108, 1003.
22. Stumm, W., and Morgan, J. J., "Aquatic Chemistry," Second Edition, Wiley, New York, 1981.
23. Neal, C., and Thomas, A. G., J. Hydrol., 1985, 79, 319.
24. Edmonds, T. E., and Coutts, G., Analyst, 1983, 108, 1013.
25. Fuesko, J., Toth, K., Pungor, E., Kunovits, J., and Puscbaum, H., Anal. Chim. Acta, 1987, 194, 163.
26. Hongbo, C., Hansen, E. H., and Růžička, J., Anal. Chim. Acta, 1985, 169, 209.
27. Madsen, B. C., and Doller, D. W., Anal. Chem., 1987, 59, 127.

Flow Injection Amperometric Detection Based on Ion Transfer Across a Water - Solidified Nitrobenzene Interface for the Determination of Tetracycline and Terramycin

Huamin Ji and Erkang Wang*

Changchun Institute of Applied Chemistry, Chinese Academy of Sciences, Changchun, Jilin 130021, People's Republic of China

An accurate, convenient and fast method is described for the determination of tetracycline and terramycin in drugs by flow injection amperometric detection based on ion transfer across a water - nitrobenzene interface solidified with poly(vinyl chloride) and agar. When a constant potential is applied both antibiotics transfer across the interface, the process being facilitated by protons, with a linear current response for 2–200 μM solutions of tetracycline and 5–300 μM solutions of terramycin. The coefficients of variation for 22 replicate injections of 0.2 mM solutions of tetracycline and terramycin are 1.2 and 2.5%, respectively. The results obtained are in good agreement with those given by a biological assay (the relative standard deviation is less than 1%). A total of 60 samples could be determined in 1 h.

Keywords: *Tetracycline and terramycin determination; flow injection analysis; amperometric detection; ion transfer; water - solidified nitrobenzene interface*

Since its introduction by Nagy et al.,[1] flow injection analysis (FIA) has attracted considerable interest as a method for fast, repetitive and reproducible analysis.[2,3] Apart from the detection mode of electroanalysis,[4,5] other methods such as absorbance,[6] fluorescence[7] and luminescence[8] have been employed for detection in FIA. Amperometric detection in conjunction with FIA and liquid chromatography (LC - EC) has been widely used for the determination of electroactive substances.[9–11]

Tetracyclines are widely used antibiotics that are routinely determined by means of antimicrobial assay,[12] although other methods such as fluorimetry[13] and spectrophotometry[14] have also been reported. However, the biological assay is very complicated and time consuming. Voltammetry at the interface of two immiscible electrolyte solutions has been used by Kozlov and Koryta[15] for the determination of tetracyclines. We have previously described the determination of terramycin and erythromycin using cyclic voltammetry and chronopotentiometry with cyclic linear current scanning at a water - nitrobenzene interface.[16–18]

A preliminary study of ion transfer across a polymer gel - liquid interface and its use as a voltammetric detector for a flow system has been reported by Marecek et al.[19] This paper describes a thin-layer amperometric detector based on ion transfer across a water - solidified nitrobenzene (W/SNb) interface. The transfer process and its application to the determination of tetracycline (TC) and terramycin [oxytetracycline (OT)] have been investigated using FIA; an accurate, fast and convenient method has been developed.

Experimental

Apparatus

Fig. 1 shows a three-electrode thin-layer flow-through cell that is similar to a conventional amperometric detector.[9] The reference and auxiliary electrodes were positioned downstream of the mobile aqueous phase. The solidified nitrobenzene phase consists of part of the working electrode with an interface area of 7.07 mm^2. The Ag - AgCl electrode was placed in an aqueous solution solidified by the addition of agar containing a 0.05 M tetrabutylammonium chloride (TBACl)

solution and was brought into contact with the solidified nitrobenzene (PhNO$_2$) phase by using a 0.05 M tetrabutylammonium tetraphenylborate (TBATPB) solution as the supporting electrolyte. In this way the Ag - AgCl electrode served as both reference and auxiliary electrodes for the PhNO$_2$ phase and was connected to the terminal of the working electrode in the three-electrode potentiostat. The potentiostat used as the detector controller was laboratory-built[10] and the flow injection peaks were recorded on a Model LZX-204 recorder (Dahua, Instrument Factory, Shanghai). The flow injection system consisted of a JASCO LCP-350 pump and a laboratory-made injection valve with a 20-μl sample loop. All measurements were made at laboratory temperature (20 ± 2 °C).

Reagents

A solution of 0.1 M KH$_2$PO$_4$ and 1 mM EDTA was used as the mobile phase and the pH was adjusted with H$_3$PO$_4$ or KOH. Nitrobenzene was used after purification by extraction. The other reagents were used as received. The solidified nitrobenzene phase was prepared according to the method of Marecek et al.[19] National standards of tetracycline and terramycin were
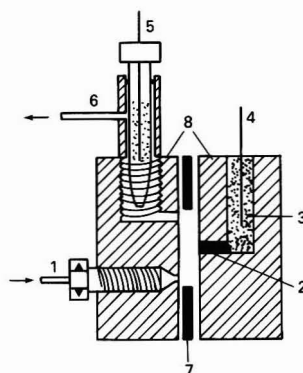
Fig. 1. Schematic diagram of the thin-layer flow-through cell. 1, Solution inlet; 2, 0.05 M TBATPB (PhNO$_2$) + PVC + agar; 3, 0.05 M TBACl (H$_2$O) + agar; 4, Ag - AgCl, working electrode; 5, Ag - AgCl + 0.05 M TBACl, reference electrode; 6, solution outlet, auxiliary electrode; 7, PTFE gasket (100 μm); and 8, PTFE cell bodies

---

* To whom correspondence should be addressed.

used and the antibiotic samples were kindly donated by the Jilin Institute of Pharmaceutical Inspection, Jilin, China. All aqueous solutions were prepared in doubly distilled water.

Analysis of Samples

A buffer solution consisting of 0.1 M KH_2PO_4 and 1 mM EDTA (pH 2.0) was used as the mobile phase in the analysis of the samples. A 0.100-g amount of the sample or TC and OT standard was dissolved in 10 ml of 0.1 M HCl, diluted to 25 ml with water and further diluted 100-fold with the mobile phase (the final concentration is *ca.* 0.2 mM). Using a flow-rate of 0.5 ml min⁻¹ and a potential of 0.430 V, 20 µl of the sample or standard solution were injected after the base line had been allowed to stabilise for 40 min. The amount of TC and OT in the antibiotic samples was calculated by comparing the peak heights given by the sample and standard. By using this procedure, 60 samples could be determined in 1 h. An aliquot of the standard solution was injected every 10 min in order to check the accuracy of the measurements.

Results and Discussion

Response Characteristics

Tetracyclines are zwitterions. Hence, the amino group of tetracycline can accept a proton ($pK_a = 3.3$) to give a protonated tetracycline complex which has a polycyclic structure (Fig. 2) with hydrophobic properties. When a potential is applied to the W/SNb system, the protonated cations can be transferred across the interface. Fig. 3 shows flow injection peaks for TC and OT at an applied potential of 0.40 V, which corresponds to the current required for transfer of the cations from the mobile aqueous phase to the solidified nitrobenzene phase. As can be seen from Fig. 3, the peaks are sharp and, therefore, easy to measure. The peak currents are 45.5 and 9.5 nA for TC and OT, respectively.

The equation describing the current response of the thin-layer amperometric detector can be written as[20]

$$i = 1.47nFC(DA/b)^{\frac{2}{3}}U^{\frac{1}{3}} \qquad .. \quad .. \quad (1)$$

where A is the electrode area and b is the height of the thin layer. It can be seen that the current is directly related to the

R_1	R_2	R_3	R_4	
H	OH	H	OH	tetracycline
H	OH	OH	OH	oxytetracycline

Fig. 2. Structure of TC and OT
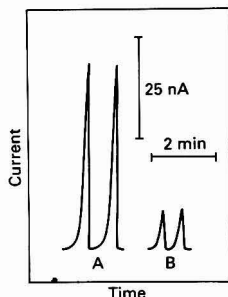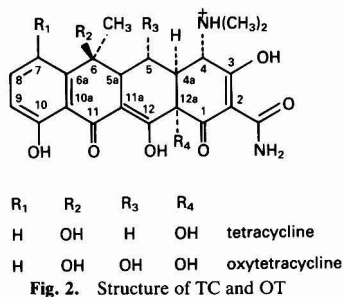
Fig. 3. Flow injection peaks for (A) 0.2 mM TC and (B) OT. Mobile phase, 0.1 M KH_2PO_4 + 1 mM EDTA, pH 2.0; Potential, 0.40 V

concentration of the analyte (C), the diffusion coefficient (D) and the bulk flow-rate (U) for a given flow cell. The theoretical logarithmic dependence of the current on the flow-rate is $\frac{1}{3}$; this result was also obtained when a glassy carbon electrode was used.[10] With the W/SNb interface detector, it was found that the current decreased from 114 to 100 nA for TC and from 38 to 35 nA for OT at flow-rates varying from 0.3 to 1.2 ml min⁻¹. A similar effect has also been observed for both tetramethylammonium (TMA) and ReO_4^- ions and for acetylcholine (ACh) at the same interface.[21] The glassy carbon electrode detector coated with polymers such as Nafion[10] or polyvinylpyridine[22] shows a similar flow-rate dependence to that of the W/SNb interface detector. It was concluded[21] that mass transport is controlled by the diffusion of analytes in the polymer film. Hence, by analogy, it is reasonable to assume that the response current for TC and OT at the W/SNb interface is also controlled by diffusion of the analytes in the solidified nitrobenzene phase rather than in the aqueous solution. This is in contrast to the results obtained for voltammetry at a water - nitrobenzene (W/Nb) interface.[16]

The effect of the applied potential on the response current (hydrodynamic voltammogram) for TC and OT is shown in Fig. 4. When the applied potential is less positive than 0.10 V, no response is observed. Both compounds reach their maximum response at 0.45 V and a peak current is observed (Fig. 4) that is probably due to the interaction of the analytes with the electrolyte (TBATPB) in the nitrobenzene phase at a more positive potential. The optimum potential was found to be in the range 0.40–0.45 V for analytical application. The similar shape of the hydrodynamic voltammograms shown in Fig. 4 suggests that TC and OT have similar transfer characteristics at the W/SNb interface. However, a much larger peak was observed for TC than for OT (Fig. 3), indicating that the diffusion behaviour of the analytes in the solidified nitrobenzene phase is markedly different; this was not apparent from voltammetry at a W/Nb interface.

As reported previously,[16] the shape of the voltammograms is affected considerably by the pH of the aqueous phase. This dependence is due to the fact that tetracyclines are zwitterions and so only the cations are able to transfer across the interface. Similar results were obtained with the flow-through detector, as shown in Fig. 5. The current response shows little variation in the (protonated) pH range 1–2.5 for OT and 2–4.5 for TC. The peaks diminish when the pH of the mobile aqueous phase is greater than 6 and 4.5 for TC and OT, respectively, showing that deprotonation of the cations is occurring.

Analytical Applications

Preliminary experiments have shown that the W/SNb interface detector described here can be used continuously for at least 1 week, with only a gradual decrease in the response due to the loss of electrolyte in the solidified nitrobenzene phase. Using a pH 2.0 phosphate buffer as the mobile phase and an applied potential of 0.40 V, the coefficients of variation for 22
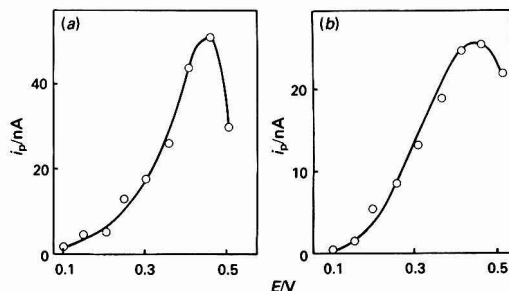
Fig. 4. Hydrodynamic voltammograms of (a) TC and (b) OT. Conditions as in Fig. 3.
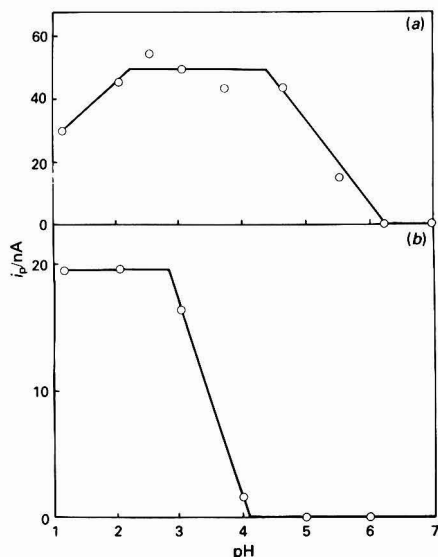
Fig. 5. Influence of pH of the mobile phase on the response of (a) TC and (b) OT. Conditions as in Fig. 3

Table 1. Determination of TC and OT in several drugs

Sample		FIA - EC/ $\mu g\,mg^{-1}$	Biological assay/ $\mu g\,mg^{-1}$	Relative standard deviation,%*
TC 807035A	..	892 ± 8	889	+0.3
TC 970309A	..	921 ± 16	928	−0.7
OT 840551	..	$844 + 3$	845	−0.1
OT 84031 ..	..	884 ± 5	877	+0.8
OT 84033 ..	..	879 ± 10	875	+0.5

* Our results were compared with those given by a microbiological assay performed by the Jilin Institute of Pharmaceutical Inspection, China.

replicate injections of 0.2 mм TC and OT were 1.2 and 2.5%, respectively.

A linear response was found in the concentration range 2–200 μM TC and 5–300 μM OT with regression equations $i(\mathrm{nA}) = 0.184C_{\mathrm{TC}} + 0.06$, $r = 0.9995$ and $i(\mathrm{nA}) = 0.112C_{\mathrm{OT}} + 0.07$, $r = 0.9990$, respectively. The detection limit is *ca.* 20 ng for TC and 50 ng for OT. When the concentration is such that a response current greater than 100 nA is produced, linearity is lost owing to the resulting high resistance in the solidified nitrobenzene phase.

The above experiment demonstrates that the W/SNb interface detector can be used for the determination of TC and OT. Therefore, the TC and OT contents in antibiotic samples can be determined using FIA with amperometric detection. Table 1 shows the results obtained, which are in good agreement with those given by a biological assay, the relative standard deviation being less than 1%. The proposed method is simpler and more accurate than that using a water - nitrobenzene interface[15,16] and demonstrates the advantages of FIA.

In conclusion, FIA with amperometric detection, based on ion transfer across a water - solidified nitrobenzene interface, is an effective method for the determination of tetracycline and terramycin in drugs. The method can be extended to other substances that are able to transfer across the interface, such as chlortetracycline and erythromycin. In conjunction with liquid chromatography, it could become an accurate and effective method for the study of biological processes.

References

1. Nagy, G., Feher, Z., and Pungor, E., *Anal. Chim. Acta*, 1970, **52**, 47.
2. Růžička, J., and Hansen, E. H., *Anal. Chim. Acta*, 1975, **78**, 145.
3. Pacey, G. E., and Bubnis, B. P., *Trends Anal. Chem.*, 1987, **6**, 165.
4. Kissinger, P. T., *Anal. Chem.*, 1977, **49**, 447A.
5. Cox, J. A., and Kulkarni, K. R., *Talanta*, 1986, **33**, 911.
6. Betteridge, D., *Anal. Chem.*, 1978, **50**, 832A.
7. Mosbach, K., and Danielsson, B., *Anal. Chem.*, 1981, **53**, 83A.
8. Ranger, C. B., *Anal. Chem.*, 1981, **53**, 21A.
9. Kissinger, P. T., and Heineman, W. R., "Laboratory Techniques in Electroanalytical Chemistry," Marcel Dekker, New York, 1984, pp. 611–635.
10. Ji, H., and Wang, E., *J. Chromatogr.*, 1987, **410**, 111.
11. Stulik, K., and Pacakova, V., "Electroanalytical Measurements in Flowing Liquids," Wiley, New York, 1987.
12. Dornbush, A. C., and Abbey, A., *in* Kavanagh, F., *Editor*, "Analytical Microbiology," Volume 2, Academic Press, New York, 1972, p. 365.
13. Kelly, R. G., and Hoyt, K. B., *Z. Klin. Chem. Klin. Biochem.*, 1969, **7**, 152.
14. Levine, J., Garlock, E. V., and Fischbach, H., *J. Am. Pharm. Assoc.*, 1949, **38**, 473.
15. Kozlov, Y. N., and Koryta, J., *Anal. Lett.*, 1983, **16**, 255.
16. Wang, E., and Liu, Y., *J. Electroanal. Chem.*, 1986, **214**, 459.
17. Wang, E., Liu, Y., and Jiang, Y., *in* Conan, K. N. L., *Editor*, "Proceedings of the Symposium on Electrochemical Sensors for Biomedical Applications," The Electrochemical Society, Pennington, 1986, pp. 35–46.
18. Wang, E., and Sun, Z., *Trends Anal. Chem.*, 1988, **7**, 99.
19. Marecek, V., Janchenova, H., Colombini, M. P., and Pappoff, P., *J. Electroanal. Chem.*, 1987, **217**, 213.
20. Elbicki, J. M., Morgan, D. M., and Weber, S. G., *Anal. Chem.*, 1984, **56**, 978.
21. Wang, E., and Ji, H., *Electroanalysis*, in the press.
22. Wang, J., Golden, T., and Tuzhi, T., *Anal. Chem.*, 1987, **59**, 740.

Determination of Trace Amounts of Aluminium in Tap Water by Spectrophotometry After Collection on a Membrane Filter Using Chrome Azurol S and Zephiramine

Kunio Ohzeki, Takashi Uno, Isoshi Nukatsuka and Ryoei Ishida
Department of Chemistry, Faculty of Science, Hirosaki University, 036 Hirosaki, Japan

A sensitive and selective spectrophotometric method for the determination of aluminium(III) using Chrome Azurol S and Zephiramine is described. The ion-pair precipitate formed between Zephiramine and perchlorate ions is effective for the enrichment of aluminium(III) on a membrane filter as its ternary complex with Chrome Azurol S and Zephiramine. The solid-state absorbance of the complex on the membrane filter is measured at 640 and 700 nm against a blank thin layer and the difference is calculated. Although the calibration graph does not obey Beer's law good reproducibility is observed, the relative standard deviation for 0.10 µg of aluminium(III) in a 20-ml sample volume being 3.1% (n = 5). A ligand buffer solution, composed of *trans*-cyclohexane-1,2-diaminetetraacetic acid and an excess of zinc(II), is effective for masking interferences from foreign ions, particularly iron(III). The method has been applied to the determination of aluminium in tap water.

Keywords: *Aluminium determination; ion-pair precipitate; spectrophotometry; membrane filter; tap water*

The sensitivity of the spectrophotometric determination of a metal ion with a triphenylmethane dye, such as Catechol Violet (CV), Chrome Azurol S (CAS) and Eriochrome Cyanine R (ECR), can be increased by the presence of a cationic surfactant such as cetylpyridinium (CP) chloride, cetyltrimethylammonium (CTA) chloride and Zephiramine (Zeph).[1] The effects of cationic surfactants on these sensitised systems have been reviewed.[2] For the determination of aluminium(III), methods based on CAS - CTA,[3] CV - CTA,[4] CAS - Zeph,[5] ECR - Zeph[6] and CAS - CP[7] have been reported. The ECR - CTA method has been used in conjunction with flow injection analysis.[8]

We have been concerned with increasing the sensitivity of spectrophotometry for the determination of trace amounts of metals by selective enrichment of the metal as a coloured species on a thin layer of ion-exchange resin[9-13] or a membrane filter.[14,15] The coloured species is concentrated as a circular thin layer and determined directly by spectrophotometry or densitometry. The aim of this work was to develop a sensitive and selective method for the spectrophotometric determination of aluminium(III) using CAS and Zephiramine. The sensitivity of the method is enhanced by the enrichment of aluminium(III) on a membrane filter as its ternary complex with CAS and Zephiramine. The selectivity of the method is increased by using a ligand buffer solution[15,16] composed of *trans*-cyclohexane-1, 2-diaminetetraacetic acid (CyDTA) and an excess of zinc(II). The proposed method was applied to the determination of aluminium in a tap water sample at the µg l^{-1} level.

Experimental

Apparatus

A Hitachi 150–20 spectrophotometer was used for measuring the absorbance of the aluminium(III) - CAS - Zeph complex fixed on the membrane filter. A Hitachi–Horiba Type M-7$_{\mathrm{II}}$ pH meter was used for the measurement of pH. A Toyo KG-25 filter holder, with a Toyo membrane filter of cellulose nitrate (0.2 µm pore size), was used for collecting the ternary complex together with the Zephiramine - perchlorate ion-pair precipitate by filtration under suction. A Yamato Model WAR Auto Still was employed to purify the water used; water was first passed through a semi-permeable membrane and then distilled. Disposable polypropylene beakers (Despo-cup,

Iuchi, Japan) were used as received. PTFE beakers were immersed overnight in 2 M nitric acid before use.

Reagents

All reagents used were of analytical-reagent grade. Permeated, distilled water was further distilled once before use.

Aluminium(III) standard solution, 1000 p.p.m., *pH* 1. Prepared by dissolving 17.5827 g of aluminium(III) potassium sulphate dodecahydrate, $AlK(SO_4)_2 \cdot 12H_2O$, in dilute hydrochloric acid and diluting to 1000 ml. A working solution containing 1.00 µg ml^{-1} of aluminium(III) was prepared by appropriate dilution of the stock solution, maintaining a pH of 1.

Chrome Azurol S solution, 1.0 mM. CAS was obtained from Dojindo (Kumamoto, Japan) and used as received.

CyDTA solution, 50 mM, *pH* ca. 6. Prepared by dissolving *trans*-cyclohexane-1,2-diaminetetraacetic acid monohydrate (CyDTA, Dojindo) in water containing sodium hydroxide.

Zinc(II) - CyDTA solution, *pH* 4.0. Prepared by mixing 100 ml of a 50 mM CyDTA solution with 100 ml of a 250 mM zinc(II) nitrate solution. The pH was adjusted by the addition of *ca.* 0.8 ml of 10 M sodium hydroxide solution.

Zephiramine solution, 10 mM. Prepared by dissolving tetradecyldimethylbenzylammonium chloride dihydrate (Dotite Zephiramine, Dojindo) in water containing 1.0 mM CyDTA.

Sodium perchlorate solution, 3.0 M. Prepared by dissolving sodium perchlorate monohydrate in water containing 1.0 mM CyDTA.

Ammonium acetate solution, 2.0 M. Prepared by dissolving ammonium acetate in water containing 1.0 mM CyDTA.

General Procedure

A 20-ml aliquot of an acidified sample solution (pH *ca.* 2) containing 0.20 µg of aluminium(III) was placed in a 150-ml polypropylene beaker and 2 ml of the zinc(II) - CyDTA solution were added. The pH of the resulting solution was about 2.5. The mixture was allowed to stand for 10 min after which time 2 ml of ammonium acetate solution were added to adjust the pH of the solution to about 6. Then, 0.25 ml of CAS, 1 ml of sodium perchlorate and 2 ml of Zephiramine solutions were added successively. The whole was mixed well

by swirling and then allowed to stand for about 15 min. The aluminium(III) - CAS - Zeph complex together with the Zephiramine - perchlorate ion-pair precipitate was collected on a membrane filter of 0.2 μm pore size (for economy, a membrane filter of 47 mm i.d. was divided into two halves and each half was used) by filtration under suction. Hence, the ternary complex was concentrated on the membrane filter as a circular thin layer 17 mm in diameter. The membrane filter was stored wet for about 15 min on a filter-paper impregnated with water. A blank thin layer was prepared using the same procedure except that no aluminium(III) was added. The wet membrane filter holding the Al(III) - CAS - Zeph complex was placed on a glass plate attached to the sample-side window of the detector of the spectrophotometer, and the wet membrane filter holding the blank thin layer was placed on a glass plate attached to the reference-side window. The absorbances were measured at 640 and 700 nm, and the difference was calculated.

Determination of the Solubility Product of the Ion-pair Precipitate Formed Between Zephiramine and Perchlorate Ions

A 10 mM Zephiramine solution ($f = 1.16$) was prepared by dissolving the Dotite reagent in water. A 25 mM perchlorate solution ($f = 0.998$) was prepared by dissolving sodium perchlorate monohydrate in water and the factor was determined gravimetrically by using tetraphenylphosphonium chloride as precipitant.[17] The procedure for the determination of the solubility product was as follows. A suitable volume of the 10 mM Zephiramine solution was placed in a 100-ml calibrated flask and 20 ml of a 1.00 M sodium chloride solution were added to adjust the ionic strength. The mixture was diluted to about 90 ml with water and an aliquot of the 25 mM sodium perchlorate solution was added so that the concentration of NaClO$_4$ in the solution was the same as that of Zephiramine. The mixture was made up to the mark with water. The ionic strength of the resulting solution was 0.2 and the initial concentrations of Zephiramine and perchlorate ions were both about 0.1 mM (see Table 1). The whole was mixed well, left to stand for 10 min in a water-bath at 20 ± 0.1 °C and then filtered through a membrane filter of 0.65 μm pore size. The first 40-ml portion of the filtrate was discarded and the next 5-ml portion was analysed for Zephiramine using the reported method.[14]

Determination of Total Aluminium in Tap Water

A tap water sample was taken after running the water for more than 1 h. A 5-ml aliquot of the tap water sample was placed in a 100-ml PTFE beaker and 1 ml of 0.1 M hydrochloric acid was added. The solution was covered with a PTFE watch-glass and heated on a hot-plate at about 65 °C for 30 min. After cooling, the solution was diluted to about 20 ml with water. The determination of aluminium was then carried out as described under General Procedure.

Determination of Filtrable Aluminium in Tap Water

A 400-ml portion of a tap water sample was filtered, with the aid of a plastic filter holder, through a membrane filter of 0.45 μm pore size under suction. Then, 100-ml portions of the filtrate were taken successively and a 5-ml aliquot of each 100-ml fraction was analysed as described under Determination of Total Aluminium in Tap Water.

Results and Discussion

Extraction of the Ternary Complex on a Membrane Filter

The solubility product of the [Zeph$^+$][ClO$_4^-$] ion-pair precipitate was found to be 1.76×10^{-9} as shown in Table 1.

Table 1. Results of the determination of the solubility product of the ion-pair precipitate formed between Zephiramine and perchlorate ions. Ionic strength, 0.2; temperature, 20 °C

Initial concentration of Zephiramine and perchlorate ions /μmol l^{-1}	Zephiramine found in solution /μmol l^{-1}	Solubility product
80.4	44.5	1.98×10^{-9}
104.0	40.4	1.63×10^{-9}
116.0	41.0	1.68×10^{-9}
	Mean:	1.76×10^{-9}
	Standard deviation:	$\pm 0.19 \times 10^{-9}$
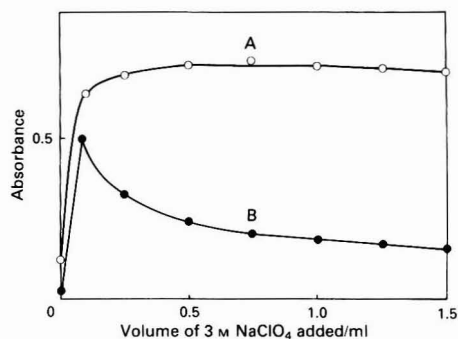
Fig. 1. Effect of perchlorate ion on the extraction of aluminium(III) as the Al - CAS - Zeph complex from solution on a membrane filter. Except for the amounts of sodium perchlorate, the other conditions were the same as those given under General Procedure. A, Sample thin layer vs. blank thin layer; and B, blank thin layer vs. membrane filter
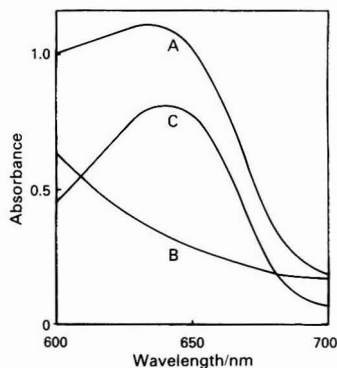
Fig. 2. Absorption spectra of the Al - CAS - Zeph complex in a thin layer of an ion-pair precipitate of Zephiramine and perchlorate ions. Thin layers were prepared as described under General Procedure. A, Sample thin layer containing 0.20 μg of aluminium vs. membrane filter; B, blank thin layer vs. membrane filter; and C, sample thin layer vs. blank thin layer

Therefore, it was expected that in the presence of a large excess of perchlorate ion (with respect to Zephiramine) almost all the Zephiramine ions, except for those involved in the formation of the aluminium(III) - CAS - Zeph complex, would be precipitated quantitatively. It was further expected that the ternary aluminium(III) - CAS - Zephiramine complex would be co-precipitated with the Zephiramine - perchlorate ion-pair precipitate and concentrated on the membrane filter by filtration. Perchlorate ion was found to have a significant effect on the extraction of the ternary complex, as shown in Fig. 1. The recovery of the complex on the membrane filter increased with increasing amounts of perchlorate ion added and reached a maximum at a molar ratio of perchlorate to Zephiramine ions ranging from 75 to 150. On the other hand,
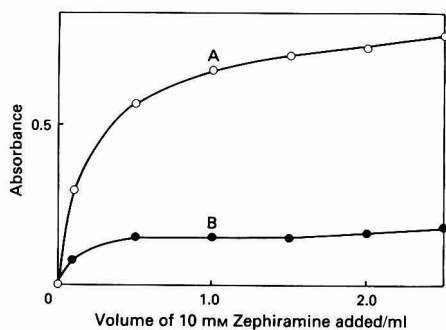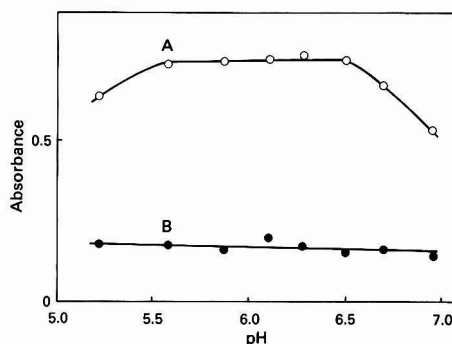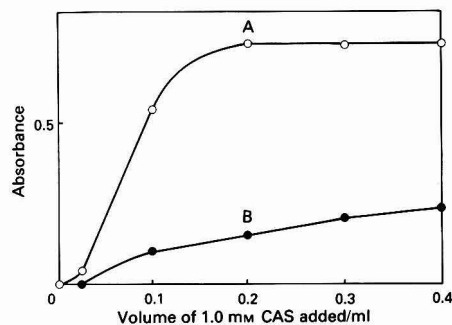
Fig. 3. Effect of Zephiramine on the extraction of aluminium(III) as the Al - CAS - Zeph complex on a membrane filter. Except for the amounts of Zephiramine, the other conditions were the same as those given under General Procedure. A, Sample thin layer vs. blank thin layer; and B, blank thin layer vs. membrane filter

the blank value initially increased and then decreased with increasing amounts of perchlorate ion, as shown in Fig. 1. The decrease in the blank value was probably due to the competition between the CAS anion and the perchlorate ion for the Zephiramine cation. The ternary complex together with the ion-pair precipitate could be collected effectively using membrane filters with pore sizes in the range 0.20–0.65 μm.

The absorption spectrum of the ternary complex fixed on a membrane filter had a maximum at 640 nm as shown in Fig. 2. As the composition of the aluminium(III) - CAS - CTA ternary complex is reported to be 1:2:4,[6] the same composition could be expected for the aluminium(III) - CAS - Zeph complex.

Effect of Zephiramine

The effect of Zephiramine on the extraction of aluminium-(III) as the Al^{III} - CAS - Zeph complex was studied by adding various amounts of Zephiramine in the presence of a large excess of perchlorate ion. The absorbance of the thin layer on the membrane filter was increased as increasing amounts of Zephiramine were added, as shown in Fig. 3. The sharp increase in the absorbance was mainly due to an increase in the recovery of aluminium as the ternary complex, which in turn was due to the increasing amounts of Zephiramine added. The addition of large amounts of Zephiramine resulted in only a gradual increase in the absorbance mainly because of an increase in the effective optical path-length as the thickness of the thin layer of the precipitate increased.

Effect of pH

The dependence of the absorbance on the pH of the medium was examined (Fig. 4). The pH was adjusted with the use of 1 M acetic acid, 1 M ammonium acetate solution and 1 M ammonia. After extraction of the Al^{III} - CAS - Zeph complex, as described under General Procedure, the pH of the filtrate was measured. The maximum absorbance of the ternary complex was obtained in the pH range 5.6–6.5, whereas the blank value was almost constant in the pH range studied.

Effect of CAS

A maximum and constant absorbance for 7.4 nmol of aluminium was obtained in the presence of a 27-fold molar excess of CAS over aluminium, as shown in Fig. 5. The blank absorbance, however, gradually increased with increasing CAS concentration.

Ligand Buffer Solution

In nature, aluminium almost always occurs as compounds with iron. As iron(III) can also form a ternary complex with CAS and Zephiramine, which interferes in the determination of

Fig. 4. Effect of pH on the extraction of aluminium(III) as the Al - CAS - Zeph complex on a membrane filter. Except for the solution pH, the other conditions were the same as those given under General Procedure. A, Sample thin layer vs. blank thin layer; and B, blank thin layer vs. membrane filter

Fig. 5. Effect of CAS on the extraction of aluminium(III) as the Al - CAS - Zeph complex on a membrane filter. Except for the amounts of CAS, the other conditions were the same as those given under General Procedure. A, Sample thin layer vs. blank thin layer; and B, blank thin layer vs. membrane filter
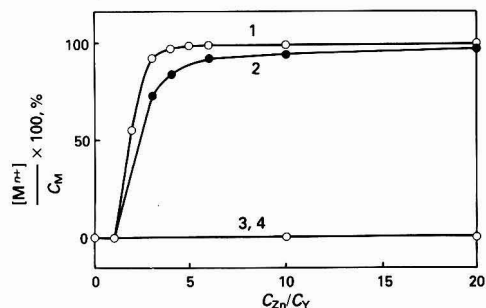
Fig. 6. Effect of zinc(II) on the complexation of aluminium(III) and iron(III) with CyDTA and EDTA. 1, Al^{III} - CyDTA; 2, Al^{III} - EDTA; 3, Fe^{III} - CyDTA; and 4, Fe^{III} - EDTA. C_{Zn} and C_Y denote the total concentrations of zinc(II) and CyDTA or EDTA, respectively. The total concentration of each ion, C_M, is assumed to be much less than the total concentration of either CyDTA or EDTA

aluminium,[1] it is necessary to mask the effect of iron before aluminium can be determined satisfactorily. 1,10-Phenanthroline[6,8] and 2,2'-bipyridyl[7] have been used for this purpose; however, the masking of interferents as small or non-coloured species is preferable. In this work a ligand buffer solution composed of CyDTA and an excess of zinc(II) was examined to test its effectiveness in masking iron(III).

The logarithmic values of the stability constants of the binary CyDTA complexes with aluminium(III), zinc(II) and iron(III) are reported to be 17.6, 18.7 and 29.3, respectively.[18] From these values it is expected that, in the presence of an excess of zinc(II) over CyDTA, the formation of a CyDTA
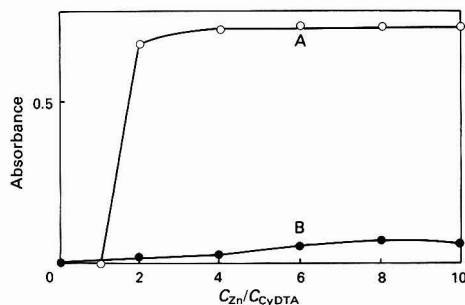
Fig. 7. Effect of zinc(II) on the formation of the Al - CAS - Zeph and Fe^{III} - CAS - Zeph complexes in the presence of CyDTA. A, Aluminium(III), 0.20 µg; and B, iron(III), 20 µg; CyDTA, 50 µmol. Except for the amounts of zinc(II), the other conditions were the same as those given under General Procedure
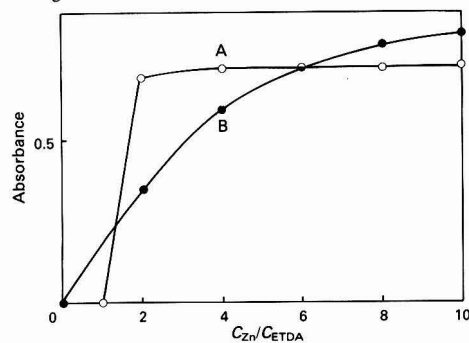
Fig. 8. Effect of zinc(II) on the formation of the Al - CAS - Zeph and Fe^{III} - CAS - Zeph complexes in the presence of EDTA. A, Aluminium(III), 0.20 µg; and B, iron(III), 20 µg; EDTA, 50 µmol
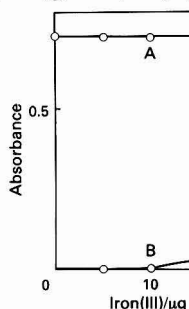
Fig. 9. Effect of a ligand buffer solution for masking the effect of iron(III). A, In the presence of 0.20 µg of aluminium(III); and B, in the absence of aluminium(III). Other conditions were the same as those given under General Procedure

complex with aluminium(III) will be suppressed, whereas iron(III) will be complexed quantitatively with CyDTA. On the basis of theoretical considerations of the actions of the ligand buffer solution,[15,16] it was predicted that a five-fold excess of zinc(II) over the total concentration of CyDTA would be required to satisfy the above conditions (see Fig. 6). If the excess of zinc(II) does not affect the determination of aluminium(III) with CAS, if the rate of formation of the iron(III) - CyDTA binary complex is reasonably fast and if the complex once formed does not react with CAS, then it should be possible to determine aluminium(III) without interference from iron(III). For comparison, the effect of zinc(II) on the formation of EDTA complexes is also illustrated in Fig. 6.

Effect of CyDTA and Zinc(II)

The effect of CyDTA and zinc(II) on the formation of the aluminium(III) - CAS - Zephiramine ternary complex was
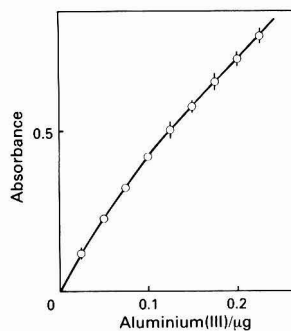
Fig. 10. Calibration graph for the determination of aluminium. Error bars indicate 95% confidence limits ($n = 5$)
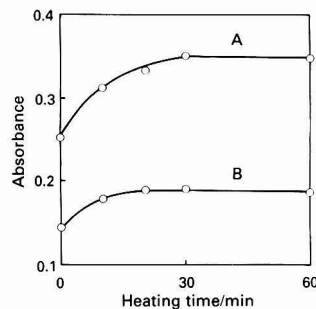
Fig. 11. Effect of heating time on the determination of aluminium in a tap water sample. Sample volumes: A, 10.0; and B, 5.0 ml. Heating temperature, *ca.* 65 °C

studied by adding a fixed amount of CyDTA to solutions containing a constant amount of aluminium(III) or iron(III) and various amounts of zinc(II). When the molar ratio of zinc(II) to CyDTA was less than 1, aluminium(III) complexed with CyDTA and formation of the ternary complex with CAS and Zephiramine was completely suppressed, as shown in Fig. 7. However, when the molar ratio of zinc(II) to CyDTA was increased beyond 4, the colour of the Al^{III} - CAS - Zeph complex reached a maximum and remained constant, whereas the formation of the corresponding iron(III) ternary complex was largely suppressed. When CyDTA was added before the addition of an excess of zinc(II), the colour development of the Al^{III} - CAS - Zeph complex was slow and did not reach a maximum even after 30 min.

The effect of EDTA was also examined for comparison purposes (Fig. 8). It was found that EDTA was not effective in masking iron(III) and that the formation of the Al^{III} - CAS - Zeph complex was not affected by EDTA in the presence of more than a four-fold excess of zinc(II) over EDTA. These results seem to conflict with the theoretical prediction given by Fig. 6. This discrepancy is probably due to the slow rate of formation of the iron(III) - and aluminium(III) - EDTA complexes.[19]

Effect of Iron(III)

The standing time required to eliminate the interfering effect of iron(III) was examined with the use of a ligand buffer solution composed of 25 mM CyDTA and 125 mM zinc(II). When 2 ml of the ligand buffer solution were added to a 20-ml sample aliquot, the maximum masking effect was attained after a standing time of more than 10 min, and up to 10 µg of iron(III) could be masked successfully, as shown in Fig. 9. Although large amounts of iron(III) could not be masked satisfactorily, it was still possible to determine 0.2 µg of aluminium(III) in the presence of up to a 100-fold excess of iron(III).

Effect of Sample Volume

The recovery of aluminium(III) as its ternary complex with CAS and Zephiramine was investigated using different sample volumes. The absorbance of a thin layer prepared from a solution containing 0.2 µg of aluminium(III) increased almost linearly from 0.705 to 0.750 absorbance units with increasing sample volumes over the range 10–30 ml. The volume of the sample was, therefore, adjusted to 20 ml before the addition of the ligand buffer solution.

Effect of Temperature

The effect of the temperature of the reaction mixture on the determination of aluminium(III) as the ternary complex was examined. The absorbance of a thin layer prepared from a solution containing 0.2 µg of aluminium(III) decreased as the

Table 2. Effect of foreign ions on the determination of aluminium(III). Al^{III}, 0.2 µg; sample volume, 20 ml. Reagents added: Zn^{II} (125 mM) - CyDTA (25 mM), 2 ml; ammonium acetate, 2 M, 2 ml; CAS, 1 mM, 0.25 ml; sodium perchlorate, 3 M, 1 ml; and Zephiramine, 10 mM, 2 ml

Ion			Added as	Tolerance ratio to 0.2 µg of aluminium(III)	Relative error, %*
Li^I	..	..	LiCl	50	+2.3
K^I	..	..	KCl	50	+3.2
Be^{II}	..	..	$BeCl_2$	0.5	+34.5
				0.1	+9.5
Mg^{II}	..	..	$MgCl_2$	12 000	+0.9
Ca^{II}	..	..	$CaCl_2$	20 000	+3.2
B^{III}	..	..	H_3BO_3	50	+2.5
Si^{IV}	..	..	Na_2SiO_3	50	+0.5
P^V	..	..	$(NH_4)_2HPO_4$	50	+4.2
Ti^{IV}	..	..	$Ti(SO_4)_2$	50	−3.5
V^V	..	..	NH_4VO_3	50	−1.8
Cr^{VI}	..	..	$K_2Cr_2O_7$	50	+0.9
Cr^{III}	..	..	$K_2Cr_2(SO_4)_4$	10	−5.8
				5	−1.6
Mn^{II}	..	..	$MnCl_2$	50	−0.4
Fe^{II}	..	..	$(NH_4)_2Fe(SO_4)_2$	1	−24.2
				25†	+1.0
Co^{II}	..	..	$CoCl_2$	50	+1.2
Ni^{II}	..	..	$NiCl_2$	50	−0.1
Cu^{II}	..	..	$CuSO_4$	50	+0.1
Ga^{III}	..	..	$Ga(NO_3)_3$	50	+0.2
Ge^{IV}	..	..	K_2GeO_3	50	+2.6
As^V	..	..	Na_2HAsO_4	50	+4.4
As^{III}	..	..	$NaAsO_2$	50	−1.7
Mo^{VI}	..	..	$(NH_4)_6Mo_7O_{24}$	50	+3.2
Rh^{III}	..	..	$Rh(NO_3)_3$	10	−22.3
				1	−0.6
Pd^{II}	..	..	$PdCl_2$	50	+0.8
Cd^{II}	..	..	$CdCl_2$	50	+1.0
In^{III}	..	..	$In(NO_3)_3$	50	+0.1
Sn^{II}	..	..	$SnCl_2$	50	−0.4
Sb^{III}	..	..	$SbCl_3$	50	−3.5
Pt^{IV}	..	..	H_2PtCl_6	50	+1.8
Hg^{II}	..	..	$HgCl_2$	50	+0.5
Tl^I	..	..	$TlNO_3$	50	+2.6
Pb^{II}	..	..	$Pb(NO_3)_2$	50	+4.4
F^-	..	..	NaF	50	−35.9
				25	−7.1
				10	−3.5

* Calculated using the equation

$$\left[\left(\frac{A - A_{0.175}}{A_{0.225} - A_{0.175}} \times 0.050 + 0.175\right) - 0.200\right] \times \frac{100}{0.200}$$

where A is the net absorbance observed in the presence of each foreign ion and $A_{0.225}$ and $A_{0.175}$ are the net absorbances for 0.225 and 0.175 µg of aluminium(III), respectively; these values were 0.798 and 0.656, respectively, based on the calibration graph.

† A 25-µl aliquot of 3% hydrogen peroxide was added.

temperature of the solution increased; the absorbances were 0.860 at 12 °C, 0.769 at 15 °C, 0.737 at 18 °C and 0.705 at 23 °C. Consequently, a low and constant temperature should be employed for the determination of aluminium(III). However, for simplicity, the whole procedure was carried out at room temperature, which gave solution temperatures in the range 18–20 °C.

Colour Stability

The stability of the colour of the Al^{III} - CAS - Zeph complex was studied for various standing times after the addition of Zephiramine. The maximum absorbance was attained after 12 min and the colour was stable for up to 60 min. The colour of the ternary complex when fixed on a membrane filter was also stable for at least 60 min provided that the filter was kept wet with water.

Calibration Graph

A calibration graph for the determination of aluminium(III) was prepared as described under General Procedure. As the solid-phase absorbance observed here was due to both absorption and scattering of light, the graph did not obey Beer's law, as shown in Fig. 10. The relative standard deviation was 3.1% ($n = 5$) and 2.4% ($n = 5$) for 0.10 and 0.20 µg of aluminium, respectively. The mean and standard deviation of the blank absorbance measured against a membrane filter was 0.173 ± 0.007 absorbance units ($n = 32$), and the limit of detection, based on three times the standard deviation of the blank, was found to be 0.004 µg of aluminium(III). A semi-quantitative determination of aluminium at the ng ml^{-1} level could easily be carried out with the naked eye by observing the differences in the colour of the Al^{III} - CAS - Zeph complex fixed on a membrane filter.

Table 3. Determination of aluminium in tap water

Water sample*	Amount taken/ml	Aluminium(III) added/µg	Absorbance†	Aluminium in tap water, p.p.b.
1	5.0	—	0.189	8.2
	5.0	—	0.191	8.3
	5.0	—	0.185	8.0
	10.0	—	0.354	8.3
	10.0	—	0.346	8.1
				Mean: 8.16
				SD: ±0.11
2	5.0	—	0.210	9.2
	5.0	0.10	0.566	9.1
	7.5	—	0.278	8.5
	7.5	0.10	0.613	8.1
				Mean: 8.72
				SD: ±0.52
3	5.0	—	0.189	8.2
	5.0	0.10	0.550	8.1
	7.5	—	0.264	8.0
	7.5	0.10	0.594	7.3
	10.0	—	0.334	7.8
	10.0	0.10	0.670	8.0
				Mean: 7.90
				SD: ±0.32
4	5.0	—	0.188	8.2
	5.0	0.10	0.566	9.1
	7.5	—	0.274	8.3
	7.5	0.10	0.601	7.6
				Mean: 8.30
				SD: ±0.62

* Samples were taken on four different days.

† Absorbance was measured against a reagent blank in the range 640–700 nm.

Effect of Foreign Ions

The effect of foreign ions, other than iron(III), was studied (Table 2). Apart from beryllium(II), chromium(III), rhodium(III) and fluoride ion, all other cations and anions tested had no affect on the determination of aluminium(III). A small positive error was still observed even when the amount of beryllium(II) was reduced to 0.02 µg in the determination of 0.20 µg of aluminium. The tolerance limits of chromium(III), rhodium(III) and fluoride ions in the determination of 0.20 µg of aluminium(III) were 1.0, 0.2 and 2.0 µg, respectively. Iron(II) reacted with CAS in the presence of Zephiramine to form an intense blue complex whose absorption maximum was at a longer wavelength than that of the corresponding aluminium complex. Consequently, in the presence of iron(II) the absorption spectrum was generally shifted to a longer wavelength and hence the absorbance difference between 640 and 700 nm was reduced, *i.e.*, a negative error was observed in the determination of aluminium. The adverse effect of iron(II), however, was successfully eliminated by its oxidation to iron(III) with hydrogen peroxide. The effect of EDTA and nitrilotriacetic acid (NTA) was also examined; the determination of 7.4 nmol (0.20 µg) of aluminium was not affected by the presence of a 5 molar excess of EDTA or NTA.

Determination of Aluminium in Tap Water

The effect of heating time on the determination of aluminium in a tap water sample was examined. A constant and maximum absorbance was attained after heating 5- and 10-ml aliquots of the sample for more than 20 and 30 min, respectively (see Fig. 11). The results of the determination of aluminium in a tap water supplying our laboratory are summarised in Table 3. The recovery of 0.10 µg of aluminium added to various sample aliquots was 98.0 ± 6.8% ($n = 7$). No contamination was found from the ambient air or the PTFE vessel used during the heating procedure. The total amount of aluminium found on four different days was in the range 7.9–8.7 ng ml^{-1}, the mean being 8.27 ng ml^{-1}.

Effect of Filtration

The effect of filtration on the determination of aluminium in tap water was studied. The total amount of aluminium found in each 100-ml fraction of a filtered tap water sample was almost constant and the mean value of the total concentration of aluminium in the filtrate was 2.3 ng ml^{-1} as shown in Table 4. As the total concentration of aluminium in the tap water sample was found to be 9.5 ng ml^{-1} and if the total aluminium in the filtrate is termed "filtrable aluminium," then the ratio of filtrable to total aluminium in the tap water sample is found to be about 0.24. The effect of filtration on the determination of iron in the tap water sample was also examined (Table 4). The determination of iron was carried out by densitometry after its enrichment as the iron(III) - ammonium pyrrolidinedithiocarbamate complex on a thin layer of anion-exchange resin.[15]

Table 4. Determination of filtrable aluminium and iron in a tap water sample. The total concentrations of aluminium and iron were found to be 9.5 and 101 ng ml^{-1}, respectively

Filtrate		Aluminium found /ng ml^{-1}	Iron found /ng ml^{-1}
1st 100-ml	..	1.9	16.2
2nd 100-ml	..	2.2	14.1
3rd 100-ml	..	2.7	11.1
4th 100-ml	..	2.3	8.1

The total amount of iron in the tap water could be determined after standing an acidified (pH about 1) 20-ml portion of the sample at room temperature for more than 10 min. The concentration of iron found was 101 ng ml^{-1}. As the amount of iron in each 100-ml fraction of the filtrate decreases with an increase in the number of fractions taken, so the significance of the term "filtrable iron" also decreases. However, it is interesting to note that about 75% of the total amount of aluminium and more than 90% of the total amount of iron in the tap water sample were removed by filtration with a membrane filter.

References

1. Cheng, K. L., Ueno, K., and Imamura, T., "Handbook of Organic Analytical Reagents," CRC Press, Boca Raton, FL, 1982, p. 53.
2. Diaz Garcia, M. E., and Sanz-Medel, A., *Talanta*, 1986, **33**, 255.
3. Shijo, Y., and Takeuchi, T., *Bunseki Kagaku*, 1968, **17**, 61.
4. Chester, J. E., Dagnall, R. M., and West, T. S., *Talanta*, 1970, **17**, 13.
5. Nishida, H., and Nishida, T., *Bunseki Kagaku*, 1972, **21**, 997.
6. Marczenko, Z., and Jarosz, M., *Analyst*, 1982, **107**, 1431.
7. Sampson, B., and Fleck, A., *Analyst*, 1984, **109**, 369.
8. Royset, O., *Anal. Chem.*, 1987, **59**, 899.
9. Shriadah, M. M. A., Kataoka, M., and Ohzeki, K., *Analyst*, 1985, **110**, 125.
10. Shriadah, M. M. A., and Ohzeki, K., *Analyst*, 1985, **110**, 677.
11. Shriadah, M. M. A., and Ohzeki, K., *Analyst*, 1986, **111**, 555.
12. Matsuhisa, K., and Ohzeki, K., *Analyst*, 1986, **111**, 685.
13. Matsuhisa, K., and Ohzeki, K., *Analyst*, 1986, **111**, 1175.
14. Ohzeki, K., and Yamagishi, M., *Analyst*, 1985, **110**, 1517.
15. Ohzeki, K., Toki, C., Ishida, R., and Saitoh, T., *Analyst*, 1987, **112**, 1689.
16. Tanaka, M., *Anal. Chim. Acta*, 1963, **29**, 193.
17. Willard, H. H., and Perkins, L. R., *Anal. Chem.*, 1953, **25**, 1634.
18. Ringbom, A., "Complexation in Analytical Chemistry," Wiley, New York, 1963, p. 311.
19. Ueno, K., "Cheletometric Titration" (in Japanese), Nanko-do, Tokyo, 1972, pp. 245 and 307.

Versatile Manifold for the Simultaneous Determination of Ions in Flow Injection Analysis

Peter C. Hauser, Susie S. Tan, Terence J. Cardwell and Robert W. Cattrall
Analytical Chemistry Laboratories, Department of Chemistry, La Trobe University, Melbourne, Victoria 3083, Australia

Ian C. Hamilton
BHP Central Research Laboratories, Newcastle, New South Wales 2287, Australia

A flow injection analysis system is described for the simultaneous determination of several ions in a single sample using a combination of potentiometric and spectrophotometric detection. A composite manifold has been designed consisting of a flow cell containing four ion-selective electrodes and two spectrophotometric transducer flow cells. The system has been applied to the determination of K^+, Ca^{2+}, NH_4^+, Cl^-, NO_3^- and PO_4^{3-} ions in a number of plant nutrient solutions.

Keywords: *Simultaneous multi-ion determination; flow injection analysis; multiple ion sensing*

There is a continuing need for faster and more diverse analytical techniques in many branches of science. The number of components that need to be determined in a single sample is increasing. Flow injection analysis is one technique that has greatly increased the throughput of samples and the application of this technique is expanding rapidly. The use of simultaneous determination in flow injection analysis has an obvious advantage in that it decreases the time required to obtain analyses for a range of analytes in a particular sample; however, so far relatively little work has been carried out in this area.[1]

Recently, we described a system based on detection with ion-selective electrodes that could be used to determine, simultaneously, a number of ions in a single sample. This system was applied to a sample (30 µl) containing two cations and two anions.[2,3] Although ion-selective electrodes are undoubtedly useful detectors in flow injection analysis, they are not available for all ions and suffer from interferences. Consequently, certain ions are best determined using spectrophotometric detection. Some examples are PO_4^{3-}, NH_4^+ and Mg^{2+} ions, which are important in plant nutrition.

The work described in this paper was aimed at expanding our original ion-selective electrode based system to include spectrophotometric detection. A composite system has been developed and applied to the simultaneous determination of K^+, Ca^{2+}, NH_4^+, Cl^-, NO_3^- and PO_4^{3-} ions in a number of plant nutrient solutions.

Experimental

Methods and Materials

Potentiometric measurements

The ionic strength adjustment buffer consisted of 0.2 M sodium acetate (May and Baker, analytical-reagent grade). The reference stream was 0.1 M sodium acetate containing 0.005 M NaCl (BDH, AnalaR grade). Standards were prepared using $CaCl_2.2H_2O$ (BDH, AnalaR grade) and KNO_3 (Mallinckrodt, analytical-reagent grade).

Ion-selective membranes

These were based on PVC; literature formulations[4,5] were used with the following reagents: K^+, valinomycin; Ca^{2+}, neutral carrier ETH 1001; and NO_3^-, tetradodecylammonium nitrate. Chloride was determined with an Ag - AgCl electrode.

Gas diffusion method

The indicator was prepared by adding 10 ml of a 0.1 M sodium hydroxide solution to 0.1 g of Cresol Red and 0.3 g of Thymol Blue (both May and Baker) and diluting to 200 ml with de-ionised water. A 10-ml volume of this solution plus 0.5 ml of a solution containing 13.8 g l⁻¹ of NaH_2PO_4 were diluted to 500 ml and the pH was adjusted to 5.0 with dilute HCl (BDH, AnalaR grade). Standards were prepared using NH_4Cl (BDH, AnalaR grade).

Molybdenum blue method

The acidic molybdate solution consisted of 0.005 M ammonium molybdate (May and Baker, analytical-reagent grade) and 0.4 M nitric acid (BDH, AnalaR grade). A 1% m/V ascorbic acid (BDH, AnalaR grade) solution in de-ionised water was used. Standards were prepared using KH_2PO_4 (May and Baker, analytical-reagent grade).

Plant nutrient solutions

These were made up in de-ionised water according to the compositions given by Douglas[6] using the following reagents: KNO_3, $MgSO_4.7H_2O$, $(NH_4)_2HPO_4$, NH_4NO_3, $(NH_4)_2SO_4$, K_2SO_4 (all Mallinckrodt, analytical-reagent grade), $Ca(NO_3)_2$, $NaNO_3$, $CaSO_4.2H_2O$ (all Ajax Chemicals, analytical-reagent grade), KH_2PO_4 (May and Baker, analytical-reagent grade), superphosphate (calcium orthophosphate, BDH, GPR), $CaCl_2.2H_2O$ (BDH, AnalaR grade) and $CaHPO_4$ (Ajax Chemicals, laboratory-reagent grade).

Multi-ion Detector System

The system for the simultaneous determination of K^+, Ca^{2+}, NO_3^- and Cl^- potentiometrically and NH_4^+ and PO_4^{3-} spectrophotometrically in a single sample (60 µl) combines the previously described ion-selective electrode sensor cell[2,3] with two spectrophotometric transducers. Also included in the system is a gas diffusion unit and a Perspex merging - splitting unit (90 mm long, 25 mm wide and 40 mm deep) containing six T-shaped junctions (channels 0.5 mm in diameter) with inlet and outlet connections to allow merging and splitting of the streams. The detectors and other units are mounted on an aluminium diecast box (185 mm long, 115 mm wide and 55 mm deep) and the electronic components are mounted inside the box with the outputs connected to the data acquisition system.

A schematic diagram of the manifold is shown in Fig. 1. The sample is injected into the carrier stream which flows to the
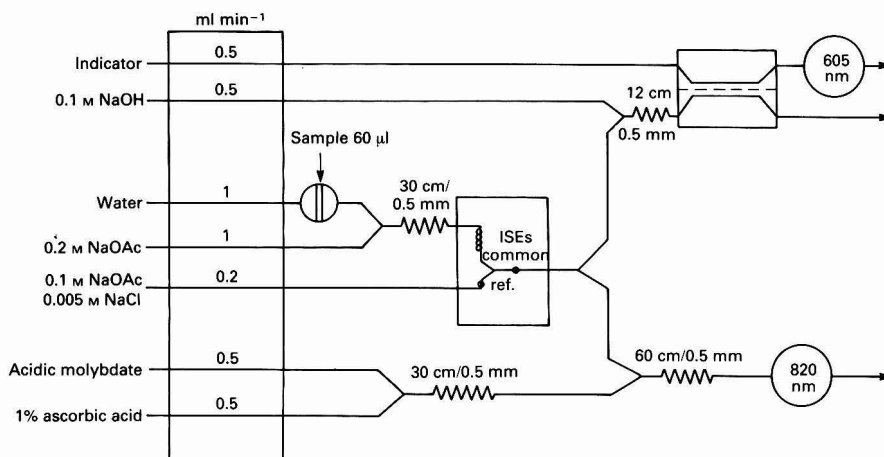
Fig. 1. Composite manifold for potentiometric and spectrophotometric detection

ion-selective electrode cell and the emerging stream is split at a T-junction in the merging - splitting unit. Each half of the carrier - sample stream is then mixed with the appropriate reagents for the spectrophotometric procedures. As different back-pressures exist in the two spectrophotometric halves of the manifold, which could cause an uneven division of the flow, reproducible splitting of the carrier stream after its passage through the potentiometric cell is crucial. Flow-rates were not optimised for the spectrophotometric procedures but were determined by the flow-rate in the ion-selective electrode flow cell and by the flow resistances in the sections of the manifold associated with the spectrophotometric methods. Splitting of the carrier stream was found to be reproducible and constant in all experiments.

Connections were made with Teflon tubing using standard fittings (Cheminert) and the sample was introduced by means of a Rheodyne 5020 Teflon injector. Solutions were transported to the manifold with a Gilson Minipuls II peristaltic pump. All carrier and reagent solutions were degassed by stirring under vacuum for about 10 min.

Potentiometric sensor cell[2,3]

This consists of two Perspex blocks with a contact area of about 3.5×3.0 cm separated by a Teflon gasket, which maintains the cell volume at 7 μl. PVC membranes were cast from tetrahydrofuran solutions on to silver wire contacts in one half of the cell. A fourth silver contact was anodised to make the Cl^- electrode. The reference electrode was also an anodised silver wire with its own electrolyte stream (0.1 M sodium acetate - 0.005 M NaCl). A platinum wire was used to earth the differential amplifier. Impedance converters were placed very close to the ion-selective electrodes in order to reduce noise.

Spectrophotometric transducers

Betteridge and co-workers[7-9] have shown that spectrophotometric detectors for flow injection analysis can be constructed very cheaply using light-emitting diodes (LEDs) and phototransistors. The LEDs have a relatively narrow emission band width of about 30 nm and hence impart a degree of spectral selectivity. Different types of LEDs (blue, green, yellow, amber, red and infrared) are available and it has been suggested that these can cover the range of wavelengths used in most spectrophotometric procedures.[8] Other reports on the successful application of such optoelectronic detectors to flow injection analysis have appeared recently.[10-15]

The design of spectrophotometric transducers is based on that reported by Freeman et al.[15] and includes fibre optic cables to separate the optoelectronic components from the flow cell itself. This approach was chosen because it allowed a rigorous separation of the electronic circuitry from the wet chemistry. Also, more efficient light coupling can be achieved because the active diameter of the fibre optic cable (1 mm) allows it to be inserted directly into the detector flow cell and dedicated phototransistors and infrared LEDs are available for the fibre optic cable. The Perspex optical detector flow cell is shown in Fig. 2 and the special adaptor needed to couple LEDs other than the infrared type is also depicted. The design facilitates the easy changeover of LEDs. The optical detector was covered with black masking tape to exclude stray light. The circuitry for the spectrophotometric transducers was adapted from an original design by Betteridge et al.[7] and the output voltage was made compatible with the data acquisition system, which was originally designed for use with ion-selective electrodes.

Gas diffusion cell

A gas diffusion cell, similar to that described by van der Linden,[16] was included in the system specifically for the determination of NH_4^+ as ammonia by spectrophotometric detection. Flow channels (65 mm long, 2 mm wide and 0.1 mm deep), machined in two identical Perspex blocks (90 mm long, 25 mm wide and 15 mm deep), were separated by commercial Teflon tape (8 mm wide, approximately 5×10^{-3} mm thick) which was used as the gas permeable membrane. The two halves of the cell were clamped together using six screws. This cell can also be used for the determination of other diffusible species such as HF, CO_2, SO_2, HCN and acetic acid.

Data acquisition system[2,3]

This was controlled by an Apple IIe microcomputer and could be used to measure transient signals from up to eight channels at a rate that was fast enough for flow injection analysis. The system consisted of a multiplexer, instrumentation amplifier and sample and hold circuitry, analogue to digital converter and offset and gain controls. Software programs were written in FORTH language, mainly because of its speed of execution and capability for low level applications, which avoided the use of tedious machine language routines. The software was a slight modification of that described previously[2,3] and allowed the additional input channels from the two spectrophotometric transducers to be incorporated.
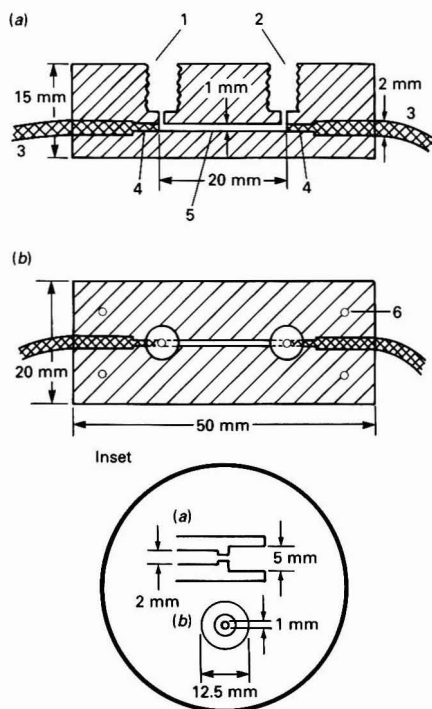
Fig. 2. Spectrophotometric transducer: 1 and 2, inlet and outlet; 3, plastic-covered fibre-optic cable (2 mm o.d., 1 mm i.d.; Tandy/Radio Shack, Cat. No. 276-228); 4, stripped section of cable; 5, flow channel (cell volume 15 μl); and 6, mounting holes. Inset: adaptor, (*a*) cross-section and (*b*) top view

Fig. 3. NH_4^+ - gas diffusion calibration graph

Results and Discussion

Spectrophotometric Procedures

Ammonium

The potentiometric determination of NH_3 with a gas sensing probe has been applied in flow injection analysis[17] but was not always satisfactory,[18,19] mainly because of the slow response times. Also, it is impossible to incorporate this probe in our electrode flow cell, not only because of the configuration, but also because of the need to use solutions of high pH. Because of these difficulties, spectrophotometric procedures for the determination of NH_4^+ were investigated. The indophenol blue method[20-22] is a direct method that relies on the reaction of the sample with an alkaline solution of phenol and hypochlorite. This method was tested for use in our system and it was found that a relatively long second reaction coil was needed to achieve reasonable sensitivity, resulting in a long residence time. Also, we encountered difficulties with the background, which were similar to those described previously by Slanina *et al.*[18] and which may be due to refractive index effects. Hence the indophenol blue method was not considered satisfactory for use with our composite manifold.

Better results for the determination of NH_4^+ were obtained with a simpler method which involved using the gas diffusion cell in conjunction with spectrophotometric detection and an indicator. The manifold and the method were adapted from that described by Cardwell *et al.*[23] It was found necessary to add phosphate buffer to the indicator stream in order to reduce the sensitivity and hence to cover the desired concentration range. A typical calibration graph is shown in Fig. 3 and demonstrates that the method can be used over the range 0.5–25 mg l^{-1} of NH_4^+. The response curve, not surprisingly, resembles a titration curve. The standard deviation of the
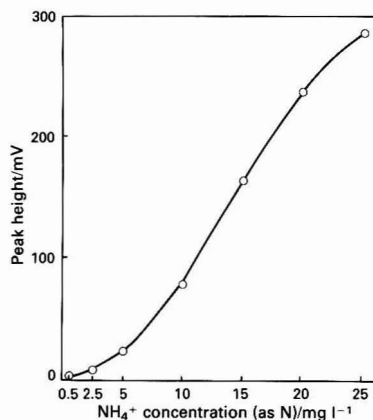
calibration is about 2 mV ($n = 5$) over the entire range, which represents about 1% in the concentration over most of the range and about 10% below 5 mg l^{-1}.

Phosphate

Both the molybdenum yellow[17] and molybdenum blue methods[12,14,15,17] have been used in flow injection analysis. The molybdenum blue method is widely used in flow analysers[24] and has been applied in combination with LED - spectrophotometric detection.[12,14,15,25] The simpler molybdenum yellow method was not successful with our system because it lacks sensitivity; also, the blue LED that was used in the detector has a peak maximum at 480 nm, whereas the optimum wavelength for the yellow method is 362 nm.[17] Further, phototransistors are relatively insensitive in the shorter wavelength regions.

The absorption maximum of molybdenum blue is 824 nm[25] and so use of the infrared LED, which is designed to couple with the fibre optic cable and which has a wavelength maximum of 820 nm, is ideal. A typical calibration graph is shown in Fig. 4 which demonstrates the high sensitivity of the method even though the graph is non-linear. The standard deviation for five injections is about 1–2 mV over the entire range, which represents about 2% in the concentration. A decrease in sensitivity of about 10% over a period of 4 h is observed, which must be due to precipitation of the molybdate complex as the original response can be restored by flushing the manifold with dilute ammonia.

The use of the red LED at 660 nm, which is the wavelength used by most workers with conventional detectors[17,26] and LEDs,[12,14] gives a similar calibration graph. Varying all the flow-rates individually between 0.5 and 4.0 ml min^{-1} produced no change in the non-linearity, suggesting that this was not due to failure to optimise the flow-rates. The Beer - Lambert law is only obeyed for a narrow spectral band pass and, as the LEDs have relatively broad spectral bands, this seems the more likely explanation for the curvature. It is worth noting that Betteridge[8] claimed that the LED based optoelectronic detectors were not successful for the determination of phosphate using this method but no explanation was given. However, our work and the work of others[12,14,15] does not support this claim.

Analysis of nutrient solutions

The proposed system was used for the determination of K^+, Ca^{2+}, NH_4^+, Cl^-, NO_3^- and PO_4^{3-} ions in some typical plant nutrient solutions. The composition of these solutions were as

Table 1. Analysis of some plant nutrient solutions

| Solution | Measured ion/mg l⁻¹ | | | | | | | | | | | | Other ions present/mg l⁻¹ | | |
| | NO_3^- | | NH_4^+ | | PO_4^{3-} | | K^+ | | Ca^{2+} | | Cl^- | | Na^+ | Mg^{2+} | SO_4^{2-} |
	Theoretical	Measured	Theoretical	Measured	Theoretical	Measured	Theoretical	Measured	Theoretical	Measured	Theoretical	Measured	Theoretical	Theoretical	Theoretical
I	227	224 (5)*	34.1	32 (5)	37.7	41.0 (1.5)	313	340 (2)	164	169 (4)	—	—	—	49.5	196
II	172	157 (3)	59.9	61.0 (1.6)	116	112 (3.5)	314	324 (1)	226	220 (4)	—	—	—	49.7	196
III	10.9	15.0 (3)	17.9	16.0 (12)	20.1	20.0 (2.5)	52.8	49.0 (1)	52.2	53.0 (2)	—	—	130	7.0	186
IV	50.8	46.0 (5)	50.8	46.0 (5)	39.7	38.0 (0.8)	142	149 (2)	265	265 (4)	—	—	—	16.1	575
V	—	—	197	200 (1.7)	112	104 (1.4)	107	115 (2)	218	212 (6)	—	—	—	28.2	918
VI	196	180 (6)	145	148 (1.1)	42.9	40.0 (1.3)	198	192 (1)	91.6	89.0 (8)	—	—	—	29.4	116
VII	67.8	70.0 (3)	35.6	38.0 (4.6)	39.3	36.0 (2.8)	179	179 (1)	16.9	21.0 (5)	138	144 (1)	668	44.7	397
VIII	152	154 (4)	22.6	21.0 (4.8)	72.2	73.0 (2.4)	140	145 (1)	182	189 (9)	—	—	—	172	32.8
IX	30.1	25.0 (4)	21.4	20.0 (13)	207	210 (2.9)	262	254 (1)	43.1	49.0 (2)	57.3	61.0 (1)	—	73.7	365
r		0.9966		0.9998		0.9982		0.9965		0.9987					

* Values in parentheses are the relative standard deviations (%).
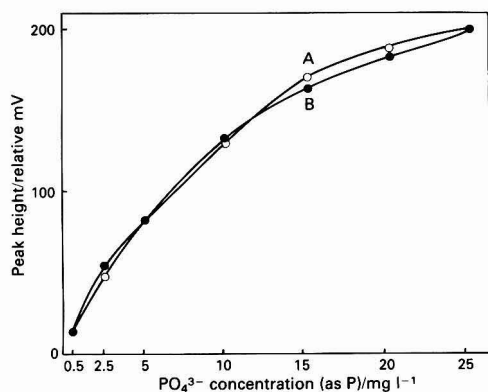
Fig. 4. PO_4^{3-} - molybdenum blue calibration graph: A, 820 and B, 660 nm

given by Douglas[6] and were chosen to cover a wide concentration range of the ions studied. It should be noted that these solutions had to be diluted ten-fold to bring the phosphate levels into the range of the molybdenum blue method. The measurement of six ions in a single sample injection took 45 s. The results are shown in Table 1 (column 2 in each instance) together with the values calculated from the known composition of each solution (column 1). The relative standard deviations are shown in parentheses and the correlation coefficient (r) for the theoretical and measured values for each ion is given at the foot of each column. Table 1 also shows the levels of other ions (Mg^{2+}, Na^+ and SO_4^{2-}) present in the samples.

In general, there is good agreement between the calculated and found values and the relative standard deviations are acceptable particularly when the complexity of the system is considered. This work demonstrates the feasibility of simultaneous multi-ion determination using flow injection analysis and shows that it is possible to design manifolds which combine potentiometric and spectrophotometric detection and which allow a wide range of cations and anions to be determined in a single sample. The advantages in terms of sample throughput and speed of analysis are obvious.

Simultaneous multi-ion determination using flow injection analysis is a much cheaper and simpler method than ion chromatography and has the added advantage of being able to determine both cations and anions simultaneously.

References

1. Luque de Castro, M. D., and Valcárcel Cases, M., *Analyst*, 1984, **109**, 413.
2. Cardwell, T. J., Cattrall, R. W., Hauser, P. C., and Hamilton, I. C., *Proc. 9th Aust. Symp. Anal. Chem.*, 1987, **1**, 72.
3. Cardwell, T. J., Cattrall, R. W., Hauser, P. C., and Hamilton, I. C., *Anal. Chim. Acta*, in the press.
4. Amman, D., Morf, W. E., Anker, P., Meier, P. C., Pretsch, E., and Simon, W., *Ion-Sel. Electrode Rev.*, 1983, **5**, 3.
5. Wright, J. A., and Bailey, P. C., *in* Pungor, E., and Buzas, I., *Editors*, "Ion-selective Electrodes," Elsevier, Amsterdam, 1978, p. 603.
6. Douglas, G. S., "Advanced Guide to Hydroponics," Peltham, London, 1985, pp. 172–182.
7. Betteridge, D., Dagless, E. L., Fields, B., and Graves, N. F., *Analyst*, 1978, **103**, 897.
8. Betteridge, D., *Fresenius Z. Anal. Chem.*, 1982, **312**, 441.
9. Betteridge, D., Cheng, W. C., Dagless, E. L., David, P., Goad, T. B., Deans, D. R., Newton, D. A., and Pierce, T. B., *Analyst*, 1983, **108**, 1.
10. Hooley, D. J., and Dessy, R. E., *Anal. Chem.*, 1983, **55**, 313.
11. Thomsen, J., Johnson, K. S., and Petty, R. C., *Anal. Chem.*, 1983, **55**, 2378.
12. Trojanowicz, M., Augustyniak, W., and Hulanicki, A., *Mikrochim. Acta*, 1984, **II**, 17.
13. Johnson, K. S., Beehler, C. L., and Sakamoto-Arnold, C. M., *Anal. Chim. Acta*, 1986, **179**, 245.
14. Worsfold, P. J., Clinch, J. R., and Casey, H., *Anal. Chim. Acta*, 1987, **197**, 43.
15. Freeman, P. R., Hart, B. T., and McKelvie, I. D., *Proc. 9th Aust. Symp. Anal. Chem.*, 1987, **2**, 782.
16. van der Linden, W. E., *Anal. Chim. Acta*, 1983, **151**, 359.
17. Růžička, J., and Hansen, E. H., *Anal. Chim. Acta*, 1975, **78**, 145.
18. Slanina, J., Bakker, F., Bruyn-Hes, A., and Mols, J. J., *Anal. Chim. Acta*, 1980, **113**, 331.
19. Krug, F. J., Růžička, J., and Hansen, E. H., *Analyst*, 1979, **104**, 47.
20. Stewart, J. W. B., and Růžička, J., *Anal. Chim. Acta*, 1976, **82**, 137.
21. Hansen, E. H., Krug, F. J., Ghose, A. K., and Růžička, J., *Analyst*, 1977, **102**, 714.
22. Basson, W. D., *Fresenius Z. Anal. Chem.*, 1982, **331**, 23.
23. Cardwell, T. J., Carey, M. F. Cattrall, R. W., Hamilton, I. C., Iles, P. J., Payne, W. R., and Snow, R. J., *Proc. 9th Aust. Symp. Anal. Chem.*, 1987, **2**, 774.
24. Smith, K. A., and Scott, A., *in* Smith, K. A., *Editor*, "Soil Analysis," Marcel Dekker, New York, 1983, p. 157.
25. Imasaka, T., Kamikubo, T., Kawabata, T., and Ishibashi, N., *Anal. Chim. Acta*, 1983, **153**, 261.
26. Růžička, J., and Stewart, J. W. B., *Anal. Chim. Acta*, 1975, **79**, 79.

Simultaneous Determination of Iron(III) and Total Iron by Flow Injection Analysis Using Kinetic Spectrophotometry With Tiron

Rokuro Kuroda, Tadashi Nara and Koichi Oguma
Laboratory for Analytical Chemistry, Faculty of Engineering, University of Chiba, Chiba, Japan

Two flow injection analysis systems have been developed for the simultaneous spectrophotometric determination of iron(III) and total iron using Tiron as the colour developing reagent. The first system uses a single detector with two flow cells aligned with the same optical path to yield two peaks corresponding to iron(III) and total iron in the sample. The sample throughput is high (60 samples h^{-1}) with a precision of 0.35% for iron(III) and 0.55% for total iron. The second system is a multi-detection system which allows 30 samples to be analysed per hour with the advantage of much simpler instrumentation.

Keywords: *Simultaneous determination of iron(III) and total iron; flow injection analysis; multi-detection system; spectrophotometry; Tiron reagent*

Flow injection analysis (FIA) has increasingly been used in various fields, owing to its high throughput, cost performance and versatility. It has also been found to be very useful for speciation studies; however, its full potential has not yet been realised. The determination of both iron(II) and iron(III) in geological[1] and biological materials[2] is a problem that has not yet been resolved. Iron(II) and iron(III) have been determined by flow injection and direct current amperometric detection with a glassy carbon electrode, in which the two valency states are differentiated by an appropriate choice of indicator potentials.[3]

A combination of spectrophotometry and atomic absorption spectrometry has been employed for the sequential determination of Fe^{II} and Fe^{III}.[4,5] The use of a valve to switch between streams, with and without a redox reagent, for the sequential determination of the oxidation states of an element has been the most common method employed for speciation and has been applied to the spectrophotometric determination of Fe^{II} and Fe^{III} with 1,10-phenanthroline - ascorbic acid.[6] A method not requiring a redox reagent and which uses selective indicator reactions for each oxidation state, with a valve to switch between the streams of buffered 1,10-phenanthroline and acetohydroxamic acid, has recently been reported.[7] Similarly, Lynch *et al.*[8] determined Fe^{II} and Fe^{III} spectrophotometrically by synchronised sample injection into two parallel flow systems, in which Fe^{II} and Fe^{III} were determined with 1,10-phenanthroline and thiocyanate, respectively. Faizullah and Townshend[9] reported a spectrophotometric system in which Fe^{II} and total iron were determined by splitting an injected sample so that a portion passed through a reductor column and a delay coil before both streams were recombined and mixed with 1,10-phenanthroline for sequential photometric detection. The use of FIA for speciation studies has been reviewed by Luque de Castro.[10]

This paper describes a simpler approach to the determination of Fe^{III} and total iron by means of spectrophotometric FIA with a single detector. The formation of a coloured complex between Fe^{III} and Tiron (sodium 1,2-dihydroxybenzene-3,5-disulphonate)[11] is used as the indicator reaction. In the presence of Tiron and acetate buffer, the oxidation of Fe^{II} is accelerated by irradiation with ultraviolet light and is complete within a very short time, so that the Fe^{III} - Tiron complex is detected immediately after the sample has been injected. The total iron, including the additional Fe^{III} produced, is detected as a satellite peak by means of two flow cells aligned with the same optical path. Another approach involves the use of a multi-detection system with a single detector, as described by Rios *et al.*[12] The indicator reaction is the same as that described above, but the entrapment of the

sample in a closed reagent system allows its repetitive passage through a single detector until it is completely dispersed into the reagent carrier solution. Iron(III) is determined from the first peak obtained and total iron, including the additional Fe^{III}, from the plateau response of the dispersed Tiron complex. When UV irradiation is employed, the second peak can be used for the determination of total iron without having to wait for complete dispersion of the Tiron complex. The sample throughput is fairly low but the system allows the simultaneous determination of Fe^{III} and total iron using simple instrumentation.

Experimental

Reagents

All chemicals used were of analytical-reagent grade.

Iron(III) and iron(II) solutions. An Fe^{III} solution (1.00 mg ml^{-1} of Fe^{III} in 0.5 M sulphuric acid) was prepared by dissolving 0.863 g of FeNH$_4$(SO$_4$)$_2$·12H$_2$O in 0.5 M sulphuric acid and diluting to 100 ml with the same acid. This solution was standardised by titration with EDTA (disodium salt) using Variamine Blue B as indicator. An Fe^{II} solution (1.00 mg ml^{-1} of Fe^{II} in 0.5 M sulphuric acid) was prepared by dissolving 0.702 g of FeSO$_4$(NH$_4$)$_2$SO$_4$·6H$_2$O in 0.5 M sulphuric acid and diluting to exactly 100 ml with the same acid. This solution was freshly prepared immediately before use.

Chromogenic reagent solution. Prepared by mixing 1.0 g of Tiron (disodium 1,2-dihydroxybenzene-3,5-disulphonate, Dojindo Laboratories, Kumamoto), 5.0 ml of 10% Triton X-100 and an acetate buffer solution (pH 4.5 or 6.0) and diluting to 500 ml with distilled, demineralised water. The acetate buffer solution was prepared by dissolving 20.5 g of anhydrous sodium acetate in 400 ml of distilled, demineralised water and adjusting to pH 4.5 or 6 by the dropwise addition of 5 M acetic acid.

Carrier solution. Sulphuric acid (0.1 M).

Working standard and synthetic solutions were prepared to be 0.1 M in sulphuric acid.

Apparatus

Single detector - two flow cell system

A schematic diagram of the FIA system is shown in Fig. 1. A single-beam spectrophotometer was used as the detector with two 1-cm flow cells aligned with the same optical path. The flow system was assembled from 1.0-mm bore Teflon tubing, except for the oxidising coil, Cm$_2$ (1.0-mm bore polyethylene tubing), the back pressure coil, b.p. (0.5-mm bore), and the

Daiflon connectors. A reciprocating pump of the double plunger type (Sanuki Kogyo DM3M-2044) was used to propel the carrier solution and the chromogenic reagent solution (pH 4.5). A six-way loop injection valve (116 µl) was used for sample injection (S in Fig. 1). A Hitachi Model 100 spectrophotometer and a Hitachi Model 056 strip-chart recorder were also used. The pulses produced by the reciprocating pump were suppressed by air dampers, D, placed just behind the pump. In order to accelerate the rate of oxidation of Fe^{II} to Fe^{III}, the oxidation coil, Cm_2, was inserted in the system. This coil was made by winding 200 cm of polyethylene tubing (1-mm bore) round a commercially available disinfection mercury lamp (Type GL-6, Matsushita Denki Sangyo, 15-mm bore, 21 cm long, 6 W) with a maximum intensity at 250 nm. The effective irradiation length was 6 cm. The coil was wrapped in aluminium foil to improve the efficiency of the irradiation process.

Multi-detection system

A schematic diagram of the multi-detection system is shown in Fig. 2 in which a single-beam spectrophotometer, D, is used with a 1-cm flow cell. The manifold was constructed with 0.5-mm bore Teflon tubing and Daiflon connectors. Peristaltic pumps (SJ-1211H, Atto), P_1 and P_2, were used to propel the chromogenic reagent solution (pH 6.0). A four-way valve, V, was used to switch the system from the open free flow mode to the closed flow mode in which the pump, P_2, allowed the trapped reagent solution to pass repeatedly through the detector, D. A mixing coil, Cm_1 (40 cm long), and removable oxidation coil, Cm_2 (50 cm long, constructed as described above for the single detector - two flow cell system), were inserted into the system.

Procedure

Single detector - two flow cell system

A 116-µl volume of the sample solution, S, is injected into the carrier stream, C (0.1 M H_2SO_4), and merges with the chromogenic reagent solution, R, at the confluence point, M (see Fig. 1). The colour-forming reaction between Fe^{III} and Tiron proceeds rapidly in the mixing coil, Cm_1, and the absorbance of the complex is monitored (560 nm) in the flow cell, fc_1. When the sample is forced to pass through the coil, Cm_2, Fe^{II} is oxidised rapidly to Fe^{III} by UV irradiation. The Fe^{III} - Tiron complex thus formed is monitored together with the complex already present at the flow cell fc_2, which is aligned with, and has the same optical path as, the flow cell, fc_1. Hence, two peaks are obtained per injection, the first corresponding to Fe^{III} and the second to the total iron.

Multi-detection system

The chromogenic reagent solution, R, is pumped through the four-way valve, V, and the loop system to waste. A 116-µl volume of the sample solution, S, is injected into the flow stream and the valve is switched to entrap the sample into the closed reagent system. The absorbance of the Fe^{III} - Tiron complex is monitored at the detector, D, and quantified from the first peak.

The sample is allowed to pass repeatedly through the detector so that damped signals are obtained; this continues until the sample is completely dispersed into the chromogenic reagent carrier solution. The total iron is determined from the second peak when the oxidation coil, Cm_2, is placed in the loop or from the plateau response of the dispersed Fe^{III} - Tiron complex by removing Cm_2 from the loop.

Results and Discussion

Tiron reacts with Fe^{III} but not with Fe^{II}. A kinetic - spectrophotometric method for the simultaneous determination of Fe^{II} and Fe^{III} with Tiron has recently been reported.[11] This work employs the same reaction, but the rapid oxidation of Fe^{II} to Fe^{III} is accomplished by UV irradiation in the flow system. Fig. 1 shows the system used for the simultaneous determination of Fe^{II} and Fe^{III} in a single sample injection; it consists of a single detector with two flow cells which are aligned and have the same optical path to the detector in the manifold. When the sample is split into two portions, both portions must reach the detector cell but at different times. In the system employed in this work the Fe^{III} in the sample meets the reagent at the point M and reacts immediately to form the Fe^{III} - Tiron complex, which is monitored during its passage through the flow cell, fc_1. Iron(II) is then oxidised rapidly and quantitatively to Fe^{III} in the oxidation coil Cm_2 where complete oxidation is achieved by UV irradiation. The Fe^{III} - Tiron complex, together with the total iron, is subsequently detected at the same detector via the second flow cell, fc_2, which is aligned with, and has the same optical path as, fc_1. The FIA signals obtained with this system are shown in Fig. 3, from which it can be seen that two peaks are obtained, the first peak corresponding to Fe^{III} in the sample and the second to the total iron. Note that Fe^{II} alone gives rise to the second peak only [Fig. 3(a) (B)]. The total iron can be determined from the second peak either by injecting a series of standard Fe^{III} solutions or a series of standard Fe^{II} solutions. The sample throughput is high, enabling 60 samples to be analysed per hour.

In this system, the flow-rates of the carrier and chromogenic reagent streams were 2.6 and 2.7 ml min^{-1}, respectively;

Fig. 1. Single detector - two flow cell system. Manifold constructed from 1.0-mm bore Teflon tubing except for b.p. (0.5-mm bore) and Cm_2 (1.0-mm bore polyethylene tubing). C, Carrier solution (0.1 M H_2SO_4); R, chromogenic reagent solution (0.2% Tiron in acetate buffer, pH 4.5); P, reciprocating pump; D, damper tube (500 cm); S, sample solution (116 µl); Cm_1, mixing coil (50 cm); fc_1 and fc_2, flow cells (31.4 µl, 10 × 2 mm); M, confluence point; Cm_2, oxidising coil (200 cm); DL, disinfection lamp (6 W); b.p., back-pressure coil (200 cm); and W, waste

Fig. 2. Multi-detection system. Manifold constructed from 0.5-mm bore Teflon tubing. R, Chromogenic reagent solution (0.2% Tiron in acetate buffer, pH 6.0); P_1 and P_2, peristaltic pumps; S, sample solution (116 µl); Cm_1 mixing coil (40 cm); V, four-way valve; D, spectrophotometric detector with a flow cell (31.4 µl, 10 × 2 mm); Cm_2, removable oxidising coil (50 cm) with DL, disinfection mercury lamp; and W, waste. Flow-rate (ml min^{-1}), 2.2 (P_1) and 2.0 (P_2)

these flow-rates are reasonably rapid and yet no oxidation of Fe^{II} occurs before the sample reaches the flow cell, fc_1. However, when both flow-rates were decreased by about 50% (*i.e.*, to 1.4 ml min^{-1} each), an appreciable peak was obtained for Fe^{II} at fc_1. The exact mechanism of the reaction between Fe^{II}, oxygen and Tiron is not known, but it has been suggested that Tiron acts as a catalyst for the oxidation of Fe^{II} and as a chromogenic complexing agent for Fe^{III}.[11] Therefore, the mixing coil, Cm_1, was constructed to be as short as possible to prevent oxidation of Fe^{II}. In contrast, the length of the oxidation coil, Cm_2, was increased to 200 cm to improve the oxidation reaction and to prevent overlapping of the first and second peaks. The rate of oxidation of Fe^{II} is dependent on pH, the reaction proceeding faster at higher pH. When a standard Fe^{II} solution was injected into the chromogenic reagent solution (R in Fig. 1) at various pH values (pH 4.5–5.5), a positive peak appeared at the same position as the first peak at a pH higher than 4.7.

The results of the simultaneous determination of Fe^{II} and Fe^{III} in their synthetic mixtures are shown in Table 1. As can be seen, Fe^{III}, total iron and Fe^{II} can be determined quantitatively (the value for Fe^{II} being obtained by calculating the difference between the values for Fe^{III} and total iron). The relative standard deviations ($n = 3$) for the determination of Fe^{III} and total iron are 0.35 and 0.55%, respectively. Owing to dispersion, and the subsequent lowering of the peak height, the precision is fairly low for the determination of total iron (second peak).

Multi-detection System

This system was used to assess the potential of this configuration for the simultaneous determination of Fe^{II} and Fe^{III}. In the multi-detection system (Fig. 2), the valve, V, can adopt two positions. In the first, the flow circulates as it would in an ordinary flow system and only one FIA peak is obtained. When V is switched to the second position, the chromogenic

reagent solution passes to waste and the sample returns to the detector. The pump, P_2, ensures the circulation of the flow. With this arrangement a number of peaks appear in accordance with the number of times that the sample passes through the detector until it is completely dispersed into the reagent solution. In this system, the first signal corresponds to the absorbance of the Fe^{III} - Tiron complex formed in the sample. During the circulation of the sample, Fe^{II} is oxidised rapidly by UV irradiation as it passes through the coil, Cm_2, and the Fe^{III} thus formed reacts with Tiron to give the second signal, which corresponds to the total iron and which can, therefore, be used to measure the total iron. However, the passage of the sample through the detector, D, increases the dispersion significantly. As shown in Fig. 4, the circulation of the flow, forced by the pump, P_2, gives rise to a multi-signal, which eventually reaches a plateau, indicating that homogenisation of the total iron - Tiron complex is complete. This absorbance plateau also allows calculation of the total iron. After measuring the first and second peaks, or the plateau height, the valve, V, is turned so that the reagent carrier solution is flushed out of the system. One cycle (*i.e.*, measurement of the first and second peaks and flushing out of the carrier) takes about 2 min, so the throughput is about 30 samples h^{-1}. The results of the simultaneous determination of Fe^{III} and Fe^{II} in synthetic mixtures are listed in Table 2, in which averages of three runs are given for each set of values. Not more than 40 µg of Fe^{III} alone can be determined owing to the very large signal produced; however, much larger amounts of Fe^{II} can be determined because there is a large dispersion of the second peak. The higher values obtained for Fe^{III} appear to be due to the contribution from Fe^{II}, which is oxidised rapidly in the Tiron - acetate buffer system. The average relative standard deviations ($n = 3$) for Fe^{III} and total iron are 1.2 and 0.61%, respectively.
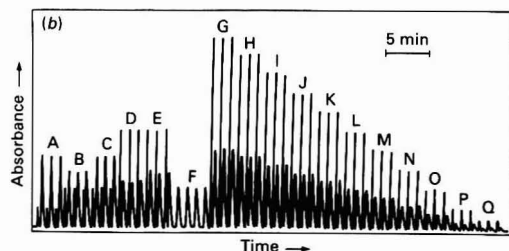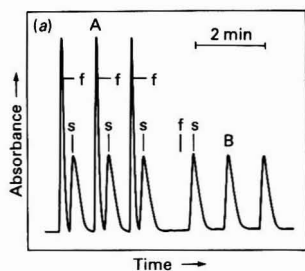
Fig. 3. Recorder traces in the single detector - two flow cell system. (*a*) Solutions of A, Fe^{III} (24 µg ml^{-1}) and B, Fe^{II} (24 µg ml^{-1}) injected three times. f, First peak; and s, second peak. Note the absence of first peaks for B. (*b*) Solutions containing Fe^{III} and Fe^{II}. Concentrations: (A) Fe^{III}, 7.92; Fe^{II}, 64.0; (B) Fe^{III}, 15.8; Fe^{II}, 40.0; (C) Fe^{III}, 15.8; Fe^{II}, 56.0; (D) Fe^{III}, 39.6; Fe^{II}, 8.00; (E) Fe^{III}, 39.6; Fe^{II}, 16.0; (F) Fe^{II}, 40.0; (G) Fe^{III}, 79.2; (H) Fe^{III}, 71.2; (I) Fe^{III}, 63.3; (J) Fe^{III}, 55.4; (K) Fe^{III} 47.5; (L) Fe^{III}, 39.6; (M) Fe^{III}, 31.7; (N) Fe^{III}, 23.8; (O) Fe^{III}, 15.8; (P) Fe^{III}, 7.92; and (Q) Fe^{III}, 3.96 µg ml^{-1}

Table 1. Simultaneous determination of Fe^{III} and Fe^{II} in synthetic mixtures (two flow cell system)

Added/µg ml^{-1}			Found/µg ml^{-1}		
Fe^{III}	Fe^{II}	Total*	Fe^{III}	Total	Fe^{II}†
7.92	16.0	23.9	8.04	24.2	16.2
7.92	40.0	47.9	8.00	47.8	39.8
7.92	64.0	71.9	8.04	71.6	63.6
15.8	40.0	55.8	16.0	55.2	39.2
15.8	56.0	71.8	16.0	71.0	55.0
39.6	8.00	47.6	39.4	47.4	8.0
39.6	16.0	55.6	39.6	55.6	16.0
7.92	8.00	15.9	8.04	16.0	7.9
15.8	16.0	31.8	16.0	31.8	15.8
31.7	32.0	63.7	31.6	63.6	32.0
0	40.0	40.0	0	39.9	39.9

* Fe^{II} plus Fe^{III}.

† Calculated by subtraction of Fe^{III} from the total iron.
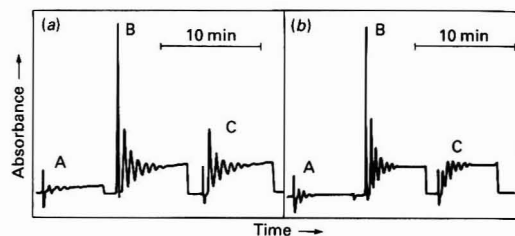
Fig. 4. Recorder traces obtained with the multi-detection system. (*a*) With UV irradiation and (*b*) without UV irradiation. A, Blank (0.1 M H_2SO_4); B, 19.7 µg of Fe^{III} per ml of 0.1 M H_2SO_4; and C, 20.2 µg of Fe^{II} per ml of 0.1 M H_2SO_4

Table 2. Simultaneous determination of Fe^{III} and Fe^{II} in synthetic mixtures (multi-detection system)

Added/µg ml⁻¹			Found/µg ml⁻¹		
Fe^{III}	Fe^{II}	Total*	Fe^{III}	Total	Fe^{II}†
With UV irradiation—					
3.95	4.04	7.99	4.30	8.24	3.94
7.90	8.08	16.0	8.58	15.8	7.2
11.8	12.1	23.9	12.4	23.6	11.2
15.8	16.2	32.0	16.9	31.6	14.7
19.7	20.2	39.9	21.0	39.6	18.6
31.6	8.08	39.7	32.2	39.2	7.0
23.7	16.2	39.9	24.4	39.5	15.1
15.8	24.2	40.0	16.2	39.4	23.2
7.90	32.3	40.2	8.13	39.2	31.1
—	20.2	20.2	0.22	19.7	19.7
Without UV irradiation—					
3.95	4.04	7.99	4.06	7.66	3.60
7.90	8.08	16.0	8.22	15.8	7.6
11.8	12.1	23.9	12.4	24.0	11.6
15.8	16.2	32.0	16.1	32.1	16.0
19.7	20.2	39.9	19.9	39.8	19.9
31.6	8.08	39.7	30.7	40.1	9.4
23.7	16.2	39.9	23.4	40.2	16.8
15.8	24.2	40.0	16.2	40.2	24.0
7.90	32.3	40.2	8.02	40.3	32.3
—	20.2	20.2	—	20.4	20.4

* Fe^{II} plus Fe^{III}.
† Calculated as the difference between total iron and Fe^{III}.

It is also possible to determine Fe^{III} and Fe^{II} simultaneously without using the Cm_2 irradiation unit. However, in this instance it takes about 7.5 min to accomplish one cycle in which total iron can be determined from the plateau absorbance caused by complete homogenisation of the Tiron - Fe^{III} complex. The results of the simultaneous determination of Fe^{II} and Fe^{III} obtained using this technique are also shown in Table 2. A series of standard Fe^{III} solutions were used for the calibration of total iron, although it is possible to use either Fe^{II} or Fe^{III} for this purpose. The accuracies are fairly good, 40 µg of total iron being determined successfully. The average relative standard deviations ($n = 3$) are 1.1% for Fe^{III} and 0.47% for total iron. However, the throughput is fairly low, *viz.*, less than 10 samples h⁻¹.

References

1. Lichte, F. E., Seeley, J. L., Jackson, L. L., McKown, D. M., and Taggart, J. E., Jr., *Anal. Chem.*, 1987, **59**, 197R.
2. Florence, T. M., *Talanta*, 1982, **29**, 345.
3. Dieker, J. W., and van der Linden, W. E., *Anal. Chim. Acta*, 1980, **114**, 267.
4. Burguera, J. L., and Burguera, M., *Anal. Chim. Acta*, 1984, **161**, 375.
5. Lynch, T. P., Kernoghan, N. J., and Wilson, J. N., *Analyst*, 1984, **109**, 839.
6. Bubnis, B. P., Straka, M. R., and Pacey, G. E., *Talanta*, 1983, **30**, 841.
7. Senior, A. T., and Glennon, J. D., *Anal. Chim. Acta*, 1987, **196**, 333.
8. Lynch, T. P., Kernoghan, N. J., and Wilson, J. N., *Analyst*, 1984, **109**, 843.
9. Faizullah, A. T., and Townshend, A., *Anal. Chim. Acta*, 1985, **167**, 225.
10. Luque de Castro, M. D., *Talanta*, 1986, **33**, 45.
11. Abe, S., Saito, T., and Suda, M., *Anal. Chim. Acta*, 1986, **181**, 203.
12. Rios, A., Luque de Castro, M. D., and Valcárcel, M., *Anal. Chem.*, 1985, **57**, 1803.

Microdetermination of Vanadium in Environmental Samples as its Ternary Complex With N-p-Aminophenyl-2-thenylacrylohydroxamic Acid and 3-(o-Carboxyphenyl)-1-phenyltriazine-N-oxide

Shahid A. Abbasi*†, A. Shahul Hameed, Prakash C. Nipaney and Rajendra Soni

Water Quality and Environment Division, Centre for Water Resources Development and Management, Kunnamangalam PO, Kozhikode 673 571, Kerala, India

Eleven hydroxamic acids together with a phenyltriazine derivative have been investigated for possible use in the extractive separation and spectrophotometric determination of vanadium(V). From the results of this investigation a method is described for the highly sensitive, selective and rapid determination of vanadium(V) at sub-microgram levels in alloy steels, minerals, animal and plant tissues and natural waters. Vanadium(V) is selectively extracted from a strongly acidic (3.5–7.5 M HCl) medium with a solution of N-p-aminophenyl-2-thenylacrylohydroxamic acid (ATHA) in chloroform. The reddish violet extract (molar absorptivity 9.1×10^3 l mol^{-1} cm^{-1} at $\lambda_{max.}$ = 550 nm) is then equilibrated with 3-(o-carboxyphenyl)-1-phenyltriazine-N-oxide at about pH 1.5. The resulting ternary complex is more highly coloured (molar absorptivity 1.55×10^4 l mol^{-1} cm^{-1} at $\lambda_{max.}$ = 455 nm) and obeys Beer's law at 455 nm over the range 0.2–15 µg ml^{-1} of vanadium(V). The extraction system enables a 25-fold enrichment of vanadium(V) to be achieved and allows the determination of the metal down to p.p.b. (ng l^{-1}) levels. The proposed method tolerates the presence of a large number of anions and cations that are normally found with vanadium in alloys, rocks, plant and animal tissues and natural waters. The applicability of the method was tested by the determination of vanadium in these matrices; ATHA was selected from 11 hydroxamic acids as it provided the maximum sensitivity and selectivity.

Keywords: *Vanadium(V) determination; hydroxamic acids; selective extraction; spectrophotometry; environmental samples*

Vanadium is a ubiquitous element and is more widely dispersed than such essential elements as zinc, copper, molybdenum and cobalt.[1] It has a mean geochemical abundance of 150 p.p.m. and is present in rocks and soils at levels ranging from 5 to 250 and 20 to 500 p.p.m., respectively.[2,3] Vanadium is, therefore, more readily accessible to most plants and animals; however, although the role of vanadium as an essential micronutrient has still to be established, there is little doubt that this element can be toxic to biological systems. There is increasing evidence of the damage caused to plants and animals through exposure to vanadium.[4,5] There is also evidence for a significant and increasing release of vanadium into the biosphere through industrial emissions and the burning of fossil fuels.[6] Whereas vanadium levels in unpolluted freshwaters are of the order of 2×10^{-4} p.p.m.,[7–9] abnormally high levels of this element have been reported in waters, plants and animals from sites affected by industrial pollution[10,11]; the reported levels of vanadium in polluted natural waters (average 1.5, maximum 7.4 p.p.m.)[8,9] are far higher than the concentration of 10^{-7} M (5.1 p.p.b.) that is thought to be physiologically significant[12] or the concentration of 0.5 p.p.m. that has been found to be toxic to fish.[5]

To facilitate further studies on the distribution and uptake of vanadium, it is essential to have a rapid, sensitive and reliable method for the determination of trace amounts of vanadium in environmental matrices.

Recently, Inoue *et al.*[13] described a method for the determination of vanadium in coal and coal fly ash employing N-m-tolylbenzohydroxamic acid. The method has moderate sensitivity ($\varepsilon = 5.0 \times 10^3$ l mol^{-1} cm^{-1}). Some of the other methods for the determination of vanadium are based on N-salicylhydroxamic acid ($\varepsilon = 8.3 \times 10^3$ l mol^{-1} cm^{-1})[14] and N-phenylcinnamohydroxamic acid ($\varepsilon = 7.8 \times 10^3$ l mol^{-1} cm^{-1}).[15] The earlier work in this area has been reviewed by

Agrawal and Jain[16] and Agrawal.[17] This paper describes our attempts to develop a more sensitive and selective method than those reported previously, and one that would be applicable to the determination of vanadium in environmental matrices.

We previously described a method for the determination of trace amounts of vanadium employing N-o-methoxyphenyl-2-thenohydroxamic acid (MTHA).[18] In the hydroxamic acids studied in this work we have introduced conjugation with the –CH=CH– group at the co-ordination site *ortho* to the heteroaromatic atom in the thiophene ring [Fig. 1(A)]. This results in an increase in the sensitivity and selectivity of the reagents relative to N-phenyl-2-thenohydroxamic acid [Fig. 1(B)].

Fig. 1(A) shows the structure of N-phenyl-2-thenylacrylohydroxamic acid (PTHA); the various derivatives of PTHA, having substituents in the *meta* or *para* positions of the benzene ring, which, together with PTHA, were investigated as reagents for the determination of vanadium, are given in Table 1. The results presented in Table 1 show that N-p-aminophenyl-2-thenylacrylohydroxamic acid (ATHA) in chloroform gives a more sensitive colour reaction with vanadium than the other analogues. The sensitivity ($\varepsilon = 9.1 \times 10^3$ l mol^{-1} cm^{-1}) is substantially enhanced by the formation of a ternary complex with 3-(o-carboxyphenyl)-1-phenyltriazine-N-oxide (CPPTNO) ($\varepsilon = 1.55 \times 10^4$ l mol^{-1} cm^{-1}). Other thenylacrylo analogues also formed ternary complexes with CPPTNO, but their sensitivities were lower than that given by
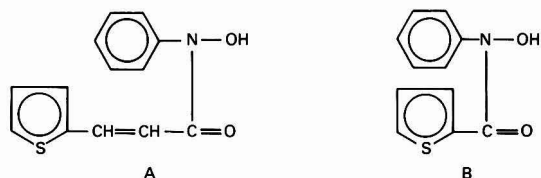
Fig. 1. (A) N-Phenyl-2-thenylacrylohydroxamic acid; and (B) N-phenyl-2-thenohydroxamic acid

---

* Concurrently Adjunct Professor, Sonoma State University, CA 94928, USA.

† Present address: School of Ecology, Pondicherry (Central) University, Pondicherry 605 001, India.

Table 1. Spectral data for the vanadium(V) - hydroxamic acid complexes in chloroform

Hydroxamic acid	λ_{max}/nm	Molar absorptivity/ $l\,mol^{-1}\,cm^{-1}$	Reference
N-p-Aminophenyl-2-thenylacrylo-	550	9.1×10^3	This work
N-p-Aminophenyl-2-thenylacrylo-	455*	1.55×10^4*	This work
N-m-Aminophenyl-2-thenylacrylo-	550	8.9×10^3	This work
N-p-Methoxyphenyl-2-thenylacrylo-	545	8.8×10^3	This work
N-m-Methoxyphenyl-2-thenylacrylo-	545	8.1×10^3	This work
N-p-Tolyl-2-thenylacrylo-	540	8.0×10^3	This work
N-m-Tolyl-2-thenylacrylo- ..	540	7.6×10^3	This work
N-Phenyl-2-thenylacrylo-	535	7.2×10^3	This work
N-p-Chlorophenyl-2-thenylacrylo-	530	6.6×10^3	This work
N-p-Bromophenyl-2-thenylacrylo-	530	6.3×10^3	This work
N-p-Iodophenyl-2-thenylacrylo-	525	6.2×10^3	This work
N-p-Nitrophenyl-2-thenylacrylo-	520	5.9×10^3	This work
N-m-Tolylbenzo-	530	5.0×10^3	13
N-Salicyl-	540	8.3×10^3†	14
N-Phenylcinnamo-	580	7.8×10^3	15

* As ternary complex with CPPTNO.
† As ternary complex with thiocyanate in isobutyl methyl ketone.

the ATHA - CPPTNO combination. In the proposed method vanadium(V) is first extracted from a 3.5–7.5 M HCl medium with ATHA into chloroform and the ternary complex with CPPTNO is formed subsequently at about pH 1.5. Vanadium can be extracted directly by using a mixture of ATHA and CPPTNO at about pH 1.5 but at this acidity the extraction is not as selective as it is at 3.5–7.5 M HCl, although at the latter acidity the mixed (ternary) complex is not formed. By employing the proposed method the sensitivity can be increased without affecting the over-all selectivity of the method.

The work described here demonstrates that the proposed method is significantly more sensitive and more widely applicable than other reported methods[13–17] for the determination of trace amounts of vanadium.

Experimental

Reagents

All chemicals were of analytical-reagent grade unless stated otherwise. The water was de-ionised and doubly distilled.

ATHA and its analogues, 0.1 M solutions in chloroform. ATHA and its analogues were prepared and purified by the general method of Tandon and Bhattacharyya.[19] These compounds were crystallised several times from benzene to a sharp, constant, melting point and were characterised by UV, IR and NMR spectroscopy as detailed elsewhere.[20] For the extraction studies 0.1 M solutions in ethanol-free chloroform were employed.

Chloroform. The chloroform was freed from ethanol by washing it several times with water and was doubly distilled after drying over fused calcium chloride.

CPPTNO, 0.05 M solution in acetone. CPPTNO was prepared and purified by the method of Majumdar and Saha.[21] A 0.05 M stock solution was prepared in acetone.

Vanadium(V), 5 × 10⁻⁴ M solution in water. A standard vanadium(V) solution was prepared by dissolving vanadium pentoxide (specpure grade) in the minimum volume of dilute ammonia solution, acidifying with sulphuric acid and diluting

to volume in the presence of a trace amount of potassium permanganate. The concentration of vanadium(V) was checked volumetrically.[22]

Apparatus

Spectra were recorded on Perkin-Elmer Model 402 and Hitachi Model 220 spectrophotometers. Spectral measurements at constant wavelengths were carried out using these instruments and an SF-4 (USSR) spectrophotometer employing matched quartz cells of 10-mm path length unless stated otherwise. The pH measurements were made on Industrial Electronics Model 092 and Elico Model PE 132 pH meters.

Extraction of Vanadium

A 25-ml aliquot of the sample solution (containing 0.2–15 p.p.m. of vanadium) and 40 ml of hydrochloric acid (6.5–11.5 M) were transferred into a separating funnel and a 10⁻³ M solution of KMnO₄ was added dropwise with gentle shaking of the funnel until the faint pink colour persisted. This procedure was followed to ensure the re-oxidation of any vanadium that might have been reduced to vanadium(IV) during storage of the sample. A 5-ml volume of ATHA solution (0.1 M) in chloroform was then added and the contents of the funnel were shaken for about 5 min. The phases were allowed to separate and the reddish violet extract was removed from the separating funnel and dried over anhydrous sodium sulphate. To ensure complete recovery of vanadium, the aqueous layer was extracted again with 5 ml of the ATHA solution and this second extract was dried and added to the first. The sodium sulphate was then washed twice with 2-ml portions of the ATHA solution to remove the final trace amounts of the vanadium complex. The combined extract was transferred into a separating funnel and 50 ml of water (adjusted to pH 1.5 ± 0.05) were added [adjustment of the pH was carried out with dilute (about 5 M) HNO₃, using an approximately 1 M NaOH solution for fine adjustment if the pH went below 1.45 after HNO₃ addition] followed by 15 ml of a 0.05 M CPPTNO

solution in acetone. The mixture was shaken for 15 min and the phases were allowed to separate. The chloroform layer was drained into a 25-ml calibrated flask, with recovery of the trapped extract as described above, and diluted to the mark. The absorbance was measured against a reagent blank at 450 nm and a calibration graph was constructed.

Determination of Vanadium in Standard Rock and Alloy Samples

To test the reliability of the proposed method, vanadium(V) was determined in standard phosphate rock (CRM 032) and alloy steels (BCS CRM 408/1 and NBS SRM 117). Weighed samples of phosphate rock were decomposed and made up into "B" solutions by the method of Shapiro and Bronnock.[18] The steel samples (0.5 g) were dissolved in dilute H_2SO_4 (1 + 4) and evaporated to a syrupy mass; the process was repeated twice with 5-ml portions of concentrated HNO_3. The solutions were heated until dense white fumes appeared. After cooling the solutions were made up to 50 ml with water and boiled to dissolve the solid organic matter; they were then filtered and made up to 250 ml with water after the addition of 25 ml of a 1 M sodium fluoride solution. Vanadium was determined as described under Extraction of Vanadium.

Determination of Vanadium in Plant and Animal Tissues and Natural Waters

Plant tissues

The plant samples were washed with 5% V/V EDTA solution and then with de-ionised water. This washing procedure is necessary to remove any particulate matter adhering to the surface so that the heavy metals absorbed by the tissues can be distinguished from those that are weakly absorbed on to the surface. Tests carried out on unwashed tissue indicated a concentration increase of between 22 and 96% compared with values obtained for washed tissue. The plant tissues were dried at 110 °C, ground and passed through a 70-mesh sieve.[23] Subsequently, three 1-g portions were taken from each sample and each portion was digested and analysed separately. Acid digestion was carried out with nitric - sulphuric - perchloric acid (10 + 1 + 4).

Animal tissues

The animal tissue samples (goat liver) were washed thoroughly with physiological saline solution before a final washing with water to remove any residual blood. The tissue samples were dried at 110 °C to a constant mass (referred to as the "dry mass") and mixed carefully to achieve homogeneity. Weighed amounts (ca. 100 mg) were heated with concentrated sulphuric acid (5 ml) on a hot-plate at 70 °C for 5 min and nitric acid was then added dropwise until no further reaction occurred. The heating was continued for a further 15 min after which the reactants were removed from the hot-plate, about 25 ml of water were added and the resulting solutions were cooled before being made up to fixed volumes with water in calibrated flasks.

Natural waters

The water samples were filtered on site through 0.45-μm membrane filter-papers and acidified to pH 1.8 with nitric acid according to standard methods.[24] The samples were analysed for vanadium as described under Extraction of Vanadium.

Results and Discussion

Choice of Extracting Solvent

Chloroform, benzene, carbon tetrachloride, butan-1-ol, isoamyl alcohol and isobutyl methyl ketone were tested as extracting solvents for the vanadium(V) - ATHA - CPPTNO system. Of these, chloroform was found to be the most

Table 2. Effect of solvent on the spectrophotometric sensitivity of the vanadium(V) - ATHA complex

Solvent		$\lambda_{max.}$/nm*	Molar absorptivity/ $l\,mol^{-1}\,cm^{-1}$
Isobutyl methyl ketone	..	470	7.2×10^3
Isoamyl alcohol	.. ..	485	7.5×10^3
Butan-1-ol	.. .. ..	485	7.5×10^3
Benzene ..	.. ..	520	8.3×10^3
Carbon tetrachloride	..	525	8.8×10^3
Chloroform	.. .. ..	550	9.1×10^3

* The solvents had a negligible absorbance at these wavelengths.
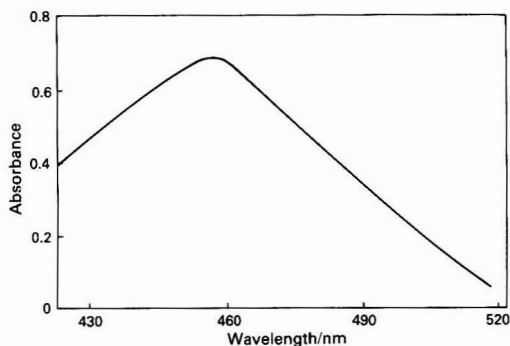
Fig. 2. Absorption spectrum of the vanadium(V) - ATHA - CPPTNO system recorded against a reagent blank

suitable because it was convenient to handle and the extracts showed maximum sensitivity in this solvent (Table 2). The alcohols and ketones were not suitable as the intensity and stability of the colour in these solvents were low. As the presence of trace amounts of ethanol in the chloroform adversely affected the colour intensity of the complex, it was essential to use ethanol-free chloroform for all extraction work.

Absorption Spectra

The absorption spectrum of the vanadium(V) - ATHA - CPPTNO system recorded against a reagent blank is shown in Fig. 2. The maximum absorbance occurs between 450 and 460 nm. At 455 nm the absorbance was reproducible and all measurements were therefore made at this wavelength. The molar absorptivity of the complex at 455 nm, based on its vanadium content, is $1.55 \times 10^4\,l\,mol^{-1}\,cm^{-1}$. The reagent blank is colourless and has a negligible absorbance in the range 380–750 nm.

Effect of Acidity, Reagent Concentration and Time of Equilibration

The extraction of the vanadium(V) complex from 2.5–7.5 M HCl is not only rapid but is also more selective than if carried out at a pH of less than 0 because at lower pH species such as iron(II), iron(III), molybdenum(VI) and uranium(VI) begin to interfere. A 0.1 M ATHA solution was found to be suitable for complete extraction of vanadium(V) within 5 + 2 min of equilibration. The optimum concentration of CPPTNO required to obtain mixed (ternary) complex formation within 15 min of equilibration at pH 1.2–1.8 was 0.05 M. Higher concentrations did not expedite or enhance the colour development.

Adherence to Beer's Law and Sensitivity

The ternary system obeyed Beer's law over the range 0.2–15 $\mu g\ ml^{-1}$ of vanadium(V). The sensitivity of the method, according to Sandell's definition,[25] was 0.003 $\mu g\ cm^{-2}$ of vanadium(V). The sensitivity can be enhanced further by up to 20 times by enrichment of the vanadium concentration through solvent extraction with ATHA from the aqueous phase into smaller volumes of the organic phase.

Table 3. Effect of foreign ions on the determination of vanadium(V). [Vanadium(V)] = 40 μg per 25 ml

Tolerance limit/ μg per 25 ml	Foreign ion
>100 000	Fluoride, chloride, phosphate, Ag^+, Li^+, Na^+, K^+, Be^{2+}, Mg^{2+}, Ca^{2+}, Ba^{2+}, Sr^{2+}, Hg^{2+}, Zn^{2+}, UO_2^{2+}, La^{3+}, Ga^{3+}, bromide, iodide, acetate
80 000	Cu^{2+}, Ni^{2+}, Co^{2+}, Mn^{2+}, Pb^{2+}, Pd^{2+}, As^{5+}, Sb^{5+}, Al^{3+}, Ce^{3+}, Th^{4+}, sulphate
60 000	Fe^{3+},* Cr^{6+}, Hf^{4+}, Sn^{4+}
30 000	Zr^{4+}, molybdate, tungstate
10 000	Ti^{4+}†

* In the presence of ascorbate (5 ml, 5% m/V) as masking agent.
† In the presence of fluoride (2 ml, 5% m/V) as masking agent.

Effect of Foreign Ions

Vanadium(V) was extracted in the presence of a large number of foreign ions and then determined to test the tolerance of the method (Table 3). The tolerance limit was set as that amount of foreign ion above which an error of more than ±2.0% occurred in the recovery of the vanadium. The results showed that a large number of ions did not interfere in ratios from 1 : 2000 to 1 : 1000 of vanadium to foreign ion. Of particular significance is the high tolerance of the method towards anions and cations such as fluoride, chloride, phosphate, iron(III), copper(II), nickel(II), cobalt(II), titanium(IV), zirconium-(IV), hafnium(IV) and uranium(VI), which are normally associated with vanadium in rocks, minerals and other environmental matrices.

Analytical Data

Vanadium was extracted from aqueous solutions of various volumes and vanadium concentrations. The studies revealed that the proposed extraction system is capable of enriching vanadium from "lean" solutions (i.e., solutions with a very low vanadium content) by up to 25 times without adversely affecting the recovery of the metal or the precision and accuracy of the determination (Table 4). This aspect effectively enhances the sensitivity of the proposed method by several orders of magnitude.

Table 4. Analytical data for the extraction and determination of vanadium(V) with ATHA - CPPTNO ($n = 8$)

Aqueous solution		CHCl₃ ATHA extract				
Volume of sample/ml	Concentration of V^V, p.p.m.	Volume of extract/ml	V^V expected, p.p.m.	V^V found, p.p.m.	Relative error, %	Standard deviation, p.p.m.
250	0.04	10	1.00*	1.015	1.5	0.01
100	0.10	10	1.00*	1.015	1.5	0.01
50	1.00	10	5.00	4.94	1.2	0.06
50	2.00	10	10.00	10.06	0.6	0.09
60	5.00	20	15.00	14.93	0.47	0.11

* Cells with a 5-cm path length were used for absorbance measurements.

Table 5. Determination of vanadium in alloy steels, rocks, animal and plant tissues and natural waters

Sample	Vanadium present (certified value), p.p.m.	Vanadium added, p.p.m.	Vanadium found, p.p.m.*	Standard deviation, p.p.m.
Alloy steel (BCS CRM 408/1) ..	310	0	307	1.01
Alloy steel (NBS SRM 117)	600	0	596	1.88
Phosphate rock (CRM 032)	153 ± 7	0	156	0.79
Radish (*Raphanus satives* L.) ..	—	0	0.098†	0.002
	—	2.00	2.101	0.005
Water hyacinth (*Eichhornia crassipes* Mart. Solms.)	—	0	0	—
	—	5.00	5.07	0.065
Goat liver	—	0	0.119	0.001
	—	2.00	2.121	0.026
Lake water	—	0	0	—
	—	0.500	0.496	0.003
	—	2.500	2.491	0.042
	—	0.050	0.051†	0.002
	—	0.005	0.005‡	0.0002
	—	0.003	0.0029‡	0.0002

* Average of six determinations.
† Cells with a 10-cm path length were used for absorbance measurements.
‡ Vanadium was enriched 20 times by solvent extraction, and cells with a 10-cm path length were used for absorbance measurements.

Stoicheiometry of the Ternary System

To establish the stoicheiometry of the ternary complex, the methods of continuous variation, molar ratio and slope ratio were employed.[26] All three methods suggested the formation of a 1 : 1 : 1 vanadium(V) - ATHA - CPPTNO complex as the colour system. The stability constant of the ternary complex, determined spectrophotometrically by the method of Harvey and Manning,[27] was 3.9×10^6.

Environmental Analysis

The results obtained for the determination of vanadium in some certified reference materials (Table 5) demonstrate the accuracy and precision of the proposed method. In other samples vanadium was determined with and without standard additions; the results indicate that the method allows the recovery of vanadium from environmental matrices with a high degree of reliability and, generally, with a relative error of less than $\pm 2\%$.

References

1. Hansen, O., *Acta Pharmacol. Toxicol.*, 1983, **52**, 3.
2. Thornton, I., *Editor*, "Applied Environmental Geochemistry," Academic Press, London, 1983.
3. Adrino, D. C., "Trace Metals in the Terrestrial Environment," Springer-Verlag, New York, 1980.
4. Morrell, B. G., Lepp, N. W., and Phipps, D. A., *Environ. Geochem. Health*, 1986, **8**, 14.
5. Abbasi, S.A., and Soni, R., *in* Chan, M. W. H., Hoare, R. W. M., Holmes, P. R., Law, R. J. S., and Reed, S. B., *Editors*, "Pollution in the Urban Environment," Elsevier, London and New York, 1987, pp. 566–574.
6. Abbasi, S. A., Soni, R., and Kunhahmed, T., "Effect of Heavy Metals on the Growth of Black Gram, *Cicer aeretenium,*" Technical Report TR-21, Centre for Water Resources Development and Management, Calicut, 1987, pp. 1–27.
7. Abaychi, J. K., and Dou Abul, A. A. J., *Water Res.* 1985, **19**, 457.
8. Nojiri, Y., Kawai, T., Otsuki, A., and Fuwa, K., *Water Res.* 1985, **19**, 503.
9. Borg, H., *Water Res.* 1987, **21**, 65.
10. Kovacs, M., Nyari, I., and Toth, L., *in* Salanki, J., *Editor*, "Heavy Metals in Water Organisms," Akademiai Kiado, Budapest, 1985, pp. 67–81.
11. Dissanayake, C. B., and Weerasooriya, S. V. R., *Int. J. Environ. Stud.*, 1986, **28**, 207.
12. Hudson, T. G. F., *in* Browning, E., *Editor*, "Elsevier Monographs on Toxic Agents," Elsevier, Amsterdam, 1974.
13. Inoue, S., Hoshi, S., and Matsubara, M., *Talanta*, 1986, **33**, 611.
14. Chatterjee, A. B., Bag, S. P., Chakrabarti, A. K., and Chakrabarti, P. R., *Mikrochim. Acta*, 1983, **II**, 307.
15. Chandravanshi, B. S., Yenesew, A., and Kebede, Z., *Anal. Chim. Acta*, 1985, **172**, 175.
16. Agrawal, Y. K., and Jain, R. K., *Rev. Anal. Chem.*, 1982, **6**, 49.
17. Agrawal, Y. K., *Rev. Anal. Chem.*, 1980, **4**, 3.
18. Shapiro, L., and Bronnock, W. W., *US Geol. Surv. Bull.*, 1962, **114A**, 45.
19. Tandon, S. G., and Bhattacharyya, S. C., *Anal. Chem.*, 1961, **33**, 1267.
20. Abbasi, S. A. *Pol. J. Chem.*, in the press.
21. Majumdar, A. K., and Saha, S. C., *Anal. Chim. Acta*, 1969, **44**, 85.
22. Vogel, A. I., "A Textbook of Quantitative Inorganic Analysis," Fourth Edition, Longmans, London, 1978.
23. Glick, D., *Editor*, "Methods of Biochemical Analysis," Volume 21, Wiley, New York, 1973, pp. 39–46.
24. Rand, M. C., Greenberg, A. E., and Tras, M. J., *Editors*, "Standard Methods for the Examination of Water and Wastewater," Fourteenth Edition, American Public Health Association, New York, 1976, p. 145.
25. Sandell, E. B., "Colorimetric Determination of Traces of Metals," Third Edition, Interscience, New York, 1959.
26. Skoog, D. A., and West, D. M., "Fundamentals of Analytical Chemistry," Third Edition, Holt, Rinehart and Winston, New York, 1976, Chapter 24.
27. Harvey, A. E., and Manning, D. L., *J. Am. Chem. Soc.*, 1952, **74**, 4744.

Determination of Antimony in Geological Samples Using Hydride Generation and Direct Current Plasma Atomic Emission Spectrometry

Paavo Perämäki and Lauri H. J. Lajunen

Department of Chemistry, University of Oulu, SF-90570 Oulu, Finland

A hydride generation technique coupled with direct current plasma atomic emission spectrometry has been used for the determination of antimony. The optimum instrumental parameters and the calibration graphs and detection limits (established for standard solutions) were determined at three different wavelengths. The interference effects of other hydride-forming elements on the determination of antimony were investigated and the method was tested on a number of Geological Survey reference materials.

Keywords: *Direct current plasma atomic emission spectrometry; hydride generation; interference effects; geological samples; antimony*

The hydride generation technique is a sensitive method in the atomic spectrometric determination of those elements which form gaseous covalent hydrides. Miyazaki *et al.* were the first workers to combine the hydride generation technique with direct current (d.c.) plasma atomic emission spectrometry. They determined arsenic and antimony in water samples with a system in which the evolved hydrides were first collected in a liquid nitrogen trap.

Since the pioneering work of Miyazaki *et al.*, a number of papers have been published, in which batch-type[2,3] or continuously working[4-6] hydride generation systems have been connected to a d.c. plasma source.

In this work, trace amounts of antimony were determined with a batch-type hydride generator coupled to a d.c. plasma atomic emission spectrometer. The interference effects of other hydride-forming elements on the determination of antimony were also studied and the method was tested on a number of US Geological Survey reference materials.

Experimental

Reagents

All chemicals used were of analytical-reagent grade and were obtained from Merck (Darmstadt, FRG), except for sodium tetrahydroborate(III), which was purchased from Fluka (Buchs, Switzerland). Demineralised, distilled water was used throughout.

Selenium and tellurium metals (1.0000 g of each) were dissolved in 20 ml of aqua regia. Germanium (0.5000 g) was added to 5 ml of 40% HF and concentrated HNO_3 was then added dropwise until dissolution was complete. Metallic tin (1.0000 g) was dissolved in a mixture of 200 ml of concentrated HCl and 5 ml of concentrated HNO_3. Bismuth (1.0000 g) was dissolved in 50 ml of concentrated HNO_3. All solutions were diluted to the appropriate volume with water in order to obtain metal concentrations of 1000 mg l^{-1}.

An antimony stock solution was prepared by dissolving 0.5000 g of metallic antimony in 5 ml of concentrated HCl and 2 drops of concentrated HNO_3. To prevent precipitation of antimony, the solution was diluted to 500 ml with 10% HCl. Finally, 1000 mg l^{-1} stock solutions of lead and arsenic were prepared by dissolving $Pb(NO_3)_2$ (1.5985 g) and As_2O_3 (1.3203 g) in water and 50 ml of concentrated HCl, respectively. Concentrated HNO_3 (10 ml) was added to the lead stock solution.

Potassium iodide and ascorbic acid solutions (1 M each) were prepared by dissolving the reagents in water. A 1 M solution of thiourea was made up in 10% HCl. A 4% m/V reductant solution was prepared by dissolving sodium tetra-

hydroborate(III) in water. The solution was stabilised by the addition of a grain of NaOH (approximate mass, 200 mg) per 50 ml of solution. A fresh solution was prepared at least every third day.

All samples were made up in 10% HCl. For antimony, the acid concentration necessary for hydride generation is not critical.[7] A freshly prepared stock solution, containing 10 mg l^{-1} of antimony, was diluted daily; potassium iodide was added to this stock solution to reduce any Sb^V present to Sb^{III} ($c_{KI} = 0.05$ M). In the optimisation of the instrumental parameters and in the interference studies, the antimony concentration in all the test solutions was 50 µg l^{-1} (with two exceptions, mentioned later). During the analysis of the reference samples, thiourea and ascorbic acid were added as a pre-reductant and masking agent, respectively.

Instrumentation

A SpectraSpan III B single-channel d.c. plasma atomic emission spectrometer (SpectraMetrics, Andover, MA, USA), equipped with a SpectraMetrics hydride generator and a Goertz 120 E chart recorder (Goertz, Vienna, Austria), was used for the measurements. The spectrometer was operated in the active diagnostic mode during the determinations.

The hydride generation system[2] consists of a reaction cell (a Büchner funnel with a glass frit), a drying tube, a hydrogen delay column, a flow meter and a special sample introduction tube. The drying tube is filled with granulated, anhydrous $CaCl_2$. The excess of hydrogen, produced in the reduction step, is passed through the delay column which is filled with Porapak Q (Waters Associates, Framingham, MA, USA). All parts of the hydride generator are connected by Tygon tubing.

Before commencing measurements with the hydride generation system, the correct wavelength for antimony is determined by aspirating a solution of antimony into the plasma via the normal sample introduction tube; this tube is then replaced by the hydride introduction assembly. (It is worth noting that special sample introduction tubes have been designed which allow both ordinary sample nebulisation and hydride introduction through the same tube, without disturbing the plasma.)[3,6] The sleeve pressure of the spectrometer was 50 lb in^{-2} and the nebuliser pressure was decreased to 15 lb in^{-2}. The plastic sample and waste tubes of the normal sample introduction system were kept closed by means of the rollers of a peristaltic pump. The argon flow-rate through the reaction cell was adjusted to 1.40 l min^{-1} using the flow meter. The instrumental parameters employed for the determination of antimony are given in Table 1.

Table 1. Instrumental settings employed for the determination of antimony

Wavelength ..	..	..	..	.. 259.805 (231.147, 206.833) nm
Entrance slit	..	..	..	.. 100×300 μm
Exit slit	..	..	..	.. 100×300 μm
PMT voltage	..	..	..	.. 650–900 V
Gain	..	..	..	.. 13–25
Recorder sensitivity		..	..	.. 20–100 mV
Chart speed ..	..	..	..	.. 1 cm min^{-1}
Reaction time	..	..	..	.. 20 s
Argon flow-rate	..	..	..	.. 1.40 l min^{-1}

Procedure

The measurement cycle is carried out as follows. A 10-ml acidified sample is introduced into the reaction vessel with an adjustable dispenser. Next, 0.5 ml of the NaBH reductant is added with a micropipette and 20 s are allowed for the generation of stibine. The purge valve is then opened and the hydride is swept into the plasma by the argon flow. The antimony emission signal is recorded by a chart recorder (it is also possible to read the peak height from the digital display of the spectrometer). After the signal has returned to the base line, the rinse valve is opened and the cell is emptied. The reaction vessel is rinsed by the addition of 10 ml of distilled water using an adjustable dispenser. Both valves are then closed and the next sample can be introduced.

At least three measurements were made on each solution and the average peak height was calculated. The anhydrous calcium chloride in the drying tube becomes moist after about 2 h of operation and must then be changed.

The geological samples (0.1–0.5 g) were accurately weighed into 50-ml calibrated flasks. Aqua regia (6 ml) was added and the flasks were kept in a sand-bath for 1.5 h at 90–110 °C. The flasks were allowed to cool and the solutions were diluted to the mark with 10% HCl. The solutions were centrifuged, then diluted further and the analyses were performed using the standard additions method. Thiourea and ascorbic acid solutions were added as pre-reducing and masking agents, respectively (the concentration of both reagents in the test solutions was 0.1 M).

Results and Discussion

Optimisation

A 4% NaBH$_4$ solution was used for hydride generation.[8] The reaction time and the volume of NaBH$_4$ reductant employed are not critical for the generation of stibine (Fig. 1). Satisfactory reproducibility can be obtained with a reaction time of about 20 s and a reductant volume of about 0.5 ml.

The position of the plasma has a large effect on the response (Fig. 2). In practice, it is difficult to maintain the plasma in exactly the same position during the analyses. However, good results can be obtained if the entrance slit is positioned at the crook of the Y-shaped plasma image.

The effect of varying the dimensions of the entrance slit was also investigated. The dimensions of the exit slit were kept constant (100×300 μm) while the width and height of the entrance slit were changed. The best signal to noise ratios were obtained when the dimensions of the entrance slit were set at 50×300 μm and 100×300 μm, the latter values giving the best results.

Fig. 3 shows the effect of varying the argon flow-rate through the reaction cell. When the flow-rate is increased, the peaks become higher and narrower. However, if the flow-rate is too high, the plasma will be disturbed. During the optimisation procedure, the argon flow-rate was set at 1.25 l min^{-1}.
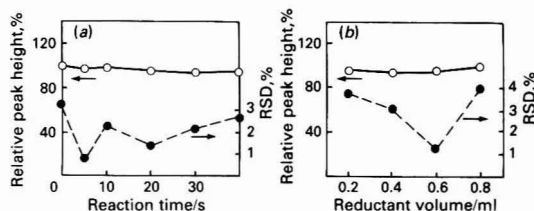
Fig. 1. Effect of (a) reaction time and (b) volume of NaBH$_4$ reductant on stibine generation. Concentration of Sb, 100 μg l^{-1}
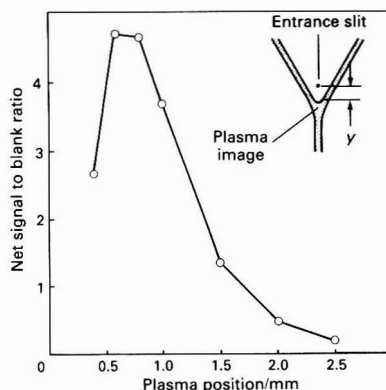
Fig. 2. Net signal to blank ratio [(signal−blank)/blank] at various plasma positions (y)
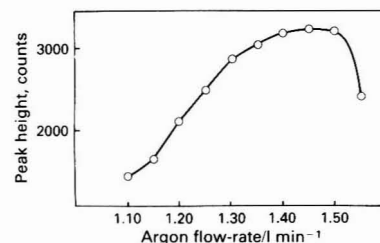
Fig. 3. Effect of varying the argon flow-rate through the reaction cell

Table 2. Detection limits and relative sensitivities for different Sb wavelengths

Wavelength/nm	Detection limit*/ μg l^{-1}	Relative sensitivity
206.833	1.0	0.26
231.147	0.3	0.57
259.805	0.2	1.00

* 10-ml sample.

Calibration Graphs

Calibration graphs for antimony were constructed at three different wavelengths, viz., 206.833, 231.147 and 259.805 nm. The calibration graphs were linear in the range studied (0–600 μg ml^{-1} of Sb). The best senstivity was obtained at a wavelength of 259.805 nm (Table 2); this wavelength was therefore selected for all further measurements. Fig. 4 shows the emission signals obtained for three dilute antimony solutions.

The precision (RSD) of the method was 7.3 and 2.0% for 5 and 50 μg ml^{-1} of Sb, respectively ($n = 10$). The detection limits given in Table 2 were obtained in aqueous solutions and correspond to the mean of the blank plus three times its standard deviation.

Matrix Ion Effects

The hydride generation technique, when used in conjunction with a d.c. plasma atomic emission spectrometer, is sensitive to interferences caused by other elements present in the sample.[2,9,10] In this work, the effect of other hydride-forming elements on the determination of antimony was studied. The
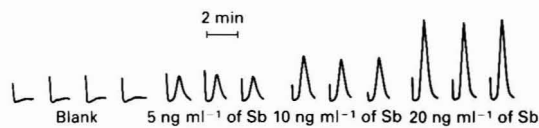
Fig. 4. Emission signals recorded for trace amounts of antimony at 259.805 nm
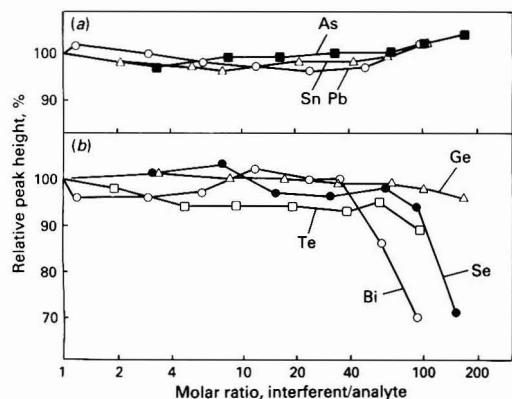
Fig. 5. Effect of hydride-forming elements on the determination of antimony

Table 3. Typical statistics of the standard additions graphs used in the determination of antimony in various geological reference materials

Sample*	Slope/counts $l \mu g^{-1}$†	Correlation coefficient
GXR-1	19.883	0.997
GXR-2	20.508	0.998
GXR-3	20.219	0.998
GXR-4	19.083	0.995

* GXR-5 was not analysed.

† Counts = digital readout of the spectrometer.

concentration of antimony in the test solutions was 50 µg l^{-1}, and increasing amounts of each of the other elements were added successively. Potassium iodide was used to reduce any Sb^V present to Sb^{III}. The iodide concentration in the final test solutions was 2.5×10^{-4} M.

It was found that only selenium, tellurium and bismuth interfered at higher concentrations in the range studied (Fig. 5). At high concentrations these elements were either reduced to the free metal or formed metal borides in the reaction vessel during the reduction step.[11] With selenium, the test solutions exhibited a reddish colour, indicating that the selenium was being reduced to the free metal by the iodide ion.

Determination of Antimony in Reference Samples

The proposed method was tested by determining antimony in several US Geological Survey reference materials. Because the interferences caused by selenium, tellurium and bismuth were not very severe, no attempt was made to eliminate them. The amounts of these three elements present in geological samples are usually in the low p.p.m. or p.p.b. range[12] and it is therefore unlikely that interference effects will be a problem. Among the samples analysed GXR-1 has the highest concentrations of bismuth, selenium and tellurium, viz., ca. 1700, 18.6 and 8.7 mg kg^{-1}, respectively.[13-15] Although the level of bismuth is fairly high, the concentration in the final test solutions is below 1000 µg l^{-1}, and hence interference is not expected.

The analyses were performed using the standard additions method. The slopes of the standard additions graphs for different samples were similar during the measurement cycle, indicating that no interferences were present (Table 3). The results of the determinations are shown in Table 4.

Because low results were obtained for the standard reference material GXR-1 (compared with the recommended value), another sample dissolution method was tried. Samples were accurately weighed into 100-ml Erlenmeyer flasks and 6 ml of aqua regia were added. The flasks were fitted with reflux condensers (to prevent evaporation of antimony) and the solutions were heated in a sand-bath for 2.5 h at 140–150 °C. The solutions were allowed to cool and the condensers were flushed with 10% HCl. The solutions were transferred quantitatively into 50-ml calibrated flasks and the analyses were performed using the standard additions method. The results obtained are given in Table 5.

A two-tailed F-test of variances[19] gave an F value of 45.45 for the GXR-1 sample, demonstrating that there is a significant difference between the two variances at the 5% level. A separate estimation of variance t-test gave a t value of −1.47.

Table 4. Results of the determination of antimony in some geological reference samples. All results expressed in mg kg^{-1}

Sample		Material	This work*	Recommended value†	ITNA†	IENA†	A‡	B§	C¶	D ‖
GXR-1	..	Jasperoid	83.1 ± 10.1, $n = 5$ (89.8 ± 1.5, $n = 3$)	124 ± 6	124 ± 3	125 ± 5	117	105	115 (122)	97.6
GXR-2	..	Soil	40.2 ± 2.3, $n = 4$ (42.5 ± 0.7, $n = 3$)	48 ± 5	50 ± 2	45 ± 4	45.7	39.6	41.04 (40.00)	43.6
GXR-3	..	Fe - Mn - W-rich deposit	38.1 ± 1.8 ($n = 4$)	40 ± 3	43 ± 2	38 ± 2	40.1	36.0		21.9
GXR-4	..	Copper mill heads	3.86 ± 0.06 ($n = 3$)	4.4 ± 0.8	4.8 ± 0.6	3.9 ± 0.6	3.32	3.6		5.1
GXR-5	..	Soil	1.57 ± 0.16 ($n = 4$)	2 ± 1	1.6 ± 0.2	2.0 ± 1.0		<1		1.6

* n = Number of determinations. For an explanation of the values in parentheses (GXR-1, GXR-2), see footnote¶.

† ITNA = instrumental thermal neutron activation; IENA = instrumental epithermal neutron activation. The recommended value is the mean of the results obtained with these two methods.[14]

‡ A. (i) HCl digestion; (ii) matrix modification with palladium in 1.4 M nitric acid; and (iii) GFAAS.[16]

§ B. (i) HCl - H$_2$O$_2$ digestion; (ii) IBMK extraction; and (iii) FAAS.[13]

¶ C. (i) Aqua regia digestion (values in parentheses: HF - HClO$_4$ - HNO$_3$ digestion); and (ii) hydride generation AAS.[17]

‖ D. (i) Volatilisation of antimony triiodide; (ii) trioctylphosphine oxide (TOPO) - IBMK extraction; and (iii) FAAS.[18]

Table 5. Effect of sample dissolution technique on the determination of antimony. All results expressed in mg kg^{-1}

Sample	Normal dissolution			Dissolution in Erlenmeyer flasks		
	Sb found	Mean	Variance	Sb found	Mean	Variance
GXR-1	81.46 92.25 87.11 88.09 66.42	83.07	10.07	88.50 91.43 89.46	89.80	1.49
GXR-2	41.87 37.29 39.33 42.24	40.18	2.32	42.40 41.92 43.27	42.53	0.68

For four degrees of freedom this indicates that there is no difference between the mean values of the results obtained with the two different sample dissolution techniques.

For the GXR-2 sample, the two-tailed F-test gave an F value of 11.51 and the variances did not differ significantly at the 5% level (the tabulated F value is 39.17). A pooled estimation of variance t-test gave a t value of -1.66; there is no evidence that the two methods give different results [for five degrees of freedom, the critical value of $|t|$ is 2.57 ($p = 0.05$)].

The reason for the low recovery of antimony from the GXR-1 sample is not known. This sample matrix has a high silicon content and hence may require treatment with hydrofluoric acid. However, good recoveries were also obtained using hydrochloric acid and aqua regia for dissolution of the samples[16,17]; it is unlikely that an interfering element is present in the GXR-1 sample (for example, both GXR-1 and GXR-3 have a high iron content).

Conclusions

A hydride generation technique used in conjunction with d.c. plasma atomic emission spectrometry was found to be a simple and sensitive method for the determination of low levels of antimony in several geological reference materials. The emission intensity of antimony was independent of the reaction time used for hydride generation, indicating that the stibine generated was stable, and hence a suitable reaction time could be selected to ensure that the hydride generation reaction was complete before the hydride was swept into the plasma. The other hydride-forming elements had only a small effect on the determination of antimony and, in the geological reference materials studied, the interference caused by these elements was negligible.

References

1. Miyazaki, A., Kimura, A., and Umezaki, Y., *Anal. Chim. Acta*, 1977, **90**, 119.
2. Häyrynen, H., Lajunen, L. H. J., and Perämäki, P., *At. Spectrosc.*, 1985, **6**, 88.
3. Boampong, C., Brindle, I. D., Ponzoni, C. M. C., *J. Anal. At. Spectrom.*, 1987, **2**, 197.
4. Panaro, K. W., and Krull, I. S., *Anal. Lett.*, 1984, **17**, 157.
5. Krull, I. S., and Panaro, K. W., *Appl. Spectrosc.*, 1985, **39**, 960.
6. Ek, P., and Hulden, S.-G., *Talanta*, 1987, **34**, 495.
7. Fernandez, F. J., *At. Absorpt. Newsl.*, 1973, **12**, 93.
8. "Hydride Generator Instruction Manual," SpectraMetrics, 1983.
9. Thompson, M., Pahlavanpour, B., Walton, S. J., and Kirkbright, G. F., *Analyst*, 1978, **103**, 705.
10. Nakahara, T., and Kikui, N., *Anal. Chim. Acta*, 1985, **172**, 127.
11. Bye, R., *Talanta*, 1986, **33**, 705.
12. Rose, A. W., Hawkes, H. E., and Webb, J. S., "Geochemistry in Mineral Exploration," Academic Press, London, 1979.
13. O'Leary, R. M., and Viets, J. G., *At. Spectrosc.*, 1986, **7**, 4.
14. Gladney, E. S., Perrin, D. R., Owens, J. W., and Knab, D., *Anal. Chem.*, 1979, **51**, 1557.
15. Chao, T. T., Sanzolone, R. F., and Hubert, A. E., *Anal. Chim. Acta*, 1978, **96**, 251.
16. Niskavaara, H., Virtasalo, J., and Lajunen, L. H. J., *Spectrochim. Acta, Part B*, 1985, **40**, 1219.
17. Aslin, G. E. M., *J. Geochem. Explor.*, 1976, **6**, 321.
18. Welsch, E. P., and Chao, T. T., *Anal. Chim. Acta*, 1975, **76**, 65.
19. Miller, J. C., and Miller, J. N., "Statistics for Analytical Chemistry," Wiley, New York, 1984.

On-line Separation of Silver With the Chelate-forming Resin Amberlite XAD-2 - PAR Prior to its Determination by Flame Atomic Absorption Spectrometry

Krystyna Brajter and Ewa Dąbek-Zlotorzyńska
Department of Chemistry, University of Warsaw, Pasteura 1, PL-02-093 Warsaw, Poland

The preparation, characteristics and analytical application of the chelate-forming resin Amberlite XAD-2 - PAR are described. The XAD-2 - PAR resin in the presence of tetren (tetraethylenepentaamine) was applied to the on-line isolation of silver prior to its determination by flame atomic absorption spectrometry. The over-all system provides signal enhancement and can be used for the rapid and selective separation and determination of silver in copper ores.

Keywords: *On-line silver determination; atomic absorption spectrometry; Amberlite XAD-2 - PAR chelating resin; copper ores*

Atomic absorption spectrometry is an accepted method for the determination of silver in ores and concentrates.[1,2] To avoid matrix interferences, which are observed in flame and electrothermal methods, preliminary analyte isolation is recommended.[1-4] Most previously described methods involve extraction for the isolation of silver before its determination by AAS,[1-4] but for many methods difficulties are observed owing to non-selective extraction of silver.[3] We consider ion exchange with the use of a chelate-forming resin to be a very promising method for the isolation of analytes from a matrix metal. These resins are prepared by immobilisation of chelating agents on various supports.[5-13]

In this work 4-(2-pyridylazo)resorcinol (PAR) immobilised on Amberlite XAD-2 hydrophobic polystyrene resin in the presence of tetren (tetraethylenepentaamine) was applied to the on-line isolation of silver prior to its determination by flame AAS. Selective separation was achieved. Using 0.5 M thiourea in 0.2 M nitric acid for elution, the over-all system provides signal enhancement and can be used for the rapid determination of silver in copper ores.

Experimental

Reagents

Amberlite XAD-2 (Aldrich) had a specific surface area of 330 m^2 g^{-1}, a pore diameter of 90 Å and a bed size of 20–60 mesh.

PAR (POCH, Poland) was recrystallised from ethanol.

Standard solutions of metal ions were prepared by dissolving appropriate amounts of analytical-reagent grade metal nitrates in doubly distilled water. The solutions were standardised by AAS against spectral standards.

Tetren was obtained as a 20% solution (Merck).

Apparatus

A Beckman Model 1272 atomic absorption spectrometer with an air - acetylene burner and a Perkin-Elmer HGA-74 graphite furnace atomiser and a Zeiss Jena Model AAS 1 spectrometer with an air - acetylene burner were used. An Elpo (Poland) Model N-517 pH meter with calomel and glass electrodes, Type G 202B (Radiometer, Denmark), were utilised, together with a peristaltic pump (DP2-2, GDR).

The column was of 6 mm i.d. and fitted with a stopcock.

Determination of Metal Ions

Metal ions were determined by means of flame and graphite furnace AAS. They were calibrated against standards pre-

pared in the same media as the samples. Zr was determined spectrophotometrically with PAR (λ = 520 nm).

Preparation of PAR Resin

The Amberlite XAD-2 resin (after washing with methanol, 6 M hydrochloric acid, water, 2 M sodium hydroxide solution and water) was shaken with 5 × 10^{-4} M PAR solution until the supernatant solution became colourless. The resin was filtered off, washed with water, air dried and stored in a refrigerator. The modified resin contained 0.04 mmol of PAR per gram of Amberlite XAD-2. It is stable for at least 3 months.

Determination of the Adsorption Isotherm of PAR

The sorption of PAR was measured under static conditions. A 0.200-g portion of Amberlite XAD-2 was moistened with methanol and then shaken with 20 ml of PAR solution of various concentrations (1 × 10^{-4}–1 × 10^{-3} M) at pH 4 for 12 h. After 24 h the equilibrium concentration of PAR in the solution was measured by spectrophotometry at 395 nm.

Sorption of PAR as a Function of pH

A 0.200-g portion of resin was moistened with methanol and then shaken for 12 h with 20 ml of 1 × 10^{-3} M PAR in the absence and presence of tetren (1 × 10^{-3} and 1 × 10^{-2} M), then the pH was adjusted with nitric acid and sodium hydroxide solution to a value in the range 2–12. The equilibrium concentration of PAR was measured by spectrophotometry after 24 h.

Resistance of XAD-2 - PAR Resin to Mineral Acid and NaOH

A 50-ml volume of mineral acid or NaOH of known concentration was passed through a column containing 0.500 g of XAD-2 - PAR resin (0.04 mmol g^{-1}) and the flow-rate was adjusted to 1.0 ± 0.2 ml min^{-1}. The concentration of complexing reagent in the effluent was measured spectrophotometrically.

Retention of Metal Ions as a Function of pH

Samples (0.200 g) of modified resin were mixed with 1 ml of methanol and 20 ml of solution containing 0.10 mg of metal ions in the absence and presence of a 10 molar excess of amine (tetren). The solutions were adjusted to appropriate pH values. After equilibrium had been attained (24 h) the concentration of metal ions was determined by AAS.

Separation Procedures (Off-line)

A 5-ml volume of solution containing a mixture of metal ions was adjusted to pH 7.2–7.7 with tetren and passed through a column of PAR resin at a flow-rate of 0.5 ml min⁻¹. The column was washed with water and 5 ml of 0.05 M tetren solution at pH 7.2–7.7. Silver was eluted with 10 ml of 0.5 M thiourea in 0.2 M nitric acid. A 4.5-cm bed height of 0.5 g of modified resin was used (0.04 mmol g⁻¹).

On-line Pre-concentration of Silver Prior to Flame AAS

All silver-containing standards were adjusted to pH 7.2–7.7 with tetren. Sample solutions were pumped through the 4.5-cm bed height of 0.5 g of modified resin (0.04 mmol per gram of resin) at the aspiration rate of the AA spectrophotometer, 8 ml min⁻¹. The resin was washed with water, 5 ml of 0.05 M tetren at pH 7.2–7.7 and water for 1 min to remove interstitial solution and to establish a base-line AA signal. Silver on the modified resin was eluted next with 10 ml of 0.5 M thiourea in 0.2 M nitric acid. The eluted silver was detected as the measured AA peak height. After elution the column was washed with water for 3 min to re-establish the base line.

Determination of Silver in Natural Samples

Sample preparation

Transfer about a 1-g sample of copper ore or brass into a beaker and add 10 ml of water and 15 ml of 2 M HNO₃. After the evolution of CO₂ and H₂S, evaporate the sample to dryness on a hot-plate. Add three further 10-ml portions of 2 M HNO₃, evaporating to dryness after each addition. Add 25 ml of nitric acid to the dry residue and heat to boiling under a cover. Filter the residue, wash twice with dilute nitric acid, combine the two filtrates and again evaporate to dryness. Dissolve the residue in 25 ml of dilute HNO₃, filter the solution into a 100-ml calibrated flask, rinse the filter-paper carefully with 25 ml of dilute nitric acid and dilute to the mark with 0.1 M HNO₃.

Method I (off-line)

Place 1 ml of the above solution in a beaker, dilute to 5 ml and adjust to pH 7.2–7.7 with tetren solution. Introduce the mixture on to a column containing 0.5 g of modified resin (0.04 mmole g⁻¹) at a flow-rate of 0.5 ml min⁻¹. Wash the column with water, 5 ml of 0.05 M tetren at pH 7.2–7.7 and water. Elute the silver with 10 ml of 0.5 M thiourea in 0.2 M nitric acid into a 100-ml flask. Determine silver by graphite furnace AAS under the following conditions: wavelength, 328.07 nm; band width, 0.7 nm; volume of sample, 10–20 µl; drying, 100 °C for 20 s; charring, 550 °C for 15–20 s.

Method II (on-line)

Place 50 ml of the above solution in a 250-ml calibrated flask, adjust to pH 7.2–7.7 with tetren solution and dilute to the mark with water. Introduce on to a column containing 0.5 g of XAD-2-PAR resin (0.04 mmol g⁻¹) 25 ml of the above solution at a flow-rate of 8 ml min⁻¹, then wash the column for 1 min with water, 5 ml of tetren at pH 7.2–7.7 and water (1 min). Elute the silver on the resin with 10 ml of 0.5 M thiourea in 0.2 M HNO₃ directly into the flame AA spectrometer at the same flow-rate.

Results and Discussion

Amberlite XAD-2-PAR chelating resin in the presence of tetren was successfully used for the on-line (and off-line) isolation of silver from matrix metals before its determination by flame AAS. The method was adopted for the determination of silver in copper ores and appeared to be precise and rapid (Table 1).

Table 1. Results for the determination of silver in natural samples (average of eight determinations; mean and range, 95% confidence limit)

| | Content of Ag, 10⁻²% | | | |
Sample	Off-line	On-line	Extraction with dithizone	AAS*
Copper ore† ..	2.21 ± 0.10	2.19 ± 0.15	—	1.80
Brass	—	1.98 ± 0.20	2.06 ± 0.26	1.39

* Without separation.
† Standard rock sample, copper ore CuPI (Institute of Geology, Warsaw). Silver concentration, 2.26 × 10⁻²%.
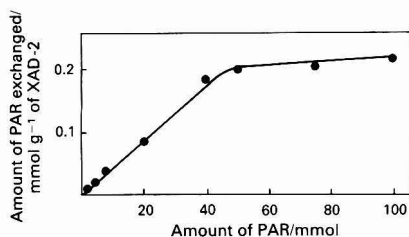
Fig. 1. Adsorption isotherm of PAR
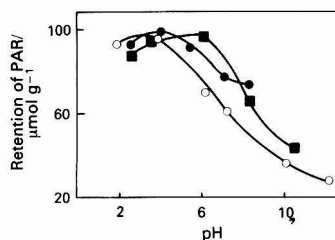
Fig. 2. Sorption of PAR as a function of pH. Tetren: (○) absent; (●) 1 × 10⁻³ M; and (■) 1 × 10⁻² M

In Fig. 1 the adsorption isotherm of PAR on Amberlite XAD-2 resin at pH 4 is presented. It indicates that the capacity of XAD-2 for PAR is 0.2 mmol g⁻¹. The maximum capacity occurs at low pH, as Fig. 2 shows. This is in agreement with the theory postulated by Cantwell and Puon[14] based on the Stern-Gouy-Chapman theory.[15] In acidic medium, protonated forms of PAR (pK_{a1} = 2.7, pK_{a2} = 5.5, pK_{a3} = 12.3),[16] owing to the zero charge on the molecules, are sorbed to a greater extent on the hydrophobic surface of XAD-2 resin than they are in a non-acidic medium. The sorption of PAR by XAD-2 is due mainly to π-π dispersion forces arising from the aromatic nature of the resin and reagent.

The PAR-modified resin is resistant to mineral acids at concentrations up to 6 M (the release of PAR from the resin phase is less then 40%). The influence of HNO₃, HCl and HClO₄ and also NaOH on the retention of PAR was investigated (Fig. 3). The following sequence of influence of mineral acids on the modified resin can be deduced: HCl > HNO₃ > HClO₄.

The influence of tetren solution on the retention of PAR was investigated at molar ratios of PAR to tetren of 1:1 and 1:10. No differences due to the presence of tetren or to better results were observed (Fig. 2).

PAR forms stable complexes with many metal ions and without a competing ligand it is convenient for group metal ion pre-concentration. We found that in the presence of tetren as
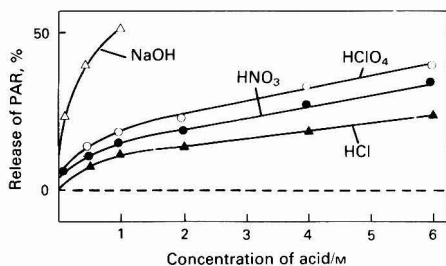
Fig. 3. Release of PAR from XAD-2 - PAR resin by mineral acids and NaOH
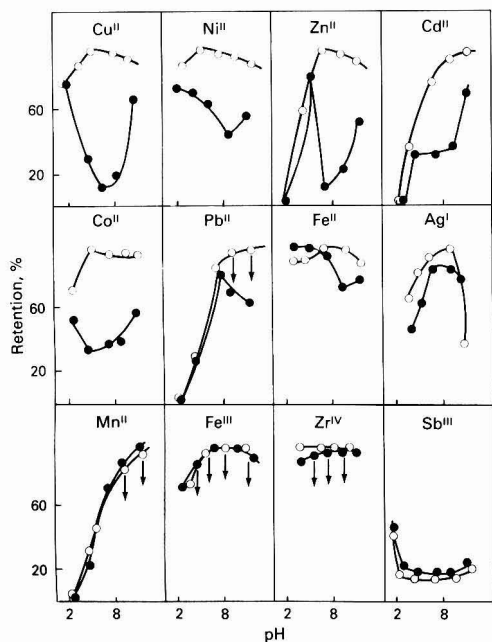
Fig. 4. Retention of metal ions on the PAR-loaded resin as a function of pH. (○) In the absence and (●) in the presence of tetren

a competing ligand, differentiation of retention of metal ions occurs. The retentions of Ag^I, Cu^{II}, Ni^{II}, Co^{II}, Mn^{II}, Zn^{II}, Cd^{II}, Pb^{II}, Fe^{II}, Fe^{III}, Sb^{III} and Zr^{IV} in the absence and presence of tetren are shown in Fig. 4. Comparison of the results shows that Ag^I in the presence of tetren is especially strongly retained on XAD-2 - PAR resin. Cu^{II} and other metal ions show a negligible affinity for the resin under these conditions.

On the basis of the different behaviours of Ag^I and Cu^{II} and other metal ions, a method for the isolation of Ag^I was worked out. Results for the separation of Ag^I from excess of other metal ions using the off-line procedure are presented in Table 2. In static measurements tetren provides a great enough differentiation of the retention of Cu^{II} and Ag^I to separate both metal ions.

The dynamic experiments showed that the molar ratio of tetren to all the matrix metals is a very important factor for the quantitative retention of silver. To optimise the conditions, a set of experiments was performed in which the Cu^{II} content was changed from 0 to 90%. It was found that if tetren is added to the feed solution with the pH maintained in the range 7.2–7.7, silver was quantitatively retained on 0.5 g of XAD-2 - PAR resin containing 0.04 mmol of PAR per gram of resin, independent of the Cu^{II} content.

Table 2. Separation of silver from other metal ions on PAR-loaded Amberlite XAD-2 (11 µg of Ag added; average of four measurements and 95% confidence limits)

Silver found/µg	Metal ion	Added/mg	Found/mg
10.9 ± 0.1	Cu	0.10	0.10 ± 0.01
10.8 ± 0.2		0.50	0.50 ± 0.01
10.8 ± 0.1		1.00	0.99 ± 0.01
10.6 ± 0.3		2.00	1.98 ± 0.02
10.8 ± 0.1	Zn	0.50	0.50 ± 0.02
10.7 ± 0.2		1.00	0.97 ± 0.02
10.7 ± 0.3		2.00	1.65 ± 0.05
10.8 ± 0.2	Ni	0.05	0.045 ± 0.002
10.8 ± 0.2		0.10	0.075 ± 0.002
10.6 ± 0.2		0.20	0.15 ± 0.02
10.9 ± 0.1	Co	0.10	0.10 ± 0.01
10.9 ± 0.1		0.20	0.20 ± 0.01
10.8 ± 0.2		1.00	0.85 ± 0.02
10.8 ± 0.2	Cu	0.50	0.50 ± 0.01
	Zn	0.10	0.10 ± 0.01
	Ni	0.05	0.044 ± 0.004
	Co	0.05	0.050 ± 0.001
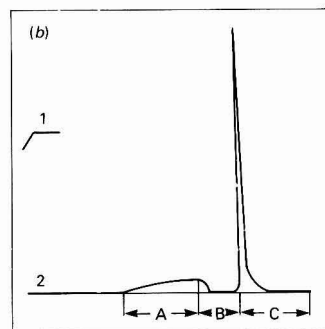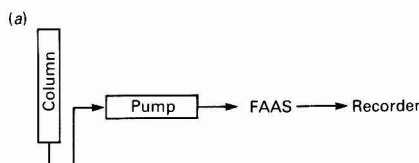
Fig. 5. (a) Schematic diagram of the flame AAS (FAAS) system. (b) 1, Direct introduction of a 0.5 p.p.m. silver solution into the FAAS system (no column); 2, on-line system. A, Introduction; B, washing; and C, elution profiles for the XAD-2 - PAR column equilibrated with a 0.5 p.p.m. silver solution

Determination of Silver

The application of flame AAS for the determination of silver after its on-line pre-concentration and separation required the correlation between the flow-rate of sample introduction into the flame AAS system and the flow-rate used in the column. To provide the maximum analytical signal of silver the characteristic flow-rate of the nebuliser of the Beckman spectrometer was used, *i.e.*, 8 ml min^{-1}.

The same flow-rate was used in the column and for sample introduction and silver elution. The other column parameters (bed height, capacity) were the same as in the off-line procedure. The change in the analytical signal of silver was recorded during the whole experimental procedure, *i.e.*, sample introduction, Cu^{II} elution and Ag^I elution. The base line and the shape of the recorded chromatograms (peak height *vs.* time) were unchanged (Fig. 5). Application of the ion-exchange isolation of silver enhanced the analytical signal of silver (Fig. 5).

Both the peak-height and the peak-area modes were used to determine the concentration of Ag^I. The peak-area mode gave better results, but it was more time consuming because of lack of a peak-area intregrator. The precision obtained with the peak-height mode is good enough and this mode was utilised in the final procedure. For the determination of silver concentrations calibration graphs were used. Standard silver solutions yielded a linear calibration graph over the range 0.1–2 p.p.m. with a correlation coefficient of 0.996. The precision was evaluated from ten replicate measurements on a 0.5 p.p.m. Ag^I solution. A relative standard deviation of 2.3% was obtained.

Column Performance

The volume of sample introduced into the column was equal to 25 ml in 3 min. Then 5 ml of 0.05 M tetren were passed through the column to elute remaining traces of Cu^{II} from the column, which took less than 1 min. Before elution of silver the column was washed with water for less than 1 min (5 ml) to remove interstitial solution and to re-establish a base-line AA signal. It was found that for elution of silver 0.5 M thiourea in 0.2 M nitric acid is very convenient; 8 ml of eluent were used (1 min), then the column was washed with 25 ml of water. The column can be used several times.

Results for the determination of silver after off-line isolation are given in Table 2. This method is more time consuming.

References

1. Viets, J. G., O'Leary, R. M., and Clark, J. R., *Analyst*, 1984, **109**, 1589.
2. Donaldson, E. M., *Talanta*, 1982, **29**, 1069.
3. Donaldson, E. M., *Talanta*, 1984, **31**, 443.
4. Donaldson, E. M., and Wang, M., *Talanta*, 1986, **33**, 233.
5. Brajter, K., and Dąbek-Złotorzyńska, E., *Fresenius Z. Anal. Chem.*, 1987, **326**, 763.
6. Brajter, K., and Dąbek-Złotorzyńska, E., *Talanta*, 1986, **33**, 149.
7. Brajter, K., and Olbrych-Śleszyńska, E., *Analyst*, 1986, **111**, 1023.
8. Brajter, K., Olbrych-Śleszyńska, E., and Staśkiewicz, M., *Talanta*, 1988, **35**, 65.
9. Leyden, D. E., and Luttrell, G. H., *Anal. Chem.*, 1975, **47**, 1612.
10. Vanderborght, B. M., and Van Grieken, R. E., *Anal. Chem.*, 1977, **49**, 311.
11. Terada, K., Matsumoto, K., and Kimura, H., *Anal. Chim. Acta.*, 1983, **153**, 237.
12. Pietrzyk, J. D., Koreff, E. P., and Rotsch, T. D., *Anal. Chem.*, 1978, **50**, 497.
13. Pietrzyk, J. D., and Chu, C. H., *Anal. Chem.*, 1977, **49**, 860.
14. Cantwell, F. F., and Puon, S., *Anal. Chem.*, 1979, **51**, 623.
15. Grahame, D. C., *Chem. Rev.*, 1947, **41**, 441.
16. Geary, W. J., Nickless, G., and Pollard, F. H., *Anal. Chim. Acta*, 1962, **26**, 575.

Characterisation of Trace Elements in Dry Depositions by Instrumental Neutron Activation Analysis

L. Morselli and S. Zappoli
Dipartimento di Chimica Industriale e dei Materiali, Università degli Studi, 40136 Bologna, Italy

M. Gallorini and E. Rizzio
CNR Centro di Radiochimica e Analisi per Attivazione, Pavia, Italy

The determination of trace elements present in dry atmospheric depositions by instrumental neutron activation analysis (INAA) is reported. Eighteen elements, As, Br, Co, Cr, V, Sb, Mn, Zn, Ce, Fe, Hf, La, Mg, Rb, Sc, Th, Na and K, were determined in 22 samples that were collected every month over 2 years (1985–87).

The results show characteristic groups of elements, *i.e.*, anthropogenic, non-anthropogenic and toxic, and elements showing seasonal variations. The results obtained offer a preliminary series of data on the natural fallout in an urban industrialised area in northern Italy.

Keywords: *Trace element determination; dry deposition; atmospheric pollution; neutron activation analysis*

Atmospheric dry depositions may be a very important source of information in environmental monitoring and related studies. The chemical characterisation of the components of atmospheric dry depositions provides essential data for: (i) atmosphere quality; (ii) types of local and long-distance pollution; (iii) effects of urban and industrial settlements; and (iv) additional information related to agriculture and meteorological factors.

The determination of the chemical species contained in these materials, such as inorganic and organic acids, organic compounds (polycyclics and pesticides), heavy metals and trace elements, plays an important role in defining not only the pollution rate but also the possible pollutant sources.[1-3]

In this paper, attention is focused on the determination of trace elements which provide useful information about the quality of the atmosphere in large urban industrialised areas. The study was carried out on samples collected every month over 2 years in the area of Bologna, a city in northern Italy with about 500 000 inhabitants. Instrumental neutron activation analysis (INAA) was employed for the determination of all the elements considered. This technique has been found to be one of the best methods for this purpose, owing to its wide multi-element capability especially when small amounts of samples have to be analysed as in this instance (10–50 mg).

The results from the multi-element analysis appear to be related strictly to possible pollutant sources such as motor vehicles, domestic heating, industrial plants and urban waste incinerators. Previous work on trace elements released into the urban atmosphere has been studied to assess possible links with the composition of atmospheric dry depositions.[4-7]

Experimental

Sampling

Atmospheric dry depositions were collected every month over a period of almost 2 years (1985–87) by means of a wet and dry sampling apparatus (MTX, Bologna, Italy). The apparatus is composed of two polyethylene vessels to sample the wet and dry depositions separately. When it is raining a rain sensor allows the dry deposition vessel to be closed with a cap and when it is not raining the wet deposition vessel is closed. The sampling site, located in the suburbs of Bologna, is bordered along an arc of 180° by a woody area.

The samples collected using this procedure are representative of the natural dry depositions and are related to monthly and seasonal variations. This technique differs from the usually adopted, high-volume collection, which may not reflect the real average of the dry fallout and the distribution

of the related elements. With this latter method, the resulting data are strictly dependent on many different parameters, *e.g.*, short collection time, filters used, aspiration speed, particle size and weather conditions at the sampling time. A series of soil samples were also collected from three different points located around the dry deposition sampler. All samples were ground, homogenised and stored in polyethylene vials before analysis.

Analysis

The following 18 elements were determined in all of the samples collected: As, Br, Ce, Co, Cr, Fe, Hf, K, La, Mg, Mn, Na, Rb, Sb, Sc, Th, V and Zn. Four of these (K, Fe, Mg and Na) were found to be present at concentration levels of a few per cent. and all other elements were determined at p.p.m. ($\mu g\ g^{-1}$) levels.

The analyses were carried out by INAA at the CNR Centre for Radiochemistry and Activation Analysis in Pavia using the Nuclear Reactor TRIGA Mark II at the University of Pavia.

Standards

A series of multi-element standard solutions were prepared with either the pure elements or their compounds dissolved in high-purity acids. The National Bureau of Standards Standard Reference Material NBS SRM 1648 Urban Particulate Matter[8] was employed as a comparison standard to check the precision and accuracy of the method. This SRM was found to be the most suitable standard material owing to its composition and chemical characteristics, which can be assumed to be very similar to those of the samples examined.

Table 1 provides a comparison of the values obtained in this study with those suggested or certified by the NBS. Except for rubidium, for which no values are provided by the NBS, all other results are in good agreement, confirming the precision and accuracy of the analyses carried out in this work.

Neutron Irradiation and Gamma Counting

Multi-standard solutions (varying from 0.5 to 1 ml) were sealed in quartz vials and irradiated among the samples. Weighed amounts of the dry depositions (20–50 mg), the soil samples (100–200 mg) and the SRM (*ca.* 80 mg) were sealed in polyethylene vials and irradiated under the following conditions.

Table 1. Analysis of NBS SRM 1648 Urban Particulate Matter. All concentrations expressed in $\mu g\ g^{-1}$ unless indicated otherwise

Element				Experimental value	NBS value
Ce	..	..	..	51 ± 5	(55)
As	..	..	..	110 ± 7	115 ± 10
Br	..	..	..	487 ± 30	(500)
Cr	..	..	..	410 ± 15	403 ± 12
Co	..	..	..	21 ± 4	(18)
Fe, %	..	..	..	3.6 ± 0.2	3.91 ± 0.10
Hf	..	..	..	4.8 ± 0.5	(4.4)
K, %	..	..	..	0.95 ± 0.07	(1.0)
La	..	..	..	38 ± 5	(42)
Mg, %	..	..	..	0.85 ± 0.05	(0.8)
Mn	..	..	..	790 ± 52	(860)
Na, %	..	..	..	0.5 ± 0.08	(0.40)
Rb	..	..	..	48 ± 4	—
Sc	..	..	..	6.2 ± 0.5	(7)
Sb	..	..	..	44 ± 3	(45)
Th	..	..	..	7.1 ± 0.8	(7.4)
V	..	..	..	123 ± 12	(130)
Zn	..	..	..	4650 ± 181	4760 ± 140

Table 2. Gamma energies (keV) and radionuclides utilised in the analyses

Element				Radionuclide analysed	γ-Line utilised (keV)	Half-life	
As	..	..	..	^{76}As	559, 657	26.4	h
Br	..	..	..	^{82}Br	777, 619	35.3	h
Ce	..	..	..	^{141}Ce	145	32.5	d
Co	..	..	..	^{60}Co	1173, 13	5.21	yr
Cr	..	..	..	^{51}Cr	320	27.8	d
Fe	..	..	..	^{59}Fe	1095, 12	45.6	d
Hf	..	..	..	^{181}Hf	482	42.5	d
K	..	..	..	^{42}K	1524	12.3	h
La	..	..	..	^{140}La	487, 159	40.2	h
Mg	..	..	..	^{27}Mg	840, 101	9.41	min
Mn	..	..	..	^{56}Mn	847, 181	2.67	h
Na	..	..	..	^{24}Na	1369	14.9	h
Rb	..	..	..	^{86}Rb	1078	18.6	d
Sb	..	..	..	^{124}Sb	603, 169	60.4	d
Sc	..	..	..	^{46}Sc	889	84.0	d
Th	..	..	..	^{233}Pa	311	27.0	d
V	..	..	..	^{51}V	1434	3.7	min
Zn	..	..	..	^{65}Zn	1115	245	d

(i) *Determination of ^{51}V, ^{56}Mn and ^{27}Mg (short-life isotopes)*

Neutron irradiation was carried out by the pneumatic facility (Rabbitt) for 1 min at a neutron (n) flux of $5 \times 10^{12}\ n\ cm^{-2}\ s^{-1}$. After a cooling period of 100 s, the resulting activities of ^{51}V and ^{27}Mg were evaluated; ^{56}Mn was counted 2 h later.

A correction for the ^{56}Mn contribution from its γ peak at 847 keV on the ^{27}Mg γ peak at 843 keV was also made by measuring the ^{56}Mn activity through its 1811 keV secondary γ peak. The Mg content was also checked using the ^{27}Mg 1013 keV γ-line.

(ii) *Determination of ^{82}Br, ^{76}As, ^{42}K, ^{24}Na and ^{140}La (medium half-life) and ^{233}Th (through ^{233}Pa), ^{141}Ce, ^{60}Co, ^{51}Cr, ^{181}Hf, ^{59}Fe, ^{86}Rb, ^{124}Sb and ^{46}Sc (long half-life)*

The samples and standards were irradiated at a neutron nominal flux of $1.2 \times 10^{12}\ n\ cm^{-2}\ s^{-1}$ in the rotating facility of the nuclear reactor for 50 h. Gamma counting of the first series (medium half-life) of radioisotopes was started after a 1-d cooling period and all the other radioelements (long half-life) were counted 2 weeks later. All gamma spectra from the irradiated samples and standards were evaluated by two Ge(Li) detectors (of 20 and 25% efficiency; 1.92 and 1.85 keV resolution at the ^{60}Co 1332.4 keV line, respectively) coupled with automatic sample changers and a Nuclear Data ND 66 computerised multi-channel analyser. In all the gamma-count-

Table 3. Concentration ranges and mean values of some major and trace elements in dry depositions and in soil samples (1985–87). Mean values and RSDs are calculated from a minimum of 10 independent measurements. Concentration in $\mu g\ g^{-1}$ unless indicated otherwise

Element		Winter (Oct.–March) Range	Mean	Summer (Apr.–Sept.) Range	Mean	Soils: range
Ce	..	16–71	21.6 ± 13.0	21–69	40.4 ± 12.0	13–17
Fe, %	..	0.8–3.2	1.66 ± 0.33	0.3–2.8	2.14 ± 0.37	0.1–3.0
Hf	..	0.6–5.6	2.34 ± 1.50	0.6–3.6	2.32 ± 0.95	0.9–3.8
La	..	5.0–21.7	12.5 ± 2.1	11.8–25.5	16.0 ± 2.1	4–25
Mg, %	..	0.4–3.2	1.8 ± 0.6	0.6–3.4	1.6 ± 1.0	0.5–3.4
Rb	..	20.0–99.5	40.3 ± 15.7	45.0–86.1	56.5 ± 8.6	15–110
Sc	..	0.6–4.2	2.4 ± 1.0	2.1–3.9	3.0 ± 0.4	0.2–10
Th	..	1.5–8.5	3.6 ± 0.8	3.8–7.2	5.0 ± 0.5	0.5–11
Na, %	..	0.64–3.3	1.1 ± 0.4	0.54–1.1	0.8 ± 0.1	ND*
K, %	..	0.4–1.2	0.8 ± 0.2	1.0–1.7	1.3 ± 0.2	ND

* ND = not determined.

Table 4. Concentration ranges and mean values of some potentially toxic trace elements in dry depositions and in soil samples (1985–87). Concentrations in $\mu g\ g^{-1}$; *cf.* Table 1

Element		Winter (Oct.–March) Range	Mean	Summer (Apr.–Sept.) Range	Mean	Soils: range
As	..	3.9–33.9	13.7 ± 8.4	2.8–20.5	7.5 ± 3.7	1.2–9.5
Br	..	20.4–269.0	160 ± 61	20.0–103.1	65 ± 27	0.5–1.5
Co	..	5.9–32.8	16.2 ± 9.5	6.5–35.8	19.5 ± 11.4	1–12
Cr	..	34.0–130.4	81 ± 23	40.0–130.0	97 ± 36	4–90
V	..	82.5–584.0	395 ± 140	53.3–260.0	110 ± 46	10–80
Sb	..	10.1–33.6	18.8 ± 5.8	7.4–47.7	16.7 ± 7.0	0.2–1
Mn	..	104–761	525 ± 140	362–849	595 ± 157	26–600
Zn	..	453–2041	980 ± 401	367–819	605 ± 117	6–25

ing series, the maximum dead-time did not exceed 15%. Table 2 lists the gamma-ray energies utilised in the analysis.

Results and Discussion

From the resulting data (more than 400 individual measurements) two groups of elements can be distinguished according to the scattering of their relative concentration values.

Table 3 lists the concentration ranges and the mean values of the elements determined in the dry deposition samples that are normally present in abundance in soil and that should not be considered as significant for pollution assessment studies. For the same elements the concentration ranges found in the analysis of three different soil samples collected near the sampling point are also given. The values are similar and do not show specific seasonal variations.

Table 4 shows the results obtained from the determination of typical polluting elements characterised by potential toxicity and that are related to industrial urban areas. They are characterised by a wide scatter in their concentrations and, in many instances, are affected by seasonal variations. A comparison with the concentration ranges found in the soil samples shows a significant increase in the dry particulates for all of them. The seasonal distributions of the elements considered are given in Figs. 1–4, where the relative concentrations are plotted on a semi-logarithmic scale against the monthly variation.

Figs. 1 and 2 show the concentration variations of some typical heavy metals. Iron, manganese and cobalt show a similar distribution over the same time period. The iron concentrations are of the order of a few per cent., while the manganese and cobalt concentrations are about 100 and a few p.p.m., respectively. Their distribution does not seem to depend on seasonal variations. The situation is completely different in Fig. 2, where the concentrations of zinc, vanadium
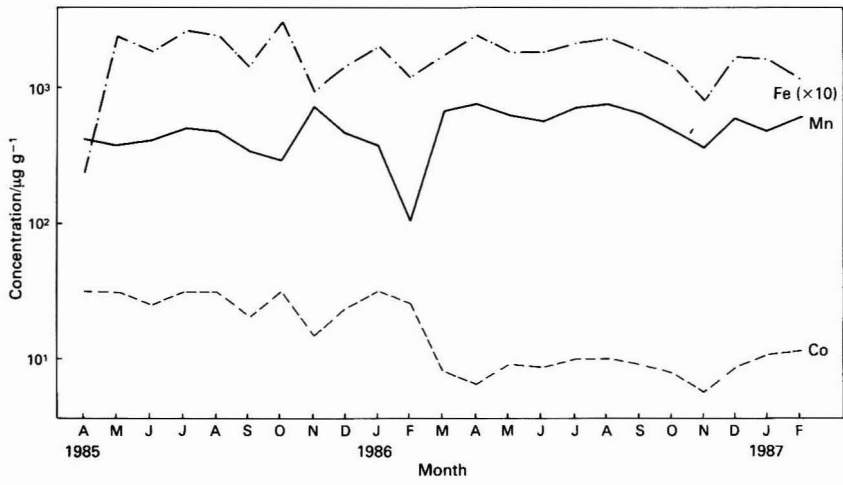
Fig. 1.   Fe (×10), Co and Mn concentration trends *versus* monthly variation (1985–87)
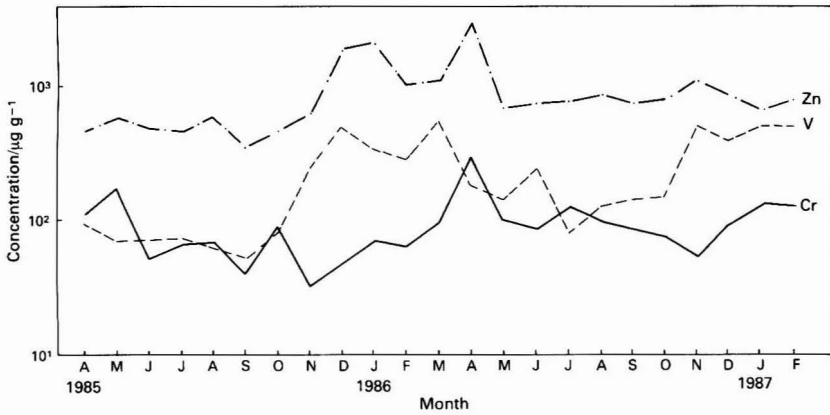
Fig. 2.   Zn, V and Cr concentration trends *versus* monthly variation (1985–87)
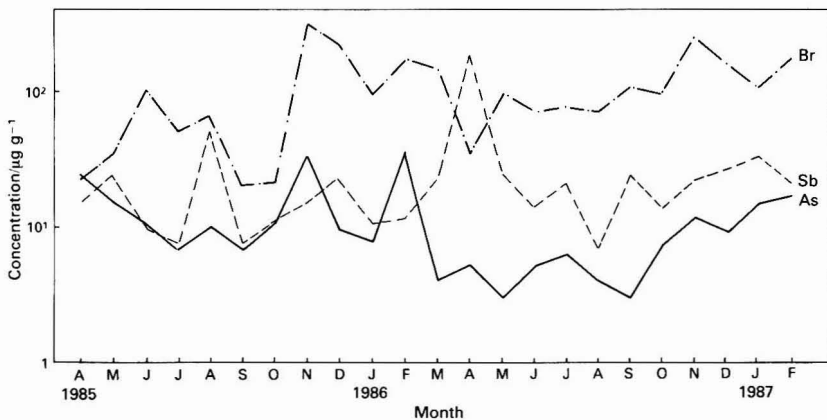
Fig. 3.   Br, Sb and As concentration trends *versus* monthly variation (1985–87)
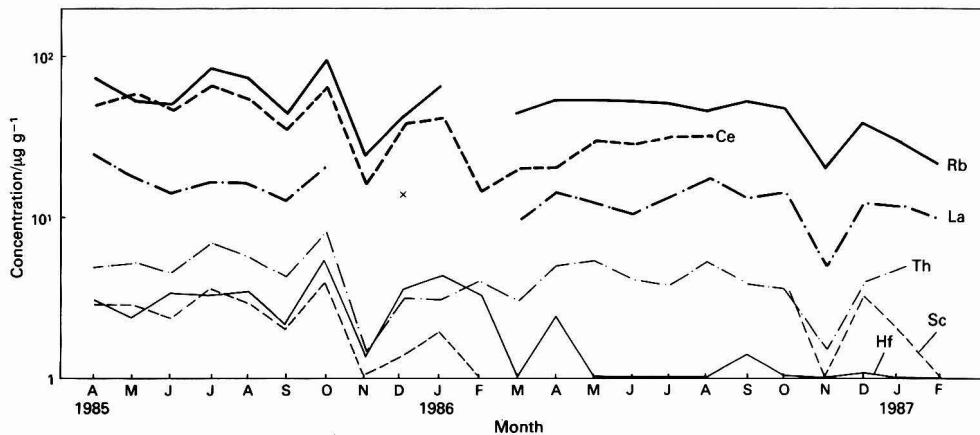
Fig. 4. Concentration trends of some non-anthropogenic elements *versus* monthly variation (1985–87)

and chromium increase during the winter months. This is particularly evident for vanadium, which shows a dramatic increase from about 60 p.p.m. in summer up to more than 500 p.p.m. in December, reflecting the incidence of domestic oil heating. Fig. 3 shows the behaviour of some non-metallic elements such as arsenic, antimony and bromine. These elements show a large scatter in their concentrations with the monthly variations and are independent of the seasonal variation. However, the higher concentrations of arsenic and bromine during the winter months may be due to the weather conditions, which, in that period, are often foggy and humid. This can increase the fallout by condensation of volatile elements or their compounds. The concentration variations of rubidium, lanthanum, cerium, thorium, scandium and hafnium, which are not related to industrial activity, are shown in Fig. 4. Except for the difference in the total concentrations, these elements show a constant and similar trend with time. In many instances their concentration ranges are the same as those found in the soils surrounding the sampling site.[9]

In conclusion, this preliminary study on natural dry depositions shows some interesting seasonal and monthly variations for six elements as shown in Figs. 2 and 3. All these elements are related to human activities and have become "normal" components in the atmosphere of urban industrialised areas. Some of them increase dramatically during different periods of the year. This applies to vanadium, bromine and zinc, which during the winter months reach values of up to 10 times higher than in other months.

At present, further information about pollution sources and their contribution to the atmosphere cannot be extrapolated from these data. For this purpose, a complete study should take into account (i) a more statistical series of results (different sampling sites in the considered area, more samples analysed and elements determined, more information on soil composition) and (ii) all the meteorological parameters (wind strength and dominant directions, air temperature and humidity and weather conditions).

Hence, the elemental characterisation and subsequent quantitative analysis of natural dry depositions does not only contribute towards the monitoring of atmosphere quality over a period of time, but can also be used to detect and identify possible sources of pollution.[10,11]

References

1. Buttler, D., "Air Pollution Chemistry," Academic Press, London, 1979, p. 63.
2. Ligocki, M. P., Leuenberger, C., and Pankow, J. F., *Atmos. Environ.*, 1985, **19**, 1609.
3. Stoessel, R. P., and Prange, A., *Anal. Chem.*, 1985, **57**, 2880.
4. Gallorini, M., Orvini, E., Rolla, A., and Burdisso, M., *Analyst*, 1981, **106**, 328.
5. Gallorini, M., Orvini, E., Di Cassa, M., Tittarelli, P., and Rolla, A., "Proceedings of the International Conference on Heavy Metals in the Environment, Amsterdam, September 1981," CEP Consultants, Edinburgh, 1981, p. 657.
6. Gallorini, M., Orvini, E., Rolla, A., and Tittarelli, P., *in* Lindberg, S. E., and Hutchinson, T. C., *Editors*, "Proceedings of the Sixth International Conference on Heavy Metals in the Environment, New Orleans, September 1987," CEP Consultants, Edinburgh, 1987, p. 15.
7. Morselli, L., Carrelli, R., Errani, E., Gallorini, M., and Rizzio, E., paper presented at the Pittsburgh Conference and Exposition, Atlantic City, March 1987.
8. "NBS Certificate of Analysis, SRM 1648 Urban Particulate Matter," National Bureau of Standards, Washington, DC, November 16, 1978.
9. Wedepohl, U. H., *in* Abrens, L. H., *Editor*, "Origin and Distribution of the Elements," Pergamon Press, London, 1968, p. 999.
10. Dams, R., Robbins, J. A., Rahn, K. A., and Winchester, J. W., "Nuclear Techniques in Environmental Pollution," International Atomic Energy Agency, Vienna, 1971, p. 139.
11. Eisenbud, M., and Kneip, T. J., "Trace Metals in Urban Aerosols," Electric Power Research Institute Report No. EPRI-117, October 1975.

Variation of Precision With Concentration in an Analytical System

Michael Thompson

Department of Chemistry, Birkbeck College, University of London, Gordon House, 29 Gordon Square, London WC1H 0PP, UK

A data set consisting of the analyses of about 700 geochemical materials for 25 elements, duplicated within-batch, has been investigated in respect of the relationship between the standard deviation of the determination and the concentration of the analytes. The data were fitted to three models of this relationship. A simple linear model with a positive intercept was found to be a good fit with nearly all of the analytes when fitted by weighted regression, but not by simple regression. A more complex relationship based on the addition of variances was found to be equally good. A suggested relationship based on a linear fit between the logarithms of the standard deviation and concentration was less satisfactory statistically, and also raised some theoretical difficulties. The choice of an appropriate model is important both from the scientific viewpoint and for data quality control purposes.

Keywords: *Precision, standard deviation, statistics, chemometrics, repeatability*

In an analytical system[1] where the test materials differ only in the concentration of the analyte, *i.e.*, there is no effective difference in the matrix or the physical state, one expects to find a definite relationship between the concentration of the analyte and the precision with which it can be determined. Nearly always one finds that the absolute precision of the determination (*i.e.*, the standard deviation σ_c) increases with concentration, *c*, whereas the relative precision [*i.e.*, relative standard deviation (RSD) = σ_c/c] decreases with concentration.

The establishment of a simple mathematical relationship between σ_c and *c* would provide analysts with a valuable tool. The precision of the system could be predicted at any given concentration by means of an equation with a small number of experimentally estimated parameters. This would allow the varying precision of a system to be specified very simply, and would provide a model that would be invaluable in data quality control schemes.

An inappropriate model, however, could give rise to seriously incorrect predictions, especially extrapolations. Moreover, it is easy to fit experimental precision data to an inappropriate model. This possibility stems from two factors, namely the relatively large uncertainties normally found in the experimental values of σ_c and the use of unweighted regression for the fitting.

In this study, some data produced over a long period for data quality control purposes are examined for compatibility with particular models. The primary task that gave rise to the data was the routine multi-element analysis of silicate materials (*i.e.*, rocks, soils and sediments) by inductively coupled plasma atomic emission spectrometry (ICP-AES). The data set used in this study consisted of results for about 700 different samples, analysed in duplicate within-batch, for 25 elements. As samples rather than reference materials were used, and as the order of analysis was completely randomised within each batch, and the data collection was automatic and uncensored, it can be taken that the results obtained represent the within-batch precision of the system in an unbiased manner, and that any conclusions arrived at are descriptive of "real analysis."

Precision Models That Have Been Proposed

Several workers have discussed equations relating standard deviation with concentration. Zitter and God[2] suggested two possible models that might be appropriate, one of which is a linear function of the form

$$\sigma_c = \sigma_0 + \theta c \quad .. \quad .. \quad .. \quad .. \quad (1)$$
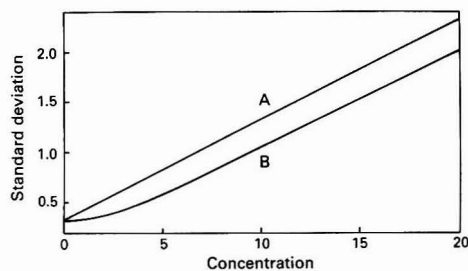
Fig. 1. Examples of model relationships between standard deviation and concentration. (A) An example of equation (1), *i.e.*, $\sigma_c = \frac{1}{3} + 0.1c$; and (B) an example of equation (13), *i.e.*, $\sigma_c = (\frac{1}{9} + 0.01c^2)^{\frac{1}{2}}$

where σ_0 is the standard deviation at zero concentration of the analyte and θ is a constant (Fig. 1). Thompson and Howarth[3-5] also used this equation as a model for routine quality control of within-laboratory geochemical data produced by atomic absorption spectrometry and spectrography. They found that the equation represented the data well. They also showed that the equation accounted well for the relationship between RSD and concentration. From equation (1),

$$RSD = \sigma_c/c = \sigma_0/c + \theta \quad .. \quad .. \quad .. \quad (2)$$

As the detection limit (c_L) is effectively defined by IUPAC[6] as the concentration equal to $3\sigma_0$, the RSD at the detection limit is given by

$$RSD_{(detection\ limit)} = \frac{1}{3} + \theta \quad .. \quad .. \quad .. \quad (3)$$

According to this model, therefore, the RSD falls with increasing concentration, in the form of a rectangular hyperbola, from the value of $\frac{1}{3} + \theta$ at the detection limit towards an asymptotic precision equal to θ. This behaviour has been qualitatively noted by several workers.[7-9] The function is illustrated in Fig. 2.

Both equations (1) and (2) can be generalised by expressing the concentration and precision in units of detection limit. The generalised concentration κ is given by $\kappa = c/c_L = c/3\sigma_0$. Insertion of this value into equation (1) gives

$$\sigma_{gen} = \frac{\sigma_c}{c_L} = \frac{1}{3} + \theta\kappa \quad .. \quad .. \quad .. \quad (4)$$

From equation (2) we obtain

$$RSD = 1/3\kappa + \theta \quad .. \quad .. \quad .. \quad (5)$$
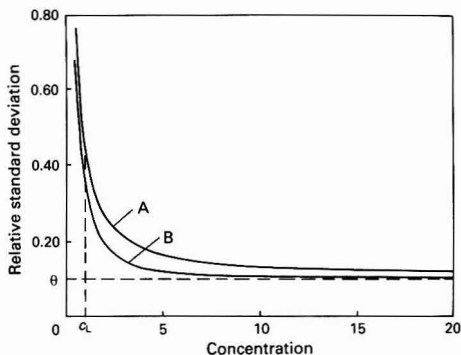
Fig. 2. Relative standard deviation as a function of concentration according to the two models illustrated in Fig. 1. Derived from (A) equation (1) and (B) equation (13)
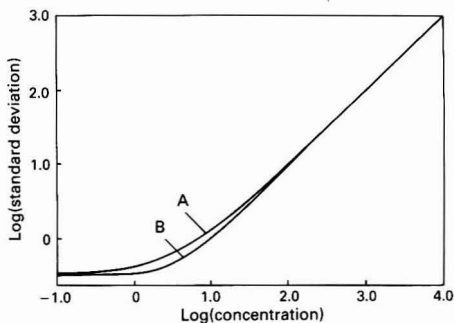
Fig. 3. Relationship between log(standard deviation) and log(concentration) implied by (A) equation (1) and (B) equation (13). The slope of both lines approaches a constant value only at concentrations well above the detection limit

The ISO Standard "The Precision of Test Methods"[10] allows the use of equation (1) or either of two alternatives:

$$\sigma_c = \theta c \quad \quad \quad \quad (6)$$

and

$$\log \sigma_c = \log k + n \log c; \quad n < 1 \quad \quad (7)$$

for relating the standard deviation of reproducibility (see below) to concentration in collaborative trials. Equation (7) can be expressed in the alternative form

$$\sigma_c = k c^n; \quad n < 1 \quad \quad \quad (8)$$

Equations (7) and (8) have been used as a basic form by other workers. Horwitz *et al.*[11] maintain that there is a general relationship between RSD and c for collaborative trials, regardless of the analyte, the matrix or the analytical method. The proposed relationship corresponds to the form

$$\sigma_c = 0.02 c^{0.8495} \quad \quad \quad \quad (9)$$

Hughes and Hurley[12] suggested that equations of the type

$$\sigma_c = k c^{0.5} \quad \quad \quad \quad (10)$$

might be appropriate for method specification and recommended the use of the parameter k as a measure of method performance in collaborative trials. Zitter and God[2] pointed out that equation (10) (with $k = 1$) would be the expected relationship in data dominated by Poissonian counting statistics, for example, near the instrumental detection limit in an XRF method.

It should be noted that in equations (6)–(10) there is no provision for an IUPAC detection limit, as in all of these models $\sigma_c = 0$ when $c = 0$. Moreover, equation (7) is other-

wise inconsistent with equation (1) in the implication that $d \log \sigma_c / d \log c$ is a constant (n). If equation (1) is taken as correct, then

$$\log \sigma_c = \log(\sigma_0 + \theta c) \quad \quad \quad (11)$$

This function describes the obtuse hyperbola shown in Fig. 3. From equation (11), it follows that

$$\frac{d \log \sigma_c}{d \log c} = \frac{1}{1 + \sigma_0/\theta c} \text{ or } \frac{d \log \sigma_{gen}}{d \log \kappa} = \frac{1}{1 + 1/3\theta\kappa} \quad (12)$$

Only when $\kappa > 100$ does this slope approach a constant value, as distinct from the implication of equation (7).

Zitter and God[2] also pointed out that in a relationship such as equation (1), showing analytical error as the sum of two independent terms, it should be the variances that are additive rather than the standard deviations, *i.e.*,

$$\sigma_c^2 = \sigma_0^2 + \theta^2 c^2 \quad \quad \quad (13)$$

This model is theoretically more satisfactory than equation (1), but obviously more difficult to use. For given values of σ_0 and θ, values of RSD predicted by equations (1) and (13) tend towards identity at both very low and high generalised concentrations (κ values). The maximum relative deviation between the two models amounts to 0.414 and occurs at a concentration of

$$c = \sigma_0/\theta \text{ or } \kappa = 1/3\theta \quad \quad \quad (14)$$

The difference between the models represented by equations (1) and (13) is shown in various forms in Figs. 1–3.

Types of Precision

In the context of collaborative trials, BS 5497[10] differentiates between two extreme types of precision, *viz.*, repeatability and reproducibility. Repeatability precision refers to "tests performed under conditions that are as constant as possible, with tests performed during a short interval of time. . . in one laboratory by one operator using the same equipment." Reproducibility precision, in contrast, refers to "tests performed in widely varying conditions, in different laboratories with different operators and different equipment."

The data examined in this study were collected under conditions that corresponded closely but not identically with "repeatability." The main differences between the conditions of this study and those of repeatability are (i) the data were produced by many different operators although all were subject to a single strict regime, (ii) the data were accumulated over a long period of time and (iii) the time interval between the duplicated analysis was not particularly short, being a random time in the range 0–6 h. The precisions estimated in this study are, therefore, referred to as "within-batch precisions."

Experimental

Instrumental Conditions

Elemental data were recorded under simultaneous multi-element conditions on an ARL 34 000 1-m vacuum ICP spectrometer. The operating conditions were as follows: forward power, 1.2 kW at 27 MHz; viewing window, a 4-mm square centred at 14 mm above the load coil; Fassel-type plasma torch; coolant flow-rate, 12.0 l min^{-1}; auxiliary flow-rate, 0.4 l min^{-1}; injector flow-rate, 1.00 l min^{-1}; Meinhard TR-30-3A concentric glass nebuliser; Scott-type double-pass spray chamber; uptake rate of test solution, 0.8 ml min^{-1} (unpumped); signal stabilisation time, 20 s; and integration time, 3×5 s. The lines used and their instrumental detection limits under the given conditions are shown in Table 1.

Test Materials

The test materials included in this study were all types of soils,

Table 1. Spectral lines and instrumental detection limits (IDL)

Analyte				Line/nm		Order	IDL/ng ml^{-1}
Li	..	..	..	670.8	I	1	3
Na	..	..	..	589.0	I	1	12
K	..	..	..	766.5	I	1	45
Rb	..	..	..	780.02	I	1	150
Be	..	..	..	313.0	II	2	0.14
Mg	..	..	..	279.1	II	2	110
Ca	..	..	..	317.9	II	2	75
Sr	..	..	..	407.8	II	1	1.2
Ba	..	..	..	455.4	II	1	11
Al	..	..	..	308.2	I	2	75
La	..	..	..	398.9	II	2	6
Ti	..	..	..	337.3	II	2	90
V	..	..	..	311.1	II	2	3
Cr	..	..	..	267.7	II	3	4.5
Mo	..	..	..	281.6	II	2	7.5
Mn	..	..	..	257.6	II	2	7.5
Fe	..	..	..	259.9	II	2	75
Co	..	..	..	228.6	II	3	11
Ni	..	..	..	231.6	II	2	17
Cu	..	..	..	324.8	I	2	3
Ag	..	..	..	328.1	I	2	4.5
Zn	..	..	..	202.5	II	2	7.5
Cd	..	..	..	226.5	II	2	4.5
Pb	..	..	..	220.3	II	2	60
P	..	..	..	178.3	I	3	45

Fig. 4. Setting of an upper limit for the concentration range of a typical element (lanthanum) to prevent the regression being affected unduly by a small proportion of very high results, *i.e.*, concentrations beyond line A. The limits were set to include about 95% of the raw data

Table 2. Concentration ranges of the elements in this study. The system detection limits (SDL) were calculated as $3\hat{\sigma}_0$, with $\hat{\sigma}_0$ derived from the variance model, where there was significant slope, otherwise from the value of $\bar{y}_i$

Analyte				SDL/µg g^{-1}	Top of range/ µg g^{-1}	Range, orders of magnitude
Li	..	..	..	0.38	60	2.20
Na	..	..	..	32	27 300	2.93
K	..	..	..	32	33 700	3.02
Rb	..	..	..	31	169	0.74
Be	..	..	..	0.041	6.3	2.19
Mg	..	..	..	29	19 800	2.83
Ca	..	..	..	56	263 000	3.67
Sr	..	..	..	0.53	880	3.22
Ba	..	..	..	2.7	790	2.47
Al	..	..	..	160	74 600	2.68
La	..	..	..	0.9	46	1.69
Ti	..	..	..	25	5400	2.32
V	..	..	..	0.75	238	2.50
Cr	..	..	..	1.7	153	1.95
Mo	..	..	..	2.5	74	1.47
Mn	..	..	..	11	870	1.90
Fe	..	..	..	65	46 600	2.86
Co	..	..	..	1.6	51	1.50
Ni	..	..	..	2.2	175	1.90
Cu	..	..	..	2.1	177	1.93
Ag	..	..	..	0.8	3.0	0.57
Zn	..	..	..	3.7	220	1.77
Cd	..	..	..	0.72	7.5	1.02
Pb	..	..	..	13	85	0.81
P	..	..	..	20	1120	1.75

rocks, river and marine sediments. They were analysed in batches of 50–200 typically.

Preparation of Test Solutions

Test portions of 0.100 g were weighed into polytetra-fluoroethylene test-tubes, and nitric acid (70% *m/m*, 2.0 ml), perchloric acid (60% *m/m*, 1.0 ml) and hydrofluoric acid (40% *m/m*, 5.0 ml) were added. The tubes were heated in a temperature-programmable block according to the following schedule: 100 °C for 3 h, 140 °C for 3 h and 190 °C for 15 h. Hydrochloric acid (5 M, 2.00 ml) was added to the dry, cooled residues, and the tubes were heated in a shallow block (30 min, 50 °C). Water (8.00 ml) was added and the tubes were stoppered and shaken briskly for a few minutes. The solutions were analysed after temperature equilibration in the instrument room.

Preparation of the test solutions and instrumental analysis were carried out by a number (>20) of different workers. However, the procedures were standardised and controlled.

Data Quality Control Protocol

Trueness was monitored by the insertion of two house reference materials and procedural blanks into the batch at pre-determined average frequencies. The within-batch precision was monitored by the duplication of a small proportion of the test materials at the weighing stage. Each batch, consisting of test materials, reference materials, blanks and duplicates, was analysed in a unique randomised order. Data from batches failing the quality control requirements were not included in this study. The precision requirement corresponded to the specification $\sigma_{gen} = \frac{1}{3} + 0.05\kappa$, as per equation (4). This requirement is considerably less strict than the precision actually obtained, and therefore some outlying results may be incorporated in the raw data.

Data Collection and Pre-processing for This Study

The analytical data for the duplicates from each batch were abstracted and dumped on to magnetic tape over the period 1982–87. The mean and absolute differences of each duplicated result were recorded to at least three significant figures.

At the end of the collection period the data were reorganised into separate files for each element.

The concentration ranges for each element were examined as histograms and as normal probability plots. Any long tails or apparent bimodality on the high side of the distribution was deleted from the data set in order to prevent the subsequent regression from being over-influenced by a small proportion of very high concentration values. Typically about 5% of the results were thus ignored. An example of this procedure is shown in Fig. 4. The concentration ranges of the data used are given in Table 2.

Results and Discussion

Estimation of Standard Deviation at Various Concentrations

The raw data were converted into estimates of standard deviation at various concentrations by the method of Thompson and Howarth.[3] The mean and absolute differences of the
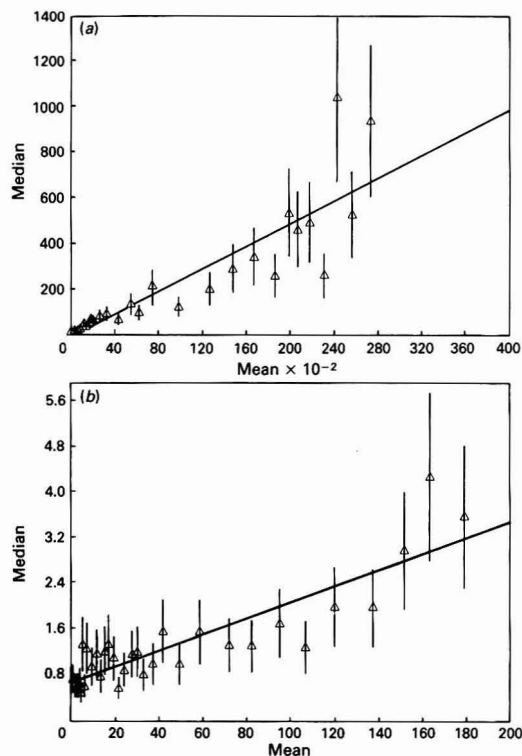
Fig. 5. Examples of the unweighted regression of standard deviation on the concentration for (a) sodium and (b) copper. A poor fit is obtained at low concentrations of sodium. Error bars show the ranges $y_i \pm se(y_i)$, where se indicates standard error. All units in $\mu g\ g^{-1}$

individual duplicates for an element were sorted into increasing order of concentration. The data were then subdivided into groups of 21 results (the number 21 was selected arbitrarily to give a convenient number of points for the final regression). Within each group (i) the mean (x_i) of the means and the median (y_i') of the absolute differences were calculated. The mean (x_i) estimates the concentration, and the standard deviation of the analysis at this concentration was estimated by $y_i = 1.048 y_i'$. The relationship between standard deviation and concentration could then be explored by a regression or similar examination of the successive values of y_i on x_i. The x_i and y_i data thus produced are subsequently referred to as the "processed data."

The factor 1.048 is derived from the properties of the normal curve of error. The use of medians eliminates the effects of a small proportion of outlying results among the duplicates.

Investigation by Unweighted Linear Regression

The relationship between standard deviation and concentration for each analyte was explored initially by means of unweighted linear regression of y_i on x_i. All elements except rubidium and silver gave significant positive slopes, as determined by the value of $t_b = |b/s_b|$ exceeding the critical values for $p = 0.05$ for the appropriate number of degrees of freedom, where b is the coefficient estimate and s_b is its standard error. This result reflects the general trend for standard deviation to increase with concentration. In the instances where no significant slope was detected, the concentration ranges of the analytes were invariably small compared with the detection limit.

Overall, however, the fits obtained by unweighted regression were poor, especially towards the bottom end of the concentration ranges. This can be seen in the example in Fig. 5. The reason for the poor fit in relation to the estimated confidence interval of each y value is that unweighted

Table 3. Results of weighted linear regression on the processed data. Statistics a and b are the intercept and coefficient of the regression, respectively. The parenthesised figures are their standard errors. VSR is the variance of the scaled residuals. The number of x_i, y_i points is n. The parameters σ_0 and θ in equation (1) are estimated by a and b, respectively

Analyte			a	$se(a)$	b	$se(b)$	VSR	n
Li	..	..	0.068	(0.040)*	0.015	(0.003)	1.09	31
Na	..	..	7.5	(2.0)	0.017	(0.001)	0.97	30
K	..	..	6.4	(2.8)	0.021	(0.001)	0.82	31
Rb	..	..	8.0	(0.73)	0.002	(0.009)*	—	30
Be	..	..	0.011	(0.002)	0.010	(0.002)	1.46	32
Mg	..	..	6.3	(1.9)	0.014	(0.001)	0.89	30
Ca	..	..	17	(3.3)	0.015	(0.002)	1.56	31
Sr	..	..	0.13	(0.054)*	0.019	(0.002)	1.10	29
Ba	..	..	0.86	(0.19)*	0.018	(0.002)	1.46	31
Al	..	..	32	(25)*	0.015	(0.002)	2.07†	30
La	..	..	0.21	(0.07)	0.032	(0.005)	1.07	30
Ti	..	..	7.1	(2.0)	0.012	(0.002)	1.73†	32
V	..	..	0.2	(0.03)	0.013	(0.0009)	0.52	28
Cr	..	..	0.47	(0.08)	0.025	(0.004)	1.47	32
Mo	..	..	0.82	(0.07)	0.021	(0.008)	1.19	30
Mn	..	..	2.6	(0.50)	0.013	(0.002)	0.56	23
Fe	..	..	17	(6.8)	0.014	(0.001)	0.92	26
Co	..	..	0.48	(0.04)	0.010	(0.002)	0.46	31
Ni	..	..	0.66	(0.08)	0.012	(0.003)	1.11	31
Cu	..	..	0.61	(0.06)	0.011	(0.002)	0.70	32
Ag	..	..	0.23	(0.02)	−0.011	(0.02)*	—	32
Zn	..	..	1.00	(0.14)	0.019	(0.003)	0.71	30
Cd	..	..	0.19	(0.012)	0.017	(0.010)	0.81	31
Pb	..	..	2.6	(0.44)	0.020	(0.014)*	—	30
P	..	..	5.8	(0.97)	0.018	(0.003)	0.85	28

* Not significantly greater than zero by a one-sided t-test at $p = 0.05$.
† Significantly greater than unity by the F-test at $p = 0.05$.
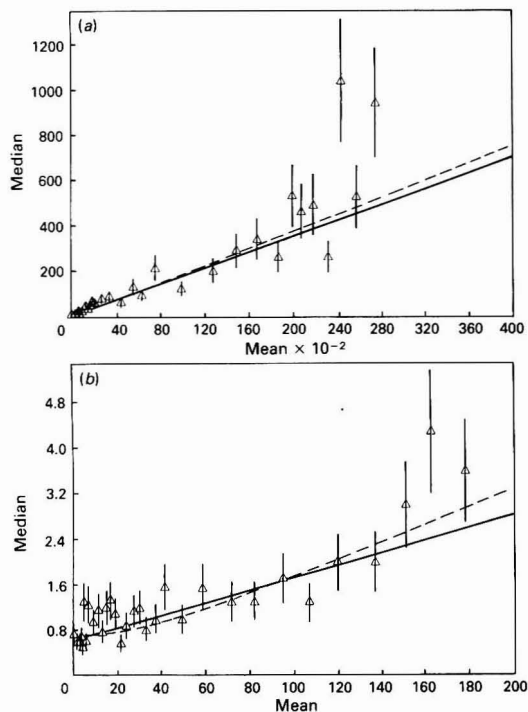
Fig. 6. Examples of the fitting of standard deviation to concentration by (solid line) weighted linear regression and by (broken line) non-linear fitting of the variance function, equation (13). (a) Sodium and (b) copper. The fit of both models at the lower end of the concentration range is good, allowing estimation of the system detection limit. All units in $\mu g\ g^{-1}$

Fig. 7. System detection limits compared with instrumental detection limits

regression takes no account of the precision of the y values. For most of the analytes considered here the concentration range spans several orders of magnitude and consequently the precisions of the y values vary greatly over the range of the x values. This condition contravenes the homoscedastic requirement of normal unweighted regression. This fact also explains the observation that the estimated intercepts of many analytes were not significantly different from zero, as judged by the value of $t_a = |a/s_a|$ (where a is the intercept estimate and s_a is its standard error), contrary to the impression gained from a visual examination of the data. It was therefore concluded that unweighted regression was not a suitable technique for the examination of this type of data.

Results from Weighted Linear Regression

The processed data for each of the analytes were examined next by weighted linear regression, as advocated in BS 5497.[10] The results are shown in Table 3. The procedure is simple and is implemented in most statistical packages.

Calculation of the weights

The y values were weighted by the reciprocal of their estimated variances. The standard error of a median absolute difference (y value) is evaluated[3] as $1.362\sigma/\sqrt{n}$. In this instance $y_i\ (= 1.048y_i')$ estimates σ_c, and n (the number of values from which the median was extracted) is 21, giving an estimated standard error of $0.3115y_i$. The variance is simply the square of this standard error.

BS 5497[10] recommends the use of weights based on variances estimated from the fitted equation. As these are unknown, an iterative procedure is used. This differs from the

method used by the author. The two methods are expected to produce similar results in this instance.

Regression slopes

Significant positive slopes were obtained for all but four of the analytes (Rb, Ag, Cd and Pb). The lack of a significant slope in these instances is the result of the limited concentration range above the detection limit of the analyte, within which there is no detectable change in precision. The b values mostly fall in the range 0.01–0.02, and with a few outliers seem to be part of a unimodal population.

The b values correspond to RSD values of 0.01–0.02 measured at concentrations well above the detection limits. This standard may seem unexpectedly good for multi-user routine analysis. However, it must be recalled that duplicate data from analytical batches failing the initial quality control were excluded from the study, and that the effects of outlying duplicates within *included* batches were virtually nullified by the median procedure. Moreover, it will be shown below that, under circumstances fulfilled by many of the analytes, weighted linear regression slightly underestimates the true asymptotic precision.

Regression intercepts and detection limits

Of the analytes giving significant slopes, all but one gave intercepts that were both significantly greater than zero at a probability of 0.05 and visually appropriate (Fig. 6). This was true even for analytes of which the concentration ranges were very large, *i.e.*, only a small proportion of the data was of the same order of magnitude as the detection limit. Where significant slopes were not obtained, values of a were estimated by $\hat{y}_i$.

As the intercept (a) estimates σ_0, the standard deviation at zero concentration, it can be used to obtain the system detection limit, which is simply 3a.[1] System detection limits (SDL) would be expected to be higher than the instrumental detection limits (IDL) multiplied by the dilution factor, and this expectation is confirmed in this study (Fig. 7) which shows an average SDL/IDL of about 4.

Goodness of fit

The goodness of fit of the weighted regressions was evaluated by examination of the scaled residuals. The scaled residuals are the residuals divided by the standard error of the y value, *i.e.*, $(y_i - \hat{y}_i)/se(y_i)$. For a good fit the scaled residuals should be randomly negative or positive for increasing values of x, their absolute magnitude should show no trend with concentration and their variance should not be significantly greater than unity. Broadly, the residuals complied with the first two of these tests, apart from those of aluminium and titanium. Table 3 shows that the same two elements alone fail the last

Table 4. Results obtained by non-linear fitting of the variance function to the processed data. Statistics a and b are from the function $y = (a + bx^2)^{\frac{1}{2}}$, where a estimates $\sigma_0{}^2$ and b estimates θ^2. VSR is the variance of the scaled residuals. VRATIO is VSR divided by the corresponding value for weighted linear regression

Analyte			a	$\hat{\sigma}_0 (= \sqrt{a})$	$b \times 10^4$	$\hat{\theta} (= \sqrt{b})$	VSR	VRATIO
Li	..	..	0.0163	0.128	2.85	0.017	1.06	1.03
Na	..	..	116	11	3.53	0.019	1.01	0.95
K	..	..	114	11	4.71	0.022	0.76	1.08
Be	..	..	1.82×10^{-4}	0.014	1.93	0.014	1.51	0.97
Mg	..	..	94	9.7	2.40	0.016	0.90	0.98
Ca	..	..	353	19	2.54	0.016	1.83*	0.86
Sr	..	..	0.031	0.18	4.19	0.021	1.19	0.93
Ba	..	..	0.82	0.91	4.15	0.020	1.57	0.93
Al	..	..	2704	52	2.73	0.017	2.07*	—
La	..	..	0.097	0.31	14.82	0.039	1.00	1.02
Ti	..	..	76	8.7	1.88	0.014	1.77*	0.98
V	..	..	0.062	0.25	2.33	0.015	0.68	0.84
Cr	..	..	0.32	0.56	9.30	0.030	1.57	0.94
Mn	..	..	13.1	3.6	3.37	0.018	0.44	1.28
Fe	..	..	462	22	2.25	0.015	1.00	0.92
Co	..	..	0.29	0.54	2.85	0.017	0.53	0.87
Ni	..	..	0.55	0.74	3.49	0.019	1.03	1.08
Cu	..	..	0.49	0.71	2.56	0.016	0.73	0.96
Zn	..	..	1.51	1.2	6.64	0.025	0.81	0.88
P	..	..	47	6.9	6.23	0.025	0.82	1.01

* Significantly greater than unity by the F-test at $p = 0.05$.

test, as judged by an F-test giving a probability of less than 0.05.*

Hence it must be concluded that a linear relationship with a positive intercept accounts satisfactorily for the variation of the standard deviation of the determination with the concentration of the analyte for most of the elements studied. The two discrepant elements are both regarded as being incompletely solubilised by the decomposition procedure, for reasons independent of this study.

The Variance Model

The processed data for each of the analytes were also fitted to the variance model [equation (13)] by means of an iterative non-linear fitting method,[13] using the same weights that were used for weighted linear regression. The results are presented in Table 4. The parameters a and b are estimated directly by the algorithm, and the values of $\hat{\sigma}_0$ and $\hat{\theta}$ are the square roots of a and b, respectively. No standard errors are produced by this method.

The values of $\hat{\sigma}_0$ and $\hat{\theta}$ are close to the values estimated by weighted linear regression for the linear model (Table 3) and individually not usually significantly different from them. Both parameters are consistently slightly higher when estimated for the variance model, but this is simply a result of the shape of the curve, as can be seen by examination of Fig. 1. The discrepancy is greatest when the top of the concentration range for an analyte falls near the maximum divergence of the two models, i.e., at a generalised concentration of $\kappa = 1/3\theta$ [from equation (14)]. Examples of analytes in this class are copper, nickel and cobalt. The discrepancy is smaller for analytes with higher concentration ranges.

In addition to being slightly higher, the θ values obtained for the variance model, considered over all of the analytes, are also more coherent, i.e., they have a smaller relative dispersion and, with a few exceptions, might be taken as being randomly sampled from a single Gaussian population. This may be the result of better over-all estimation of the asymptotic precision with the variance model.

The goodness of fit of the model was tested as before by the

variances of the scaled residuals. Only in three instances was the variance significantly greater than unity, namely for Ca, Al and Ti, and the calcium result was only marginally significant at the 0.05 level. For no analyte was the variance significantly greater or smaller than the corresponding value produced by weighted linear regression, suggesting that the two models give equally good fits to the data. This is illustrated by the fits shown in Fig. 6.

Log - Log Relationships

The processed data were converted into logarithms (base 10) and the relationships of the type expressed in equation (7) were explored by linear regression. As the $se(y_i)$ values were proportional to the y values, the data were rendered homoscedastic by the log-transform, so that weighted regression was unnecessary. The results are presented in Table 5 for all elements previously shown to demonstrate a significant relationship by weighted regression. A significant slope was obtained for every analyte.

The regression intercepts and coefficients cannot be compared directly with the results on the untransformed data. However, a measure of goodness of fit was obtained as follows. The estimated values of $\log y_i$ were converted back into estimates of y_i ($\bar{y}_i$). Then the scaled residuals r_i were formed in the usual way, i.e., $r_i = (y_i - \bar{y}_i)/se(y_i)$.

As above, the variance of the scaled residuals was compared with the theoretical value of unity that would apply to a perfect fit. The values obtained are shown in Table 5. Ten out of 21 results exceeded the critical value of the F statistic for $p = 0.05$, indicating a significant lack of fit. By comparison, for the linear model with weighted regression on untransformed data, the critical value was exceeded for only two analytes.

Further, the variances obtained here were compared with those obtained previously by weighted linear regression on the untransformed data, by forming a variance ratio for each analyte (Table 5). In every instance the variance from the log - log regression was the greater, the geometric mean of the ratio over all analytes being 1.73. Individually, five of the analytes gave ratios greater than the critical value for $p = 0.05$, and 12 of the ratios were greater than the critical value for $p = 0.1$. Therefore, it can be concluded that overall the log - log relationship gave a fit for this data set inferior to that given by weighted linear regression.

---

* In a series of 22 such tests one would expect one or two failures by chance alone. In this work the conservative measure was taken of assuming the failure to be due to lack of fit, especially as the test was supported by independent evidence.

Table 5. Results of linear regression on log-transformed processed data. Statistics a and b are the intercept and the coefficient of the regression, respectively. VSR is the variance of the scaled residuals calculated as in the text. $VRATIO$ is VSR divided by the corresponding value for weighted linear regression on untransformed data

Analyte			n	a	$b(se)$	t	VSR	$VRATIO$
Li	..	..	30	-1.13	0.68 (0.105)	6.5	4.51*	4.15*
Na	..	..	30	-0.82	0.79 (0.048)	16.2	1.70*	1.75†
K	..	..	31	-1.28	0.92 (0.054)	16.9	1.44	1.75†
Be	..	..	31	-1.52	0.55 (0.084)	6.6	2.50*	1.71†
Mg	..	..	30	-0.77	0.74 (0.047)	15.5	1.35	1.51
Ca	..	..	31	-0.47	0.73 (0.032)	22.3	1.56	1.00
Sr	..	..	29	-1.27	0.84 (0.05)	15.9	1.45	1.32
Ba	..	..	30	-0.76	0.68 (0.09)	7.8	2.53*	1.73†
Al	..	..	30	-1.70	1.03 (0.10)	10.3	5.63*	2.71*
La	..	..	30	-0.79	0.63 (0.09)	6.6	1.64*	1.53
Ti	..	..	32	0.09	0.48 (0.06)	8.2	4.22*	2.44†
V	..	..	28	-0.99	0.60 (0.05)	13.1	0.80	1.54
Cr	..	..	31	-0.52	0.53 (0.06)	8.7	2.31*	1.57
Mo	..	..	22	0.01	0.11 (0.06)	1.74	2.13*	1.79†
Mn	..	..	23	-0.36	0.51 (0.06)	9.0	1.01	1.80*
Fe	..	..	26	-0.67	0.75 (0.06)	12.3	1.04	1.13
Co	..	..	31	-0.38	0.20 (0.04)	4.8	0.48	1.03
Ni	..	..	31	-0.14	0.19 (0.05)	4.1	2.30*	2.09*
Cu	..	..	32	-0.31	0.27 (0.04)	6.4	1.55	2.21*
Zn	..	..	31	-0.46	0.50 (0.07)	7.4	1.23	1.72*
P	..	..	27	0.08	0.43 (0.07)	5.8	1.49	1.75†

* Significant at $p = 0.05$ by the F-test.
† Significant at $p = 0.1$ by the F-test.
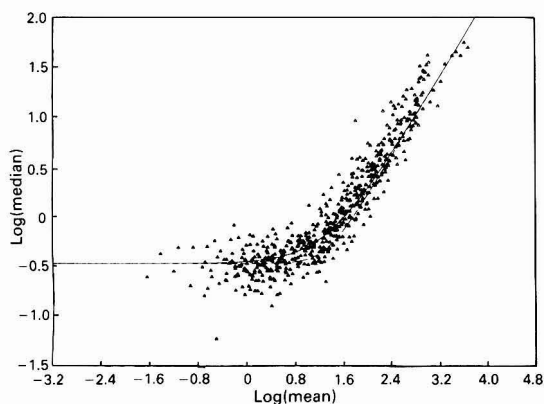
Fig. 8. Overview of the generalised processed data set on log - log axes, compared with (solid line) the theoretical generalised relationship $\sigma_{gen} = \frac{1}{3} + 0.016\kappa$ and (broken line) the generalised variance model $\sigma_{gen} = (\frac{1}{9} + 0.000256\kappa^2)^{\frac{1}{2}}$

Inspection of the regression slopes (b in Table 5) shows values between 0.1 and 1.0, depending mainly on the range of the analyte concentration above the detection limit. This situation is unlike that for slope values given by the linear model [equation (1)] or by the variance model [equation (13)], where the results are coherent and suggest a single θ parameter over most of the analytes, regardless of the detection limit. For the log - log relationship, a range of b values would be the predicted outcome of the linear model being correct, but with different generalised concentration ranges for each analyte. The intercepts are also a complex function of the precision characteristics for the system coupled with the concentration range of the analyte, and are of no fundamental significance.

Possibility of a Single Model for Most Analytes

Processed data

An overview of the whole processed data set on log - log axes

was obtained by generalising the x_i and y_i values for each analyte by dividing by the respective detection limit. However, the data for certain elements were omitted, Al, Ca and Ti because of lack of fit and La and Cr because of non-conforming values of θ. The separate data sets were then combined, log-transformed and plotted (Fig. 8). Superimposed on the points are equation (4) and the function

$$\sigma_{gen} = \left(\frac{1}{9} + \theta^2\kappa^2\right)^{\frac{1}{2}} \quad .. \quad .. \quad .. \quad (15)$$

which is the generalised form of equation (13). A value of $\theta = 0.016$ was used to represent the mean value over the analytes from Table 4.

Fig. 8 shows data extending over about four orders of magnitude from the detection limit. The data clearly conform to the linear model and to the variance model, and show the validity of the generalisation used, $i.e.$, that results for nearly all of the analytes conform to a single model, $viz.$, equation (4) or (15) with a single value of θ. Fig. 8 also shows the incorrectness of fitting a straight line to these log - log data, except at high generalised concentrations.

Raw data

The raw data for the same range of analytes are presented in Fig. 9 in the same fashion. The points are the generalised absolute differences between each pair of duplicated values $versus$ the generalised concentration. All of the raw results were included, not just those within the range of the regression of the processed results. Superimposed on the 10 194 data points are the percentiles calculated for absolute differences, assuming a model of the form of equation (15) with $\theta = 0.016$ and a Gaussian distribution of error. Broadly this diagram shows the data conforming to the model. For instance, the number of data points falling between the percentile ranges 5–50 and 50–95 are close to each other (4265 and 4224, respectively), although lower than expected. This tendency seems to apply to all concentration ranges. However, there is a considerable excess of data points above the 95th percentile, which is an unexpected distribution of results. This aspect is discussed in the next section.
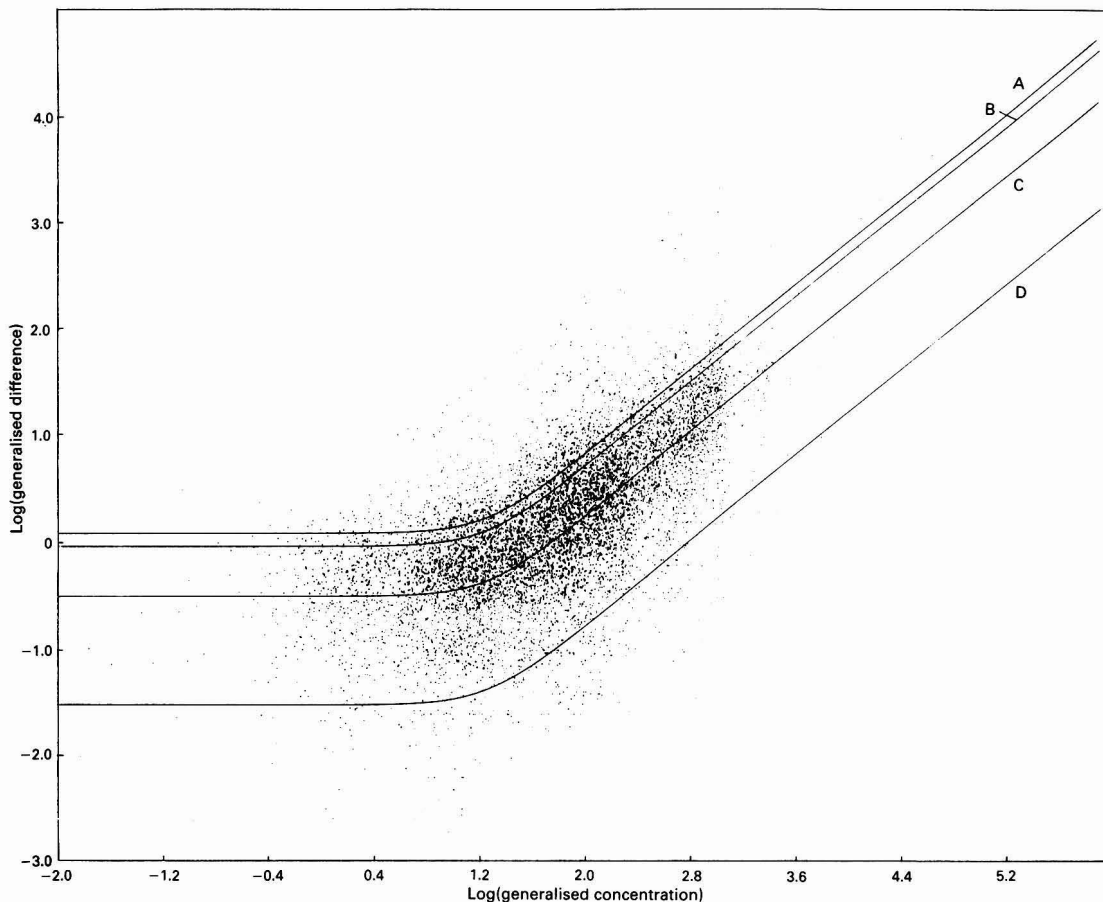
Fig. 9. Overview of the generalised raw data set (10 194 points) on log - log axes, compared with percentiles for the generalised variance model $\sigma_{gen} = (\frac{1}{9} + 0.000256\kappa^2)^{\frac{1}{2}}$. (A) 99th percentile; (B) 95th percentile; (C) median; and (D) 5th percentile

Frequency Distribution of Analytical Errors in This Study

Fig. 9 suggests a substantial deviation from the Gaussian distribution of errors. However, the data for the various analytes were standardised to a single model (*i.e.*, with a single value of θ), a factor which may have contributed to the discrepancy. The raw data were therefore investigated further. For each element the absolute <u>differences</u> were individually standardised by dividing by $\sqrt{2(\hat{\sigma}_0^2 + \hat{\theta}^2 c^2)}$ with the respective $\hat{\sigma}_0$ and $\hat{\theta}$ values taken from Table 4. The elements calcium, aluminium and titanium were not included as they did not fit the model. The elements cadmium, molybdenum, silver and rubidium were standardised with $\hat{\sigma}_0 = \bar{y}_i$ and $\hat{\theta} = 0$, as they did not show significant regression on concentration. Data sets originally conforming to a Gaussian distribution of analytical error would, by this treatment, give rise to the positive half of a standardised Gaussian curve.

Each of the 21 elements tested gave rise to the same pattern, a reduced but quasi-Gaussian pattern up to an ordinate of about 1.7σ, and an excess of points beyond this. The pattern is most clearly seen in the combined data for all of the elements (Fig. 10), which encompasses 14 805 observations. There is a deficit of observations up to about 1.7σ. However, a half-Gaussian curve reduced in height by 15% fits very closely up to this point. Beyond 1.7σ there is an excess of observations to the extent of about 300% of the expected but no sign of bimodality.
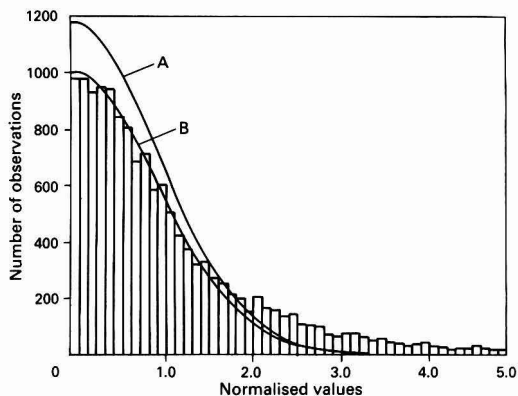
Fig. 10. Standardised absolute differences between 14 805 duplicated values compared with a half-Gaussian curve (A) and a half-Gaussian curve reduced in height by 15% (B)

The cause of this discrepancy is not known and could conceivably be an artefact of the fitting to a model, but if it is typical of analytical data generally it has serious implications in data quality control. For example, repeatability values from collaborative trials are often used as standards of precision in

statutory methods of analysis. They are calculated after an outlier rejection procedure. Duplicated data obtained in subsequent routine analysis would then tend to produce an excessive proportion of unacceptable deviations, with about one in six instances being incorrectly rejected, compared with the expected one in 20 instances. This aspect needs to be investigated further. At present there is very little information on the true frequency distribution of analytical random errors.[14]

Conclusions

Among the analytes with adequate concentration ranges, the linear model of precision gave a good account of the data and accounted for all of the major features of the variation. However, the use of weighted regression was essential, because of the heteroscedastic nature of the data. This feature is bound to cause a poor fit with unweighted regression if the concentration range is substantial. If the concentration range is smaller, less than about one order of magnitude, weighted regression helps to avoid the occasional inappropriate and apparently significant fits obtained by unweighted regression.

A model with an intercept was also essential to account for the variation for most elements. A model constrained to pass through the origin [equations (6) and (7)] could not account for the variation unless all of the data were greater than the detection limit by a factor of about 50 or more.

The variance model is sounder theoretically than the linear model, but is more difficult to work with. For the present data set it gave almost indistinguishable results. This similarity is the outcome of the large standard errors on the individual medians (y values) in the regressions. There was some indication that this non-linear model gave values of θ that were closer to the true value of the asymptotic precision than those obtained by the linear model, especially when the analyte concentration range did not exceed a value of σ_0/θ. In such an instance, the value of θ obtained by weighted linear regression could explain the observed variation well, but could not be used accurately for extrapolation to higher concentrations.

Models which imply a linear relationship between $\log \sigma_c$ and $\log c$ [equations (5)–(8)] have nothing to commend them in this study. Reasonable fits could be obtained for those analytes with relatively short concentration ranges, but such fits would be unsuitable for extrapolation. In most instances, however, the log - log plot was distinctly curved and poor fits were obtained. No fundamental meaning could be attached to the regression parameters that were estimated, as they were determined not only by the actual performance of the method, but also to an overwhelming extent by an arbitrary factor, the concentration range of the analyte. No diagnostic value could

therefore be attached to the estimated value of k in equation (7), contrary to the suggestion of Hughes and Hurley.[12]

In the broader context, it is clear that the fitting of experimental precision data must be undertaken with suitable mathematical models. The large standard errors inevitably associated with precision estimates and the short concentrations ranges often used in such studies allow reasonable fits to be made with a number of models. However, only appropriate models have parameters that are subject to scientific interpretation. The linear model seemed most suitable in this study. A more general conclusion must await further research.

There is good reason to expect that similar results could be obtained for analytical systems other than ICP-AES, but so far no other large bodies of data seem to have been examined in the manner presented here. The author would be happy to hear from other analytical scientists with access to suitable data sets.

References

1. Analytical Methods Committee, *Analyst*, 1987, **112**, 199.
2. Zitter, H., and God, C., *Fresenius Z. Anal. Chem.*, 1971, **255**, 1.
3. Thompson, M., and Howarth, R. J., *Analyst*, 1976, **101**, 690.
4. Thompson, M., and Howarth, R. J., *J. Geochem. Explor.*, 1978, **9**, 23.
5. Thompson, M., *Comput. Geosci.*, 1978, **4**, 333.
6. IUPAC, *Spectrochim. Acta, Part B*, 1978, **33**, 242.
7. Scott, R. H., and Kokat, M. L., *Anal. Chim. Acta*, 1975, **75**, 257.
8. Floyd, M. A., Halouma, A. A., Morrow, R. W., and Farrer, R. B., *Int. Lab.*, 1985, **16**, 24.
9. Ajhar, R. M., Dalager, P. D., and Davidson, A. L., *Am. Lab.*, 1976, **8**, 71.
10. British Standard 5497: Part 1: 1987, "Precision of Test Methods: Guide to the Determination of Repeatability and Reproducibility for a Standard Test Method by Interlaboratory Tests" (ISO 5725, 1986).
11. Horwitz, W., Kamps, L. R., and Boyer, K. W., *J. Assoc. Off. Anal. Chem.*, 1980, **63**, 1344.
12. Hughes, H., and Hurley, P. W., *Analyst*, 1987, **112**, 1445.
13. Head, J. H., *US Air Force Acad. Tech. Rep.*, No. 70–5, 1970, 49 pp.
14. Thompson, M., and Howarth, R. J., *Analyst*, 1980, **105**, 1188.

SHORT PAPERS

Investigation of the Negative Sulphate Peaks Obtained in the Analysis of High-concentration Chloride Solutions by Ion Chromatography

David Mealor and Isabel M. Valente
BP Research International, Sunbury Research Centre, Chertsey Road, Sunbury-on-Thames, Middlesex TW16 7LN, UK

The object of this work was to detect reliably 0.5 mg l^{-1} of sulphate in 10 g l^{-1} of chloride (the maximum amount that could be analysed) in order that 2–3 mg l^{-1} of sulphate could be detected in oil reservoir formation waters, which contain, typically, 40–60 g l^{-1} of chloride. When a solution containing 10 g l^{-1} of chloride was subjected to ion chromatography a small positive peak followed by a small negative peak occurred where the sulphate peak should have been. This made the detection and quantification of less than 2 mg l^{-1} of sulphate in 10 g l^{-1} of chloride uncertain. Investigation showed that the phenomenon was caused by sulphate contamination at the 0.01–0.02 mg l^{-1} level in the eluent. The use of a high-capacity anion-exchange pre-column to clean up the eluent eliminated the problem and allowed the desired detection limit to be achieved.

Keywords: *Brines; ion chromatography; sulphate; chloride; oil formation water*

Ion chromatography[1] is a convenient technique for the determination of common anions. Sulphate is strongly retained on the ion chromatography column whereas chloride is not[2]; therefore, it is possible to separate 5 mg l^{-1} levels of sulphate from 10 g l^{-1} of chloride[3] (Fig. 1, A). At higher concentrations of chloride, separation is poor and the sulphate peak is distorted.[4] Hence, the object of this work was to detect reliably 0.5 mg l^{-1} of sulphate in 10 g l^{-1} of chloride in order

that 2–3 mg l^{-1} of sulphate could be detected in oil reservoir formation waters with much higher sodium chloride contents. This is the natural level occurring in many such waters in the UK.

Of other common anions that could appear in the chromatogram, such as NO_2^-, NO_3^-, PO_4^{3-} and Br^-, only Br^- is at a significant level (30–100 mg l^{-1}) in formation water. All of these ions are well separated from sulphate and hence do not interfere.

When an initial attempt was made to determine such levels of sulphate in strong brine solutions a difficulty was encountered in the form of a base-line disturbance at the position of the sulphate peak. For example, Fig. 1, B, shows a chromatogram of 10 g l^{-1} of chloride (as sodium chloride) with no added sulphate. It has a narrow positive peak followed by a narrow negative peak exactly where the sulphate peak should be. This makes the detection and quantification of less than 2 mg l^{-1} of sulphate very difficult.

An investigation into this problem is described here. The cause and a method of preventing it are given. The detection limit subsequently achieved was 0.5 mg l^{-1} of sulphate in a 10 g l^{-1} chloride solution.

Experimental

Chromatograms were obtained using a Dionex Model 2000i ion chromatograph with an integral conductivity detector and a nominal 5-µl sample loop. Separations were achieved using Dionex HPIC AS3 or AS4A columns and a flow-rate of 2 ml min^{-1} of the eluent mixtures 0.003 M NaHCO$_3$ - 0.0024 M Na$_2$CO$_3$ or 0.00075 M NaHCO$_3$ - 0.0020 M Na$_2$CO$_3$, respectively. The anion suppressor was a 250 × 6 mm i.d. column. Dionex fibre and micromembrane suppressors were also used.

Sodium chloride and sodium carbonate were of Aristar grade (BDH); the other reagents were of analytical-reagent grade. All the solutions were prepared in water of conductivity 6–7 µS m^{-1} obtained from a Milli-Q reverse osmosis - ion-exchange system (Millipore).

When required a column (250 × 9 mm i.d.) of Amberlite IRA-400 strong anion-exchange resin (BDH) was positioned between the eluent reservoir and the pump, as shown in Fig. 2. It was prepared from 20–50 mesh chloride-form resin. Before use the column was treated with 1 M sodium hydroxide
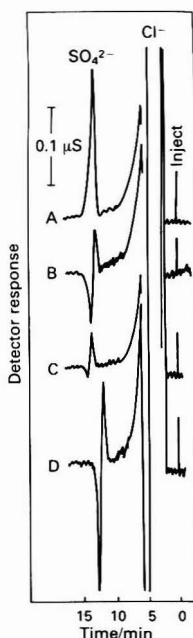
Fig. 1. Chromatograms obtained using an AS3 separator column. A, Sulphate (5 mg l^{-1}) in chloride (10 g l^{-1}); B, chloride alone (10 g l^{-1}); C, sulphate (1 mg l^{-1}) in chloride (10 g l^{-1}); and D, chloride (10 g l^{-1}) with sulphate (0.1 mg l^{-1}) added to the eluent
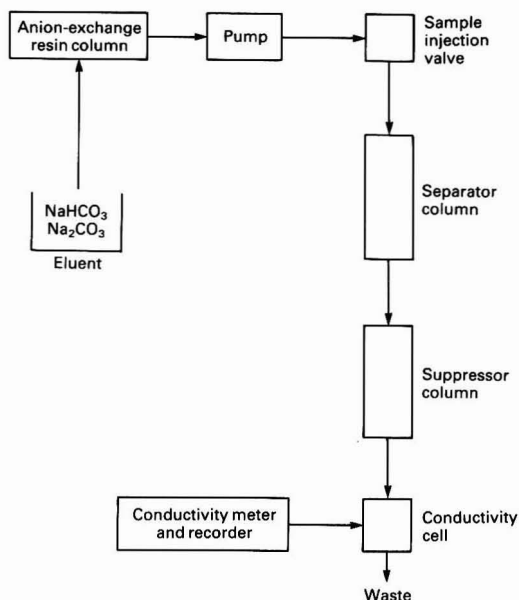
Fig. 2. Schematic diagram of the ion chromatography system for anion determination

Fig. 3. Chromatograms obtained using an AS4A separator column with 0.1 mg l^{-1} of oxalate added to the eluent. A, Oxalate (10 mg l^{-1}) in chloride solution (10 g l^{-1}); and B, chloride solution (10 g l^{-1})

solution at a flow-rate of 4 ml min^{-1} for 30 min, then similarly with 1.0 M sodium carbonate solution. It was subsequently equilibrated with the eluent off-line for about 2 h.

Procedure

For the analysis of brine samples the apparatus shown in Fig. 2 was assembled using either of the column - eluent combinations given above. A calibration graph was prepared by injecting the standards (0.5–5 mg l^{-1}) in sodium chloride solution (10 g l^{-1}) on to the column. The area of the sulphate peak was measured. The samples were diluted to contain between 5 and 10 g l^{-1} of sodium chloride before they were injected.

Results and Discussion

A chromatogram of 5 mg l^{-1} of sulphate in a solution of 10 g l^{-1} of chloride is shown in Fig. 1, A. The sulphate peak is clear of the "tail" of the chloride peak and there is apparently no reason why 0.5 mg l^{-1} of sulphate should not be detected. Only 5 µl of solution were injected so as to avoid overloading the column, which would have resulted in distorted peaks in the chromatogram. Both the AS3 and AS4A separator columns gave similar separations and had, apparently, similar capacities. However, when a 10 g l^{-1} solution of chloride, to which no sulphate had been added, was injected the chromatogram shown in Fig. 1, B was obtained. A narrow positive peak followed by a similar sized negative peak occurred at the sulphate position. A chromatogram for the separation of 1 mg l^{-1} of sulphate in a solution of 10 g l^{-1} of chloride, Fig. 1, C, shows that the negative part of the disturbance has almost disappeared whereas the positive part remains. This clearly makes the detection and quantification of sulphate impossible at this level.

By changing the chloride concentration it was found that the base-line disturbance was absent at chloride concentrations of 6 g l^{-1} and lower and present at concentrations of 7 g l^{-1} and higher. The magnitude of the effect increased with increasing chloride concentration. The effect occurred whichever suppressor was used. It was also noted that the magnitude changed with each batch of eluent. Because of this and
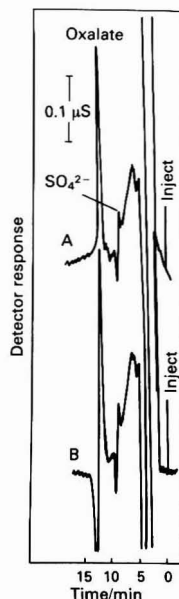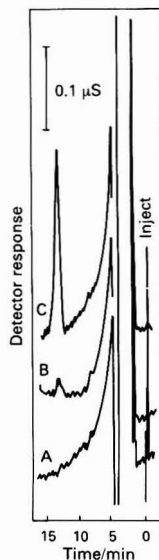
Fig. 4. Determination of sulphate in chloride solution (10 g l^{-1}). Sulphate in the eluent for the AS3 separator column is removed by in-line ion exchange. Sulphate concentration: A, 0; B, 0.5; and C, 5.0 mg l^{-1}

because the base-line disturbance always occurred at the sulphate position it was suspected that the cause of the effect was sulphate contamination of the eluent.

This possibility was investigated by adding 0.1 mg l^{-1} of sulphate to the mobile phase. When a 10 g l^{-1} chloride solution was injected on to the column much larger positive and negative peaks were observed at the sulphate position, as shown in Fig. 1, D, than had originally been obtained.

Further proof was obtained by showing that a similar effect could be produced at the elution volume of another strongly

retained ion by adding that ion to the eluent. Oxalate at 0.1 mg l^{-1} was added to the mobile phase. When a 10 g l^{-1} chloride solution was injected on to the column the chromatogram (Fig. 3, B) showed large positive and negative peaks at both the oxalate and sulphate elution volumes, the sulphate peaks being caused by the "natural" contamination of the eluent.

From the magnitude of the effect shown in Fig. 1, A, it is apparent that sulphate in the eluent at the $0.01–0.02 \text{ mg l}^{-1}$ level is sufficient to cause a base-line disturbance. To remove this contamination a column of high-capacity strong ion-exchange resin (Amberlite IRA-400) in the carbonate form was connected in-line between the eluent reservoir and the pump (Fig. 2). Sulphate from the eluent is very strongly retained on this column. Fig. 4, A shows that this column eliminated the problem and lowered the detection limit to 0.5 mg l^{-1} of sulphate in 10 g l^{-1} of chloride as shown in Fig. 4, B. Linear calibration graphs were obtained in the range $0.5–5 \text{ mg l}^{-1}$ of sulphate in a 10 g l^{-1} chloride solution using either peak-height or peak-area measurement. The effectiveness of this column is further proof that contamination of the eluent was the cause of the original problem. The ion-exchange column required re-generation after several days of continuous use.

A possible explanation of this effect is as follows. If sulphate is present as a contaminant in the mobile phase then the separator column will not be wholly in the carbonate - hydrogen carbonate form, but will be partially in the sulphate form. It is believed that when a large amount of chloride ion is injected on to the column some sulphate is displaced from the column into the mobile phase. The sulphate moves a short distance down the column with the chloride until the latter becomes diluted and no longer causes the effect. The displaced sulphate leaves a void in the sulphate concentration in the column. Both the displaced sulphate and the void pass through the column and appear at the sulphate position in the chromatogram as a positive peak overlapping a similar sized negative peak. The negative peak arises owing to a decrease in the level of sulphate in the eluent. Calculations show that when there is 0.01 mg l^{-1} of sulphate in the eluent it contributes about 0.2 μS to the background conductance of 16 μS. The peak height given by 5 mg l^{-1} of sulphate is also about 0.2 μS and hence the negative peaks can be accommodated within the sulphate background.

References

1. "Annual Book of ASTM Standards," American Society for Testing and Materials, Philadelphia, 1981, Part 31.
2. Small, H., Stevens, T. S., and Bauman, W. C., *Anal. Chem.*, 1975, **47**, 1801.
3. "Ion Chromatography Systems Applications Note 3," Dionex Corporation, Sunnyvale, CA, 1978.
4. Bynum, M. A. O., Tyree, S. Y., and Weiser, W. E., *Anal. Chem.*, 1981, **53**, 1935.

Determination of Water in Acetic and Formic Acids by the Proton Isoconcentration Technique Using the Addition Method

Mohamed Rashid Omar Karim and Thuraya Mohamed Karadaghi
Chemistry Department, College of Science, Salahaddin University, Arbil, Iraq

Two analytical procedures have been used for the determination of water in acetic and formic acids under proton isoconcentration conditions, based on a large and systematic change in the potential measurements on addition of 0–2% *m/m* of water to a mixture of propylene carbonate and 10% *V/V* acetic or formic acid containing 2×10^{-3} M perchloric acid in glacial acetic acid as a background electrolyte, using a combination pH glass electrode. The first procedure was used directly for the determination of water in the range 0–10% *m/m* and the second for the range 10–100% *m/m*. In the second procedure the dilute acids were concentrated by mixing them with dry mixtures of propylene carbonate and acetic or formic acid. The method is fast, accurate and reproducible.

Keywords: *Water determination; acetic and formic acids; addition method - proton isoconcentration technique; direct potentiometry; combination pH glass electrode*

The application of direct potentiometry to the determination of residual water in organic solvents using a pH glass electrode under proton isoconcentration conditions was first reported in 1977 independently by Kakabadse[1] and Schwabe and Queck.[2] This technique was subsequently applied to various solvents as a batch method[3-9,10] and recently in on-line monitoring.[11] The addition method in the proton isoconcentration technique (PICT) has recently been employed for the determination of water in organic solvents.[9]

In this work the addition technique was applied to the direct potentiometric determination of residual water in a mixture of propylene carbonate and 10% *V/V* acetic or formic acid under proton isoconcentration conditions and was used for the determination of water in acetic or formic acid directly in the concentration range 0–10% *m/m* and indirectly over the range 10–100% *m/m*, using a combination pH glass electrode.

Experimental

Reagents

The organic solvents were obtained from Fluka and were dried as described elsewhere.[12-14] The water contents after drying, as determined by Karl Fischer titration,[15] were 0.008, 0.01 and 0.05% *m/m* in propylene carbonate, acetic acid and formic acid, respectively. BDH laboratory-reagent grade perchloric acid, dissolved in glacial acetic acid (0.1 M in perchloric acid) and containing 0.05% *m/m* of water, was used as a stock solution.

Apparatus

Measurements were made on magnetically stirred solutions at $25 \pm 0.1\,^{\circ}$C using an Orion Model 811 digital pH - millivolt meter with a potential range of ± 1000 mV and a discrimination of ± 0.1 mV. A Hewlett-Packard 9862 calculator - plotter was used for drawing the graphs. An Orion 910-100 combination pH glass electrode was used, with a silver - silver chloride reference electrode and a saturated solution of lithium chloride in acetic acid as the electrolyte. A Schott Geräte TR 156 automatic titrator was used for the addition of water.

Preparation of Calibration Graphs

Procedure I, for the determination of water in acetic or formic acid in the range 0–10% m/m

A dried two-necked round-bottomed flask (100 ml) fitted with a combination pH glass electrode was charged with 50 ml of a dry mixture consisting of 5 ml of acetic or formic acid, 44 ml of propylene carbonate and 1 ml of perchloric acid in glacial acetic acid. Known increments of 0–1 ml of water were added using the automatic titrator and the potential was recorded immediately after each addition in a dry-box under a blanket of dry nitrogen to prevent absorption of atmospheric moisture. The potential was plotted against percentage of water. For the determination of water in acetic or formic acid, 5 ml of the sample were added with a dried pipette to a dried 50-ml calibrated flask containing 1 ml of 0.1 M perchloric acid in glacial acetic acid and the solution was diluted to the mark with dry propylene carbonate. The potential of this solution was measured after 5 min. The percentage of water in the sample was obtained directly from the calibration graph.

Procedure II, for the determination of water in acetic or formic acid in the range 10–100% m/m

A 1-ml volume of the sample was added with a dried pipette to 50 ml of a dry mixture, prepared as described under *Procedure I*, and the potential of this solution was measured after 5 min. The percentage of water in the mixture was obtained from the calibration graph and the mass of water in the sample was calculated by considering the dilutions involved.

Results and Discussion

The changes in the cell potentials (ΔE) on addition of 0–2% *m/m* of water to acetic or formic acid in the presence of 2×10^{-3} M perchloric acid in glacial acetic acid, using a combination pH glass electrode, were 60.0 and 88.0 mV, respectively (Table 1). However, this change was not large enough for an accurate determination of the residual water in these acids. A

Table 1. Change in potential, ΔE, and standard deviation ($n = 7$) for the addition of 0–2% *m/m* of water to organic solvents containing 2×10^{-3} M perchloric acid in glacial acetic acid, using an Orion 910-100 combination pH glass electrode with LiCl in acetic acid as the electrolyte

Solvent	Water concentration, % *m/m*	Mean ΔE/mV	Standard deviation/ mV
Propylene carbonate	0.20	330.2	0.89
Acetic acid	0.20	60.1	1.03
Formic acid	0.20	88.2	1.23
Propylene carbonate + 10% *V/V* acetic acid	0.20	290.3	0.95
Propylene carbonate + 10% *V/V* formic acid	0.20	305.1	1.06
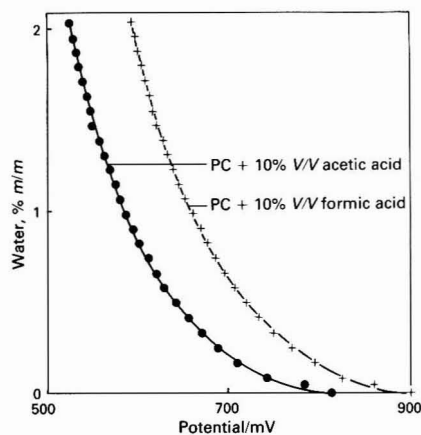
Fig. 1. Calibration graphs showing the change in potential on addition of 0–2% m/m of water to a mixture of 10% V/V acetic or formic acid with propylene carbonate containing 2×10^{-3} M perchloric acid in glacial acetic acid, using an Orion 910–100 combination pH glass electrode with a saturated solution of LiCl in acetic acid as the electrolyte

large and systematic change in the cell potential was observed on addition of 0–2% m/m of water to a mixture of 10% V/V acetic or formic acid in propylene carbonate containing 2×10^{-3} M perchloric acid in glacial acetic acid, using a combination pH glass electrode (Table 1 and Fig. 1). There may be several reasons for the large and systematic change in the cell potentials observed at high solvent concentrations for small changes in the water content.[5–7,10] The relevant experimental parameters in this work are the nature of the solvent, the nature of the acid and its concentration and the type of pH glass and reference electrodes used.

Effect of Solvent

Propylene carbonate was chosen as the solvent for mixing with acetic or formic acid to prepare the calibration graphs, owing to the higher ΔE values and lower standard deviations[9] obtained. Also, propylene carbonate is liquid over a convenient range of temperatures and is easily purified by vacuum distillation.[16] It can be seen from Table 1 that the ΔE value for formic acid is higher than that for acetic acid.[17]

Effect of Acid

In this work 2×10^{-3} M perchloric acid in glacial acetic acid was used as the background electrolyte. The interference of acetic or formic acid in the determination of water was studied by adding 1 ml of dry acetic or formic acid to a dry mixture of propylene carbonate and 10% V/V acetic or formic acid in the presence of 2×10^{-3} M perchloric acid in glacial acetic acid, as described under *Procedure II*. There was no change in the potential although an increase of 2 mV was observed when 1 ml of dry formic acid was added to pure, dry propylene carbonate containing 2×10^{-3} M perchloric acid in glacial acetic acid.

Effect of pH Glass and Reference Electrodes

The Orion 910-100 combination pH glass electrode was conditioned for 1 h in propylene carbonate containing 2×10^{-3} M perchloric acid in glacial acetic acid.[9] The reference electrode was silver - silver chloride with a saturated solution of lithium chloride in acetic acid as the internal solution.[8,9,16] It was found that leakage of water from the reference electrode into the standard solutions was negligible.[8]

Table 2. Accuracy of the determination of water by direct potentiometry for the addition of 0–2% m/m of water to a solution of 10% V/V acetic or formic acid in propylene carbonate containing 2×10^{-3} M perchloric acid in glacial acetic acid, using an Orion 910–100 combination pH glass electrode with a saturated solution of LiCl in acetic acid as the electrolyte

| Solvent | Water found, % m/m | | | Relative error, % | |
	Accurate dilution	Addition technique	Procedure	Addition technique	Karl Fischer
Acetic acid	70.02	70.62	II	+0.86	+1.20
	50.04	48.99	II	−2.10	+0.50
	25.08	24.64	II	−1.75	+2.62
	10.01	10.29	I	+2.80	+2.15
	5.43	5.61	I	+3.30	+5.61
	1.02	1.04	I	+1.96	+3.14
Formic acid	70.03	72.27	II	+3.20	—
	50.04	51.04	II	+2.00	—
	25.05	24.45	II	−2.40	—
	12.06	11.69	II	−3.10	—
	6.32	6.09	I	−3.64	—
	1.04	1.08	I	+3.85	—
	0.51	0.53	I	+3.92	—

Table 3. Limit of detection of water in acetic and formic acids by direct potentiometry for the addition of 0–2% m/m of water to a mixture of 10% V/V acetic or formic acid in propylene carbonate containing 2×10^{-3} M perchloric acid in glacial acetic acid, using an Orion 910-100 combination pH glass electrode

Solvent	Water in solvent, % m/m	Sensitivity/ mg kg^{-1} per 2 mV
Acetic acid ..	0.01	50
	0.50	92
Formic acid ..	0.05	38
	0.50	56

Accuracy of Water Determination

The results obtained for samples containing various amounts of water are shown in Table 2. In general, the accuracy of the method is satisfactory and compares favourably with that achieved by Karl Fischer titration. The use of the Karl Fischer titration technique for the determination of water in formic acid was not successful; indistinct end-points were observed during the titrations owing to a rapid reaction between formic acid and the reagent.[15] Karl Fischer titration could be used for the determination of water in acetic acid, although the end-point was not particularly stable.[8]

Limit of Detection of Water in Acetic and Formic Acids

The detection limit is based on the amount of added water that is necessary to produce a change in potential of 2 mV, *i.e.*, corresponding to approximately twice the standard deviation (Table 1). It can be seen from Table 3 that the sensitivity of the pH glass electrode to changes in the water concentration depends on the nature of the solvent and the amount of residual water in the solvent. The detection limit for water in formic acid was lower than that for acetic acid.

Conclusions

The proposed method can be used for the determination of water in acetic and formic acids. The method is characterised by accuracy and simplicity of operation and compares favourably with the Karl Fischer method. The main advantage of employing the addition method in the PICT for the determination of water in acetic or formic acid is that the time required for the analysis is reduced significantly.

References

1. Kakabadse, G. J., *Editor,* "Solvents—The Neglected Parameter," UMIST, Manchester, 1977, p. 178.
2. Schwabe, K., and Queck, C., *Z. Chem.,* 1977, **17**, 304.
3. Kakabadse, G. J., Abdulahed Maleila, H., Khayat, M. N., Tassopoulos, G., and Vahdati, A., *Analyst,* 1978, **103**, 1046.
4. Karim, M. R. O., *PhD Thesis,* University of Manchester, 1980.
5. Kakabadse, G. J., *Ion-Sel. Electrode Rev.,* 1981, **3**, 160.
6. Karim, M. R. O., *Analyst,* 1986, **111**, 1211.
7. Karim, M. R. O., and Hussain, M. A., *Analyst,* 1987, **112**, 163.
8. Karim, M. R. O., *Analyst,* 1987, **112**, 1369.
9. Karim, M. R. O., and Karadaghi, Th. M., *Analyst,* 1988, **113**, 843.
10. Nichugovskii, G. F., and Vasil'eva, V. S., *J. Anal. Chem. USSR,* 1987, **42**, 139.
11. Kakabadse, G. J., Olatoye, E. O., Perry, R., Tipping, A. E., Hall, T. F., and Waterfall, R. C., *Analyst,* 1988, **113**, 337.
12. Fujinaga, T., and Izutusu, K., *Pure Appl. Chem.,* 1971, **27**, 275.
13. Keese, R., Muller, P. K., and Toube, T. P., "Fundamentals of Preparative Organic Chemistry," Ellis Horwood, Chichester, 1982, p. 126.
14. Wehman, T. C., and Popov, A. I., *J. Phys. Chem.,* 1968, **72**, 4031.
15. Scholz, E., "Karl Fischer Titration; Determination of Water," Springer-Verlag, Berlin, 1984, p. 79.
16. Covington, A. K., and Dickinson, T., "Physical Chemistry of Organic Solvent Systems," Plenum Press, London, 1973, p. 11.
17. Ivanovskaya, I. S., Gessen, I. V., and Shul'ts, M. M., *Sov. Electrochem.,* 1968, **4**, 1172.

Inverse Spectrophotometric Detection in Flow Injection Analysis: Determination of Nitrite Using Cerium(IV) as the Chromophore

Thomas P. Lynch

BP Research Centre, Sunbury-on-Thames, Middlesex TW16 7LN, UK

The application of inverse spectrophotometric detection in flow injection is introduced and its potential illustrated by a possible application to the determination of nitrite by its reaction with cerium(IV).

A single manifold was employed with two reagent concentrations, namely 10 and 20 g l^{-1} of cerium(IV) ammonium sulphate in 0.5 M sulphuric acid. The working ranges are 10–200 and 200–1000 mg l^{-1}, respectively, for a *ca.* 30-μl sample injection and the sampling rate is between 60 and 75 injections per hour. The 200–1000 mg l^{-1} system was applied to the determination of nitrite in culture media and the results were compared with those given by a manual diazotisation method.

The same manifold with a smaller sample loop was also employed to demonstrate the extension of the technique to provide chemical back-off. A working range of approximately 2500 mg l^{-1} of nitrite can be covered anywhere between 1000 and 9000 mg l^{-1} simply by selection of a suitable reagent concentration.

Keywords: *Cerium(IV); chemical back-off; flow injection; inverse spectrophotometry; nitrite determination*

Spectrophotometry (UV and visible) was employed in over 30% of the flow injection methods listed in the Tecator 1974–1984 Bibliography[1] and it is the most widely applied detection system in the technique. In almost all of the published procedures the absorbance of the product of a reaction is measured. This paper describes an alternative approach, which we call inverse spectrophotometry, where the decrease in the absorbance of a reagent due to its reaction with the sample is measured. This highlights the advantages that can be gained over conventional spectrophotometric detection. The concept has been described briefly for two applications,[2] both of which employ cerium(IV) as the reagent chromophore.

This paper describes one of these systems, namely the determination of nitrite, and introduces the concept of chemical back-off. The main feature of this system is the ability to analyse high sample concentrations in a simple manifold without excessive prior dilution. Previous flow injection methods for nitrite are mostly based on the diazo spectrophotometric method[3,4] or on voltammetric detection.[5,6]

A method was required for the analysis of a large number of biological culture media that contained between 2 and 3 g l^{-1} of nitrite. Early efforts directed at desensitising the diazo methods (typical upper limit 0.1 g l^{-1}) met with minimal success and it was therefore decided to consider alternative chemistries that did not have the inherent sensitivity of the diazo reaction.

A classical titrimetric method for the determination of nitrite utilises the redox reaction between nitrite and cerium(IV):

$$2Ce^{IV} + NO_2^- + H_2O \rightarrow 2Ce^{III} + NO_3^- + 2H^+$$
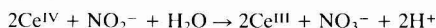
i.e.,

coloured reactant → colourless product

The application of this chemistry using inverse spectrophotometric detection is described for the determination of nitrite. The concept of chemical back-off is also introduced and advantages and possible applications of the technique are discussed.

Experimental

Reagents and Solutions

All chemicals were of analytical-reagent grade and de-ionised, distilled water was used throughout. Nitrite standards were prepared by dilution of an aqueous stock solution containing 14.996 g l^{-1} of sodium nitrite (10 000 mg l^{-1} of nitrite), which was standardised by titration with standard potassium permanganate solution.

Several cerium reagent concentrations were employed, namely 10, 20, 30, 40 and 50 g l^{-1} solutions of cerium(IV) ammonium sulphate in 0.5 M sulphuric acid.

Apparatus

A Tecator 5020 flow injection analyser was employed with a Cecil CE373 visible spectrophotometer equipped with a Hellma flow cell. The manifold was constructed using 0.8 mm i.d. tubing and an Altex micro-plumbing system (Anachem). Peak heights were recorded using both a chart recorder and the measurement facility in the Tecator instrument. Calibration data and repeatability statistics were obtained using a DEC professional microcomputer and a VG Lab Systems statistics software package.

Flow Diagram

A flow diagram of the system is shown in Fig. 1. Samples (30 μl) were injected into the carrier stream of de-ionised water prior to merging with the cerium reagent.

Results and Discussion

Inverse Spectrophotometry

The normal procedure when attempting to develop a spectrophotometric flow injection (FI) method is to produce a coloured product. For example, in the diazotisation reaction for nitrite a red product is produced by a two-step reaction. Therefore, in a conventional spectrophotometric flow injection method the base line is at zero absorbance and sample
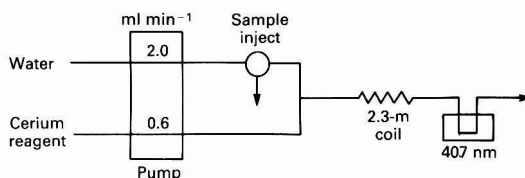
Fig. 1. Manifold for the determination of nitrite
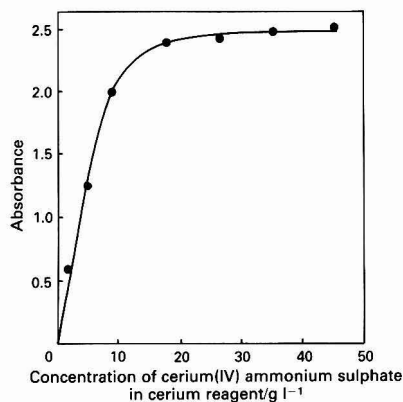
Fig. 2. Concentration *versus* absorbance graph for cerium(IV) ammonium sulphate

Fig. 3. Calibration graph for working range 200–1000 mg l^{-1} of nitrite

Table 1. Comparison of results obtained for the determination of nitrite in four culture media samples by the cerium flow injection method and a manual diazo method[7]

Sample No.	Concentration of sodium nitrite, % m/V	
	By diazo method	By cerium FIA
1	0.27	0.28
2	0.28	0.27
3	0.30	0.29
4	0.28	0.29

responses result in an increase in absorbance. In an inverse spectrophotometric method the base-line absorbance is positive and sample responses result in a decrease in absorbance.

The manifold shown in Fig. 1 was set up and the detector zeroed with only water flowing in the cerium reagent stream. Various concentrations of cerium reagent were then used and the absorbance base-line value was determined. The resulting graph of absorbance *versus* reagent concentration, shown in Fig. 2, is a typical Beer's law plot. Initial work was carried out, as in conventional spectrophotometry, on the linear part of this plot. However, it was soon realised that the plateau region of the plot can be employed in a unique way and this led to the chemical back-off concept.

Working Range 10–200 mg l^{-1} of Nitrite

The working range was covered using the manifold shown in Fig. 1 with a reagent containing 10 g l^{-1} of cerium(IV) ammonium sulphate. The best straight line through the origin of a plot of nitrite concentration (0–200 mg l^{-1}) *versus* peak height (absorbance change) gave a slope of 4.19×10^{-3} and a correlation coefficient of 0.9999.

Repeated injections ($n = 30$) of a 100 mg l^{-1} solution gave a 95% confidence interval for the mean peak height of ±0.5% relative. The sampling rate was 75 injections per hour.

The 10 g l^{-1} cerium(IV) ammonium sulphate reagent gives a base-line absorbance value of 2.12 (Fig. 2). This absorbance occurs just as the Beer's law plot begins to deviate from linearity and it was decided to investigate the possibility of using a stronger reagent to extend the high concentration working range. A reagent concentration of 20 g l^{-1} was chosen as this approximately corresponds to the beginning of the plateau on the Beer's law plot.

Working Range 200–1000 mg l^{-1} of Nitrite

This working range was covered using the 20 g l^{-1} reagent with the manifold shown in Fig. 1. A graph of nitrite concentration (200–1000 mg l^{-1}) *versus* peak height (absorbance change) was non-linear (Fig. 3) but a fourth-degree polynomial regression curve could be fitted with a correlation coefficient of better than 0.9999.

Repeated injections ($n = 30$) of a 500 mg l^{-1} solution gave a 95% confidence interval for the mean peak height of ±0.3% relative. The sampling rate was 60 injections per hour.

This system met the criteria we had set to solve our immediate problem, which was the rapid screening of nitrite in a large batch of culture media samples. The samples (1 ml) were dispensed into an autosampler cup together with 2 ml of

water as diluent and then injected into the system. A test result was taken as the mean of triplicate injections. A number of samples were analysed by a manual diazotisation procedure[7] and a comparison of the results obtained for four of these is given in Table 1.

The 20 g l^{-1} reagent concentration was chosen as it corresponded to the beginning of the plateau on the Beer's law plot. However, it soon became apparent that unlike conventional spectrophotometric methods, inverse spectrophotometry could make use of solutions with absorbances on the plateau region and this led to the concept of chemical back-off.

Chemical Back-off

In the work with the 20 g l^{-1} cerium(IV) ammonium sulphate reagent, the calibration graph flattened out at nitrite concentrations less than 200 p.p.m. This corresponds to the plateau of the Beer's law plot for the cerium reagent (Fig. 2), *i.e.*, the injection of samples with less than 200 p.p.m. of nitrite fails to consume enough reagent to move off the plateau region. Hence in effect the working calibration range has been backed-off by *ca.* 200 mg l^{-1} and it should be possible to extend the back-off by moving further along the plateau, *i.e.*, using a more concentrated cerium reagent.

Several experiments were carried out using increasing cerium reagent concentrations. The original manifold (Fig. 1) was employed but with a smaller sample loop (*ca.* 15 µl) and the plots in Fig. 4 show the working ranges for the various reagent concentrations. Each reagent covers a working range of approximately 2500 mg l^{-1} and the analyst could cover this range with a starting value of anything between 0 and 7000 mg l^{-1} using a single manifold and the appropriate reagents, and the calibration graphs could be adequately described by computer-aided polynomial regression. The obvious application of this technique is in the analysis of high concentrations
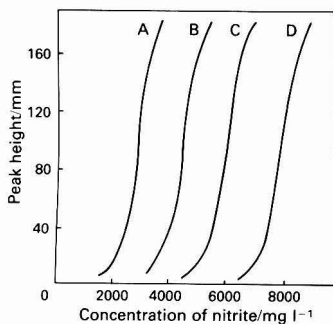
Fig. 4. Working ranges for various cerium reagent concentrations: A, 20; B, 30; C, 40; and D, 50 g l^{-1}

with a simple flow injection system. This could be particularly useful in a process control situation where product or reactant concentrations are more likely to be at the percentage rather than the parts per million level and it may be necessary to maintain levels within a confined concentration range (*e.g.*, product specification).

However, another potential application is in situations where the analyst is concerned with obtaining the greatest accuracy and precision possible, and does not require a large working range. Consider, for example, a sample that contains 6000 mg l^{-1} of nitrite and is analysed both by the method for the 10–200 mg l^{-1} range (10 g l^{-1} reagent), after prior dilution, and directly using the 40 g l^{-1} reagent as in Fig. 3.

Using the method for the 10–200 mg l^{-1} range a 60-fold dilution would bring the sample into the middle of the working range and a 0.01 change in absorbance would correspond to *ca.* 2.5 mg l^{-1} in the diluted solution or *ca.* 150 mg l^{-1} in the sample. Using the 40 g l^{-1} reagent, however, the same 0.01 change in absorbance at the 6000 mg l^{-1} level would be equivalent to *ca.* 5 mg l^{-1} in the sample, and therefore we have a potentially much more accurate method. The possibility of dilution errors is also removed with this system.

The method has also been shown to be precise in that a *ca.* 6000 mg l^{-1} nitrite solution was injected repeatedly ($n = 20$) into a 40 g l^{-1} system and a 95% confidence interval for the mean peak height of ±0.1% relative was obtained. However, problems were encountered in the application of the technique in that commercial spectrophotometers are not designed to work from full absorption to maximum transmission. The responses obtained for a particular manifold could be varied depending on the way in which the spectrophotometer had been set up. It would therefore be advisable to design a purpose-built detector, possibly based on the phototransducer type described by Sly *et al.*[8]

Conclusions

The application of inverse spectrophotometric detection in flow injection has been demonstrated and a simple manifold for the determination of nitrite at levels between 10 and 1000 mg l^{-1} has been described. The concept of chemical back-off has been introduced and its potential demonstrated for the determination of nitrite concentrations between 1000 and 9000 mg l^{-1}. Future possible applications have also been identified in the areas of process control and assay procedures.

References

1. "Flow Injection Analysis Bibliography 1974–1984," Tecator, 1985.
2. Lynch, T. P., Poster A17 presented at Flow Analysis III, Birmingham, UK, 1985.
3. Anderson, L., *Anal. Chim. Acta*, 1978, **110**, 123.
4. Gine, M. F., Bergamin, F⁰. H., Zagatto, E. A. G., and Reis, B. F., *Anal. Chim. Acta*, 1980, **114**, 191.
5. Fogg, A. G., Bsebsu, N. K., and Abdalla, M. A., *Analyst*, 1982, **107**, 1040.
6. Fogg, A. G., and Bsebsu, N. K., *Analyst*, 1984, **109**, 19.
7. "Vogel's Textbook of Quantitative Inorganic Analysis," Fourth Edition, Longman, London, 1978, p. 755.
8. Sly, T. J., Betteridge, D., Wibberley, D., and Porter, D. G., *J. Autom. Chem.*, 1982, **4**, 186.

Spectrophotometric Determination of Dissolved Oxygen in Water Through the Formation of an Argentocyanide Complex With Silver Sol*

Tarasankar Pal and Pradip K. Das

Department of Chemistry, Indian Institute of Technology, Kharagpur 721 302, India

A simple and sensitive method for the determination of dissolved oxygen (DO) in water has been developed, involving the dissolution of a gelatin-stabilised yellow silver sol formed with cyanide ion in the presence of oxygen. The coloured sol becomes colourless argentocyanide ion at the end-point. The reagent solution is fairly stable over the experimental time scale and the change in absorbance at a wavelength of 415 nm gives a measure of the concentration of dissolved oxygen in water. The effects of foreign ions on the determination indicated that the method is suitable for determining DO in both drinking and effluent waters and is free from interferences. It has the advantage of being capable of determining oxygen down to a concentration of 50 p.p.b. in water samples. The slope of the calibration graph is 0.206 A ml µg^{-1} [absorbance units per (microgram per millilitre)]. The molar absorptivity of the solution is 6.58×10^3 l mol^{-1} cm^{-1} with a relative standard deviation of 0.9%, a confidence limit (for 10 determinations) of 0.17 ± 0.001 p.p.m. and a Sandell sensitivity of 1.63×10^{-2} µg cm^{-2}.

Keywords: *Dissolved oxygen determination; silver sol; argentocyanide ion; spectrophotometry*

Several methods have been proposed for the determination of dissolved oxygen (DO) in water since the classical method of Winkler,[1] some simply being modifications of Winkler's method. Reviews detailing the theory and measurement of DO are available.[2-4] Caritt and Carpenter[2] concluded that the modified Winkler methods, although laborious and time consuming, are reliable. However, there are some serious drawbacks (*e.g.*, large sample volume, time consuming, interference from foreign ions) to both the original[1] and the modified methods.[4] In order to eliminate the drawbacks and to increase the sensitivity, several physico-chemical methods have been applied, the most significant of which are photometric determinations.[5-7] Direct photometric methods involve the oxidation of polyphenols and aminophenols or leuco-dyes[8-13] and the indirect methods involve oxidation of manganese(II) by the DO and the reaction of the resulting manganese(III) with iodide,[14] *o*-toluidine[15] or redox indicators.[16,17] In another set of methods, the manganese(III) is complexed with EDTA[18,19] or DCTA[20,21] and the resulting colour intensity is measured. Oxygen analysis by sensitive gas chromatography[22-27] has been applied not only to water, but also to other solvent systems. In this paper, a yellow silver sol is used as the colour reagent for the determination of trace amounts of dissolved oxygen in water by following the oxygen- and cyanide-dependent[28] decrease in intensity of the coloured silver sol at 415 nm. The method is best suited to the routine determination of DO in industrial and natural waters at concentrations down to 50 p.p.b. This is the first report of the determination of DO in water using a yellow silver sol in an alkaline medium.

Experimental

Reagents

All reagents used were of analytical-reagent grade and all solutions were prepared in distilled water. Silver nitrate (Glaxo) (0.84935 g) was dissolved in sufficient distilled water to make 500 ml of solution. Gelatin powder (Merck, 0.5 g) was dissolved in 100 ml of warm distilled water. To avoid microbial degradation of the gelatin solution, a fresh solution was prepared daily. Sodium cyanide (M and B, 0.12250 g) was

dissolved in 250 ml of distilled water and the solution was standardised with silver nitrate.[29] Silver sol was prepared by placing 5.0 ml of 10^{-2} M silver nitrate solution in a 400-ml beaker and adding 100 ml of 0.5% gelatin solution with stirring. The pH of the solution was adjusted to *ca.* 8 using 0.2 M NaOH solution. The silver - gelatin complex was completely reduced by *ca.* 0.02 g of ascorbic acid.[30] The sol solution was diluted to 250 ml with dilute NaOH to obtain a sol solution of *ca.* pH 8. The silver sol is very stable at room temperature and is best stored in amber bottles.[28] At $\lambda_{max.}$ (415 nm) the sol solution shows negligible scatter. Absorbance values are proportional to the sol concentration. For the purpose of degassing, oxygen-free nitrogen was used, which was further purified by passing it over hydrogen-reduced copper powder at 350 °C and through two consecutive solutions of alkaline pyrogallol.[7]

Apparatus

A Varian Cary-17D spectrophotometer was used for measuring absorbances in 1-cm quartz cells.

Procedure

Gelatin-stabilised silver sol and sodium cyanide were studied as reagents for the determination of DO. First, both reagents are degassed with oxygen-free nitrogen for 10–15 min. The nitrogen is passed through a long hypodermic needle and purged through a short needle, both inserted through the septum. Then appropriate aliquots of the two reagents (silver sol : sodium cyanide = 5 : 1 *V/V*) are placed in the spectrophotometer cell under a nitrogen atmosphere. Following injection of a sample, the spectrophotometer cell should be protected from oxygen (using stoppers) until the absorbance has been determined. Two types of water, air-saturated or oxygen-saturated water, may be used as samples to obtain a calibration graph. In our work air-saturated water was studied.

The concentration, *C*, of DO in the sample tube containing air-saturated water is calculated from the equation

$$C\,(\text{p.p.m.}) = C'\,(\text{p.p.m.}) \times \frac{v}{5000 + v} \quad .. \quad (1)$$

where C' is the concentration of oxygen in air-saturated water and v (µl) is the volume of air-saturated water injected into the spectrophotometer cell containing 5000 µl of reagent.

Air-saturated water at 25 °C contains 8.1 p.p.m. of oxygen; at other temperatures, the concentration of oxygen can be calculated from the equation [31]

$$C \text{ (p.p.m.)} = 14.161 - 0.3943t + 0.007714t^2 - 0.0000646t^3 \quad (2)$$

Once the Beer's law graph has been plotted, any value falling on, or near, the straight line can be used to derive the conversion factor (K), which can then be multiplied by the absorbance of the unknown sample of water to obtain the unknown DO value.[32] Thus,

$$\text{DO in unknown sample p.p.m. (µg ml}^{-1}) = K \times \text{corrected absorbance for the unknown sample} \quad \dots \quad (3)$$

where

$$K = \frac{\text{p.p.m. DO in the standard sample}}{\text{corrected absorbance for the standard sample}}$$

Depending on the make of spectrophotometer used, the corrected absorbance can be obtained automatically or manually by taking the difference between the absorbance of the blank and that of the unknown or standard samples. The reagents placed in the spectrophotometer cell in an atmosphere of purified nitrogen can be used as a blank. In this experiment the standard sample was taken as 120 µl of air-saturated water at 28.5 °C, *i.e.*, 170 p.p.m. of DO.

Results and Discussion

The reaction of the silver sol with cyanide may be represented as follows:

$$4Ag + 8CN^- + 2H_2O + O_2 \rightarrow 4[Ag(CN)_2]^- + 4OH^- \quad (4)$$
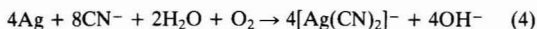
The silver sol solution was yellow when stabilised by the gelatin solution, but argentocyanide, which is readily formed in the alkaline medium, was colourless. Therefore, if silver sol and cyanide are taken in a 5 : 1 ratio in the concentration range mentioned earlier, the decrease in intensity of the yellow silver sol in the presence of oxygen is a measure of DO in the water. As the disappearance of the yellow colour is both DO- and cyanide-dependent, the sol concentrations in the test system should be sufficient for the final absorbance values to lie within the sensitive spectrophotometric region. The importance of the method is that as little as 50 p.p.b. of DO can be determined using a minimum volume (*ca.* 0.03 ml) of air-saturated water while observing the absorbance values.

Comparison With Other Methods

The methods described in the literature for the spectrophotometric determination of DO in water suffer from serious interferences from common ions, *e.g.* Fe^{2+}, Fe^{3+}, SO_3^{2-}, $S_2O_3^{2-}$ and NO_2^-.[3] The proposed method has advantages not only over Winkler's method but also over other spectrophotometric methods: (*a*) the method is simple to follow and less time consuming; (*b*) it can be used to monitor DO continuously if silver sol and cyanide ion are present in appreciable amounts; (*c*) as little as 50 p.p.b. of DO in water can be determined; and (*d*) the method does not suffer from interferences (see below).

Interferences

A brief investigation was made of the influence of common organic and inorganic compounds which usually interfere in

Table 1. Summary of interference effects on the determination of 170 p.p.b. of DO in air-saturated water

Ion	Salt	Concentration, p.p.m.	Effect on absorbance/A
Chloride	KCl	200	<0.01
Nitrate	$Ni(NO_3)_2$	250	0.01
Nitrite	$NaNO_2$	200	<0.01
Sulphate	$ZnSO_4$	250	<0.01
Hydrogen carbonate ..	$NaHCO_3$	200	<0.01
Sulphide	Na_2S	400	<0.01
Iron(II)	Mohr's salt	200	<0.01
Iron(III)	$Fe(NO_3)_3.9H_2O$	250	0.01
Manganese(II) ..	$Mn(OAc)_2$	200	<0.01
Iodide	KI	100	0.01
Carbonate ..	Na_2CO_3	200	<0.01
Phosphate ..	Na_3PO_4	200	<0.01
Calcium(II) ..	$Ca(NO_3)_2$	200	<0.01
Magnesium(II) ..	$MgSO_4$	200	<0.01
Persulphate ..	$K_2S_2O_8$	200	<0.01
Thiosulphate ..	$Na_2S_2O_3$	200	<0.01
Tartrate	Tartaric acid	350	<0.01

Table 2. Comparison of DO values obtained using Winkler's technique (A) and the proposed method (B)

Sample	Method	DO content*/ µg ml^{-1}	SD/µg ml^{-1}
Distilled water	A	7.92	0.20
	B	8.11	0.07
Water from the Ganges (pH 7.8, total dissolved solids 350 p.p.m., chloride 5.6 p.p.m.) ..	A	7.27	0.16
	B	7.35	0.01

$*n = 10$.

the determination of DO (see Table 1). The concentration of ions listed in Table 1 are those in the undiluted, air-saturated samples, 120 µl of which were injected into the spectrophotometric cell. The oxygen concentration was 170 p.p.b. Possible interferences not studied included hypochlorite, ozone and hydrogen peroxide, which are good oxidising agents.

Applications

The dissolved oxygen contents of several samples of water, *e.g.*, laboratory-distilled water and water from the Ganges (India), were determined by the standard method[1] and the proposed method. The results are given in Table 2.

References

1. Winkler, L. W., *Ber. Dtsch. Chem. Ges.*, 1888, **21**, 2843.
2. Caritt, D. E., and Carpenter, J. H., *J. Mar. Res.*, 1966, 286.
3. Degn, H., Balsiev, I., and Brook, R., *Editors*, "Measurement of Oxygen," Elsevier, Amsterdam, 1976.
4. Lindstrom, R. E., Patel, S. N., and Wilkinson, P. K., *J. Parent. Drug Assoc.*, January/February, 1980.
5. Fadrus, H., and Malý, J., *Analyst*, 1971, **96**, 591.
6. Brokenkow, W. W., and Clinc, J. D., *Limnol. Oceanogr.*, 1969, **14**, 450.
7. Duncan, A., Harriman, A., and Parter, G., *Anal. Chem.*, 1979, **51**, 2206.
8. Mackay, W. M., and Middleton, R. E., *J. Soc. Chem. Ind.*, London, 1898, **17**, 1127.
9. Tuve, R., *US Pat.*, 2 440 315, 27 April, 1948.
10. Hamlin, P. A., and Lambert, J. L., *Anal. Chem.*, 1971, **43**, 618.
11. Gilcreas, F. W., *J. Am. Water Works Assoc.*, 1935, **27**, 1166.
12. Winkler, L. W., *Z. Angew. Chem.*, 1916, **26**, 135.
13. Meyling, A. H., and Frank, G. H., *Analyst*, 1962, **87**, 60.

14. Hansen, W. J., and Pieters, H. H., *Anal. Chim. Acta*, 1948, **7**, 712.

15. McCrumb, F. R., and Kenny, W. R., *J. Am. Water Works Assoc.*, 1929, **21**, 400.

16. Banks, J., *Analyst*, 1959, **84**, 700.

17. Stones, W. F., *Chem. Ind. (London)*, 1957, 37.

18. De Corvalho, A. H., Calado, J. G., and Mowra, M. L., *Rev. Port. Quim.*, 1963, **5**, 15.

19. Rahim, S. A., and Mohamed, S. A., *Talanta*, 1978, **25**, 519.

20. Sastry, G. S., Hamm, R. E., and Pool, K. H., *Anal. Chem.*, 1969, **41**, 857.

21. Malaiyandi, M., and Sastri, V. S., *Talanta*, 1983, **30**, 983.

22. Elsey, P. G., *Anal. Chem.*, 1959, **31**, 869.

23. Natelson, S., and Stellate, R. L., *Anal. Chem.*, 1963, **35**, 847.

24. Weiss, R. F., and Craig, H., *Deep-Sea Res.*, 1973, **20**, 291.

25. Barbery, G., and Berube, Y., *Ind. Eng. Chem. Fundam.*, 1971, **10**, 632.

26. Swinnerton, J. W., Linnenbom, V. J., and Cheek, C. H., *Anal. Chem.*, 1962, **34**, 483.

27. Swinnerton, J. W., Linnenbom, V. J., and Cheek, C. H., *Anal. Chem.*, 1964, **36**, 1669.

28. Pal, T., Ganguly, A., and Maity, D. S., *Anal. Chem.*, 1986, **58**, 1564.

29. Vogel, A. I., "A Text Book of Quantitative Inorganic Analysis," Third Edition, Longmans, London, 1969, p. 272.

30. Pal, T., and Maity, D. S., *Anal. Lett.*, 1985, **18**(B9), 1131.

31. Siedel, A., *in* Linke, W. F., *Editor*, "Solubilities of Inorganic and Metal Organic Compounds." Volume II, Fourth Edition, Van Nostrand, New York, 1958, p. 1228.

32. Mohapatra, S. C., and Johnson, W. H., *Indian J. Technol.*, 1980, **18**, 219.

Analysis of Commercially Available Cheeses for the Migraine Inducer Tyramine by Thin-layer Chromatography and Spectrophotometry

Christine S. Evans, Sophie Gray and Nevcan O. Kazim
School of Biological Sciences, Thames Polytechnic, London SE18 6PF, UK

The amounts of tyramine in a variety of cheeses were measured using thin-layer chromatography and spectrophotometry. The largest concentrations were found in blue cheeses (up to 4200 µg g^{-1}), whereas soft cream cheeses did not contain measurable concentrations. Higher concentrations of tyramine were measured in cheeses that had a longer time of maturation in their preparation.

Keywords: *Tyramine; cheese, migraine inducer; thin-layer chromatography; spectrophotometry*

Tyramine in foods has been considered responsible for promoting attacks of dietary-induced migraine in susceptible subjects.[1] Cheese is commonly cited as a food to be avoided if such attacks are to be minimised, although few data are available as to the variation in tyramine content with the type of cheese.[2] Variations in amine concentrations are due to the action of microorganisms used in cheese production and the length of time of manufacture.[3] Horowitz *et al.*[4] examined nine types of cheese and found tyramine levels to vary from nil in cottage cheese to 1416 µg g^{-1} in New York State Cheddar. Other studies have shown variations in American and Canadian cheddars,[5,6] Danish Blue, American and Italian Parmesan,[6] South African cheeses[7] and Gruyère cheese,[8] but there is little information on the tyramine content of the many varieties of British manufactured cheeses. A much larger range of cheeses have become available commercially in the UK in recent years, with many international varieties commonplace in the diet, and the determination of tyramine in these products may be of interest to migraine sufferers. In this investigation a total of 30 varieties of cheese were analysed for tyramine, including cheese made from cow's, sheep's and goat's milk, which are readily available in supermarkets and delicatesson stores in the UK.

Experimental

Cheeses were obtained from various supermarkets and stores.

For the extraction of tyramine, 5 g of grated cheese were shaken with 10 ml of chloroform and 10 ml of dilute hydrochloric acid for 24 h. After leaving the emulsion to separate, the aqueous layer containing tyramine was removed. Residual tyramine in the chloroform layer was not detected, but a further extraction of the chloroform layer with acid was used routinely to ensure complete extraction.

Tyramine was separated from the aqueous extract by thin-layer chromatography on silica gel (Kieselguhr G; Merck) in butan-1-ol - glacial acetic acid - water (7.5 + 1.5 + 1.0). Standard samples of tyramine were chromatographed simultaneously, and tyramine in both standards and cheese extracts was identified on TLC plates by its R_F value (0.64) after spraying marker traces with Pauly's reagent. This reagent was prepared by mixing equal volumes of solution A, containing 4 g of sulphanilic acid, 40 ml of concentrated HCl and 400 ml of water, with solution B, containing 5% of sodium nitrite, before adding 2 volumes of 10% sodium carbonate solution.

Zones corresponding to the position of tyramine were eluted from the silica gel from both cheese samples and standard tyramine with 2 M ammonia solution, and quantified by their absorbance at 237 nm. A calibration graph for tyramine in the range 0–20 µg ml^{-1} of ammoniacal solution was prepared routinely under conditions identical with those used for the cheese samples. All cheese samples were assayed

with and without added tyramine (to the grated cheese on emulsification) and the recovery was measured as 96–101% of the added tyramine. Tyramine was measured in the cheese extracts derived from the grated cheese, which was considered representative of the whole cheese.

Noradrenaline was identified by its R_F value on TLC with butan-1-ol as solvent (0.22), and by co-chromatography with the authentic compound. Confirmation of both tyramine and noradrenaline data was made by HPLC of aqueous extracts of the cheeses after chloroform and acid extraction. A Shimadzu HPLC instrument was used with a column of Spherisorb C6 with 0.01 M orthophosphoric acid as solvent using UV detection at 280 nm.

Analysis by HPLC proved less reliable than the TLC - spectrophotometric method, with the recovery of added

Table 1. Determination of tyramine in cheeses

Type of cheese	Tyramine/ µg g^{-1}	Weeks to maturation
Cow's milk cheeses—		
Cottage cheese	ND*	
Quark (skimmed milk soft cheese)	ND	
Cream cheese	ND	
Curd cheese	ND	
Edam	216	5
Brie	240	2
Cheshire	278	3
Wensleydale	312	3
Leicester	312	11
Caerphilly	344	
Dutch Leiden	350	
Lancashire	360	3
Melbury	456	2
White Stilton	490	2
Processed cheddar	552	
Vegetarian cheddar	601	20
Derby	648	10
Mild cheddar	768	16
Lymeswold	787	
Swiss Emmental	864	20
Low-calorie cheddar (Shape)	912	10
Mature cheddar	1036	25
Italian gorgonzola	1248	
Fully matured cheddar	1440	32
Danish blue	3840	
Blue Stilton	4200	
Goat's milk cheeses—		
Saint Loup (goat's milk log)	518	
Saint Chevrier	618	
Fetta	1050	
Sheep's milk cheese—		
Roquefort	2270	

*Not detectable.

tyramine measured as 82–104%. Contaminating peaks in the samples were incompletely separated from the tyramine peak.

Results

The tyramine content of a wide range of cheeses is shown in Table 1. The highest amount of tyramine recorded was found in Blue Stilton, although all blue cheeses had considerably higher levels than non-blue varieties. Tyramine in cottage cheese, quark, cream cheese and curd cheese was below the level of sensitivity of the assay system used (1 µg g^{-1}). Information as to the length of time each type of cheese had been left to mature before distribution was supplied by J. Sainsburys, the English Country Cheese Council and Dairy Crest. In general, it was found that the longer the time of maturation of the non-blue cheeses the higher was the tyramine level, a correlation coefficient of 0.79 being found for those cheeses for which data were available. Three types of cheddar, mild, mature and fully mature, produced by the same manufacturer showed a correlation coefficient of 0.98 for tyramine content and time of maturation. Cheeses prepared from goat's milk all had a medium to high level of tyramine in comparison with non-blue cheeses prepared from cow's milk. Roquefort, a blue cheese made from sheep's milk, contained a high level of tyramine, 2270 µg g^{-1}, which was comparable to levels found in blue cheeses made from cow's milk.

Detection of other phenolic amines in the cheese samples showed that two of the cheeses tested contained an additional basic Pauly-positive component. This was present in both Leicester and Melbury varieties and was identified as noradrenaline (3,4-dihydroxyphenylethanolamine) on the basis of co-chromatography with the authentic compound using both TLC and HPLC techniques. Both cheeses contained less than 100 µg g^{-1} of this amine.

Discussion

This study has confirmed that different types of cheese contain different levels of tyramine. The highest levels were found in blue cheeses, to which a second mould is added in the processing of these products, whereas no tyramine was detected in the milder cottage and cream cheese products. The non-blue cheeses showed intermediate levels of tyramine which correlated with the length of time involved in their maturation, increasing amounts of tyramine being noted particularly in the cheddar cheeses which are produced as mild, mature and fully mature varieties. Two cheeses, Leicester and Melbury, also contained small amounts of a second phenolic amine, noradrenaline. It is likely that there could be an additive effect of the two amines in these cheeses in inducing attacks of dietary migraine, as they are structurally similar.

Although the causes of dietary-induced migraine have not been elucidated fully, tyramine has been implicated as a contributory factor. The avoidance of foods which are known to be high in tyramine can relieve both the intensity of migraine attacks and their frequency. Little information is available to the consumer about the chemical composition of foodstuffs and this study may allow susceptible migraine sufferers to moderate their intake of tyramine by selecting low-tyramine varieties of cheese in preference to those high in tyramine.

References

1. Hanington, E., in Smith, R., Editor, "Background to Migraine and Second Migraine Symposium," Heinemann, London, 1967, p. 10.
2. Smith, T. A., Food Chem., 1981, 6, 169.
3. Kosikowski, F. V., Sci. Am., 1985, 252, 66.
4. Horowitz, D., Lovenburg, W., Engleman, K., and Sjoerdsma, A., J. Am. Med. Assoc., 1964, 188, 1108.
5. Koehler, P. E., and Eitenmiller, R. R., J. Food Sci., 1978, 43, 1245.
6. Sen, N. P., J. Food Sci., 1969, 34, 22.
7. Kaplan, E. R., Sapeika, N., and Moodie, I. M., Analyst, 1974, 99, 565.
8. Price, K., and Smith, S. E., Lancet, 1971, 1, 130.

BOOK REVIEWS

British Pharmacopoeia 1988. Volumes I and II
British Pharmacopoeia Commission. Pp. xlii + 1575. H.M. Stationery Office. 1988. Price £130. ISBN 0 11 320837 5.

The British Pharmacopoeia has provided authoritative standards for the quality of substances and preparations used in medicine and pharmacy since 1864, and this new edition is the fourteenth.

Volume I includes medicinal and pharmaceutical substances and IR reference spectra (previously published separately). Volume II contains sections on formulated preparations, blood products, immunological products, radiopharmaceuticals and surgical materials. The 24 Appendices give procedures for testing compliance with the standards.

The Pharmacopoeia contains 2100 monographs, of which 495 are edited versions of those in the European Pharmacopoeia. Major changes have been made to the Formulated Preparations section in order to produce standards that apply to a range of products of similar type rather than to a product manufactured to a fixed formulation. This is intended to allow greater flexibility so that some auxiliary ingredients that may be undesirable in particular circumstances can be omitted. These modifications and other changes of emphasis have led to a substantially revised collection of General Notices.

New Monographs include human insulin, aprotinin, a proteolytic enzyme inhibitor, and aprotinin injection; the β-adrenoceptor antagonist atenolol and atenolol tablets; the oral hypoglycaemic agent glipizide and glipizide tablets; the tranquilliser temazepam; the antispasmodic agent mebeverine hydrochloride and mebeverine tablets; and, together with monographs for tablets, the hypotensive agent prazosin hydrochloride and the antacid hydrotalcite. Also included is a general monograph for pressurised inhalations which include a test for deposition of the emitted dose.

With a world-wide circulation of over 25 000, the BP is of immense importance to all those involved with pharmaceutical and medicinal chemistry and analysis, and this new edition is to be welcomed.

P. C. Weston

Methods of Enzymatic Analysis. Third Edition. Volume XI. Antigens and Antibodies 2
Edited by Jürgen Bergmeyer and Marianne Grassl. Pp. xxvi + 508. Verlag Chemie. 1986. Price DM315. ISBN 3 527 26501 X (VCH Verlagsgesellschaft); 0 895273 241 6 (VCH Publishers).

Enzymes were first described as labels in immunoassays for antigens and antibodies in 1971. Since then a large number of qualitative and quantitative enzyme immunoassays (EIA) for both large and small molecules have been described. This new volume in Bergmeyer's established "Methods in Enzymatic Analysis" series is devoted to EIAs for antigens and antibodies in chlamydial, bacterial, fungal and parasitic diseases. The assays mainly use either horseradish peroxidase or alkaline phosphatase as the label, but an application of β-galactosidase as a label for a monoclonal antibody against soybean mosaic virus is also presented. The description of the various EIA methods is thorough and includes background information, method design, equipment, reagents and solutions, international reference methods and standards, procedures and method validation. A particularly useful feature of this book is that several of the contributors give details of assay optimisation. For example, Karlsson and co-workers describe

the optimisation of antibody coating conditions (antibody concentration, pH) for polystyrene microtitre plates and incubation times for sample and conjugate in an EIA for *Salmonella* sp. antibody.

This book is an excellent source of practical information on selected EIAs and a useful resource for anyone designing new EIAs.

L. J. Kricka

Manual of Pesticide Residue Analysis. Volume 1
Edited by Hans-Peter Thier and Hans Zeumer. Pp. xvi + 433. VCH. 1987. Price DM128. ISBN 3 527 27010 8.

This is an excellent compendium, now published in very readable English, of pesticide residue methods, both compound specific and multi-residue, as practised in the Federal Republic of Germany. This first volume of an intended series concentrates mainly on well established methodology for the "older" pesticides, some of which, such as DDT, are not, or should not be, extensively used in Europe. Later volumes, it is stated, will deal with more recently introduced pesticides and, presumably, more recently developed methodology.

Part 1 of this volume is a clear and concise exposition of topics such as calibration, recovery, limits of detection and determination, the obtaining and preparation of samples and finally the presentation of reports of analyses. All these areas are so often misunderstood or badly executed even by experienced workers but are the bedrock of good residue analyses.

Part 2 describes a series of clean-up methods of wide utility and forms a useful basis for any analyst presented with a pesticide - substrate combination that has not been investigated before.

Part 3 describes specific methods for individual or small groups of related pesticides which are not amenable to inclusion in the multi-residue methods described in Part 4.

Twenty-one "multi-residue" methods are described in Part 4 but some of these, such as that limited to the phthalimide fungicides and that for surface residues of ethylene and propylene bisdithiocarbamate fungicides, are of such limited range that perhaps they would have been better included in Part 3 or even have had a separate section to themselves.

On the whole this is a book to be recommended to experienced workers for reference when moving into pesticide - substrate combinations not previously examined and to new entrants to the increasingly important field of pesticide residue monitoring.

D. F. Lee

Selective Sample Handling and Detection in High-performance Liquid Chromatography. Part A
Edited by R. W. Frei and K. Zech. *Journal of Chromatography Library, Volume* 39A. Pp. xii + 457. Elsevier. 1988. Price Dfl 240; $117. ISBN 0 444 42881 X.

With the continuing rapid advances in HPLC column technology it tends to be forgotten that the analytical column has two "ends," *viz.*, sample treatment and detection, which have lagged behind somewhat in their development. This book is a timely reminder that the scope of HPLC analysis can be considerably broadened by considering pre-column and post-column treatments. The important point is that many of these procedures can be carried out on-line.

The book, which is the first of a two-volume series, is divided into eight chapters. The first two chapters deal mainly with on-line sample handling techniques, one chapter concentrating on the determination of organic compounds in water

and the other on the determination of drugs and metabolites in biological matrices. Both chapters describe methods involving pre-column and valve switching arrangements incorporating solid - liquid extraction substrates. The third chapter continues the theme of using solid surface chemistry, pre- and post-column, for controlling selectivity and sensitivity, concentrating on the immobilisation of compounds on silica substrates. The range of substrates available, immobilisation techniques and the use of solid-phase reactors is fully discussed.

The remaining chapters concentrate mainly on detection processes. Chapter 4 deals with the derivatisation of organic analytes to enhance detection by UV - visible, luminescence or electrochemical measurement. In contrast, Chapters 5 and 6 are concerned with the latest developments in detector hardware. The first reviews photodiode array systems coupled to powerful microprocessors for data processing and manipulation and the second focuses on electrochemical detectors, in particular cell design and operation. Chapter 7 further develops the "pumpless" post-column reactor concept with a review of solid-phase reactors, although the main emphasis is on the source of band broadening. The final chapter rounds off the volume with a detailed critical review of the commercial instrumentation and applications available for post-column reaction detectors.

I fully endorse the Editors' comment that the book is a mine of information and will be a valuable companion not only to those who are already involved in a lot of HPLC work but also to those seeking alternative methods and needing an insight into the scope of HPLC methods. However, few of the examples involve inorganic applications. Perhaps this will have more emphasis in the second volume, although surprisingly no indication was given of the contents of Part B.

P. Jones

Laser Raman Spectroscopy. Analytical Applications
Halina Barańska, Anna Łabudzińska and Jacek Terpiński. Pp. 271. Ellis Horwood and PWN Polish Scientific Publishers. 1987. Price £38.50. ISBN 0 85312 339 X (Ellis Horwood); 0 470 20829 5 (Halsted Press).

For some years there has been an increasing need for a book that deals with the analytical applications of Raman spectroscopy, a technique which has a considerable diversity of analytical applications both in industry and academia. The title of this book might lead one to suppose that this shortfall has at last been rectified, but unfortunately this is not the case. The book contains nine chapters. Of these, the first three cover the theory and instrumentation and the last two cover fundamental concepts and a selected atlas of spectra (66

compounds in total). This leaves two chapters covering qualitative identification of organic and inorganic compounds (62 and 9 pp., respectively), one on quantitative analysis (17 pp.) and one covering selected applications (9 pp.). Hence, of the total 271 pp. of the book less than 100 pp. deal with analytical applications, and most of these relate to the qualitative analysis of organic compounds, which can normally be achieved more reliably, more rapidly and with greater sensitivity by other techniques. The main reason for the failure of the book to live up to its title is that it is a recent translation of a 1981 publication and contains no references later than 1979. As the analytical application of Raman spectroscopy is a rapidly developing area the value of the book to the analyst is minimal.

The theoretical background of the Raman effect and group theory are covered in a reasonably thorough manner and, together with the chapter on fundamental concepts, form the most useful part of the book, although they have relatively little relevance to the analytical aspects discussed. The deficiencies of the book first become apparent in Chapter 3, which deals with instrumentation and experimental techniques.

The use of dye lasers is scarcely mentioned and the use of pulsed laser systems not at all. Other omissions, mainly relating to the age of the book, are Fourier transform Raman spectroscopy, the use of fibre-optics, multi-channel detectors and combined double - single monochromator systems. All of the industrial spectrometers discussed are obsolete and several of the instrument manufacturers mentioned no longer manufacture Raman spectrometers. The problem of fluorescence is only dealt with in a perfunctory manner and no mention is made of the use of picosecond gating, the use of near infrared lasers or computer simulation in this context. The analytical value of surface-enhanced and resonance-enhanced Raman spectroscopy is not considered.

The organic identification chapter is adequate, but the classic work of Dollish, Fateley and Bentley is probably still a more useful source of this sort of information. The outdated nature of the book is again exhibited in the chapter relating to inorganic compounds, where great advances have been made in recent years, particularly relating to catalyst and semiconductor studies. The chapter on quantitative analysis is also inadequate and does not cover the value of stabilised laser outputs in this context, especially for time-resolved studies. The chapter relating to specific applications covers several unrealistic examples which could all have been done much better by other techniques. Finally, the atlas of 66 Raman spectra adds nothing to the value of the book, and much more useful collections of spectra are available elsewhere.

To sum up, this book would probably have been useful 10 years ago, but is so out of date and so inadequate in its coverage of analytical applications that it does very little to advance the use of Raman spectroscopy in this area.

D. L. Gerrard

CUMULATIVE AUTHOR INDEX
JANUARY–OCTOBER 1988

FOLD HERE

THE ANALYST READER ENQUIRY SERVICE OCT'88

For further information about any of the products featured in the advertisements in this issue, please write the appropriate number in one of the boxes below.
Postage paid if posted in the British Isles but overseas readers must affix a stamp.

PLEASE USE BLOCK CAPITALS LEAVING A SPACE BETWEEN WORDS *Valid 12 months*

1 NAME

2 COMPANY

PLEASE GIVE YOUR BUSINESS ADDRESS IF POSSIBLE. IF NOT, PLEASE TICK HERE

3 STREET

4 TOWN

5 COUNTY
POST CODE

6 COUNTRY

7 DEPARTMENT
DIVISION

8 YOUR JOB TITLE
POSITION

9 TELEPHONE NO

OFFICE USE ONLY   REC'D   PROC'D

FOLD HERE

Postage
will be
paid by
Licensee

Do not affix Postage Stamps if posted in Gt. Britain,
Channel Islands, N. Ireland or the Isle of Man

2

BUSINESS REPLY SERVICE
Licence No. WD 106

Reader Enquiry Service
The Analyst
The Royal Society of Chemistry
Burlington House, Piccadilly
LONDON
W1E 6WF
England

The Analyst

The Analytical Journal of The Royal Society of Chemistry

CONTENTS